

Lead 3-9-85

Proceedings of the Vertical Axis Wind Turbine (VAWT) Design Technology Seminar for Industry

Sidney F. Johnston, Jr., Editor

Prepared by
Sandia National Laboratories
Albuquerque, New Mexico 87185 and Livermore, California 94550
for the United States Department of Energy
under Contract DE-AC04-76DP00789



Issued by Sandia National Laboratories, operated for the United States Department of Energy by Sandia Corporation.

NOTICE: This report was prepared as an account of work sponsored by an agency of the United States Government. Neither the United States Government nor any agency thereof, nor any of their employees, nor any of their contractors, subcontractors, or their employees, makes any warranty, express or implied, or assumes any legal liability or responsibility for the accuracy, completeness, or usefulness of any information, apparatus, product, or process disclosed, or represents that its use would not infringe privately owned rights. Reference herein to any specific commercial product, process, or service by trade name, trademark, manufacturer, or otherwise, does not necessarily constitute or imply its endorsement, recommendation, or favoring by the United States Government, any agency thereof or any of their contractors or subcontractors. The views and opinions expressed herein do not necessarily state or reflect those of the United States Government, any agency thereof or any of their contractors or subcontractors.

Printed in the United States of America
Available from
National Technical Information Service
U.S. Department of Commerce
5285 Port Royal Road
Springfield, VA 22161

NTIS price codes
Printed copy: A15
Microfiche copy: A01

SAND80-0984
Unlimited Release
Printed August 1980

Distribution
Category UC-60

PROCEEDINGS OF THE VERTICAL AXIS
WIND TURBINE (VAWT) DESIGN TECHNOLOGY
SEMINAR FOR INDUSTRY

April 1, 2, and 3, 1980
Albuquerque, New Mexico

Sidney F. Johnston, Jr., Editor

ABSTRACT

The objective of the Vertical Axis Wind Turbine (VAWT) Program at Sandia National Laboratories is to develop technology that results in economical, industry-produced, and commercially marketable wind energy systems. The purpose of the VAWT Design Technology Seminar for Industry was to provide for the exchange of the current state-of-the-art and predictions for future VAWT technology. Emphasis was placed on technology transfer of Sandia's technical developments and on defining the available analytic and design tools.

ACKNOWLEDGMENTS

The Seminar Coordinator expresses his appreciation to Dr. Maurice Katz, Director of the Office of Solar Power Applications, Department of Energy, Washington, DC, for being the principal luncheon speaker; also to Dr. Richard Braasch and Mr. Emil Kadlec of the Advanced Energy Projects Division of Sandia National Laboratories, who helped outline the Seminar procedures. Thanks are due to Mr. George P. Tennyson of the DOE/Albuquerque Operations Office for his welcoming address.

Sheila Guynes, secretary of the Advanced Energy Projects Division at Sandia National Laboratories, deserves special thanks for her tireless attention to innumerable details necessary to the success of the Seminar.

Projectionists W. C. Garcia and H. J. Landis of Sandia National Laboratories and G. Hauge of the University of New Mexico made the visual aids flow effortlessly and in tune with the presentations in spite of some not-so-apparent difficulties.

The personnel of the Albuquerque Hilton Inn and Convention Center provided excellent facilities and many amenities.

To the many other employees of Sandia National Laboratories a special thanks; without them the Seminar would not have been possible.

Sidney F. Johnston, Jr.
Seminar Coordinator
Sandia National Laboratories
Division 4715

CONTENTS

	Page
Foreword - George Tennyson	5
Introduction - Dr. Maurice Katz and William C. Reddick	7
I. OVERVIEW OF VAWT PROGRAM R. H. Braasch	22
II. DESIGN CHARACTERISTICS OF CURRENT AND FUTURE VAWT SYSTEMS	44
Current and Future Design Characteristics of Vertical Axis Wind Turbines E. G. Kadlec	45
17 Meter Vertical Axis Wind Turbine (VAWT) R. D. Grover	55
Design Characteristics of the DOE/ALCOA-17 Meter Turbine R. O. Nellums	67
Intermediate Vertical Axis Wind Turbine (VAWT), 1 Megawatt R. D. Grover	118
Control Algorithm Investigations G. M. McNerney	124
III. STRUCTURAL DESIGN OF VAWT SYSTEMS	137
Overview of Available Techniques for VAWT Struc- tural Design Analyses W. N. Sullivan	138
Static Blade Analysis of the DOE/Alcoa Low-Cost 17 Meter Turbine W. N. Sullivan	146
VAWT Rotor Structural Dynamics Analysis Methods D. W. Lobitz	156
Design of VAWT Drive Train for Torque Ripple Control R. C. Reuter, Jr.	176
Guy Cable and Foundation Design Techniques T. G. Carne	195

	Page
IV. AERODYNAMIC PERFORMANCE OF VAWT SYSTEMS	214
Vertical Axis Wind Turbine Aerodynamic Performance Prediction Methods P. C. Klimas	215
Measured Aerodynamic and System Performance of the 17 Meter Research Machine M. H. Worstell	233
Possible Aerodynamic Improvements for Future VAWT Systems P. C. Klimas	259
V. SYSTEM ENGINEERING AND ECONOMICS	274
Summary of VAWT Economic Studies and Optimization Techniques R. O. Nellums	275
Possible Improvements in VAWT Economics E. G. Kadlec	289
VI. SESSION VI	295
Experimental Measurements	
Instrumentation of the 17 Meter Research Turbine M. T. Mattison	296
Instrumentation for the 17 Meter Low-Cost VAWT M. T. Mattison	305
Currently Available Instrumentation Software Collection and Analysis Packages on the 17 Meter Research Turbine G. M. McNerney	317
APPENDIX A -- Seminar Brochure Invitations and Response	329
APPENDIX B -- Industry Personnel Representing and Affiliation	330
Bibliography	331

Foreword

George P. Tennyson

The Vertical Axis Wind Turbine (VAWT) Design Technology Seminar for Industry was held because we in the Department of Energy (DOE) believe in the potential competitive viability of VAWTs, and our contractors have technical data, procedures, and experience to share toward the achievement of that viability. Our policy is not merely to develop wind turbines but to encourage the wide use of wind power. The information available through our program is aimed at accomplishing just that, and any contract we let -- past, present, and in the foreseeable future -- must fit in with that policy. However, within the programmatic and budget constraints required by the Legislative and Executive branches, we expect a strong growth in the VAWT program in Fiscal Years FY80, FY81, and FY82. In 1980 we are experiencing a 50% program growth over the year's initially approved plans. This includes the initiation of the medium-scale VAWT development by issuing announcements in Commerce Business Daily and preparation of the Request for Proposals.

In FY81, we expect to see the program grow by a factor of between three and five from the expanded 1980 figure. In FY82 we expect further growth in the VAWT effort provided there is overall wind program growth, and there is substantial evidence that there will be. I am not sure that we can grow by a factor of three to five every year, but we can surely try. That is, as long as the economic promise of the VAWTs is as good as, or better than, their competitors'.

But achievement isn't just programs and paperwork, it's people in action. I would be less than honest or gracious if I did not publicly acknowledge a few of the individuals who have worked very hard to bring the VAWT technology to reality and the consequent recognition of the necessity for this meeting and the procurements to follow. Special recognition is

due to Sandia's Dick Braasch, ably assisted by Emil Kadlec and Bill Sullivan, and supported by Glen Brandvold and Jim Scott. Dean Graves of DOE/ALO also gave his enthusiastic support.

There was a review panel that included representatives from NASA, DOE Headquarters, Sandia, a number of contractors, and some consultants. It was this review panel's objectivity that finally brought merit out of obscurity to recognition.

The DOE Headquarters Program Manager, Bill Reddick, although relatively new to the VAWT effort, may just have had the deciding impact. At least, prior to his appointment as Program Manager no such mid-size VAWT development had been approved.

Without Lou Divone's support, of course, there would have been no meeting. Or for that matter without any of these people, or you. Guiding a program from its initial stages to a point where significant progress is evident takes a tremendous amount of energy and effort which all of the above generously contributed.

But in the end it is the contractors and subcontractors who make it happen. We are all here to put you in the best possible position to contribute to making the VAWT one of America's future alternative energy tools.

Introduction

Dr. Maurice Katz

In the early 1970s, the federal government's support of solar programs was mostly research and development oriented. Between \$2 and \$4 million were spent by the National Science Foundation and other agencies for solar R&D and, of that, only about \$300,000 was for wind energy systems. The Vertical Axis Wind Turbine (VAWT) Program did not exist.

In 1977 when the Department of Energy (DOE) was formed, the solar budget had risen sharply. About \$100 million was appropriated, the total wind program was about \$15 million, and \$1.5 million was supporting the VAWT Program. DOE organized the solar program under two assistant secretaries: one for high technology long-term technologies and the other for near-term technologies and commercialization activities. The new reorganization puts an end to this split and adds a commercialization emphasis to all solar programs, both long-term and short.

The solar program approved by the Secretary of Energy earlier this year is organized by market sector and reports to a single deputy assistant secretary. The market sectors are for solar applications for buildings, for industry, and for solar power applications. Technology program cradle-to-grave management is carried out within these market sectors. Thus active, passive, and photovoltaic systems are assigned to the buildings sector; biomass and solar thermal energy to the industrial sector; and wind and ocean systems to the solar power applications office which also has responsibility for all solar technology interface with the utility market. Thus technical development and market development fall under one management. This should go far to smooth communication between developers and customers. An alcohol fuels market sector office is also included in the solar program.

The FY81 budget will be the first managed in this new structure. The Presidential request provides for over \$650 million in solar program funds of which \$87 million is for wind energy systems, and about \$8 million is included for the VAWT Program. In addition, about \$900 million is requested elsewhere in the federal budget to accelerate solar technology acceptance. Such programs as tax and other incentives are included.

What does this new structure mean for the wind energy program? The key lies in the market sector approach. We are attempting to achieve the President's goal of displacing 1.7 quads of oil annually by the year 2000 with wind energy. For this to happen, we estimate that about 25,000 large wind machines (greater than 100 kW rated capacity) and 1.6 million small wind machines will have to be operating by that year. The total private sector market for all these machines will come to about \$35 billion by the turn of the century.

Clearly, only a program guided by market sector considerations can hope to achieve these goals. Thus I would expect to see increased emphasis in government support for strictly commercialization activities. These would include expanded demonstration programs and expanded emphasis on information dissemination, market development, field evaluations, and reduction of institutional barriers. The recent ruling by the federal energy regulatory commission to require the purchase of power from small producers is an excellent example of reducing nontechnical barriers. Current legislation under consideration by Congress is expected to lead to a significant cost sharing program for wind commercialization.

In summary, it is clear that the nation's energy future requires the application of wind and other solar technologies. It is also clear that success in this field cannot be achieved without committed cooperation between government and the private

sector. We are beginning to see excellent examples of such cooperation. In Clayton, New Mexico, a 200 kW Mod OA windmill has already provided over 1/2 million kWh to the local municipality grid and can supply over 10% of the electricity sold by the municipality. The optimism of the local officials for this solar technology application is indeed heartening. In 1979, 51 utilities across the nation were participating in 83 wind application projects. This participation was 50% higher than that in the previous year. Some utilities have also been including wind systems in their expansion plans. Both large centralized systems and small distributed consumer-owned systems are considered.

In closing, our energy problems must and will be solved. The President's goals for solar energy are challenging but achievable. The indicators for wind applications are positive and I am personally convinced that continued cooperation among researchers, manufacturers, utilities, consumers, and government will lead to success.

William C. Reddick

The Wind Energy Systems Division of the Department of Energy (DOE) strongly believes in and supports the Vertical Axis Wind Turbine (VAWT) Program. We see an increase in emphasis on wind system technology as a result of the efforts by Sandia National Laboratories and its supporting contractors. As a consequence of this progress, DOE is increasing its support of the VAWT Program to ensure that this alternative wind turbine technology will be available to the public and private sector. Our development, cost, and energy goals for wind energy systems are as follows:

Objective

- To expedite the development and commercialization of reliable, cost-effective wind systems to contribute a significant quantity of energy to our nation's needs.

Energy Goal

- 1.7 quads/year by 2000 estimated in the domestic policy review.
- 10%-15% of President's 20% goal.

Cost Goals

- Status: 15 to 30¢/kWhr
- Second-Generation: 8¢/kWhr (1980 prototype) and 4¢/kWhr (production).
- Third-Generation: 5 to 6¢/kWhr (1983 prototype) and 3¢/kWhr (production).

This introduction is an abbreviated version of what is happening in the VAWT Program, but I hope it will communicate the fact that we are making measurable progress in the wind program. Of course, the VAWT Program is the proof that we are trying to provide a broad spectrum of technologies in the wind energy area (Fig. 1).

It is quite fortunate that we do have Sandia National Laboratories and other facilities in the field to implement and manage the technical programs. DOE decided that decentralization is the most effective method for managing a large number of high technology projects. I believe this decentralization policy has proven very effective. If we in Washington had to concentrate on day-to-day management of the technical projects, we would not be nearly as close to developing cost-effective machines as I believe we are today.

The objective of the wind program, as we see it today, is not to just foster or bring about the development of wind energy. We believe that wind energy technology will eventually be developed without government involvement. Therefore, it is our job to accelerate the development, demonstration, and market development process. The President has set a wind energy goal of 1.7 quads per year by the year 2000. To achieve this goal we believe the cost of energy (COE) from wind machines must be lowered to approximately 3-5 cents per kWhr. The experimental machines that we have developed to date, both the horizontal axis and the low-cost

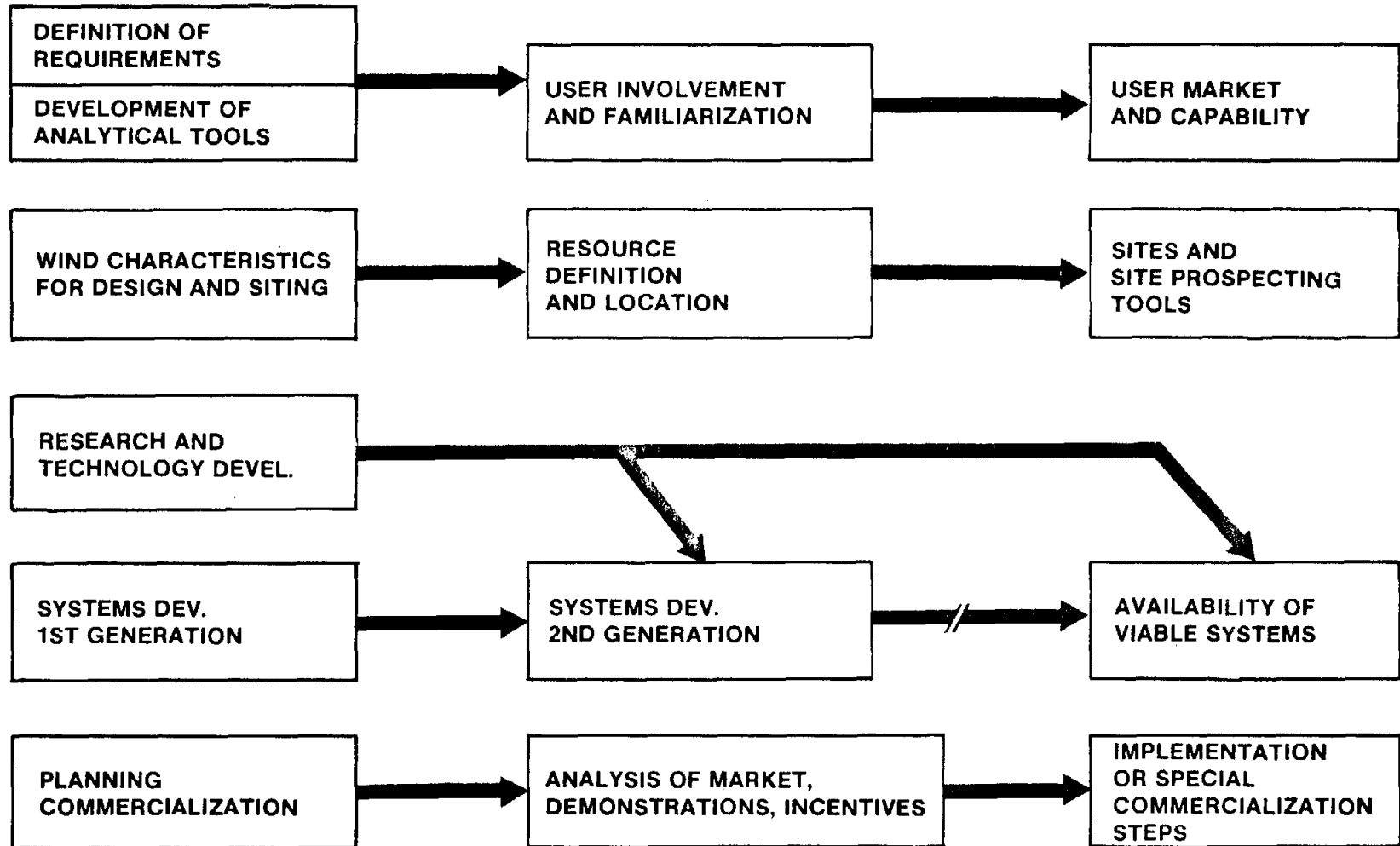


Figure 1. Wind Program Overview

vertical axis machines that will be tested starting this fall, have COEs in the range of 15 to 30 cents. Although that cost range might be lowered with the low-cost Darrieus, the machines that we are testing today like the Mod 1 and the Mod 0As are in that range. We are looking forward to our second-generation of machines having COEs of approximately 8 cents for an experimental prototype and about 4 cents for production quantities. Finally, the third-generation machines should bring the costs down to 3-5 cents making wind energy economically competitive and, therefore, more widely acceptable to future users (private individuals, utilities, and for agricultural applications).

Figure 2 shows the decentralization structure for the Wind Systems Program. Although the figure identifies us as the "Wind Systems Branch," we have since been designated as the "Wind Systems Division." This change is important for us since the Wind Systems Division is now not only responsible for developing the technology, but will also manage the market development activities as well.

As stated previously, the field facilities handle the technical management of the Wind Systems Program. The Solar Energy Research Institute (SERI) manages the market studies and institutional analyses program, and the innovative concepts program. The innovative concepts program provides an avenue for those inventors with promising concepts for wind power to have their inventions evaluated by

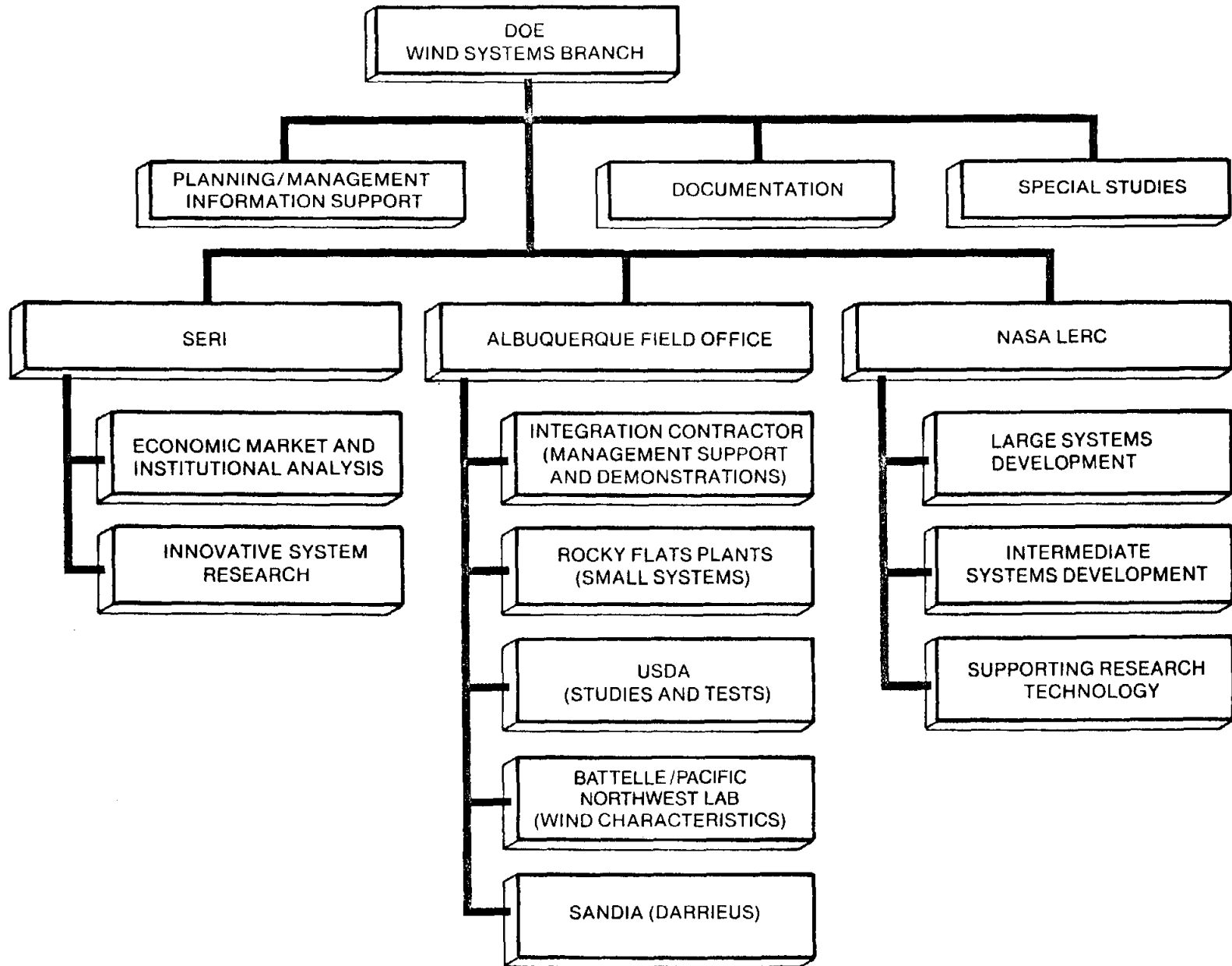


Figure 2. Wind Systems Branch Management Organization

the government. For those concepts that show the potential for high payoff, the DOE may develop experimental machines for testing. We do not believe that we have the last word in how to utilize wind power; therefore, we keep the door open so that new ideas can be developed if they prove to be cost-effective and viable.

Next, we have the Albuquerque Operations Office that functions as our field program manager for Sandia National Laboratories, Rocky Flats, USDA, and Pacific Northwest Laboratories. Rocky Flats has responsibility for developing and testing small systems. We have an agricultural activity at the U.S. Department of Agriculture, the Wind Characteristics Program at Pacific Northwest Laboratories, and Sandia National Laboratories with the VAWT Program. Finally, NASA has the responsibility for developing the large and intermediate-scale machines.

Figure 3 is an overview of the program in terms of our program strategy both from a technology development perspective and also from a market development perspective, which is commonly referred to as commercialization. The first area includes market studies, requirements analyses and those kinds of study activities that are necessary for the government to assure itself that the program will meet the needs of the industry and the end-users. As these studies are completed we will make them available to the users and the producers to help them in their decision making process, market planning, and planning for wind systems utilization.

- TESTING OF ALL 1, 8, AND 40 KW PROTOTYPES UNDERWAY
- DEDICATION OF MOD-0A 200 KW MACHINE HAWAII
- BEGIN UTILITY OPERATIONAL TEST OF MOD-1
2 MW MACHINE
- COMPLETE INSTALLATION OF FIRST MOD-2 2.5 MW
MACHINE
- AWARD OF MOD-5 ADVANCED MULTIMEGAWATT WIND
TURBINES
- ISSUE RFP FOR MOD-6 ADVANCED MULTIPURPOSE
MEDIUM SCALE WIND TURBINE PROJECT
- BEGIN TESTING OF FIRST LOW-COST DARRIEUS
- COMPLETE WIND ATLASES
- COMPLETE LARGE WIND TURBINE SITING HANDBOOK

Figure 3. Federal Wind Program FY80 Accomplishments

Secondly, we have the wind characteristics program element. I think this is one of the more important areas of the program in terms of our (DOE) ability to foster and accelerate the use of wind energy. This program provides not only information for the potential users but it also provides information for the design and development of machines.

Then, of course, we have the hardware programs where we develop the technology that leads to the production of engineering or demonstration models. Product improvement is part of this effort as we go through the various stages or generations of technology development.

Finally, we have what we call commercialization. This type of activity, as you probably know, is new to the Federal Government. It would probably be better to say that what we are doing is developing a product (wind energy technology), and then helping the private and public sector with the marketing (i.e., market development) and utilization of that product. In terms of actual marketing of the technology, in the commercial sense, I really don't think the government is structured to accomplish that task. I think commercialization is a private sector function.

Over the past two years the budget for the Wind Energy Program has increased (Fig. 4). In FY81 we expect a considerable increase in the funding for the overall wind program -- in the area of \$80-100 million. The funding levels

	<u>FY79</u>	<u>FY80</u>	<u>FY81</u>
1. RESEARCH AND ANALYSIS	\$ 6.3M	\$ 8.8M	\$ 7.7M
2. WIND CHARACTERISTICS	\$ 4.4	4.7	6.2
3. TECHNOLOGY DEVELOPMENT	8.9	9.9	17.7
4. ENGINEERING DEVELOPMENT	33.9	19.8	48.4
5. IMPLEMENTATION & MARKET DEVELOPMENT	4.7	2.0	7.0
	—	—	—
OPERATING EXPENSE	58.2	45.2	87.0
CAPITAL EQUIPMENT & CONSTRUCTION	1.4	18.1	
	—	—	—
TOTAL	<u>59.6</u>	<u>63.3</u>	<u>87.0</u>

Figure 4. Wind Energy Structure

for the VAWT program will not be discussed because they are included in the Technology Development and Engineering Development Programs.

In terms of the program structure and content of the program elements discussed herein, the different activities and their areas of responsibility are as follows:

- Research and Analysis: Provides analyses, assessments, models, and studies to support decision-makers at the manufacturing, end-user, regulator, and legislative levels.
- Wind Characteristic: Provides wind characteristics information that directly affects siting, operation, and economics for both large and small systems.
- Technology Development: Improves the performance and lowers the cost of wind systems and improves their technical performance.
- Engineering Development: Designs, fabricates, and tests a series of progressively more advanced experimental wind systems with improved capabilities leading to systems capable of commercial production and acceptance by the industry and end-users.
- Implementation and Market Development: Implements end-user supports, outreach programs, and end-user-oriented field evaluation and system performance demonstrations which generate and accelerate private

and public sector interest while supporting manufacturer growth and capitalization in the early commercial development years.

It might be asked why there is \$18.1 million for construction in FY80, and in FY79 and FY81 the level is much less. The reason this apparent anomaly exists is that Congress decided that the Mod 2 should be included in the capital equipment and construction category, rather than in engineering and development.

What is being done with all this taxpayers' money? Figure 4 provides a breakdown of what has been accomplished and what we expect to accomplish in FY80. At Rocky Flats we are testing the 1, 8, and 40 kW prototypes, and plan to test the low-cost Darrieus in the summer of 1980. We expect to dedicate the Mod OA in Hawaii some time in July 1980. The Mod 1 is currently in testing at Boone, North Carolina. The lessons we have learned with the Mod 1 have been very helpful in providing information and engineering data that were used in the design of the Mod 2. We expect to install and have first rotation of the Mod 2, the 2.5 MW machine at Goodnoe Hills, Washington by the end of this year. We have selected General Electric and Boeing as the two contractors for the Mod 5, our advanced megawatt machine (in the area of 4 - 4.5 MW). Requests for Proposals were released in the spring of 1980 and we hope to have a contract by fall. We will begin testing of the low-cost Darrieus, which is about a 50 - 60 kW machine, at Rocky Flats some time in the summer of 1980.

The area that I mentioned previously, and that I find to be very important to the eventual wide-scale commercial use of wind technology, is the Wind Characteristics Program. Two very important products will be completed this year: (1) the wind atlases -- there will be 12 atlases with one for each region of the U.S. and its territories. These will be published some time before the end of the year; and (2) a handbook for large systems, a sort of "do it yourself" step-by-step procedure for those organizations that are interested in assessing the wind energy available and determining whether wind energy is economically feasible or not for them. We also hope to have this published before the end of the summer.

DOE believes that there is a promising future for the VAWT Program. Our commitment to the Mod 6V has shown that we are committed to the development of this technology. We have currently authorized Sandia to continue studies on the developmental possibilities of a large VAWT. If the work that we do on the Mod 6V proves to be successful, we certainly will be in a better position to convince our management to go forward with a large-scale VAWT Program.

SECTION I
OVERVIEW OF VAWT PROGRAM
R. H. Braasch

OVERVIEW OF VAWT PROGRAM

Richard H. Braasch

The purpose of this seminar is to attempt to transfer to industrial organizations the progress that has been achieved on vertical axis wind turbine technology. The purpose for transferring this technology is with regard to a future procurement to be initiated by Sandia National Laboratories in the near future for an intermediate size machine.

The organizational approach selected for this seminar is outlined in Fig. 1. Separate sessions of this seminar will review design characteristics of current and future systems, structural design, aerodynamic performance, system engineering and economics, and experimental measurements. In addition, a tour of operational test machines at Sandia National Laboratories will be conducted and open discussion groups will be conducted on items of interest in aerodynamics, systems, structural, and example problem solving.

Figure 2 is a copy of an advertisement that Sandia National Laboratories recently placed in the Commerce Business Daily. The main features of this advertisement are outlined in Fig. 3. Namely, Sandia National Laboratories will begin the procurement of an advanced intermediate size machine. The program will be called the Mod 6V and the specific machine type will be limited to a vertical axis wind turbine of the Darrieus type. Requests for quotations on this procurement will be issued by Sandia National Laboratories during May 1980. Responses generated by the Commerce Business Daily advertisement will be used to generate a source list of companies interested in participating

in this procurement activity. Companies interested in being considered for participation on a contract basis in the program are invited to send a statement of qualification concerning applicable design, fabrication capabilities, and experience by April 14, 1980 to the individual noted in the Commerce Business Daily advertisement. The scope of the program includes design, fabrication, installation, and testing of one to three machines over a 59 month time period.

The sessions associated with this seminar were shown in Fig. 1. The first session, Design Characteristics of Current and Future VAWT Systems, is outlined in Fig. 4. Current systems include the 17 meter research machine, the DOE/ALO-Alcoa machine, the 5 meter test machine, and the 2 meter wind tunnel test machine. Presentations will be given on the 17 meter research machine and the DOE/ALO-Alcoa machine. The other two machines are available for inspection during the tour of the test site. Figure 5 provides a description of the DOE/ALO-Alcoa machine.

Future systems being considered are the Mod 6V program which was just previously mentioned and initial activities related to planning for the procurement from industry of a large-scale machine.

The items being emphasized on current and future systems are listed in Fig. 4. All of the items listed are directed toward lowering the cost of energy produced from vertical axis wind turbines. Studies done to date that include the incorporation of these items into future designs indicate that the cost of energy can be reduced approximately a factor of two relative to estimates for current designs. This first session will discuss many of these items in considerable detail.

The basic features of current vertical axis wind turbine machine design are listed in Fig. 6. Collectively, these features constitute the configuration and characteristics of

vertical axis wind turbines that have been judged to most effectively reduce the cost of energy generated by these machines.

In the Darrieus type machine, the blades are curved such that the blade flatwise stresses are reduced to the point that the flatwise stresses are not controlling the fatigue life of the machine. In addition, the blades are attached at both ends. This reduces root loads by providing multiple paths for the aerodynamic-generated loads to enter the drive train. A two-bladed rotor has been selected over rotors with larger numbers of blades since it is estimated to be of lower cost, easier and less costly to erect, and the number of natural frequencies of the system are less and believed to be easier to control. The blades are constructed using an extruded aluminum process. Large extrusions have been quoted at less than two dollars per pound. In an extrusion process used for blades, the tooling required is controlled by the blade chord dimension. Hence, tooling costs are minimal.

The rotor height-to-diameter ratio has been selected at 1.5. Large height-to-diameter ratio forces the rotor to run at higher rotational rates. This reduces required transmission torque rating for machines of a given power rating.

Large diameter, thin-wall, steel towers are used because the lowest weight structure for the tower is achieved in this fashion. In addition, tower bending and torsional stiffness necessary to control the rotor speeds associated with natural frequency crossings of concern are satisfied.

Current designs employ a stiff; that is, high cable tension, cable support system. Reduction of cable tension and cable damping mechanisms will be discussed in various papers at the seminar.

The base tower employs a minimum amount of structural steel to raise the height of the rotor. Studies have indicated that

it is more profitable to build a slightly larger rotor than to raise the height of the rotor by increasing the base structure. By minimizing the base structure, a compact drive train assembly located at ground level is achieved. This can be assembled in a factory and delivered to the erection site. This will simplify the on-site erection. In addition, the rotor is assembled in the horizontal position and rotated into position onto the base. The need to lift individual items to height and assemble is greatly reduced.

Both induction and synchronous motor starting and power generation have been investigated and either approach can be used.

Vibratory stress levels due to gravity are minimal in a Darrieus vertical axis wind turbine. Also, steady state stress levels due to gravity can be controlled by designing the shape of the blade to account for sag due to gravity. The DOE/ALO-Alcoa machine includes these features. A VAWT does experience large aerodynamic load variations which increase with increasing windspeed. Lead lag stress levels at the blade roots are low at low to moderate windspeeds and generally increase with increasing windspeeds. Also, since the VAWT experiences large aerodynamic load variation, concern for gusting is not particularly great because the machine basically is always working in such an environment.

The second section of this seminar addresses the structural design of VAWT systems. Figure 7 notes the major items receiving emphasis. Basically, we are attempting to estimate machine fatigue life based upon an understanding of static and vibratory stress levels experienced during normal operating conditions. In addition, survival during extreme environmental conditions is addressed. Development of static and dynamic analysis tools are being pursued as is an understanding of natural modes of vibration for these structures and the ability to excite these natural frequencies with rotor-provided excitation. Also,

emphasis is being placed on gathering experimental structural data and comparing it to analytic predictions.

The third section of this seminar reviews the aerodynamic performance of VAWT systems. Figure 8 overviews the aerodynamic program activities. Wind tunnel tests have been conducted providing parametric performance and wake measurements on an operating 2 meter diameter rotor. Also, wind tunnel data on blade sections have been gathered. Field test data have been gathered on numerous characteristics of VAWT operation using the 17 meter, 5 meter, and 2 meter systems installed at the Sandia test site. To support this activity, computational tools have been developed for use with VAWT's. Three levels of performance prediction and two levels of load prediction will be discussed. In addition, blade section aerodynamic characteristic computational tools have been obtained from NASA and are available for providing basic airfoil section data.

Current emphasis in the aerodynamics area is directed toward understanding the effects on performance and loads introduced by the unsteady aerodynamics experienced in the VAWT. Also, emphasis on tailoring aerodynamic performance characteristics by use of unsymmetric blades and blade mounting geometry are being investigated.

The fourth section of this seminar reviews the system engineering and economics associated with VAWT systems. As noted in Fig. 9, emphasis is placed on component performance and cost modeling, system optimization and trade-off studies, identification of productive items to pursue to improve the performance or cost-effectiveness of VAWT design, and determination of the expected cost of energy associated with VAWT technology.

The fifth section of this seminar reviews experimental measurements and the equipment employed. The data system currently utilized at the Sandia test site will be described.

In addition, the data system being constructed for testing the DOE/ALO-Alcoa 100 kW_e machine will be described.

Following the above five noted sections of this seminar, a tour of the Sandia wind turbine test site will be conducted and open discussion groups will be conducted on items of interest in aerodynamics, systems, structural, and example problem solving.

VERTICAL AXIS WIND TURBINE
DESIGN TECHNOLOGY
SEMINAR FOR INDUSTRY

PURPOSE: TECHNOLOGY TRANSFER TO INDUSTRY OF MATERIAL BENEFICIAL IN PREPARING RESPONSES TO POSSIBLE FUTURE PROCUREMENTS ON DARRIEUS-TYPE VERTICAL AXIS WIND TURBINES

APPROACH: REVIEW

- DESIGN CHARACTERISTICS OF CURRENT AND FUTURE VAWT SYSTEMS
- STRUCTURAL DESIGN OF VAWT SYSTEMS
- AERODYNAMIC PERFORMANCE OF VAWT SYSTEMS
- SYSTEM ENGINEERING AND ECONOMICS
- EXPERIMENTAL MEASUREMENTS

TOUR

- OPERATIONAL MACHINE INSTALLATION

OPEN DISCUSSION GROUPS

- AERODYNAMICS
- SYSTEMS
- STRUCTURAL
- EXAMPLE PROBLEMS

FIGURE 1

COMMERCE BUSINESS DAILY ADVERTISEMENT

DESIGN, FABRICATION, INSTALLATION AND TESTING OF A DARRIEUS VERTICAL AXIS WIND TURBINE. DESIGN, FABRICATION, INSTALLATION AND TESTING OF AN ADVANCED INTERMEDIATE SCALE DARRIEUS VERTICAL AXIS WIND TURBINE, THE MOD 6V. THIS 59 MONTH PROGRAM WILL ENCOMPASS THE DESIGN, FABRICATION AND INSTALLATION OF ONE MACHINE IN 35 MONTHS WITH THE OPTION TO OBTAIN ONE OR TWO ADDITIONAL MACHINES. THE PROGRAM WILL INCLUDE CONSIDERATION FOR ANY COST SHARING PROPOSALS RECEIVED. SANDIA IS SEEKING INTEREST AND INVOLVEMENT OF QUALIFIED FIRMS AND TEAMS OF FIRMS IN THIS ACTIVITY. RESPONSES TO THIS ADVERTISEMENT WILL BE USED TO GENERATE A SOURCE LIST FOR A REQUEST FOR QUOTATION (RFQ) TO BE ISSUED APPROXIMATELY MAY 1980. THE RFQ WILL INCLUDE A REQUEST FOR TECHNICAL PROPOSAL. COMPANIES INTERESTED IN PARTICIPATING IN THIS ACTIVITY ON A CONTRACT BASIS ARE INVITED TO SEND APPROPRIATE INFORMATION OR STATEMENT OF QUALIFICATION CONCERNING APPLICABLE SYSTEM DESIGN AND FABRICATION CAPABILITIES AND EXPERIENCE. RESPONDENTS MUST IDENTIFY WHETHER THEY ARE LARGE OR SMALL BUSINESS. WRITTEN RESPONSES ARE DUE BY APRIL 14, 1980. RESPONSES RECEIVED AFTER THAT DATE MAY NOT BE CONSIDERED. ANY INFORMATION FURNISHED WILL BE CONSIDERED BY SANDIA NOT TO BE COMPANY SENSITIVE OR PROPRIETARY. THIS IS NOT A REQUEST FOR PROPOSAL. THERE IS NO INTENT TO PAY FOR INFORMATION FURNISHED IN RESPONSE TO THIS ANNOUNCEMENT. A SEMINAR COVERING THE PRESENT AND FUTURE DARRIEUS TECHNOLOGY WILL BE HELD IN ALBUQUERQUE, NEW MEXICO APRIL 1, 2, AND 3, 1980. THE SEMINAR COORDINATOR IS SIDNEY JOHNSTON, ORGANIZATION 4715; TEL. 505/844-7553. (065)

SANDIA LABORATORIES, PO BOX 5800, ALBUQUERQUE, NM 87185.

ATTN: H. L. CRUMLEY, DIVISION 3721

FIGURE 2

MOD 6V PROGRAM

MACHINE TYPE: DARRIEUS VERTICAL AXIS WIND TURBINE

PURPOSE: PROCUREMENT OF AN ADVANCED INTERMEDIATE SCALE MACHINE

PROCUREMENT METHOD: RESPONSE TO A REQUEST FOR QUOTATION (RFQ) TO BE ISSUED BY SANDIA LABORATORIES IN APPROXIMATELY MAY 1980.

OBTAINING RFQ: RESPONSES TO COMMERCE BUSINESS DAILY (CBD) ADVERTISEMENT WILL BE USED TO GENERATE A SOURCE LIST FOR THIS RFQ

RESPONSE REQUIRED: COMPANIES INTERESTED IN PARTICIPATING IN THIS ACTIVITY ON A CONTRACT BASIS ARE INVITED TO SEND APPROPRIATE INFORMATION OR STATEMENT OF QUALIFICATION CONCERNING APPLICABLE SYSTEM DESIGN AND FABRICATION CAPABILITIES AND EXPERIENCE BY APRIL 14, 1980 TO THE INDIVIDUAL NOTED IN THE CBD ADVERTISEMENT

PROGRAM SCOPE: DESIGN, FABRICATION, INSTALLATION, AND TESTING OF ONE TO THREE MACHINES

TIME SCALES: DESIGN, FABRICATION, AND INSTALLATION OF FIRST MACHINE - 35 MONTHS;
TESTING OF FIRST MACHINE - 24 MONTHS

FIGURE 3

CURRENT AND FUTURE VAWT SYSTEMS

CURRENT SYSTEMS

- 17 METER RESEARCH MACHINE
- DOE/ALO-ALCOA MACHINE
- 5 METER TEST MACHINE
- 2 METER WIND TUNNEL TEST MACHINE

FUTURE SYSTEMS

- MOD 6V: INTERMEDIATE SIZE
- LARGE-SCALE MACHINE

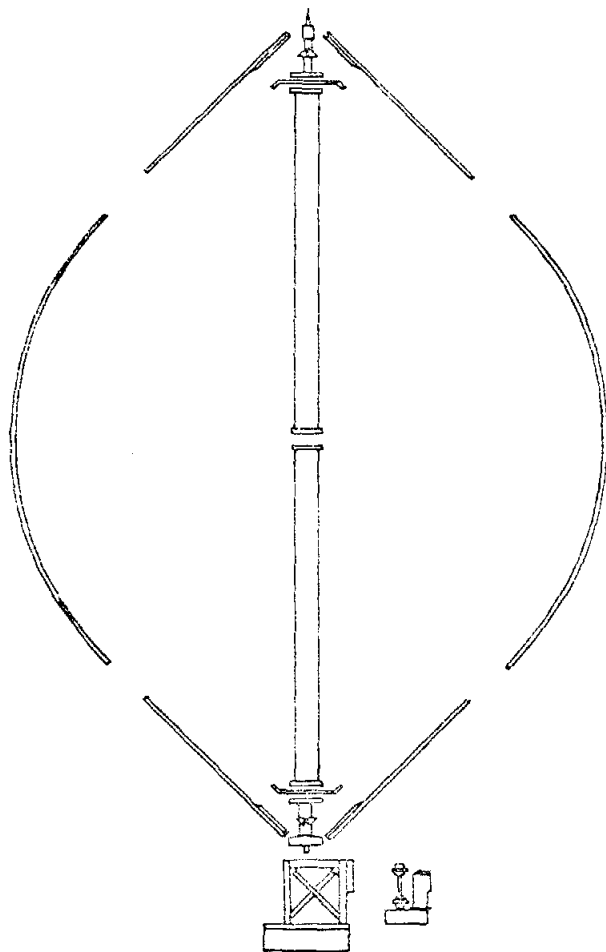
EMPHASIZE

- SYSTEM WEIGHT REDUCTION
- REDUCTION OF OVER SPECIFIED SYSTEM REQUIREMENTS
- REDUCED STRUCTURAL CONSERVATISM
- STRUCTURAL DYNAMICS
- REDUCED SUPPORT SYSTEM CABLE TENSION
- REDUCTION OF PEAK POWER PRODUCTION
- INCORPORATION OF OBSERVED HIGH EFFICIENCY PERFORMANCE
- REDUCED ANCHOR AND FOUNDATION REQUIREMENT
- SIMPLIFIED INSTALLATION AND ERECTION PROCEDURES
- LOW-COST FABRICATION PROCEDURES
- CONFIGURATION OPTIMIZATION

FIGURE 4

LOW-COST 17-METRE FABRICATION - ALCOA

MACHINE PARTS LAYOUT



MACHINE CHARACTERISTICS

Rated Electric Power	100 kW, 3-Phase, 60 Hz, 460 V
Rated Windspeed at 30' Ref.	13.8 m/s (31 mph)
Cut-In Windspeed at 30' Ref.	5.4 m/s (12 mph)
Shutdown Windspeed	26.8 m/s (60 mph)
Turbine rpm	51.5
Rotor Height	25.15 m (82.5 ft)
Number, Type of Blade	2, NACA 0015
Blade Chord	0.61 m (24 in.)
kWh/yr at 15-mph site	235,000
Capacity Factor	0.27
System Weight, Less Concrete	24,600 lb
kWh/lb at 15-mph Site	9.6
\$/lb FOB Factory, 100 Units/yr	2.12

FIGURE 5

BASIC FEATURES OF CURRENT VAWT DESIGNS

- BLADES ARE CURVED TO REDUCE FLATWISE STRESSES
- BLADES ARE ATTACHED AT BOTH ENDS
- TWO-BLADED ROTOR
- EXTRUDED ALUMINUM BLADES
- BLADE TOOLING CONTROLLED BY BLADE CHORD DIMENSION
- HEIGHT-TO-DIAMETER RATIO EQUAL TO 1.5
- LARGE DIAMETER, THIN-WALLED STEEL TOWER
- STIFF CABLE SUPPORT SYSTEM
- MINIMUM BASE TOWER
- DELIVERS MECHANICAL POWER AT GROUND LEVEL
- SIMPLIFIED ERECTION
- INDUCTION OR SYNCHRONOUS MOTOR STARTING AND POWER GENERATION
- NO VIBRATORY STRESS LEVELS DUE TO GRAVITY
- LARGE AERODYNAMIC LOAD VARIATIONS

FIGURE 6

STRUCTURAL DESIGN OF VAWT SYSTEMS

EMPHASIS

- STATIC AND VIBRATORY STRESS LEVELS DURING NORMAL OPERATING CONDITIONS
- FATIGUE LIFE ASSESSMENT
- SURVIVAL DURING EXTREME ENVIRONMENTAL CONDITIONS
- SYSTEM NATURAL FREQUENCY PREDICTION AND EXCITATION
- DEVELOPMENT OF STATIC AND DYNAMIC ANALYSIS CAPABILITY
- VERIFICATION AND CORRELATION OF ANALYTIC PREDICTIONS WITH EXPERIMENTAL DATA

FIGURE 7

AERODYNAMIC PERFORMANCE OF VAWT SYSTEMS

WIND TUNNEL TESTS

- PARAMETRIC PERFORMANCE AND WAKE MEASUREMENTS OF 2-M SYSTEM
- BLADE SECTION CHARACTERISTICS

FIELD TESTS

- PERFORMANCE OF 17-M, 5-M, AND 2-M SYSTEM: 2 AND 3 BLADED
- CAMBERED SECTION BLADES ON 5-M SYSTEM
- BLADE MOUNTED ACCELEROMETER ON 17-M SYSTEM
- DRAG BRAKES ON 5-M SYSTEM
- SIMULATED BLADE WELDS AND JOINTS ON 5-M SYSTEM

COMPUTATIONAL DEVELOPMENT

- PERFORMANCE: 3 LEVELS
- LOADS: 2 LEVELS
- BLADE SECTION CHARACTERISTICS PREDICTION

CURRENT EMPHASIS

- UNSTEADY AERODYNAMIC EFFECTS ON PERFORMANCE AND LOADS
- UNSYMMETRIC BLADE INVESTIGATIONS
- TAILORING OF PERFORMANCE CHARACTERISTICS
- WAKE MEASUREMENTS

FIGURE 8

SYSTEM ENGINEERING AND ECONOMICS

EMPHASIS

- COMPONENT PERFORMANCE AND COST MODELING
- SYSTEM OPTIMIZATION AND TRADE-OFF STUDIES
- IDENTIFICATION OF PROGRAM ACTIVITIES TO PURSUE
- COST OF ENERGY DETERMINATION

FIGURE 9

EXPERIMENTAL MEASUREMENTS

EMPHASIS

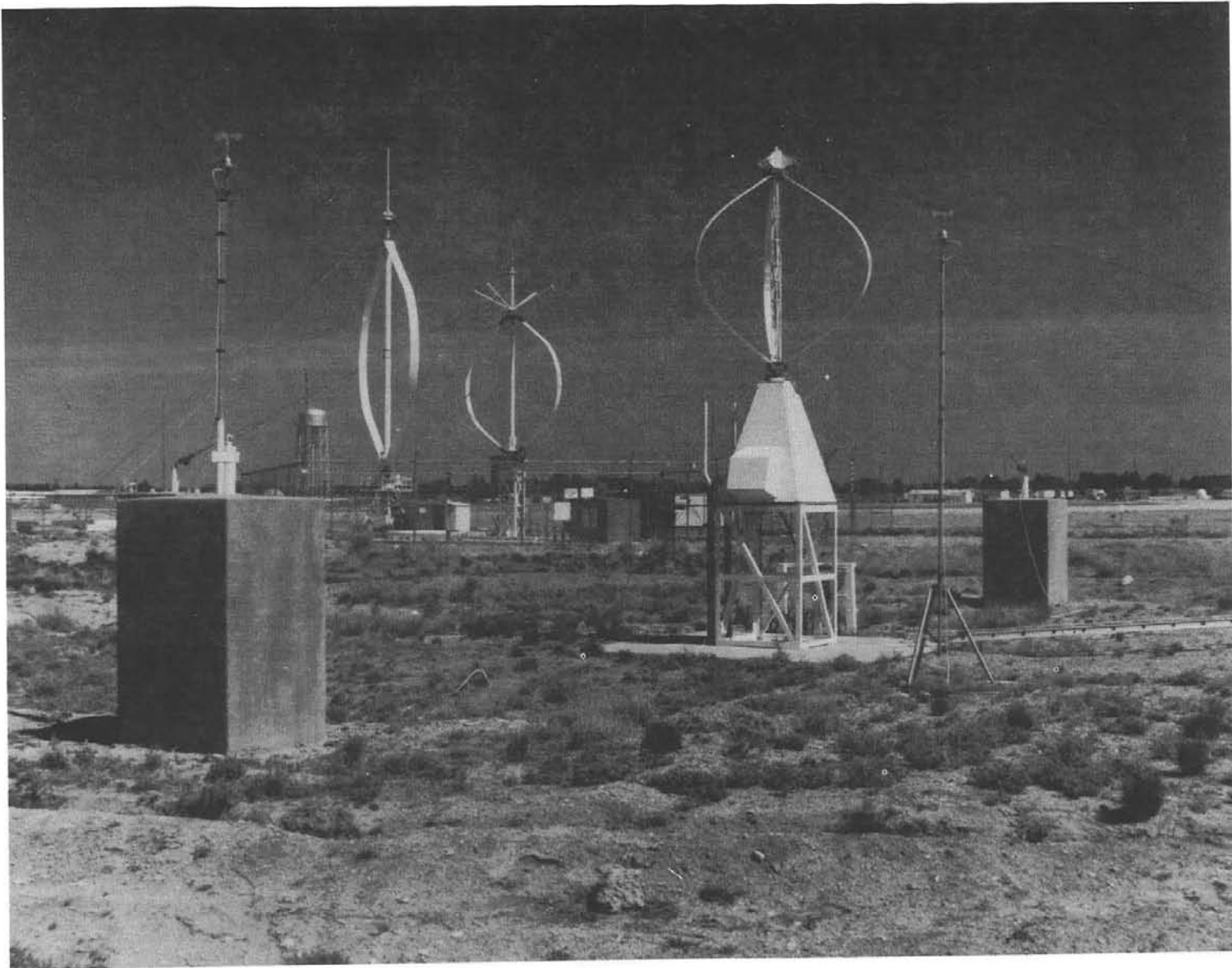
- DATA SYSTEM FOR RESEARCH TESTING
 - MACHINE CONTROL
 - DATA ACQUISITION
 - DATA STORAGE AND RETRIEVAL
 - DATA REDUCTION
 - SOFTWARE
 - USER ORIENTED
 - RAPID TESTING AND EVALUATION

- DATA SYSTEM FOR TESTING OF DOE/ALO-ALCOA 100 kW_E DESIGN

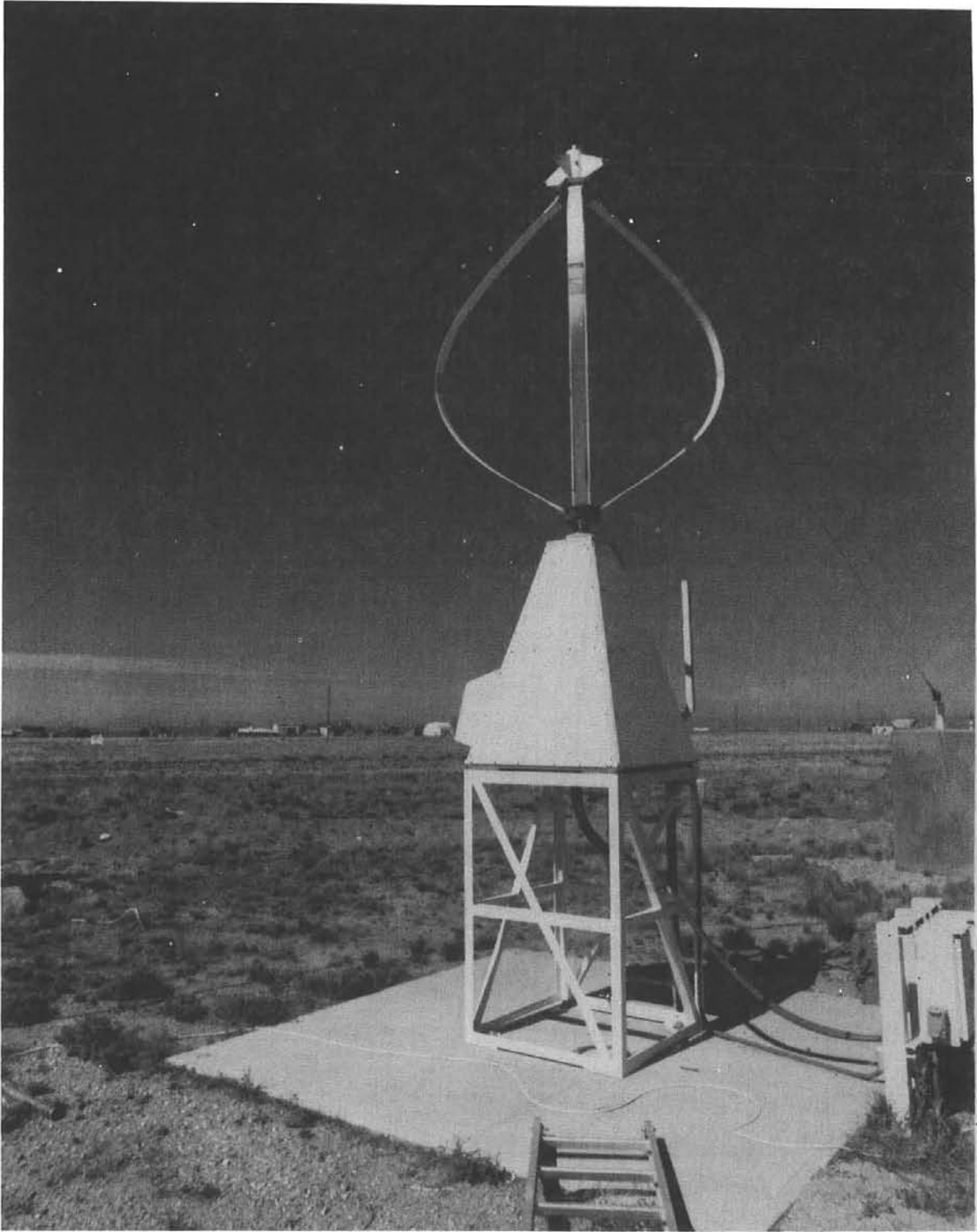
FIGURE 10



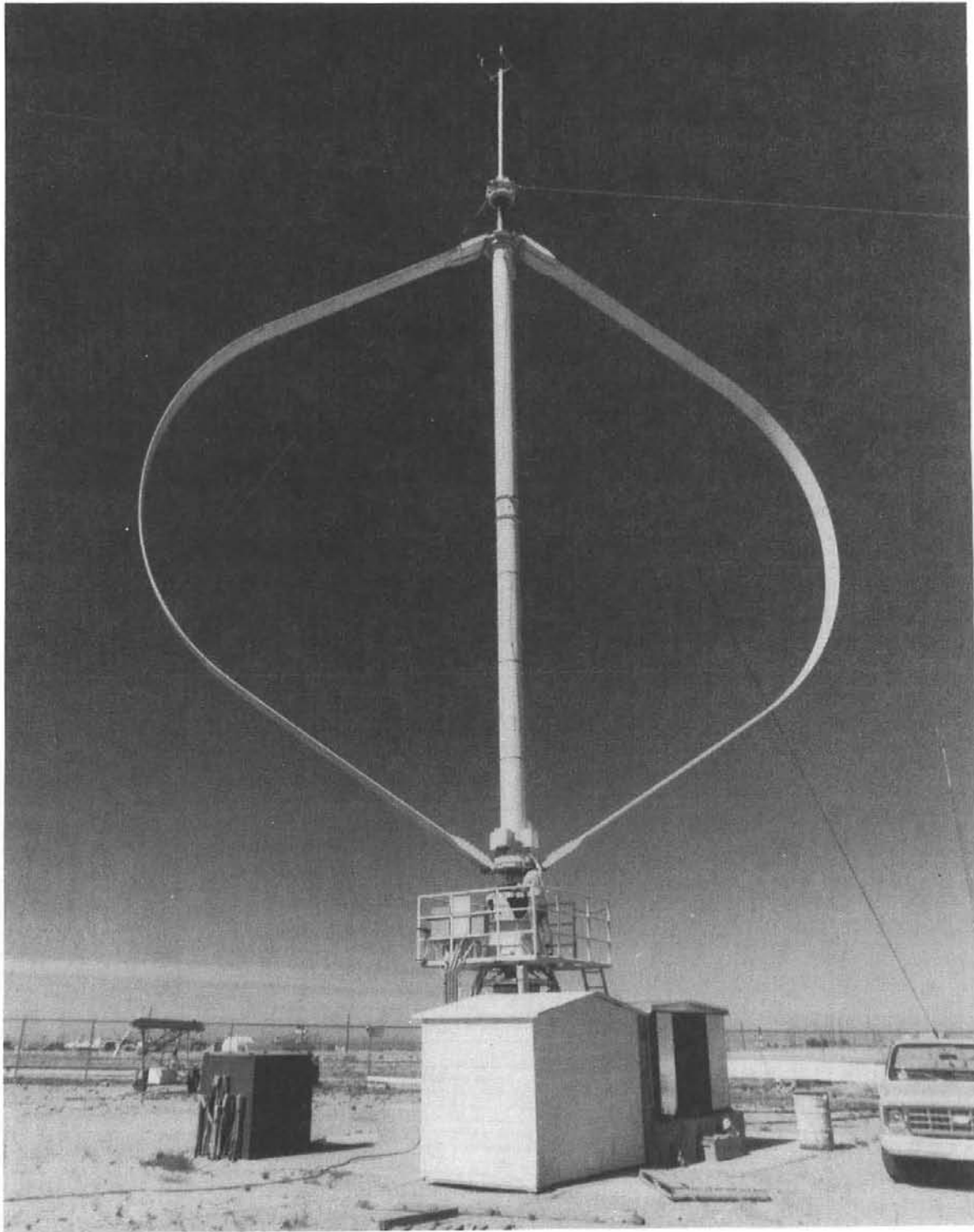
The Darrieus wind turbine generator research testing laboratory at Sandia National Laboratories. A view of the vertical axis wind turbines (VAWT) 2 meter, 5 meter, and 17 meter systems that are the primary lift-driven machines supporting the research and technology for the developing of large wind turbines for the United States Department of Energy.



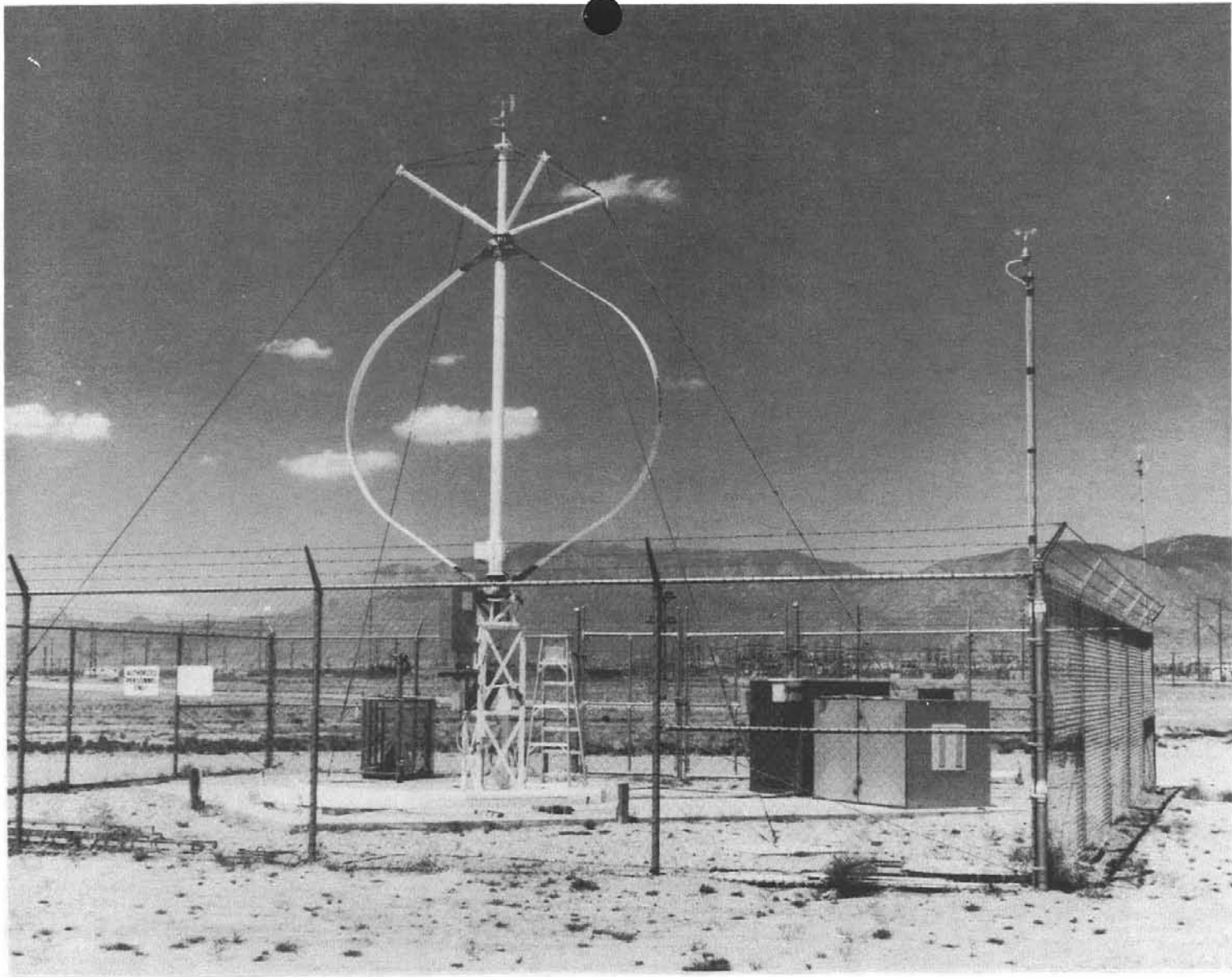
Sandia National Laboratories began its VAWT experiments in 1974 with the design of a 5 meter turbine. Since that time, a 2 meter and a 17 meter turbine have been added to the wind generator research program. The turbine control building, located a short distance from the wind turbine installations, contains the control equipment, and data gathering and recording instrumentation for the turbines.



This Sandia National Laboratories experimental 2 meter Darrieus wind turbine serves as an aerodynamic blade flutter research test unit, and a wind tunnel model to demonstrate equivalence and credibility to data collected during field tests. This lift-driven airfoil test bed is so designed that the mechanical arrangement is less compact than an operational unit, thus giving more experimental flexibility.



This Sandia National Laboratories 17 meter research turbine is designed to operate with one, two, or three blades, with or without struts, and generates 80 kW of electrical power.



Sandia National Laboratories 5 meter Darrieus wind turbine may be operated with either one, two, or three blades and has been in operation at Sandia since 1974. This VAWT develops 3 kW of electrical power.

SECTION II
DESIGN CHARACTERISTICS OF CURRENT
AND FUTURE VAWT SYSTEMS

CURRENT AND FUTURE DESIGN CHARACTERISTICS OF VERTICAL AXIS WIND TURBINES

Emil G. Kadlec

Introduction

As a U.S. Department of Energy (DOE) laboratory, Sandia National Laboratories is developing Darrieus VAWT technology with the ultimate objective of economically feasible, industry-produced, commercially marketed wind energy systems. The first full cycle of development is complete, and resulting current technology designs have been evaluated for cost-effectiveness¹ (Fig. 1). First-level aerodynamic, structural, and

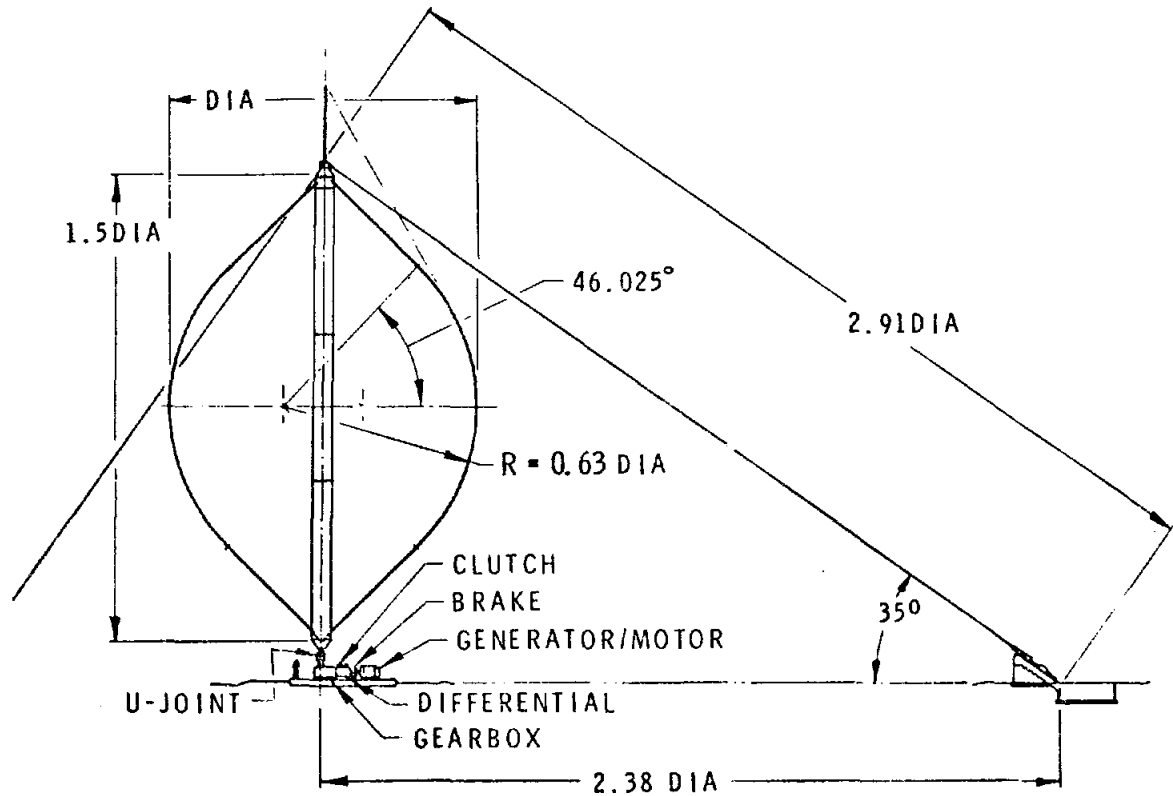


FIGURE 1. General Configuration of Turbine Used in Economic Study

system analyses capabilities have evolved during this cycle to support and evaluate the system designs. This presentation describes the characteristics of current technology designs and potential improvements identified in this first cycle.

Characteristics of the Current VAWT Designs

Inherent in the current design characteristics are specifications, design philosophy, conservatism, and low-cost manufacturability. In defining goals for the characteristics of future designs, it is important to examine current practice to identify areas that may produce substantial improvements. A qualitative review of the current design characteristics will be made in this section.

Specifications

The most notable specification is the use of a 60 mph cutoff windspeed and a 150 mph parked rotor survival windspeed. These were chosen to add a degree of conservatism to the then available static blade analysis.

The designs are intended to operate grid connected at constant rotational speed with the grid providing load and frequency control.

The current designs are generally optimized for a 15 mph average windspeed distribution.

Synchronous or induction generators are specified.

Design Philosophy

The blade designs have converged to aluminum extrusions using uniform wall thickness and constant planform. Multiple extrusions are welded together to achieve large chord dimensions (Fig. 2). The current designs utilize wall thickness ratios (wall thickness/chord) of .008 - .01.

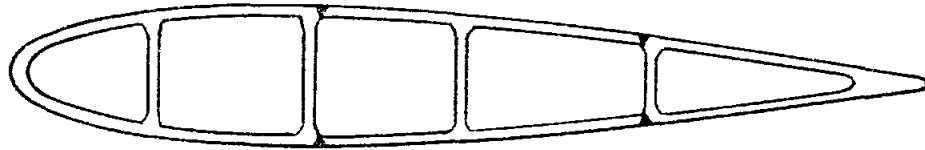


FIGURE 2. Existing Technology Blade Cross-Section

The current designs set cable tension high so that the cable vibrational frequencies are above the excitation frequencies.

Symmetric airfoil sections have been used such as the NACA 0012, 0015, and 0018 with a "take what you get" approach on aerodynamic performance.

Conservatism

As mentioned earlier, high operating and survival windspeeds are used to add a degree of conservatism.

The buckling factor of safety used for the tower is 10.

A factor of safety of two is applied to aluminum extrusion fatigue properties.

Low-Cost Manufacturability

Extruded aluminum blade construction uses low-cost, mass production techniques.

Spiral welded, thin wall steel tubes are used for rotating towers.

Standard components and sub-components are used to take advantage of established production techniques and prices.

General Features

The current designs are generally two-bladed with a height-to-diameter ratio of 1.5. The blade shape is a straight-circular arc-straight approximation of a troposkien which

retains most of the advantages of the troposkien and is easier to fabricate.

A standard speed increaser is used to couple the low speed turbine shaft to the high speed shaft of the generator.

The current designs tend toward the use of three guy cables except in cases where using an increased number allows the use of standard small hardware.

A disk brake system incorporating standard heavy equipment calipers is included in the design to stop the wind turbine for a design condition of 20% overspeed with maximum wind loading.

The current electrical systems are grid-connected, 3 phase, with 480V or 4160V outputs depending on system size. The designs call for the use of synchronous or induction generators, the choice depending on system considerations or cost.

Electrical starting is utilized. Several methods have been used in actual practice. These methods all use an induction machine as a motor starter and are listed as follows:

1. Full voltage start then generate with same machine.
2. Reduced voltage start then generate with same machine.
3. 1 and 2 above but generate with synchronous generator.
4. Pony motor start - Drive to partial operating speed with small motor, use wind power to achieve operating speed.

An option of bringing a synchronous or induction machine up to operating speed under no load conditions and then using mechanical clutching to bring the rotor up to operating speed has been investigated. This option has the advantage of controlling the torque applied to the drive train within the normal operating limits of the drive train.

Torque ripple which is due to cyclic aerodynamic loading has been successfully controlled (10-20%) by providing a soft component in the drive train to place the drive train resonant frequency well below the frequency of the aerodynamic excitation.

Goals for Characteristics of Future VAWT Systems

Attempting to define the characteristics of future wind turbines is certainly speculative. However, defining goals for characteristics is important, since reasonable goals give direction to the research and development program and if properly selected are keys to achieving the overall goal of reliable, cost-effective systems. Reviews of the current design characteristics in design studies and the recently completed economic study¹ have revealed a number of desirable changes and goals that could result in lowering the cost of energy. These are identified and discussed in this section.

Specification

The next-generation wind turbine will be designed to operate with a cut-off windspeed of 40 mph instead of 60 mph and to a parked rotor survival windspeed of 120 mph instead of 150 mph. These specifications are consistent with those used for large horizontal axis wind turbines and represent a reasonable envelope. While some energy above 40 mph will be lost, the cost saving by reduction of specifications more than compensates for the reduction in energy capture.

Future designs will tend to be optimized for windspeed distributions below 15 mph. This will tend to make the Darrieus attractive to a wider range of markets while presenting a challenge to the designer to reduce the cost of energy.

Design Philosophy

Processes and materials for producing blades other than extruded aluminum may be explored. The candidates include (but are not limited to) stretch/roll formed steel and glass-reinforced plastic (GRP) "pultrusion." Both these processes are good matches to a non-twisting, non-tapering shape and start with relatively cheap raw materials. Other processes may emerge as promising candidates after emphasis is placed on reducing blade fabrication costs.

Next-generation designs utilizing multiple aluminum extrusions may have average wall thickness ratios (blade thickness/chord) of .004 to .005. This can be achieved by using the thicker wall extrusions at the chord leading and trailing edges and the thinner wall extrusions at center chord (Fig. 3). The

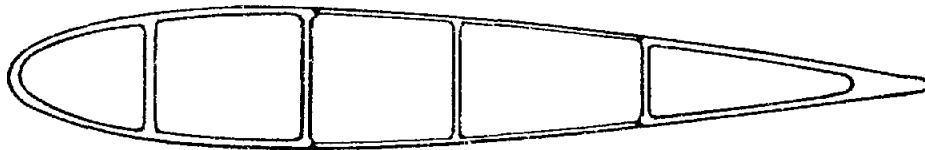


FIGURE 3. Variable Wall Blade Section

average thickness would also be reduced near the equator since the structural requirements near the equator are less than those near the blade root. Of course, structural requirements of the blade in general are reduced because of the specification change. The net effect of these changes combined could reduce the blade weight as much as 50%.

A goal for the second-generation is the reduction of cable tension. This will require that turbine excitation frequencies be between cable frequencies. Simple damping devices may be employed. The net effect should be a reduction in bearing, support structure, cable, anchor, and tower requirements, and consequently, costs.

Several aerodynamic changes are desirable to reduce the cost of energy. Among these are changes that will:

- Increase the maximum power coefficient.
- Move the tip speed ratio associated with stall regulation closer to the tip speed ratio of the maximum power coefficient (stall regulation would occur at lower wind speed).

The recent studies have assumed a maximum power coefficient (C_{pmax}) of 0.39. Test results² using the extruded NACA 0015 blades on the 17-m research turbine are showing maximum power coefficients of 0.41 to 0.42. Changing the power coefficient curve to correspond to a change in C_{pmax} from 0.39 to 0.41 increases the total energy by 5%. The rated power and total energy are increased while the operating speed remains unchanged. Further improvements in C_{pmax} may be achieved by using non-symmetric airfoils.

Moving the stall or regulation tip speed ratio closer to the maximum C_p tip speed ratio increases the operating speed, drops the rated windspeed, and reduces equipment costs. Achievement of these goals in combination would increase energy capture while reducing equipment costs.

Conservatism

The buckling factor of safety used for the tower should be 5 which is standard practice. The current designs are based on a buckling safety factor of 10.

General Features

Future studies will be conducted to determine if cost reductions can be made in the design or application of speed increasers. These studies will emphasize the matching of wind turbine requirements and speed increaser capabilities to change any conservative practices that may be in use. Also

shared functions, such as thrust bearings, housings, etc. by integrating designs, may yield cost reduction. Since the speed increaser represents a large fraction of a system cost, these studies could be fruitful.

Emphasis will be placed on installation procedures, techniques, and design features that will reduce the cost of installing wind turbines.

Design features that enhance the ease of maintenance, reduce maintenance requirements, and generally reduce operating and maintenance (O&M) costs will be incorporated.

Impact of Goals

In order to assess the impact of some of these potential changes or goals, a study of weights and costs was made of an intermediate class Darrieus wind turbine. This study used the system model VERS16¹ and its derivative ECON16. A fixed geometry and size were chosen so that no optimization was permitted on size, solidity, and height-to-diameter ratio. A 14 mph median windspeed Weibull distribution was chosen. Optimization was allowed on tipspeed and rating.

The effects were estimated of reduced specifications, changed philosophy, and already-achieved aerodynamic characteristics. The changes that affected the structural requirements and costs were the following reductions: (1) windspeed, (2) cable tension, (3) buckling safety factor, and (4) blade wall thickness ratio.

The aerodynamic characteristics examined were the increase of the C_{pmax} from 0.39 to 0.41 (already demonstrated on the 17-m research turbine) and the effect of moving the tipspeed ratio (λ) at stall (regulation) closer to the tipspeed ratio at the maximum power coefficient (C_{pmax}). The value chosen was

$\frac{\lambda_{reg}}{\lambda_{cpm}} = 0.7$. The current value is between 0.5 - 0.55.

The effects of the structural type changes were as follows:

Weight Reduction

Blades	50%
Tower and Bearings	53%
Tiedowns	45%
Speed Increaser	10%
Generator	10%
Overall System	43%

The total energy was reduced by about 2% and the system rating was reduced by 10%.

When the aerodynamic effects were added to the above changes and the system was reoptimized, the blade, tower, and tiedown weights were not affected, the transmission weight was reduced an additional 6% to a 16% reduction, and the generator weight was increased by 7% resulting in a 3% reduction. The system rating increased to 97% of the original and the total energy increased 13% to 11% over the original.

Clearly, these effects are very significant and the characteristics producing these effects should be goals for the next-generation designs.

References

1. Economic Analysis of Darrieus Vertical Axis Wind Turbine Systems for the Generation of Utility Grid Electrical Power -- Vol. 1: W. N. Sullivan, Executive Summary; Vol. 2: idem, The Economic Optimization Model; Vol. 3: R. D. Grover and E. G. Kadlec, Point Designs; and Vol. 4: W. N. Sullivan and R. O. Nellums, Summary and Analysis of A. T. Kearney and Alcoa Laboratories Point Design Economic Studies, SAND78-0962 (Albuquerque, NM, Sandia National Laboratories, 1979).
2. See M. H. Worstell, "Measured Aerodynamic and System Performance of the 17-m Research Machine," pp. 233.

17 METER VERTICAL AXIS WIND TURBINE (VAWT)

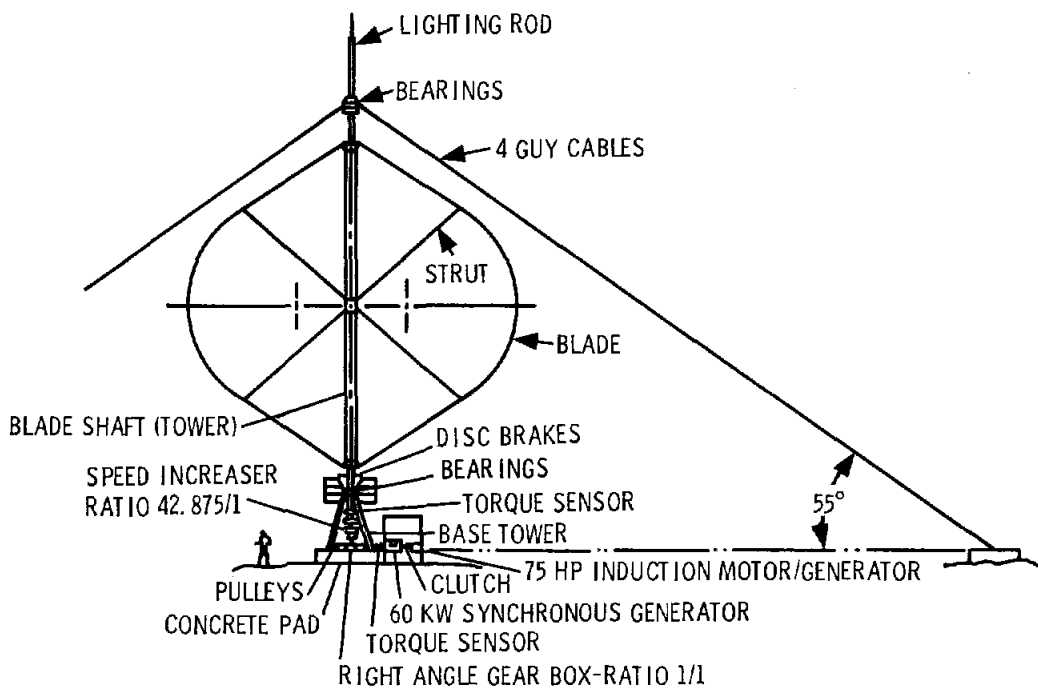
Robert D. Grover

A 17 meter research VAWT was designed and built at Sandia Laboratories in 1976-1977. This turbine is located on Kirtland Air Force Base East, at 106 degrees 33 minutes west longitude and 35 degrees 3 minutes north latitude. The turbine is located on a concrete pad at an elevation of 5440.6 feet above sea level.

Mounted on top of the concrete pad (Fig. 1) is a 4000 pound welded structural steel base that houses the two bearings that support the bottom of the turbine. These bearings are Timken tapered roller bearings, one of which has a thrust capacity of 90,000 pounds and a radial capacity of 50,000 pounds. The other bearing has a radial capacity of 50,000 pounds and a thrust capacity of 30,000 pounds. The 50,000 pound radial capacity of each bearing is to produce a turbine shaft bending moment load capability. These bearings are spaced about four feet apart in the base and support the lower rotating shaft of the turbine.

The lower shaft is seven feet long, weighs 2500 pounds, and is of welded structural steel construction. The top of the bottom shaft has a flange that supports the blade shaft (tower), and is bolted to the blade shaft by a matching flange on the blade shaft. The blade shaft is of welded structural steel construction with a twenty inch outside diameter, one inch thick wall, and weighs six tons.

The top shaft is bolted to the top of the blade shaft like the bottom shaft is bolted to the blade shaft. The top shaft



17 METER VAWT H/D 1/1

FIGURE 1

is of welded steel construction, weighs 2500 pounds, and is seven feet long. The top shaft is supported by a set of Timken bearings exactly like the bottom bearings. The top bearing housing is of welded steel construction and is attached to the four guy cables that support the side loads at the top of the turbine. Both the top and the bottom bearings may be replaced without tearing the turbine down.

The guy cables are one inch diameter steel bridge strand with a breaking strength of 120,000 pounds. The guy cables are one hundred and twenty two feet long and weigh 265 pounds each. The four cables are attached to four blocks of concrete as anchors at ground level and the cables form a 35 degree angle with the ground. There is a load cell at the bottom end of each guy cable to determine cable tension and a turnbuckle at the end of each load cell to achieve cable tension.

The turbine blades are 17 meters tall and 17 meters in diameter for a height-to-diameter ratio of one to one. The bottom of the blades are located five meters above the concrete base pad.

The first blades tested on the 17 meter VAWT were made by Kaman Aerospace of Bloomfield, Connecticut. These blades had the cross-section of a helicopter blade with aluminum extrusions for the leading and trailing edges and a center core of paper honeycomb with fiberglass skins (Fig. 2). The blades had pin joint supports and struts were required to support the blades on the blade shaft. The blades had a chord length of 21 inches and a symmetrical airfoil shape of NACA 0012. These blades were tested in both the two- and three-bladed configurations, and the blades weighed 1140 pounds each.

Beneath the bottom shaft was a torque sensor that was isolated from the drive shaft by rubber flexible couplings on both ends of the torque sensor. Beneath the torque sensor was

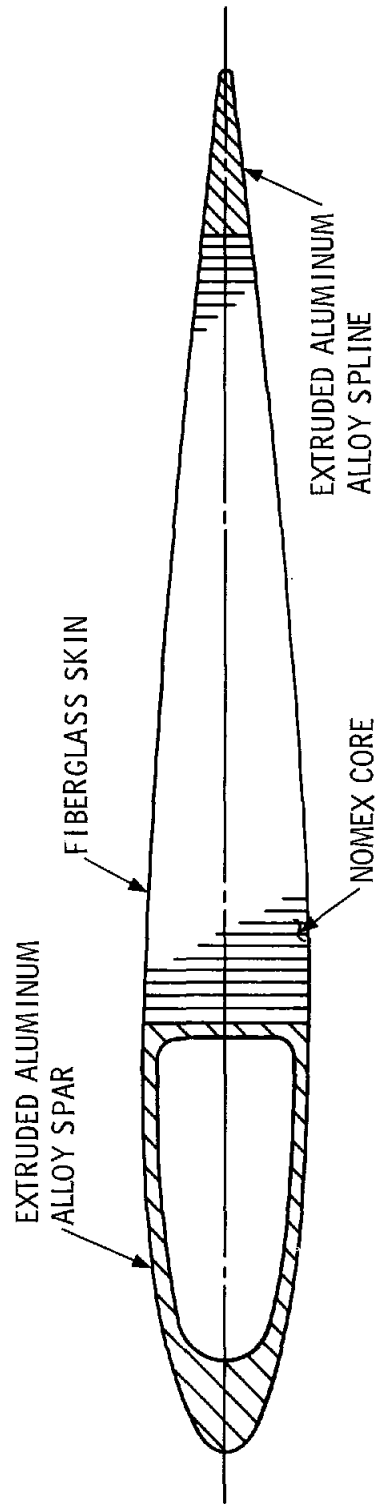


FIGURE 2

a three stage planetary transmission with each stage having a gear ratio of 3.5 to 1 for a total unit gear ratio of 42.875 to 1. Beneath the transmission was a right angle bevel gearbox, with a gear ratio of one to one, to change the power train direction from vertical to horizontal. This horizontal shaft led to a set of toothed pulleys and a toothed belt. With five pulleys, the speed ratio of the shaft could be changed from .706 to 1 to 1.417 to 1 in thirteen discrete steps. From the pulley, the shaft continued to a torque sensor that was isolated by two rubber flexible couplings. Next in line in the power train was a 60 kW synchronous generator which was attached to a 75 horsepower motor/generator by a clutch. Since the VAWT cannot reliably self-start, the induction motor was used to start the VAWT as well as being used as an induction generator.

The generators operated at 1800 rpm, and with the pulleys, belt, and transmission ratios, the turbine could be operated from 29.6 to 59.5 rpm in thirteen discrete steps.

This equipment was tested for about one year in the two-bladed configuration, and for about one more year in the three-bladed configuration. The turbine weighed about 19 tons, with about 12 tons of rotating hardware.

The 17 meter VAWT has a lightning protection system to protect the turbine support bearings at the top and bottom of the blade shaft when the turbine is struck by lightning. This system consists of a lightning rod (air terminal) at the top of the turbine, with carbon brushes on a slip ring attached to copper cables which form a circuit around the top bearings to the guy cables and the blade shaft. The bottom ends of the guy cables are connected to the grounding system by copper cables. At the bottom of the blade shaft is another slip ring with carbon brushes and copper cable to form a circuit around the bottom bearings to the grounding system. The grounding

system consists of ten foot long, one inch diameter, copper plated steel rods, driven into the ground every four feet around the base of the turbine and out to the bottom of each guy cable with the copper cable welded to each rod and attached to the guy cables and bottom carbon brushes on the bottom slip ring. This extensive grounding system was required by the local soil resistivity.

Statistically, the turbine should sustain a lightning strike once every 2-1/2 years at this location. Since the study was referenced back to Benjamin Franklin, it was felt to be quite safe. The turbine was struck by lightning four times in the first three months of operation, which was considered wonderful since it would not then get struck again for 10 years.

The next set of blades purchased for the 17 meter VAWT were extruded aluminum blades made by Alcoa. These blades were extruded in one piece and shipped to Sandia Laboratories in an 80 foot straight length. The blades were then bent to the proper shape near the turbine site. The blade was bent by placing the blade against two posts that were located about four feet apart and pressing on the blade between the posts with a hydraulic cylinder. After pressing with the hydraulic cylinder to yield the material, the blade was moved an increment of two inches and pressed again. This process was repeated until the desired length of curvature was achieved. This method was called "incremental bending." These blades weighed 1400 pounds each. These blades had a 24 inch chord and a NACA 0015 airfoil (Fig. 3).

Aluminum plates were bolted to the ends of the blades and the plates were bolted to the 17 meter blade shaft. These blades were bolted rigidly to the blade shaft since there were no pin joints and therefore no need for struts (Fig. 4).

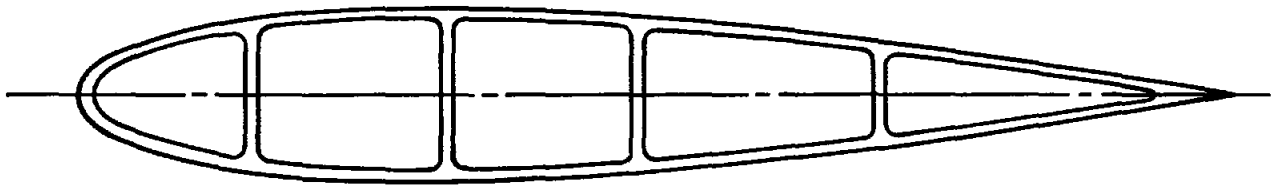


FIGURE 3

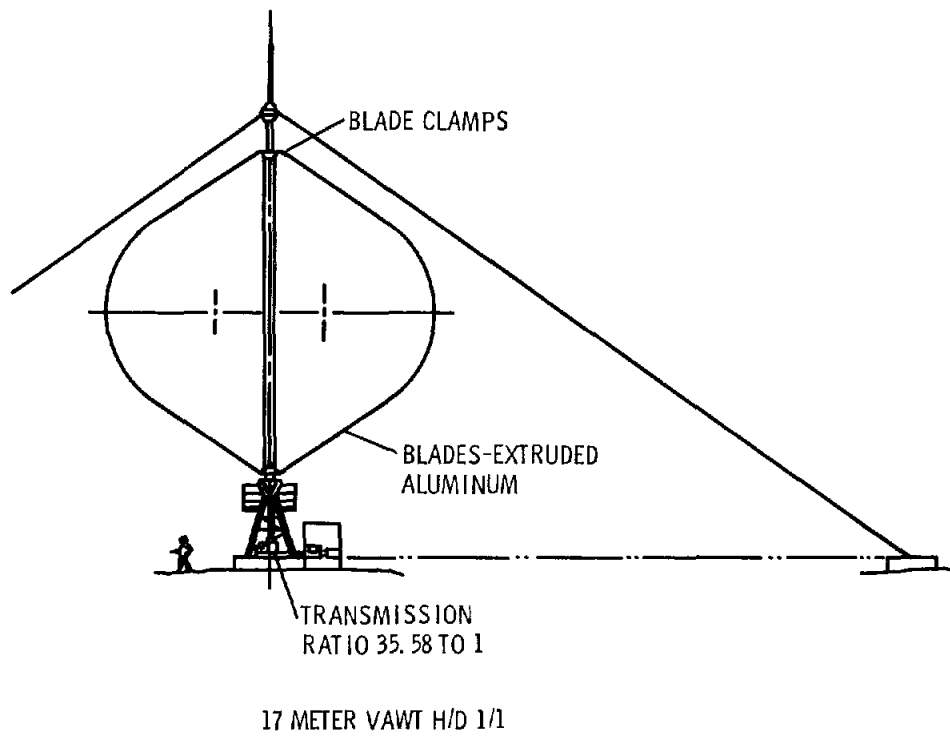


FIGURE 4

The turbine has been tested for about one year in the two-bladed configuration with the extruded blades, and will be changed to the three-bladed configuration sometime in the future.

At the time the blades were being changed from the Kaman to the Alcoa blades, the planetary transmission and right angle gearbox were replaced by a three stage right angle bevel gear transmission with a speed change ratio of 35.58 to 1. With six pulleys, that permit speed change ratios from .59 to 1 to 1.7 to 1, the turbine speed can be changed from 29.75 rpm to 86 rpm in 21 discrete steps, but the speed is limited to 54.81 rpm and 12 discrete steps.

The brake system for stopping the turbine is a hydraulically operated disc brake. There are two 36 inch diameter, three-quarter inch thick, steel discs with four hydraulic calipers on each disc. One disc is for normal stopping and is called the proportional brake, and the other disc is for emergency stopping in case of power loss, broken shaft, or excessive windspeed. The brake was designed to stop the turbine in a 90 mile per hour wind with a 25 percent turbine overspeed.

The 17 meter VAWT is being redesigned at the present time and will be rebuilt into what is thought to be a more up-to-date design as indicated by study and testing. The main features of this rebuild are as follows (Fig. 5):

1. A height-to-diameter ratio of 1.5 to 1 - This produces more power per pound of material used because more of the blade is located at a larger diameter.
2. Thinner walled blade extrusions - By tailoring the blade cross-section to the stress levels, the blade can be made thinner. It looks like the blades for this 50 percent higher turbine can be made lighter in weight than the present 17 meter blades.

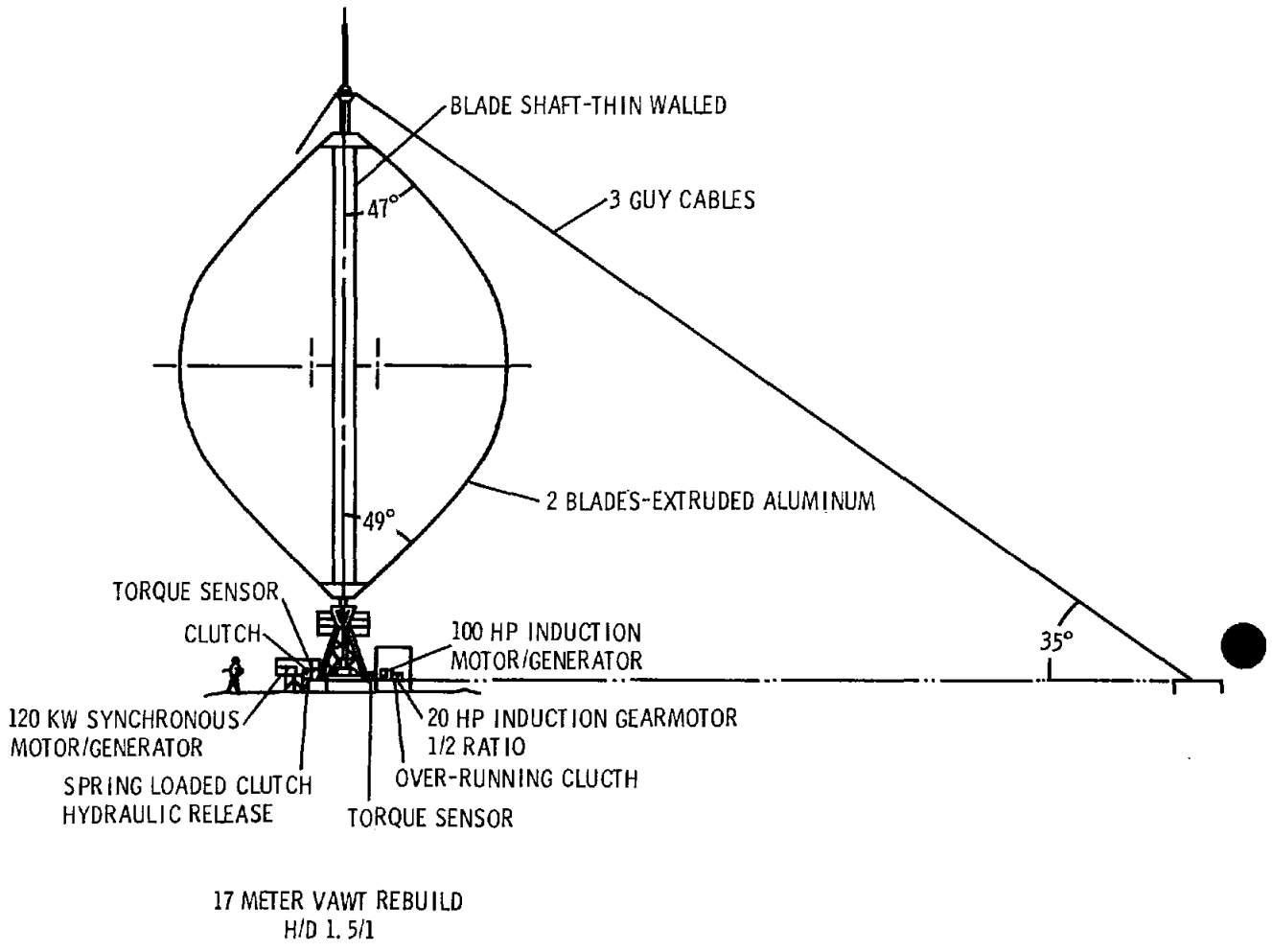


FIGURE 5

3. Two blades - A third blade does not increase electrical output enough to pay for the third blade.
4. Nonsymmetrical extruded aluminum blades - By making the inside airfoil of the blade different than the outside blade airfoil, a higher power coefficient may be achieved.
5. Larger diameter, thinner walled blade shaft (tower) - This design achieves a larger cross-sectional moment of inertia per pound of material used. Even though this shaft is 50 percent longer than the present 17 meter shaft, it will weigh about ten percent as much.
6. Three guy cables - Three guy cables are cheaper than four.
7. Pony motor - A 20 horsepower induction gear motor will be attached to the aft end of the 100 horsepower induction motor by an overrunning clutch. This motor will be used to start the turbine and will draw less current than the larger motor. This motor will bring the turbine up to about half speed and the wind will be permitted to bring the turbine up to full speed. This will permit a turbine start with less line surge.
8. Clutch - A clutch will be placed between the synchronous generator and the transmission to permit the synchronous generator to be brought up to full speed and synchronized before trying to start the turbine. Since a synchronous generator used as a motor has very low starting torque, this design will allow the motor to achieve full speed and high torque before trying to start the turbine.

9. Blade angle - With a straight line circular arc blade shape, the blade will be attached to the turbine to produce minimum blade stress due to gravity and centrifugal force at rated operating speed. To permit the sag due to gravity, the blade will be attached to the turbine at a 47 degree angle at the top of the blade, and at a 49 degree angle at the bottom of the blade.

DESIGN CHARACTERISTICS OF THE DOE/ALO-ALCOA 17 METER TURBINE

Robert O. Nellums

Introduction

The design, fabrication, and erection of four 17 meter diameter vertical axis wind turbines is being conducted by Alcoa Laboratories under contract to DOE/ALO with Sandia Laboratories as technical monitor. The major goal of the 17-m program is demonstration of a cost-effective Darrieus VAWT designed and built by private industry. A preliminary design for the system was completed and documented¹ prior to the start of fabrication in September of 1979. Fabrication of the first unit is scheduled for completion in June of 1980 and erection/check out of the first unit should be completed by September of 1980.

This paper will summarize the design characteristics of the 17-m including modifications which have recently occurred and modifications which are under consideration for the remaining three units scheduled for fabrication this summer.

17 Meter Configuration Summary

Parameters of the 17-m turbine are summarized in Table 1 and detailed design specifications are included as an appendix to this paper. As shown in Fig. 1, the rotor consists of two curved extruded aluminum blades cantilevered at each end against a tubular steel support tower. The rotor turns on an upper bearing fixed horizontally by three guy wires and a lower spherical roller bearing which supports the tower load. Both bearings allow tower pivoting. A flexible coupling

17-M CONFIGURATION

ROTOR DIAMETER	17.0 M (56.0 FT)
ROTOR HEIGHT	25.1 M (82.5 FT)
SWEPT AREA	284 M ² (3060 FT ²)
ROTOR GROUND CLEARANCE	2.7 M (9 FT)
OVERALL HEIGHT	29 M (95 FT)
OPERATING SPEED	51.5 RPM
SYSTEM MASS LESS FOUNDATION	12127 KG (26,741 LB)
NUMBER OF BLADES	2
BLADE MATERIAL	6.35 MM (0.25 IN) WALL ALUMINUM EXTRUSION 6063-T6
AIRFOIL SECTION AND CHORD LENGTH	0.616 M (24.24 IN) CHORD NACA 0015, TRAILING EDGE RADIUSED FOR 0.610 M (24 IN) CHORD LENGTH
BLADE LENGTH	30.92 M (101.46 FT) PER BLADE
BLADE EXTRUSION MASS	833.8 KG (1833 LB) PER BLADE
BLADE TO BLADE JOINTS	2 RIVETED JOINTS PER BLADE
BLADE TO TOWER CONNECTION	CANTILEVERED STIFFBACK WELDED TO BLADE
TOWER MATERIAL	SPIRAL WELDED STEEL TUBE
TOWER OD	0.762 M (30 IN)
TOWER WALL THICKNESS	4.77 MM (.188 IN)
SPEED INCREASER	3 STAGE PARALLEL SHAFT
SPEED INCREASER RATIO	35.068:1
MOTOR/GENERATOR	112 kW (150 HP) SQUIRREL CAGE INDUCTION
BRAKE	SINGLE DISC DUAL INDEPENDENT CALIPER
BRAKE TORQUE CAPACITY	60,000 Nm (44,000 FT-LB)
BRAKE DISSIPATION CAPACITY:	
SERVICE	1.02×10^6 J ($.75 \times 10^6$ FT-LB)
EMERGENCY	4.07×10^6 J (3×10^6 FT-LB)
NUMBER OF GUY CABLES	3
CABLE ANGLE (TO HORIZONTAL)	35°
CABLE DIAMETER	22.2 MM (.875 IN)
CABLE PRETENSION	$.135 \times 10^6$ N (30,300 LB)
CABLE LENGTH	48.8 M (160 FT)

TABLE 1

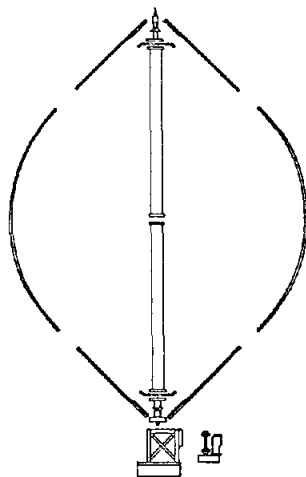


FIGURE 1. 17-m Configuration

transmits rotor output to a parallel shaft constant ratio gearbox which drives an 1800 rpm induction motor/generator through a second flexible coupling. Braking is provided on the high speed shaft. Rotor speed is regulated to 51.5 rpm through synchronous operation of the motor/generator in the power grid. Microcomputer control provides automatic shutdown under fault conditions and a manual/automatic option for wind-speed run conditions.

17-m Design Update

Several additions or modifications were incorporated in the design drawings since the design was reported¹. The major changes are:

1. Blade stresses in the neighborhood of the tower joint were reduced by changing the angle between blade and tower at the joint from 46.02° to 47° top and 49° bottom.
2. The stiffback, which is welded to the blade end, was extended up the blade by one foot to reduce weld stresses.
3. The blade to blade joints were modified in the number and type of fasteners and by shifting the joint location along the blade to a predicted point of minimum stress.
4. The 30 inch diameter tower tube of .219 inch wall thickness was changed to a .188 inch wall thickness.
5. The guy cable tensioner has been redesigned for manual tensioning and simplified tension measurement.
6. A replaceable nitrogen bottle has replaced the air compressor for pressurizing the hydraulic system.
7. The automatic control system design has been completed.

Additional modifications are under consideration for future design. Several important examples are:

1. Eliminate copper lightning protection slip rings to use underlying steel.
2. Relocate the lower tower tube-to-shaft transition by adding a flange immediately above the lower bearing to facilitate fabrication and erection.
3. Use lower capacity lower loss bearings.
4. Redesign ministrut connection to stiffback.
5. Use seam versus spiral welded tower tube.
6. Redesign steel support base for more economic use of steel and incorporate integral drive train.
7. Monitor windspeed with two anemometers rather than one.
8. Incorporate reduced current starting.
9. Modify auto mode low wind start to average power threshold rather than average wind.

Key 17-m Design Details

Several design details of the 17-m contribute significantly to the low-cost concept and will be discussed here. The blade and tower are the largest turbine assemblies and their construction advantages are discussed in Tables 2 and 3. The transmission, an \$11,000 item, is a standard frame parallel shaft gearbox which was determined to offer the best combination of efficiency, dependable performance, and cost. The guy cable anchors are "dead man" type requiring seven cubic yards of concrete for three anchors. Still lower cost is potentially available from steel auger type anchors which are under investigation.

The drive train has been designed for full voltage direct starting which results in heavy starting currents but potentially saves several thousand dollars compared to a low voltage starter. The brake has been mounted on the transmission high speed shaft which reduces brake cost and allows the brake to be mounted simply as an overhung load on the transmission shaft. These factors are believed to outweigh

EXTRUDED ALUMINUM BLADE CHARACTERISTICS

1. DEMONSTRATED TECHNIQUE
2. SMOOTH AIRFOIL SURFACE AND ACCURATE CROSS SECTION
3. HOLLOW INTERIOR WITH WEBBING MAY BE TAILORED FOR DESIRABLE SECTION PROPERTIES
4. EXCELLENT MATERIAL UNIFORMITY
5. ACCEPTABLE BENDING, WELDING, AND FASTENING PROPERTIES
6. 1980 1st QUARTER EXTRUSION PRICE WAS \$1.73/LB + \$2500 SET-UP FOR 24" CHORD

TABLE 2

SPIRAL WELDED TOWER TUBE

1. KNOWN STRUCTURAL AND AERODYNAMIC PROPERTIES
2. READILY AVAILABLE
3. ADAPTABLE TO FLANGE JOINTS ALIGNED AT FACTORY
4. ESTIMATED COST OF \$.46/LB FOR TOWER RAW TUBE

TABLE 3

the disadvantages of sending braking loads through the transmission and of risking loss of braking capability in the event of low speed shaft or transmission failure. The cost of supplying hydraulic brake power has been lowered by the use of bottled gas pressure. The lower rotor bearing was specified to be a single spherical roller bearing costing \$1294. The bearing housing is simplified because a single bearing carries axial and radial loads and pivots to eliminate the need for moment capability. The transmission service factor has been designed to 1.5 to allow for starting and braking loads and for torque ripple estimated to be 20 to 25% at rated power. Methods for reducing torque ripple below this amount did not appear cost-effective.

The blade to tower connection is made through a factory aluminum weld to an extruded stiffback which is believed to

offer a lower cost potential than the use of fasteners at the blade. On the other hand, rivets were specified for the blade to blade joint using extruded inserts to avoid impairing the blade aerodynamics. This method is compatible with the requirement for joining in the field. However, the rivets are costly and alternate means are being sought for blade to blade joints.

Table 4 summarizes the vendor component costs per unit as

ESTIMATED COMPONENT COSTS FOR THE 17-M PROGRAM

DOES NOT INCLUDE ELECTRICAL CONTROLS, COSTS REPRESENT ACTUAL OR ESTIMATED BILLINGS TO PROGRAM CONTRACTORS AND DO NOT INCLUDE ORDERING COSTS, PROGRAM CONTRACTOR PROFIT OR OVERHEAD, ENGINEERING COST, TRANSPORTATION COST, PROGRAM MANAGEMENT COSTS, OR ANY OTHER COSTS ASSOCIATED WITH THE MAJOR CONTRACTORS.

PURCHASED PARTS	VENDOR COST PER TURBINE
GEARBOX	\$11,002
ALUMINIUM BLADES AND ATTACHMENTS	10,025
STRUCTURAL STEEL	6,222
RIVETS	3,500
BRAKE HARDWARE	3,074
SHAFT COUPLINGS	2,082
SPIRAL WELD TUBE	2,080
GUY CABLES AND FITTINGS	1,483
BEARINGS	1,483
MOTOR/GENERATOR	1,335
MISCELLANEOUS	2,875
	<hr/>
TOTAL RAW MATERIAL	45,216
FACTORY LABOR LESS PROFIT BUT INCLUDING OVERHEAD (PER TURBINE)	53,000
	<hr/>
TOTAL FACTORY COST	98,216

TABLE 4

estimated in the DOE contract for four 17-m turbines. They represent cost estimates of vendor supplied hardware and fabrication subcontract estimates not including subcontractor profit. The total estimated cost of the 17-m program for Phase I and II is 1.8 million dollars.

17-m Operation

Table 5 contains the rated characteristics of the 17-m VAWT. The 100 kW output rating was selected conservatively. Figure 2 shows the estimated power versus windspeed characteristic for the turbine based upon the computer code PAREP.²

17-M OPERATING PARAMETERS

RATED ELECTRIC POWER	100 KW, 3-PHASE, 480 V, 60 Hz
TORQUE AT RATING	21, 130 NM (15,585 FT-LB)
RATED WINDSPEED	13.86 m/s (31 MPH)
CUT-IN WINDSPEED	5.8 m/s (13 MPH)
SHUTDOWN WINDSPEED	OPERATOR SELECTED UP TO 26.8 m/s (60 MPH) MAX.
TURBINE RPM	51.5

TABLE 5

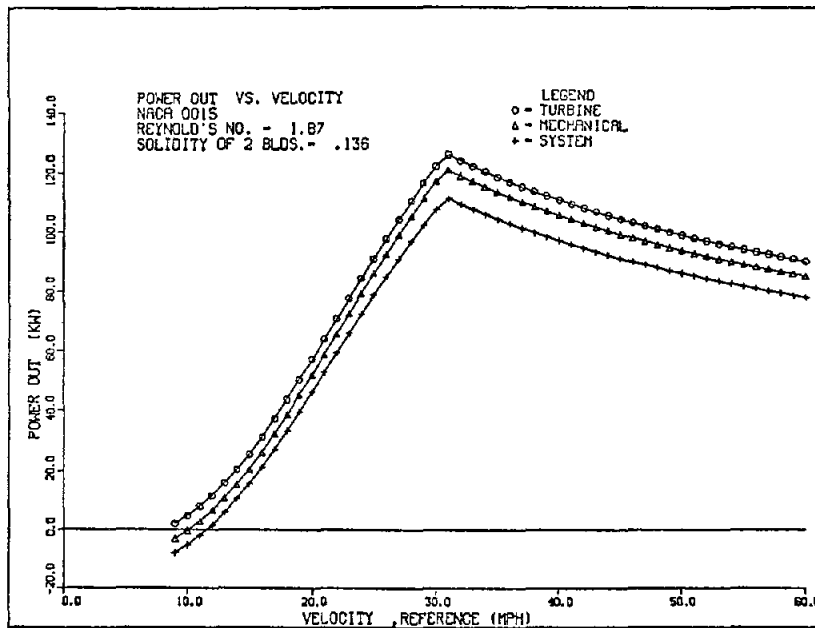


FIGURE 2. 17-m Output Power vs Windspeed from PAREP

These data indicate a rated output of 111 kW electrical. In comparison to PAREP, both experimental test data and preliminary output from Strickland's aerodynamic model³ indicate that even greater output efficiency may occur.

Operation of the turbine is to be regulated through a microprocessor-based control system. This system is designed to detect the fault conditions in Table 6 and automatically shut down. In addition to manual operation, an automatic mode may be selected which will start the turbine whenever average windspeed exceeds a selectable threshold. Once started

EMERGENCY SHUTDOWN CRITERIA

GENERATOR OVERLOAD
TURBINE OVERSPEED
EXCESSIVE WINDSPEED
INCORRECT START-UP SEQUENCE
LOSS OF TACHOMETER SIGNAL
SERVICE BRAKE FAILURE
PARKING BRAKE FAILURE
GRID POWER LOSS
MICROPROCESSOR FAILURE
EXCESSIVE VIBRATION
MANUAL EMERGENCY STOP

TABLE 6

on auto operation, the turbine will stop if the wind average falls more than 2 mph below the selected start threshold.

During startup, the turbine is estimated to reach synchronous speed within 12 to 15 seconds, drawing approximately one kilowatt-hour of power from the grid. Under normal operation, braking should require less than seven seconds. Under an emergency overspeed condition, a maximum of 15 seconds are required for brake action to stop the turbine. Taking into account the control algorithm and start-up power, the turbine is expected to lose about 7% of the annual energy potential when on auto, compared to the power predicted by summing the positive portion of the power curve over the annual windspeed distribution.⁴

Structural Analysis Overview

The 17-m structural analysis conducted by Alcoa on the 17-m design is summarized in Table 7. Table 8 lists the loading conditions which were established as a basis for the analysis. A detailed discussion of the analysis is contained in Ref. 1. In addition to reviewing the Alcoa analysis, Sandia performed the system modal, blade, and torque ripple analyses independently of Alcoa.

STRUCTURAL ANALYSIS PERFORMED

SYSTEM MODE FREQUENCIES

BLADE LOADS

BLADE BENDING RESIDUAL STRESSES

BLADE FLUTTER ANALYSIS

TOWER LOADS

TORQUE RIPPLE

ENVIRONMENTAL HAZARDS: ICE, EARTHQUAKE, TEMPERATURE, LIGHTNING

TABLE 7

LOADING CONDITIONS FOR 17-M LOW-COST VAWT

1. "NORMAL" OPERATING CONDITION 51.5 RPM, 60 MPH WIND
2. "DESIGN" CONDITION 75 RPM, 80 MPH WIND
3. PARKED ROTOR, 120 MPH WINDS "GUARANTEED" SURVIVAL
4. PARKED ROTOR, 150 MPH WINDS RESIST STEADY 150 MPH WIND WITHOUT DAMAGE

TABLE 8

Current 17-m Program Status

Fabrication of the first 17-m VAWT is proceeding within cost and schedule goals.

This unit is to be installed at the Rocky Flats Wind Systems Test Center during July and August of 1980. After check out and operational testing, this system will be turned over to Rocky Flats for long-term testing. Utilizing first unit fabrication experience, the design is currently under review for value engineering. Units 2, 3, and 4 are to be fabricated at the completion of value engineering for installation late in the fall of 1980.

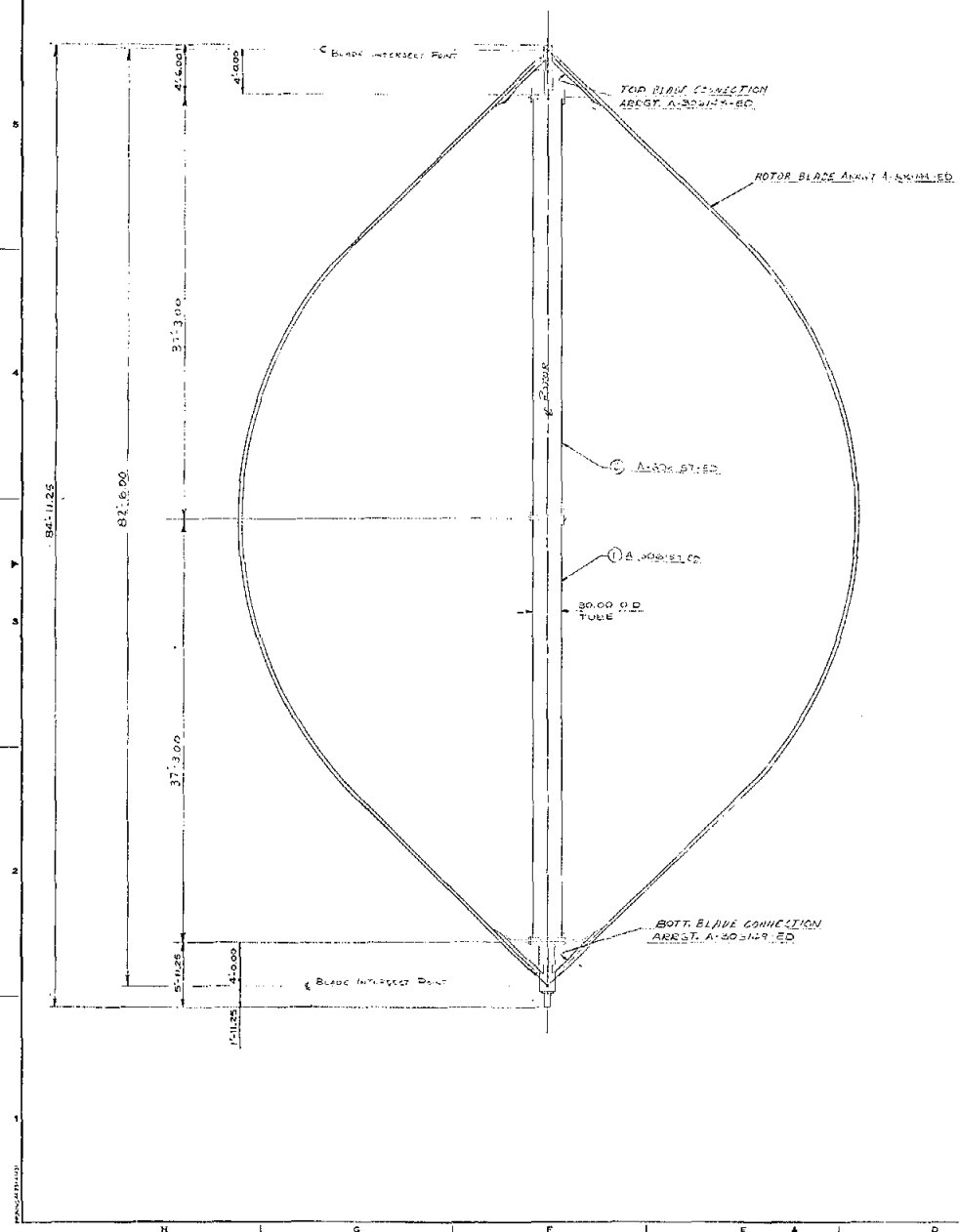
References

1. Design and Fabrication of a Low-Cost Darrieus Vertical Axis Wind Turbine System, Phase I - Technical Report, ALO-4272 (Albuquerque, NM: U.S. Department of Energy, 1980).
2. T. M. Leonard, A User's Manual for the Computer Code PAREP, SAND79-0431 (Albuquerque, NM: Sandia Laboratories, 1979).
3. P. C. Klimas, VAWT Aerodynamic Performance Prediction Methods, pp. 215.
4. G. M. McNerney, "Control Algorithm Investigations," pp. 124.

APPENDIX

The 17 Meter Detail Design

A-306142-ED



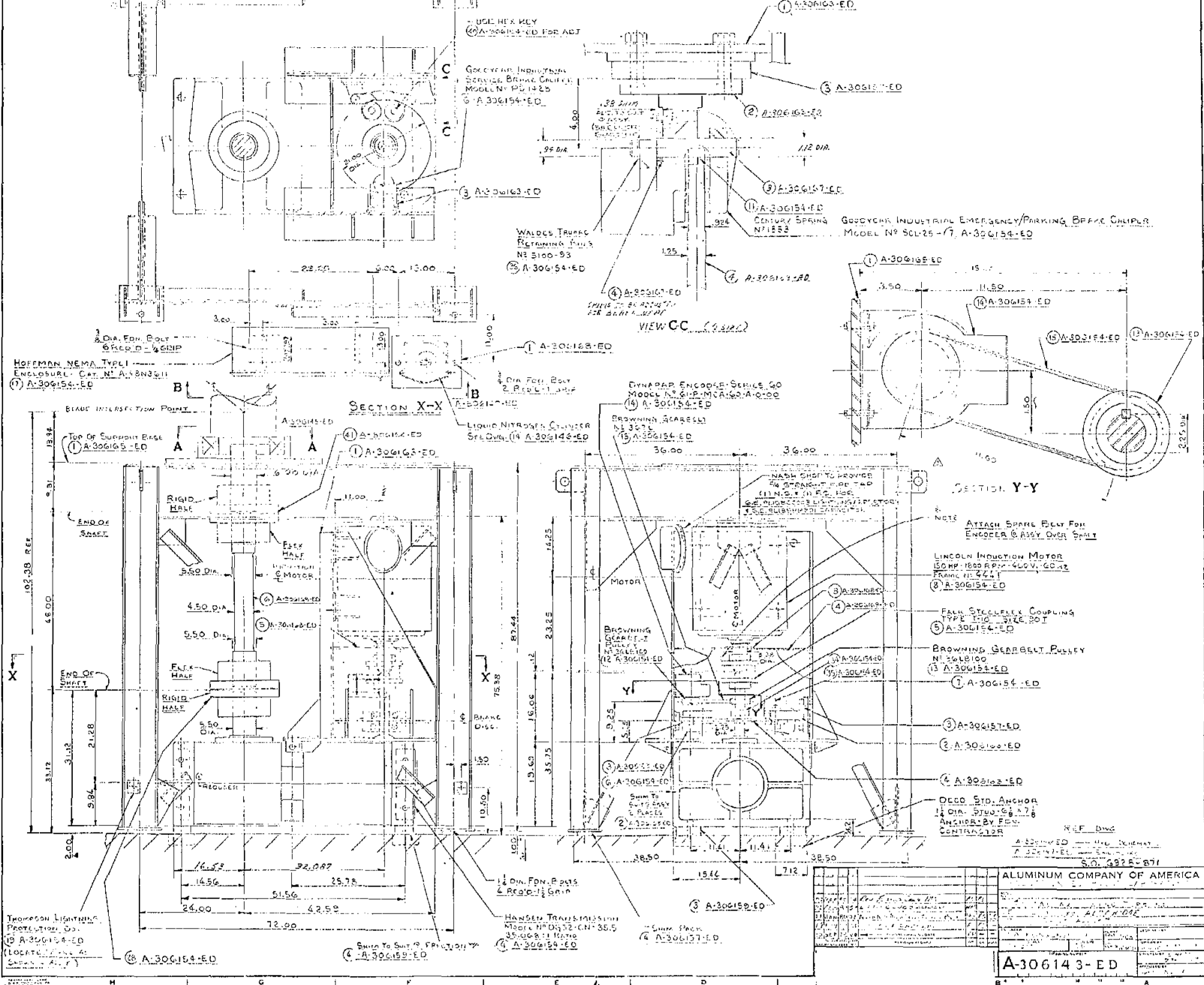
- NOTES:**
1. THE CENTER LINE OF ANY SECTION MUST NOT DEVIATE MORE THAN .001" FROM THE THEORETICAL ϕ OF THE ROTOR ASSEMBLY.
 2. FOR THE ASSEMBLY OF ANY TWO SECTIONS THE ϕ OF EACH SECTION MUST NOT DEVIATE MORE THAN .001" FROM EACH OTHER.
 3. FOR ASSEMBLY OF THE TOP & BOTT. BLADE CONNECTIONS TO THE CENTER TUBE SECTIONS, THE S.W.T. (S.W.T. E.D.T. BLADE CONNECTIONS) MUST NOT BE OUT OF LINE WITH THE THEORETICAL ϕ MORE THAN .25" THE TANGENT POINT BEING THE MOUNTING SURFACES.
 4. THE ϕ OF THE TOP & BOTT. BLADE CONNECTIONS USED FOR SECTIONS ONE BLADE MUST NOT BE OUT OF LINE WITH EACH OTHER MORE THAN .022"
 5. ROUNDOFF OF THE PIN FLANGE ON THE ASSEMBLED TORQUE TUBE SHALL NOT EXCEED .020" AT THE DIAMETER.



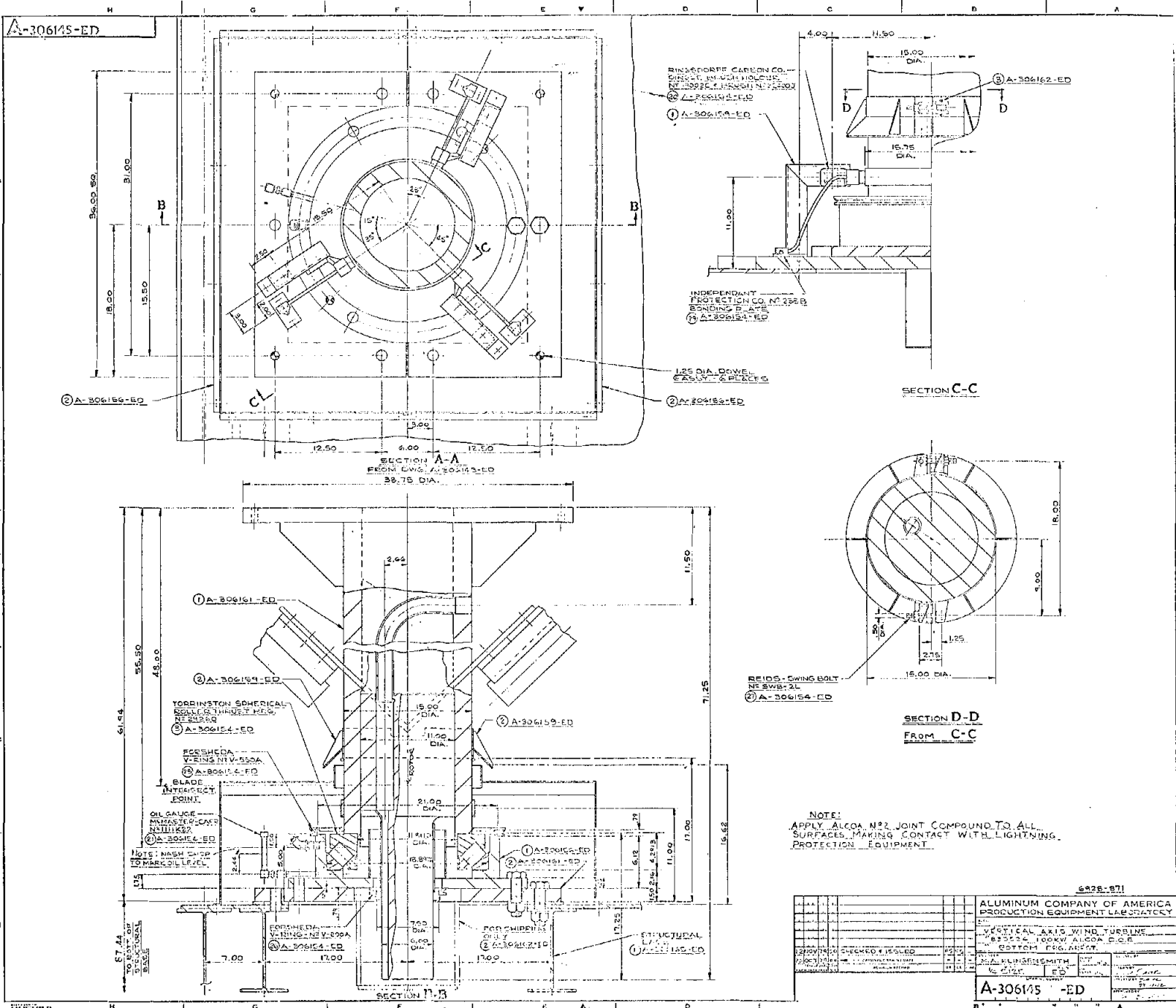
50 6928-971

ALUMINUM COMPANY OF AMERICA	
PRINCIPAL ENGINEERING LABORATORY	
DATE	APR 11 1944
BY	W. J. BROWN
CHECKED	W. J. BROWN
APPROVED	W. J. BROWN
DESIGNED	W. J. BROWN
DRAWN	W. J. BROWN
MANUFACTURED	ALUMINUM COMPANY OF AMERICA
QUANTITY	1
SCALE	AS SHOWN
A-306142 - ED	

A-306143-ED



A-306143-ED



A-30615-ED

RINDORFF CARBON CO. - DISK 11, IN. DIA. HOLE DIA. 1.5000, 2. IN. DIA. HOLE DIA. 1.5000
 (1) A-30615A-ED
 (2) A-30615B-ED

INDEPENDANT PROTECTION CO. NO. 2352B
 BEARING PLATE
 (3) ASSOCIATED

1.25 DIA. DOWEL
 EASILY TO BE PLACED

YORRINSTON SPHERICAL BEARING 3 IN. DIA. T. 1.5000
 (1) A-306161-ED
 (2) A-306162-ED
 (3) A-306163-ED

FRISHCOA WINDING INT. 1.5000
 (4) A-306164-ED

BLADE INTERSECT POINT

OIL GAUGE - MAINTENANCE CHECK MONTHLY
 (5) A-306165-ED

NOTE: NASH CAP TO BE USED TO MARK OFF LEVEL

FORMER DIA. 1.5000
 (6) A-306166-ED

FOR CHIMNEY ONLY
 (7) A-306167-ED

STRUCTURAL LUG
 (8) ASSOCIATED

826-871

DESIGNED BY	DATE	APPROVED BY	DATE
CHECKED BY	DATE	APPROVED BY	DATE
TESTED BY	DATE	APPROVED BY	DATE
INSPECTED BY	DATE	APPROVED BY	DATE

ALUMINUM COMPANY OF AMERICA
 PRODUCTION EQUIPMENT LABORATORY

VERTICAL AXIS WIND TURBINE
 100KW ALCOA P.E.R.
 BOTTOM PLATFORM

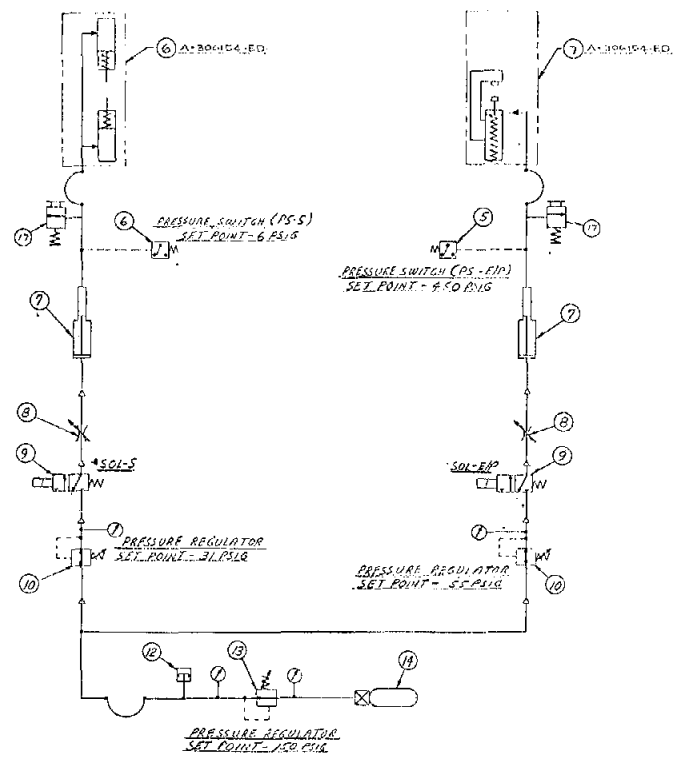
DRG. NUMBER: A-30615-ED
 DATE: 11/15/54
 BY: J. H. SMITH
 CHECKED BY: J. H. SMITH
 APPROVED BY: J. H. SMITH

A-30615 -ED

A-306146-ED

SERVICE BRAKE

EMERGENCY/PARK BRAKE



BRAKING SYSTEM

THERE ARE TWO SEPARATE BRAKING SYSTEMS. THE EMERGENCY/PARKING BRAKE IS A SYSTEM WITH SPRING APPLIED BRAKE LINES. HYDRAULIC PRESSURE, APPLIED THROUGH AN AIR-OIL INTERFACER, IS USED TO RELEASE THE BRAKE. THE SECOND SYSTEM IS A SERVICE BRAKE FOR BRAKING DURING NORMAL OPERATIONAL OPERATION. THE SERVICE BRAKE IS APPLIED WITH HYDRAULIC PRESSURE PROVIDED THROUGH AN AIR-OIL INTERFACER. EACH SYSTEM OPERATES INDEPENDENTLY. OPERATION OF THE BRAKES WHEN THE SYSTEM IS PARKED, DURING START-UP, FOR NORMAL SERVICE BRAKING AND IN EMERGENCY CONDITIONS IS DISCUSSED BELOW.

PARKED POSITION

WHEN IN THE PARKED POSITION, CONTROL VALVES SOL-EP AND SOL-S ARE DE-ENERGIZED WITH DOWNSTREAM PRESSURE VENTED TO ATMOSPHERE. WITH ZERO PRESSURE DOWNSTREAM OF THE CONTROL VALVES, THE SPRING ACTIVATED EMERGENCY/PARKING BRAKE CALIPER IS APPLIED TO THE DISC AND THE SERVICE BRAKE DISENGAGED. WITH ZERO PRESSURE DOWNSTREAM OF CONTROL VALVES, SOL-EP AND SOL-S PRESSURE SWITCHES PS-EP AND PS-S ARE OPEN. IN THE OPEN POSITION, PS-EP PREVENTS START-UP OF THE SERVICE SYSTEM.

START-UP/TURBINE

TO START-UP, CONTROL VALVE SOL-EP IS ENERGIZED APPLYING PRESSURE TO AND DIS-ENGAGING THE EMERGENCY/PARKING BRAKE.

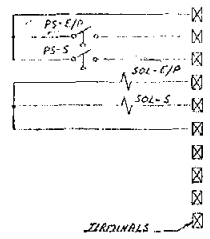
WITH PRESSURE AT THE EMERGENCY/PARKING BRAKE CALIPER, PS-EP IS CLOSED PERMITTING SYSTEM START-UP. ON START-UP, THE SERVICE BRAKE CONTROL VALVE SOL-S IS DE-ENERGIZED AND PRESSURE SWITCH PS-S IS OPEN.

NORMAL OR SERVICE BRAKING

TO STOP THE TURBINE AT NORMAL SERVICE CONDITIONS, CONTROL VALVE SOL-S IS ENERGIZED, APPLYING PRESSURE TO AND ENGAGING THE SERVICE BRAKE CALIPER. PRESSURE AT THE SERVICE BRAKE CALIPER PRESSURE SWITCH PS-S RELAYING POWER TO THE INTERFACER. ONCE THE TURBINE IS STOPPED WITH THE SERVICE BRAKE, EMERGENCY/PARKING CONTROL VALVE SOL-EP IS DE-ENERGIZED ENGAGING THE EMERGENCY/PARKING BRAKE CALIPER AND CONTROL VALVE SOL-S IS DE-ENERGIZED DIS-ENGAGING THE SERVICE BRAKE.

EMERGENCY BRAKING

STOPPING OF EMERGENCY BRAKING IS ACCOMPLISHED BY DE-ENERGIZING EMERGENCY/PARKING BRAKE CONTROL VALVE SOL-EP, ALLOWING PRESSURE FROM AND ENGAGING THE EMERGENCY/PARKING BRAKE CALIPER.



ELECTRICAL SCHEMATIC

PART 1 - HYDRAULIC AND ELECTRICAL SCHEMATIC

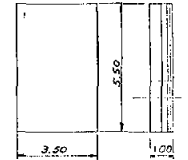
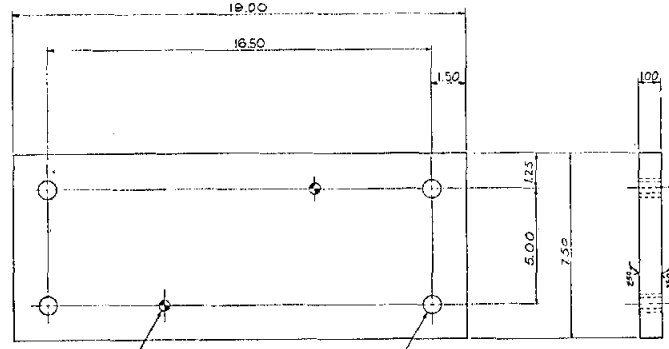
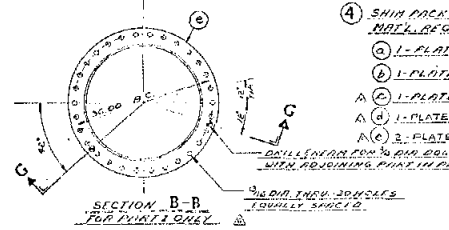
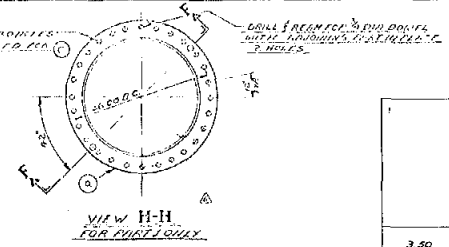
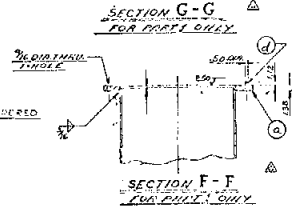
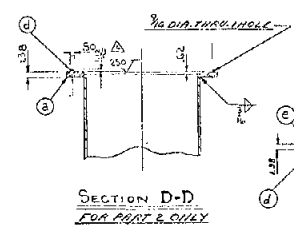
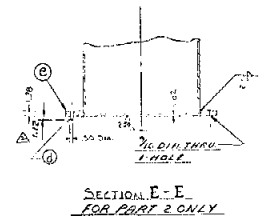
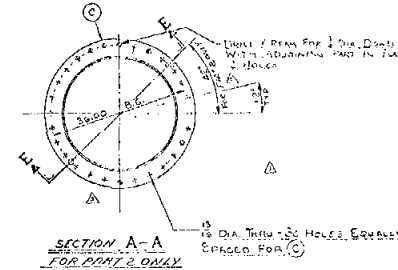
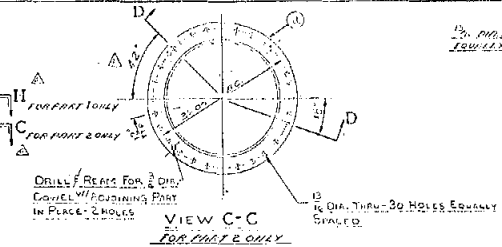
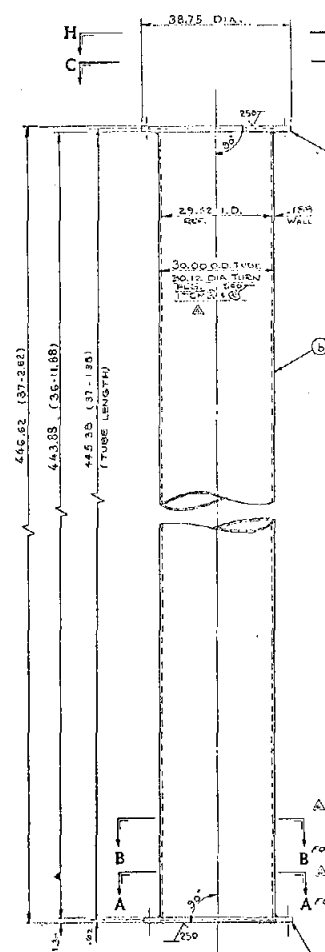
NO.	QTY	DESCRIPTION	REVISED
5	1	PRESSURE SWITCH PS-E/P, NORMALLY OPEN, ADJUSTABLE OPERATING RANGE 300-1000 PSIG OR RISKY PRESSURE AND 240-940 PSIG ON DE-CRATED PRESSURE, RATED MAXIMUM PRESSURE 5000 PSIG, 1/4 IN. NPT AND 1/4 IN. NPT, 120 VOLT, HEATH-ROD MODEL NO. 1011 WITH 1/4 INCH ALUMINUM PRESSURE PLATE (OR EQUAL)	2
6	1	PRESSURE SWITCH PS-S, NORMALLY OPEN, ADJUSTABLE OPERATING RANGE 0-75 PSIG OR RISKY PRESSURE AND 240-940 PSIG ON DE-CRATED PRESSURE, RATED MAXIMUM PRESSURE 5000 PSIG, 1/4 IN. NPT AND 1/4 IN. NPT, 120 VOLT, HEATH-ROD MODEL NO. 1011 WITH 1/4 INCH ALUMINUM PRESSURE PLATE (OR EQUAL)	2
7	2	POWER CLUSTER, ON LINE'S ONLY WITH N.H. BY PDS PORTED MASTER CYLINDER, PDS-201 PART 8-11, WITH RIGHT HAND MOUNTING BRACKET, WAGNER ELECTRIC CORPORATION PART NO. 3-30275	
8	2	FLOW CONTROL VALVE, 1/4 INCH SIZE, IN-LINE, 4 FLO SERIES FC MODEL 2701 (OR EQUAL)	
9	2	SOLENOID VALVE, 3-WAY, 2 POSITION, NORMALLY CLOSED 120 VOLT, CIRCULE SEAL CARTRIDGE NO. 5341-82000	
10	2	PRESSURE REGULATOR, 1/4 INCH NPT, PRIMARY PRESSURE 175 PSIG AND SECONDARY ADJUSTABLE RANGE 2-100 PSIG WITH 0-100 PSIG SECONDARY PRESSURE GAUGE, ROTEX MODEL NO. FOR REGULATOR 11-010-040 AND FOR PRESSURE GAUGE 18-013-008 (OR EQUAL)	
12	1	RUPTURE DISC UNIT, 1/2 INCH NPT SCREW TYPE WITH ALUMINUM DISC TO RUPTURE AT 700 PSIG AT -50 TO +150°F, FINE MESH PROTECTIVE SCREEN, 304L, 304 STAINLESS WITH CARBON STEEL LEGS (OR EQUAL)	
15	1	GAS CYLINDER REGULATOR, 1/4 INCH NPT PRIMARY PRESSURE UP TO 5000 PSI, SECONDARY PRESSURE ADJUSTMENT RANGE 0-175 PSI WITH 0-500 PSIG SECONDARY PRESSURE GAUGE AND 0-300 PSIG PRIMARY PRESSURE GAUGE AND CYLINDER VALVE CONNECTION FOR INFINITI, MORGAN PART NO. FOR REGULATOR 11-010-040, FOR SECONDARY PRESSURE GAUGE 18-013-008, FOR PRIMARY PRESSURE GAUGE 18-013-007, AND FOR CYLINDER CONNECTION 18-008-003	
14	1	LITHIUM NITROGEN CYLINDER 9-1/4 INCH DIAMETER BY 60 INCHS LONG, 500 SET AT 2600 PSIG TO BE OBTAINED FROM VENDOR AT SITE	165
15	1	HYDRAULIC BRAKE FLUID, HEAVY DUTY NON-PETROLEUM TYPE SAE STANDARD -1703-C, D.O.O. TYPE 3, US GOVERNMENT SPECIFICATION 99-8-60C (B)	
17	2	SOLENOID VALVE - 120VAC SERIES FC MODEL 4000 PSI PRESSURE RATING	

S.O. 6928-872 S.O. 6928-874
S.O. 6928-871 S.O. 6928-873

NO.	QTY	DESCRIPTION	REVISED
1	1	ALUMINUM COMPANY OF AMERICA PRODUCTION EQUIPMENT LABORATORY	
2	1	VERTICAL AXIS WIND TURBINE	
3	1	25 HP 115V 60 HZ ALCOHOL BURNER	
4	1	BRINE RECIRCULATION SYSTEM HYDRAULIC	
5	1	BRINE SOLUBLE	
6	1	M. & PLUMBERS SUPPLY	

A-306146-ED

A-306157-ED



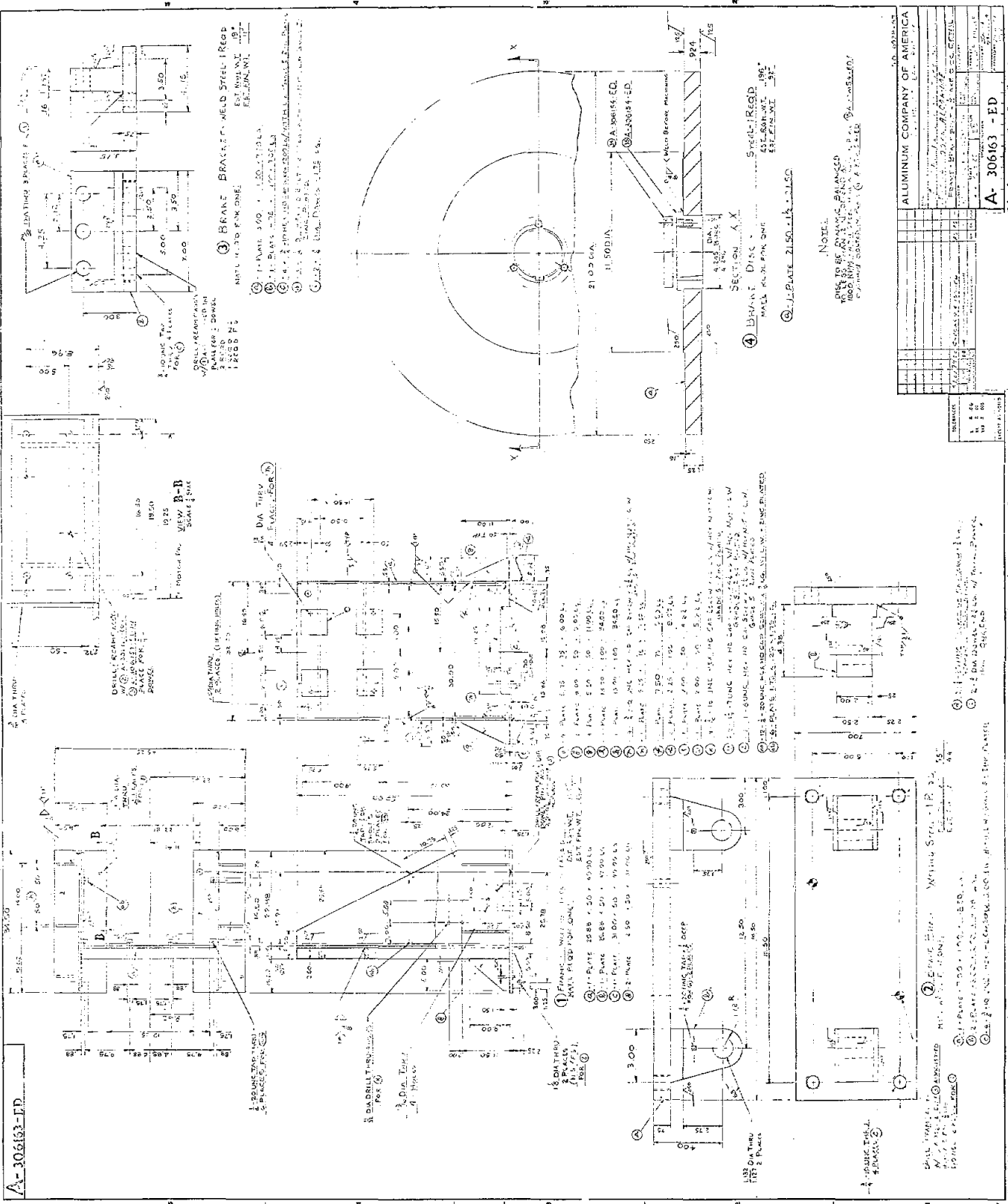
- 1 ROTOR TUBE - BOTTOM SECTION - WELDED STEEL - 1 REQ'D
MATERIAL REQ'D FOR ONE EST. RM. WT. 2710*
EST. FIN. WT. 2632*
- 2 1-PLATE 38.75 x 1/2 x 38.75 LG.
- 3 1-FOSTER WELD PIPE 30 O.D. x 1.58 WALL x 445.30 (37-1.30) LG.
NEEDS GRADE B PLAIN END SQUARE END (STRAIGHTNESS TO C. 24 IN 10 FT) PRE-ORDERED
- 4 22-#10 UNF x 1.00 Lg. BETHLEHEM A-225 TYPE 1 BOLT 1/2 A-325 FULL WASKER
HEAVY HEX ANCH. NUT - GALVANIZED
- 5 2-#10 DIA. DRILL 1.25 LG.
- 6 1-PLATE 38.75 x 1/2 x 38.75 LG.
- 7 ROTOR TUBE - TOP SECTION - WELDED STEEL - 1 REQ'D
MATERIAL REQ'D FOR ONE EST. RM. WT. 2710*
EST. FIN. WT. 2318*
SAME AS PART NO. 1 EXCEPT ITEM (C) IS NOT REQUIRED

- 8 SHIM PACK - STEEL SHIM STOCK - 4 REQ'D
MATERIAL REQ'D FOR ONE EST. FIN. WT. 4*
- 9 1-PLATE 3.50 x 1/2 x 5.50
- 10 1-PLATE 3.50 x 1/2 x 5.50
- 11 1-PLATE 3.50 x 1/2 x 5.50
- 12 1-PLATE 3.50 x 1/2 x 5.50
- 13 2-PLATE 3.50 x 1/2 x 5.50

- 14 3-STEEL PLATE - STEEL - 1 REQ'D
MATERIAL REQ'D FOR ONE EST. RM. WT. 50*
EST. FIN. WT. 46*
- 15 1-PLATE 7.50 x 1/2 x 19.00 LG.

G938-B71	
ALUMINUM COMPANY OF AMERICA	
EQUIPMENT LABORATORY	
DATE	APR 19 1954
BY	W. J. BROWN
CHECKED BY	W. J. BROWN
APPROVED BY	W. J. BROWN
DESIGNED BY	W. J. BROWN
DRAWN BY	W. J. BROWN
SCALE	AS SHOWN
TITLE	A-306157-ED

A-306163-1P



- ③ BRAKE BRACKET WELD STEEL-1 REED
EST. INVT. 107
RE-EXAMINE 111
- NYLON H-30 FOR ONE
- ① 1/2" PLATE 300 x 120 x 1/8
 - ② 1/2" PLATE 300 x 120 x 1/8
 - ③ 1/2" PLATE 300 x 120 x 1/8
 - ④ 1/2" PLATE 300 x 120 x 1/8
 - ⑤ 1/2" PLATE 300 x 120 x 1/8
 - ⑥ 1/2" PLATE 300 x 120 x 1/8
 - ⑦ 1/2" PLATE 300 x 120 x 1/8
 - ⑧ 1/2" PLATE 300 x 120 x 1/8
 - ⑨ 1/2" PLATE 300 x 120 x 1/8
 - ⑩ 1/2" PLATE 300 x 120 x 1/8

- ④ BRAKE DISC
WELD STEEL-1 REED
EST. INVT. 107
RE-EXAMINE 111
- ⑤ PLATE 2150 x 14 x 1/8

NOTE:
DISC TO BE ANNEALED
1800 MIN. AT 1000°F.
COLD CHILLED
COLD CHILLED

ALUMINUM COMPANY OF AMERICA	
DATE	10/20/50
BY	W. J. ...
CHECKED	...
APPROVED	...
DESIGNED	...
DRAWN	...
ESTIMATED	...
PROJECT	...
ORDER NO.	...
QUANTITY	...
PRICE	...
TOTAL	...
A-306163-ED	

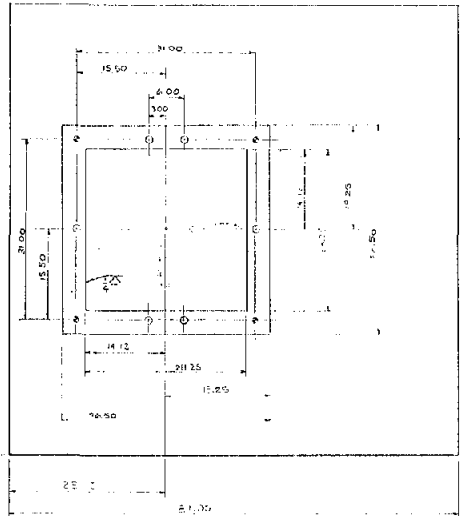
A-306165-ED

Direct Beam for LMA Storage
ASSEMBLY WITH PART A-306165-ED
WITH PLATE 1/4" THICK

1 1/2" DIA. TIRU
6" LONG
WITH PLATE
1/4" THICK

1 1/2" DIA. DRILL TIRU
4" LONG

SEE DETAIL
A

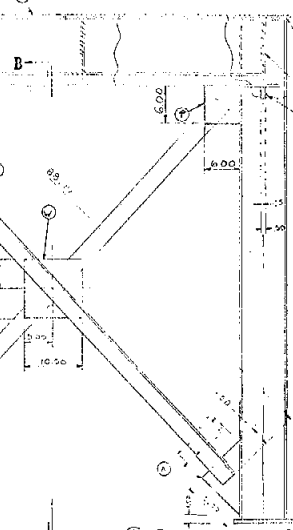


DETAIL A



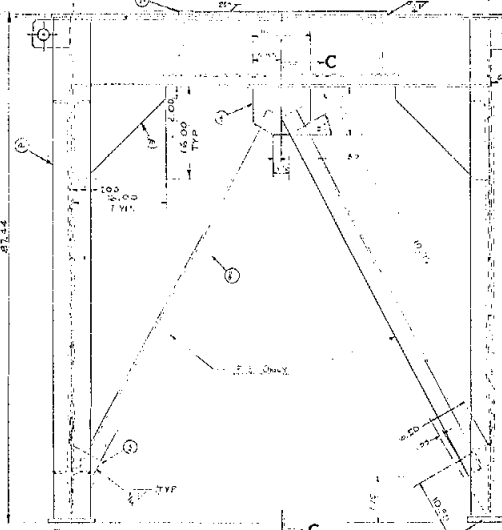
SECTION B-B

- ① A - WF 10.00 x 21.00 x 136.00
- ② A - WF 10.00 x 21.00 x 136.00
- ③ A - WF 12.00 x 27.00 x 144.00
- ④ A - WF 12.00 x 27.00 x 144.00
- ⑤ A - WF 10.00 x 21.00 x 136.00



SECTION B-B

- ① ROTOR SUPPLY BASE - WELDED STEEL - 1/4" THICK
MATERIAL FOR ONE:
- ① 1/4" PLATE 10.00 x 74.00 x 100.00
 - ② 1/4" PLATE 10.00 x 74.00 x 100.00
 - ③ 1/4" PLATE 10.00 x 74.00 x 100.00
 - ④ 1/4" PLATE 10.00 x 74.00 x 100.00
 - ⑤ 1/4" PLATE 10.00 x 74.00 x 100.00
 - ⑥ 1/4" PLATE 10.00 x 74.00 x 100.00
 - ⑦ 1/4" PLATE 10.00 x 74.00 x 100.00
 - ⑧ 1/4" PLATE 10.00 x 74.00 x 100.00
 - ⑨ 1/4" PLATE 10.00 x 74.00 x 100.00
 - ⑩ 1/4" PLATE 10.00 x 74.00 x 100.00
 - ⑪ 1/4" PLATE 10.00 x 74.00 x 100.00
 - ⑫ 1/4" PLATE 10.00 x 74.00 x 100.00
 - ⑬ 1/4" PLATE 10.00 x 74.00 x 100.00
 - ⑭ 1/4" PLATE 10.00 x 74.00 x 100.00
 - ⑮ 1/4" PLATE 10.00 x 74.00 x 100.00
 - ⑯ 1/4" PLATE 10.00 x 74.00 x 100.00
 - ⑰ 1/4" PLATE 10.00 x 74.00 x 100.00
 - ⑱ 1/4" PLATE 10.00 x 74.00 x 100.00
 - ⑲ 1/4" PLATE 10.00 x 74.00 x 100.00
 - ⑳ 1/4" PLATE 10.00 x 74.00 x 100.00
 - ㉑ 1/4" PLATE 10.00 x 74.00 x 100.00
 - ㉒ 1/4" PLATE 10.00 x 74.00 x 100.00
 - ㉓ 1/4" PLATE 10.00 x 74.00 x 100.00
 - ㉔ 1/4" PLATE 10.00 x 74.00 x 100.00
 - ㉕ 1/4" PLATE 10.00 x 74.00 x 100.00
 - ㉖ 1/4" PLATE 10.00 x 74.00 x 100.00
 - ㉗ 1/4" PLATE 10.00 x 74.00 x 100.00
 - ㉘ 1/4" PLATE 10.00 x 74.00 x 100.00
 - ㉙ 1/4" PLATE 10.00 x 74.00 x 100.00
 - ㉚ 1/4" PLATE 10.00 x 74.00 x 100.00
 - ㉛ 1/4" PLATE 10.00 x 74.00 x 100.00
 - ㉜ 1/4" PLATE 10.00 x 74.00 x 100.00
 - ㉝ 1/4" PLATE 10.00 x 74.00 x 100.00
 - ㉞ 1/4" PLATE 10.00 x 74.00 x 100.00
 - ㉟ 1/4" PLATE 10.00 x 74.00 x 100.00
 - ㊱ 1/4" PLATE 10.00 x 74.00 x 100.00
 - ㊲ 1/4" PLATE 10.00 x 74.00 x 100.00
 - ㊳ 1/4" PLATE 10.00 x 74.00 x 100.00
 - ㊴ 1/4" PLATE 10.00 x 74.00 x 100.00
 - ㊵ 1/4" PLATE 10.00 x 74.00 x 100.00
 - ㊶ 1/4" PLATE 10.00 x 74.00 x 100.00
 - ㊷ 1/4" PLATE 10.00 x 74.00 x 100.00
 - ㊸ 1/4" PLATE 10.00 x 74.00 x 100.00
 - ㊹ 1/4" PLATE 10.00 x 74.00 x 100.00
 - ㊺ 1/4" PLATE 10.00 x 74.00 x 100.00
 - ㊻ 1/4" PLATE 10.00 x 74.00 x 100.00
 - ㊼ 1/4" PLATE 10.00 x 74.00 x 100.00
 - ㊽ 1/4" PLATE 10.00 x 74.00 x 100.00
 - ㊾ 1/4" PLATE 10.00 x 74.00 x 100.00
 - ㊿ 1/4" PLATE 10.00 x 74.00 x 100.00



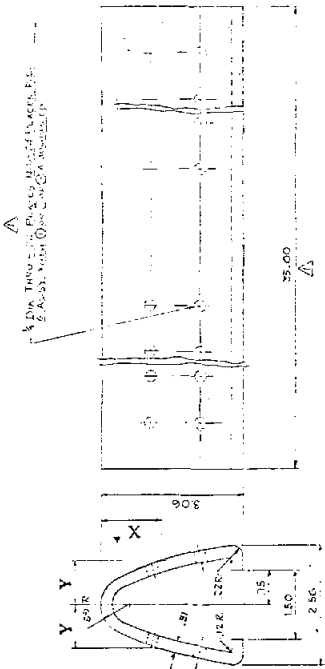
SECTION C-C

NO.	DESCRIPTION	QTY	UNIT	WEIGHT
1	1/4" PLATE 10.00 x 74.00 x 100.00	1	SQ. FT.	10.00
2	1/4" PLATE 10.00 x 74.00 x 100.00	1	SQ. FT.	10.00
3	1/4" PLATE 10.00 x 74.00 x 100.00	1	SQ. FT.	10.00
4	1/4" PLATE 10.00 x 74.00 x 100.00	1	SQ. FT.	10.00
5	1/4" PLATE 10.00 x 74.00 x 100.00	1	SQ. FT.	10.00
6	1/4" PLATE 10.00 x 74.00 x 100.00	1	SQ. FT.	10.00
7	1/4" PLATE 10.00 x 74.00 x 100.00	1	SQ. FT.	10.00
8	1/4" PLATE 10.00 x 74.00 x 100.00	1	SQ. FT.	10.00
9	1/4" PLATE 10.00 x 74.00 x 100.00	1	SQ. FT.	10.00
10	1/4" PLATE 10.00 x 74.00 x 100.00	1	SQ. FT.	10.00
11	1/4" PLATE 10.00 x 74.00 x 100.00	1	SQ. FT.	10.00
12	1/4" PLATE 10.00 x 74.00 x 100.00	1	SQ. FT.	10.00
13	1/4" PLATE 10.00 x 74.00 x 100.00	1	SQ. FT.	10.00
14	1/4" PLATE 10.00 x 74.00 x 100.00	1	SQ. FT.	10.00
15	1/4" PLATE 10.00 x 74.00 x 100.00	1	SQ. FT.	10.00
16	1/4" PLATE 10.00 x 74.00 x 100.00	1	SQ. FT.	10.00
17	1/4" PLATE 10.00 x 74.00 x 100.00	1	SQ. FT.	10.00
18	1/4" PLATE 10.00 x 74.00 x 100.00	1	SQ. FT.	10.00
19	1/4" PLATE 10.00 x 74.00 x 100.00	1	SQ. FT.	10.00
20	1/4" PLATE 10.00 x 74.00 x 100.00	1	SQ. FT.	10.00
21	1/4" PLATE 10.00 x 74.00 x 100.00	1	SQ. FT.	10.00
22	1/4" PLATE 10.00 x 74.00 x 100.00	1	SQ. FT.	10.00
23	1/4" PLATE 10.00 x 74.00 x 100.00	1	SQ. FT.	10.00
24	1/4" PLATE 10.00 x 74.00 x 100.00	1	SQ. FT.	10.00
25	1/4" PLATE 10.00 x 74.00 x 100.00	1	SQ. FT.	10.00
26	1/4" PLATE 10.00 x 74.00 x 100.00	1	SQ. FT.	10.00
27	1/4" PLATE 10.00 x 74.00 x 100.00	1	SQ. FT.	10.00
28	1/4" PLATE 10.00 x 74.00 x 100.00	1	SQ. FT.	10.00
29	1/4" PLATE 10.00 x 74.00 x 100.00	1	SQ. FT.	10.00
30	1/4" PLATE 10.00 x 74.00 x 100.00	1	SQ. FT.	10.00
31	1/4" PLATE 10.00 x 74.00 x 100.00	1	SQ. FT.	10.00
32	1/4" PLATE 10.00 x 74.00 x 100.00	1	SQ. FT.	10.00
33	1/4" PLATE 10.00 x 74.00 x 100.00	1	SQ. FT.	10.00
34	1/4" PLATE 10.00 x 74.00 x 100.00	1	SQ. FT.	10.00
35	1/4" PLATE 10.00 x 74.00 x 100.00	1	SQ. FT.	10.00
36	1/4" PLATE 10.00 x 74.00 x 100.00	1	SQ. FT.	10.00
37	1/4" PLATE 10.00 x 74.00 x 100.00	1	SQ. FT.	10.00
38	1/4" PLATE 10.00 x 74.00 x 100.00	1	SQ. FT.	10.00
39	1/4" PLATE 10.00 x 74.00 x 100.00	1	SQ. FT.	10.00
40	1/4" PLATE 10.00 x 74.00 x 100.00	1	SQ. FT.	10.00
41	1/4" PLATE 10.00 x 74.00 x 100.00	1	SQ. FT.	10.00
42	1/4" PLATE 10.00 x 74.00 x 100.00	1	SQ. FT.	10.00
43	1/4" PLATE 10.00 x 74.00 x 100.00	1	SQ. FT.	10.00
44	1/4" PLATE 10.00 x 74.00 x 100.00	1	SQ. FT.	10.00
45	1/4" PLATE 10.00 x 74.00 x 100.00	1	SQ. FT.	10.00
46	1/4" PLATE 10.00 x 74.00 x 100.00	1	SQ. FT.	10.00
47	1/4" PLATE 10.00 x 74.00 x 100.00	1	SQ. FT.	10.00
48	1/4" PLATE 10.00 x 74.00 x 100.00	1	SQ. FT.	10.00
49	1/4" PLATE 10.00 x 74.00 x 100.00	1	SQ. FT.	10.00
50	1/4" PLATE 10.00 x 74.00 x 100.00	1	SQ. FT.	10.00

ALUMINUM COMPANY OF AMERICA
600 SOUTH GOWER ST. PHOENIX, ARIZONA

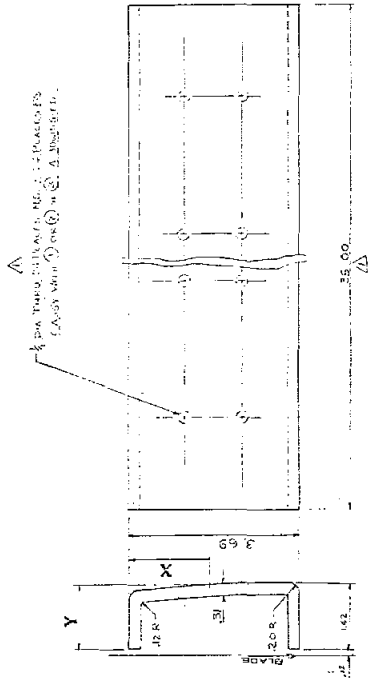
A-306165 - ED

A-306159-ED



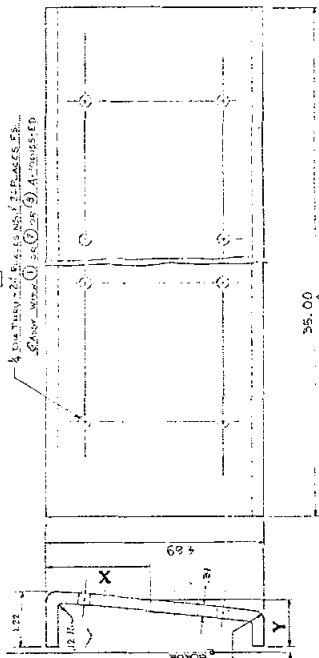
INCHES	FRACTIONS
1/16	1/16
1/8	1/8
3/16	3/16
1/4	1/4
5/16	5/16
3/8	3/8
7/16	7/16
1/2	1/2
5/8	5/8
3/4	3/4
7/8	7/8
1	1

① BLADE INSERT - 5061-T6 ALUM. EXTRUSION - 1/4 REED.
3.50" WIDE



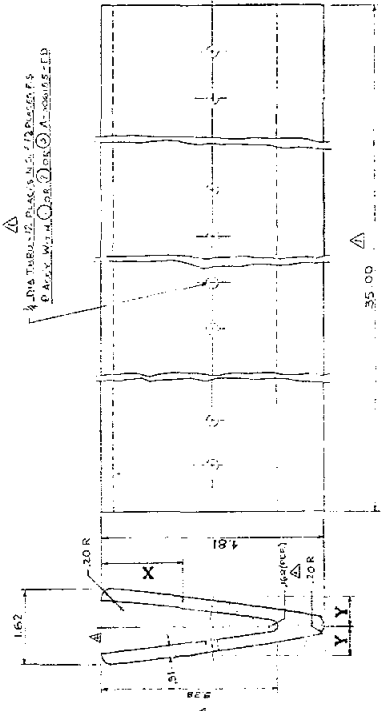
INCHES	FRACTIONS
1/16	1/16
1/8	1/8
3/16	3/16
1/4	1/4
5/16	5/16
3/8	3/8
7/16	7/16
1/2	1/2
5/8	5/8
3/4	3/4
7/8	7/8
1	1

② BLADE INSERT - 5061-T6 ALUM. EXTRUSION - 1/4 REED.
3.69" WIDE



INCHES	FRACTIONS
1/16	1/16
1/8	1/8
3/16	3/16
1/4	1/4
5/16	5/16
3/8	3/8
7/16	7/16
1/2	1/2
5/8	5/8
3/4	3/4
7/8	7/8
1	1

③ BLADE INSERT - 5061-T6 ALUM. EXTRUSION - 1/4 REED.
4.89" WIDE



INCHES	FRACTIONS
1/16	1/16
1/8	1/8
3/16	3/16
1/4	1/4
5/16	5/16
3/8	3/8
7/16	7/16
1/2	1/2
5/8	5/8
3/4	3/4
7/8	7/8
1	1

④ BLADE INSERT - 5061-T6 ALUM. EXTRUSION - 1/4 REED.
4.81" WIDE

ALUMINUM COMPANY OF AMERICA
ALUMINUM DIVISION
1000 ALUMINUM BUILDING
P.O. BOX 1000
PHOENIX, ARIZONA 85001

DATE	REV.	BY	CHKD.
10/15/59	1	J. H. W.	J. H. W.
10/15/59	2	J. H. W.	J. H. W.
10/15/59	3	J. H. W.	J. H. W.
10/15/59	4	J. H. W.	J. H. W.
10/15/59	5	J. H. W.	J. H. W.
10/15/59	6	J. H. W.	J. H. W.
10/15/59	7	J. H. W.	J. H. W.
10/15/59	8	J. H. W.	J. H. W.
10/15/59	9	J. H. W.	J. H. W.
10/15/59	10	J. H. W.	J. H. W.

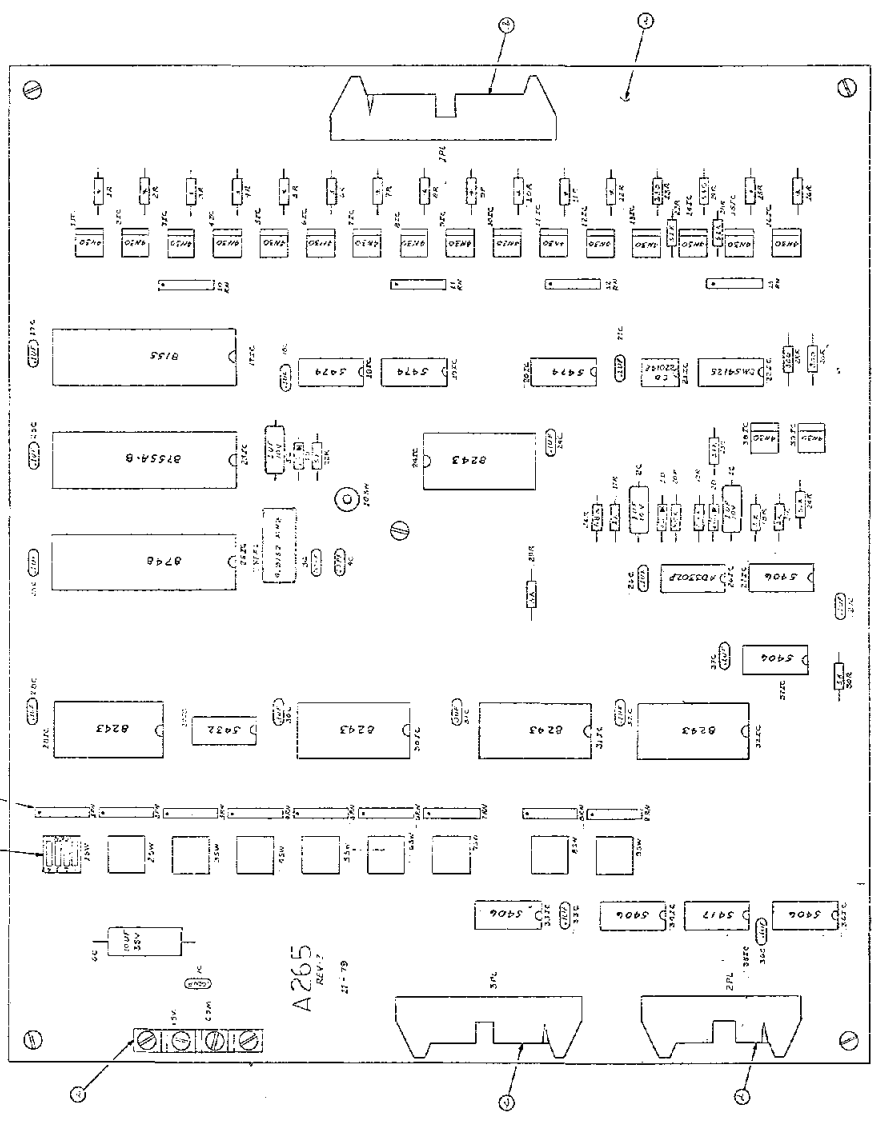
A-306159-ED

A-306367-1D

SILL OF MATERIAL

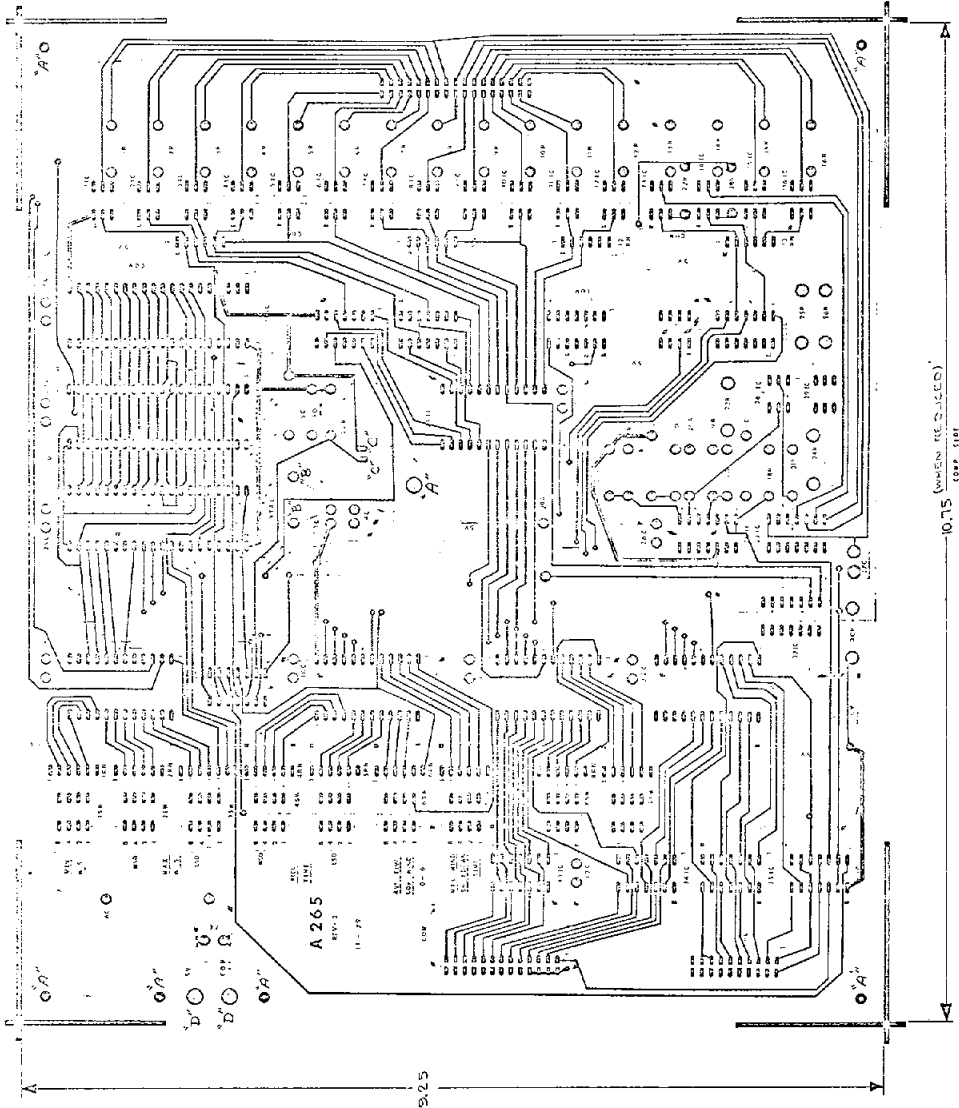
NO.	DESCRIPTION	QTY.	UNIT	REMARKS
1
2
3
4
5
6
7
8
9
10
11
12
13
14
15
16
17
18
19
20
21
22
23
24
25
26
27
28
29
30
31
32
33
34
35
36
37
38
39
40
41
42
43
44
45
46
47
48
49
50
51
52
53
54
55
56
57
58
59
60
61
62
63
64
65
66
67
68
69
70
71
72
73
74
75
76
77
78
79
80
81
82
83
84
85
86
87
88
89
90
91
92
93
94
95
96
97
98
99
100

A. TO BE LISTED ON IMPR. DRAWING
(CARRY MATERIAL LISTS TO DRAWING)



8667-10-31
 MAR 13 1950
 ALUMINUM COMPANY OF AMERICA
 175 BROADWAY, NEW YORK 17, N.Y.
 A-306367-ED

A-506368-ED



REVISION RECORD

NO.	DATE	DESCRIPTION
1	11-2-78	REVISED TO SHOW CHANGES
2	11-2-78	REVISED TO SHOW CHANGES
3	11-2-78	REVISED TO SHOW CHANGES
4	11-2-78	REVISED TO SHOW CHANGES
5	11-2-78	REVISED TO SHOW CHANGES
6	11-2-78	REVISED TO SHOW CHANGES
7	11-2-78	REVISED TO SHOW CHANGES

NOTE: DIMENSIONS TO BE MAINTAINED THROUGHOUT THE LIFE OF THE BOARD.
 BOARD TO BE MANUFACTURED BY THE ALUMINUM COMPANY OF AMERICA.

ALUMINUM COMPANY OF AMERICA

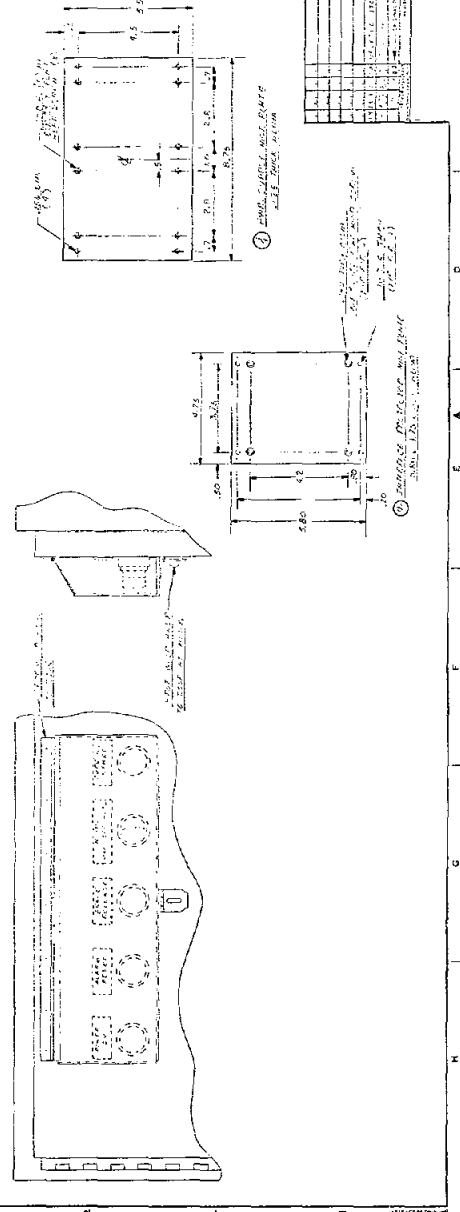
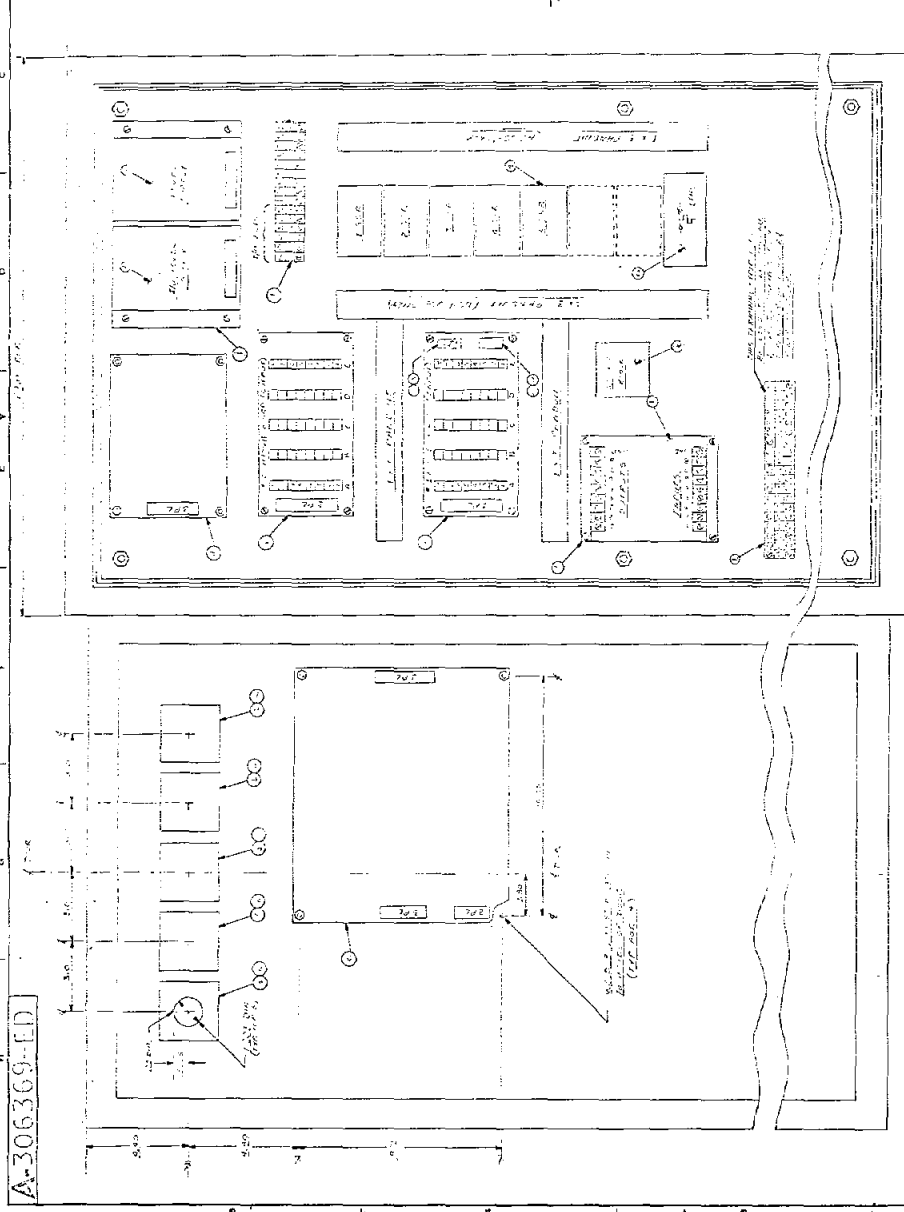
ASSIGNED: A-506368-ED
 DATE: 11-2-78
 DRAWN BY: [Name]
 CHECKED BY: [Name]
 APPROVED BY: [Name]

ALUMINUM COMPANY OF AMERICA

A-506368-ED

BILL OF MATERIALS

NO.	DESCRIPTION	QTY.	UNIT	REMARKS
1	ALUMINUM SHEET 1/4" THICK	100	SQ. FT.	
2	ALUMINUM SHEET 1/8" THICK	200	SQ. FT.	
3	ALUMINUM SHEET 1/16" THICK	50	SQ. FT.	
4	ALUMINUM ANGLE 1/2" X 1/2"	10	LINEAL FT.	
5	ALUMINUM ANGLE 3/8" X 3/8"	20	LINEAL FT.	
6	ALUMINUM ANGLE 1/4" X 1/4"	30	LINEAL FT.	
7	ALUMINUM ROD 1/4" DIA.	5	LINEAL FT.	
8	ALUMINUM ROD 3/8" DIA.	10	LINEAL FT.	
9	ALUMINUM ROD 1/2" DIA.	5	LINEAL FT.	
10	ALUMINUM ROD 3/4" DIA.	5	LINEAL FT.	
11	ALUMINUM ROD 1" DIA.	5	LINEAL FT.	
12	ALUMINUM ROD 1 1/4" DIA.	5	LINEAL FT.	
13	ALUMINUM ROD 1 1/2" DIA.	5	LINEAL FT.	
14	ALUMINUM ROD 2" DIA.	5	LINEAL FT.	
15	ALUMINUM ROD 2 1/2" DIA.	5	LINEAL FT.	
16	ALUMINUM ROD 3" DIA.	5	LINEAL FT.	
17	ALUMINUM ROD 3 1/2" DIA.	5	LINEAL FT.	
18	ALUMINUM ROD 4" DIA.	5	LINEAL FT.	
19	ALUMINUM ROD 4 1/2" DIA.	5	LINEAL FT.	
20	ALUMINUM ROD 5" DIA.	5	LINEAL FT.	
21	ALUMINUM ROD 5 1/2" DIA.	5	LINEAL FT.	
22	ALUMINUM ROD 6" DIA.	5	LINEAL FT.	
23	ALUMINUM ROD 6 1/2" DIA.	5	LINEAL FT.	
24	ALUMINUM ROD 7" DIA.	5	LINEAL FT.	
25	ALUMINUM ROD 7 1/2" DIA.	5	LINEAL FT.	
26	ALUMINUM ROD 8" DIA.	5	LINEAL FT.	
27	ALUMINUM ROD 8 1/2" DIA.	5	LINEAL FT.	
28	ALUMINUM ROD 9" DIA.	5	LINEAL FT.	
29	ALUMINUM ROD 9 1/2" DIA.	5	LINEAL FT.	
30	ALUMINUM ROD 10" DIA.	5	LINEAL FT.	



NOTES:
 1. DIMENSIONS ARE GIVEN IN FEET AND INCHES.
 2. ALL DIMENSIONS ARE TO FACE UNLESS OTHERWISE NOTED.
 3. ALL DIMENSIONS ARE TO CENTER UNLESS OTHERWISE NOTED.

SEE PAGE 51
 CLASSIFIED - SECURITY INFORMATION

MAR 13 1960
 PROJECT: BIRMINGHAM UNIVERSITY

ALUMINUM COMPANY OF AMERICA

A-306369-ED

INTERMEDIATE VERTICAL AXIS WIND TURBINE (VAWT), 1 MEGAWATT

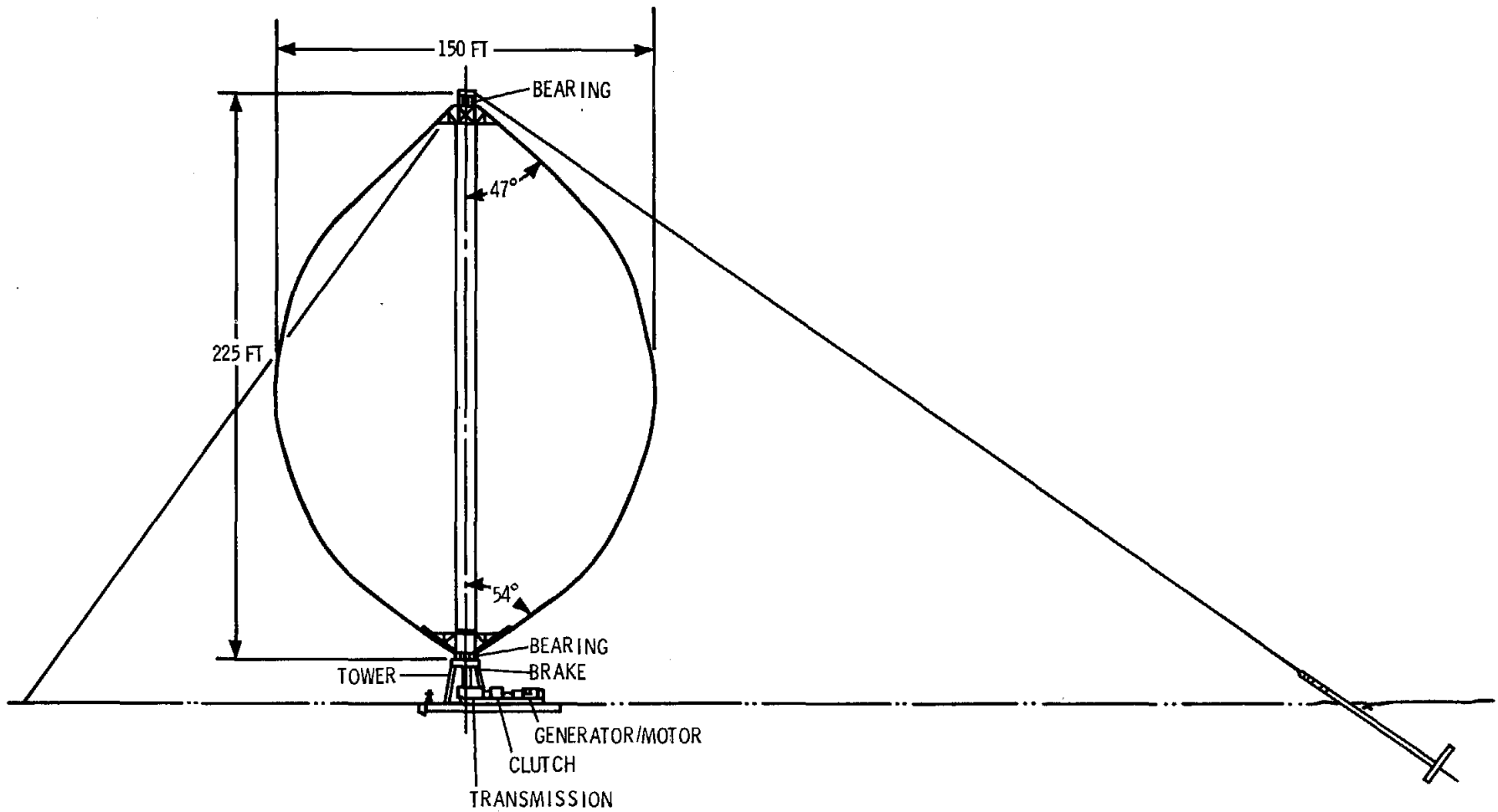
Robert D. Grover

Sandia Laboratories is in the process of designing an intermediate sized VAWT that will be in the one megawatt range at a wind velocity of 30 miles per hour. This turbine will be 150 feet in diameter and 225 feet high (Fig. 1).

The blades will have a symmetrical airfoil shape of NACA 0015 or a selected nonsymmetrical airfoil shape as determined by study and testing. The blades will have a 70 inch chord and will be made of extruded aluminum with several extrusions required to make up the length of the chord. With extrusions that can be made in a 15 inch diameter extrusion die, the 70 inch chord would require six extrusions, Fig. 2. These extrusions will be either welded or riveted together and made in shippable lengths of about 50 feet. The curved portions of the blades will be bent at the turbine site. With the welded design the blade will be bent after welding, and with the riveted design the extrusions will be bent before riveting.

To achieve minimum blade stress under centrifugal and gravity loading, the blades will be attached to the shaft at an angle of 47 degrees at the top of the blade, and 54 degrees at the bottom of the blade. These blades will weigh 18 tons and will be clamped rigidly to the blade shaft.

The blade shaft (tower) will be eight feet in diameter and have a wall thickness of .150 inch. This gives the largest practical cross-sectional moment of inertia for the amount of material used to withstand induced stresses. This shaft will



INTERMEDIATE VAWT
 1 MEGAWATT

FIGURE 1

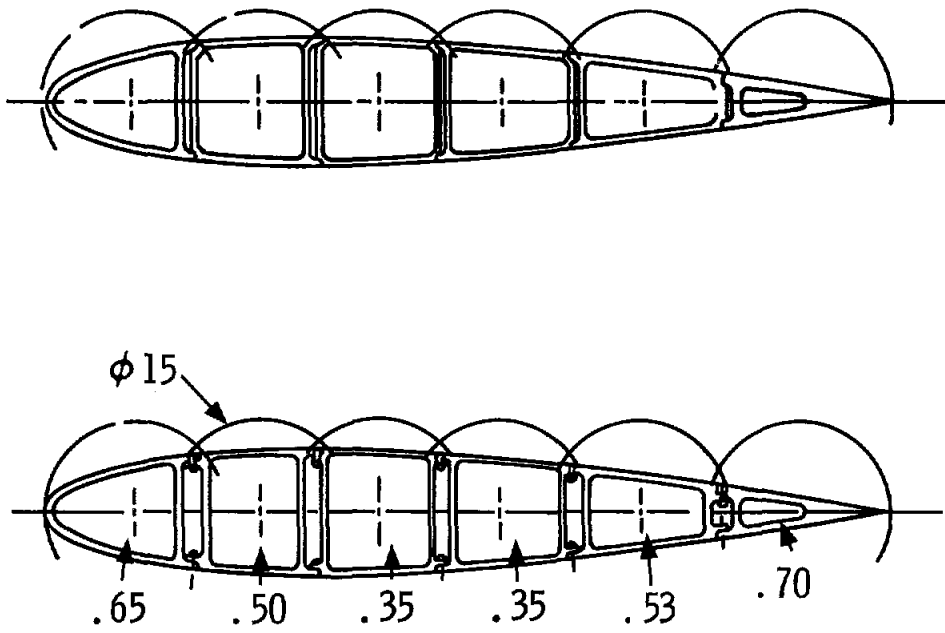


FIGURE 2

be 200 feet long, will be made in sections of welded structural steel, and weigh 15 tons.

At the top and bottom of the blade shaft will be bearings to permit rotation of the blade shaft. The bearings selected for this design are manufactured by Rotek, Incorporated. These bearings have the capability of withstanding a thrust, a radial, and a moment loading, simultaneously, with a single bearing. The bearing is bolted to a flat surface on the rotating part and to a flat surface on the stationary part. The bearings for this design are six feet in diameter and each weighs one ton.

The top of the turbine will be held stationary by three guy cables. These cables will be three and three-eighths inches in diameter, 440 feet long, weigh five tons each, and have a breaking strength of 663 tons. These cables will be steel bridge strand anchored to the ground by concrete deadmen. The bridge strand is used because of its rigidity. It has a modulus of elasticity of up to 24,000,000 pounds per square inch.

The rated torque for this turbine is 425,000 foot pounds at the low speed shaft. The torque can almost double in a high wind and a runaway turbine. The turbine can runaway from a loss of power, a broken shaft, or a broken transmission. To stop a runaway turbine in a high wind, a braking torque of three times rated torque must be applied.

The energy that must be absorbed by the brakes is the kinetic energy of rotation plus the aerodynamic energy produced by the turbine during the braking stop. The rated kinetic energy of this turbine will be about 5,000,000 foot pounds. A 20 percent overspeed will raise the kinetic energy of the turbine to about 7,000,000 foot pounds. To stop this turbine in 15 seconds, in a 90 mile per hour wind, with a 20 percent turbine overspeed, a torque of 1,200,000 foot pounds is required. This requires a braking system that will absorb 20,000,000 foot pounds of energy.

A brake disc made of structural steel for stopping this turbine has an outside diameter of eight feet, an inside diameter of three feet, a thickness of one inch, and weighs 1600 pounds. Structural steel was selected because of ease of manufacture, cost of material, lack of temper requirements, and lack of temper loss during operation.

The brake was put on the low speed shaft to avoid turbine loss due to transmission failure and to lower disc stress due to centrifugal loading.

The brake is a straightforward design with tradeoffs to be studied of the following items:

- 1 - Stopping time
- 2 - Energy to be absorbed
- 3 - Brake disc material
- 4 - Disc stress due to centrifugal loading
- 5 - Disc stress due to differential thermal expansion
- 6 - Disc stress due to braking shear stress
- 7 - Stopping torque
- 8 - Amount of brake disc material

The generator can be used as a motor to start the turbine. The motor can be connected to the turbine by a clutch which permits the motor to be brought up to speed and synchronized before the clutch is engaged. The clutch can be designed by the same method as the brake. The clutch design for this turbine will be made of structural steel and will be one inch thick, 42 inches in diameter, weigh 365 pounds, and absorb 5,000,000 foot pounds of energy to start the turbine in 12 seconds at rated torque.

The clutch is a spring loaded hydraulically released mechanism that requires hydraulic pressure only while starting the turbine.

The transmission will have a speed change ratio of 96 to 1 for an 1800 rpm generator and a turbine speed of 18.75 rpm. For a selected Philadelphia Gear Corporation transmission, the transmission will be 4.5 feet high, 7 feet wide, 10.5 feet long, and weigh 23 tons. This transmission is a three stage, right angle bevel gear design, which permits the transmission, the clutch, and the motor to be mounted on the same concrete foundation.

CONTROL ALGORITHM INVESTIGATIONS

Gerald M. McNerney

Introduction

A computer model has been developed using real data to simulate automatic control of the 17-m vertical axis wind turbine (VAWT). The purpose of this model is to find the best algorithm to be used for starting and stopping a turbine operating on computer-based automatic control. Although this model is still in the early stages of development and the results are preliminary, some trends are clear and should be of interest to anyone building a production wind turbine.

Computer Model

The computer model which simulates the 17-m VAWT in automatic control is based on two sources of experimental data collected at the DOE/Sandia VAWT site. The first data source is a set of electric power versus windspeed data collected from the 17-m turbine induction motor at 50.6 rpm. Electric power data are used since they are the quantity of interest in energy production. A plot of the power versus windspeed data used is given in Fig. 1.

The second source of data used is a collection of 890 hours of .5 Hz time series data of windspeed over 43 periods during weekends and nights of summer-fall 1979. The probability density function is plotted versus windspeed for the wind data in Fig. 2. The mean value of the wind data is 11.1 mph which is above the actual Albuquerque mean annual windspeed.

TURBINE POWER FUNCTION

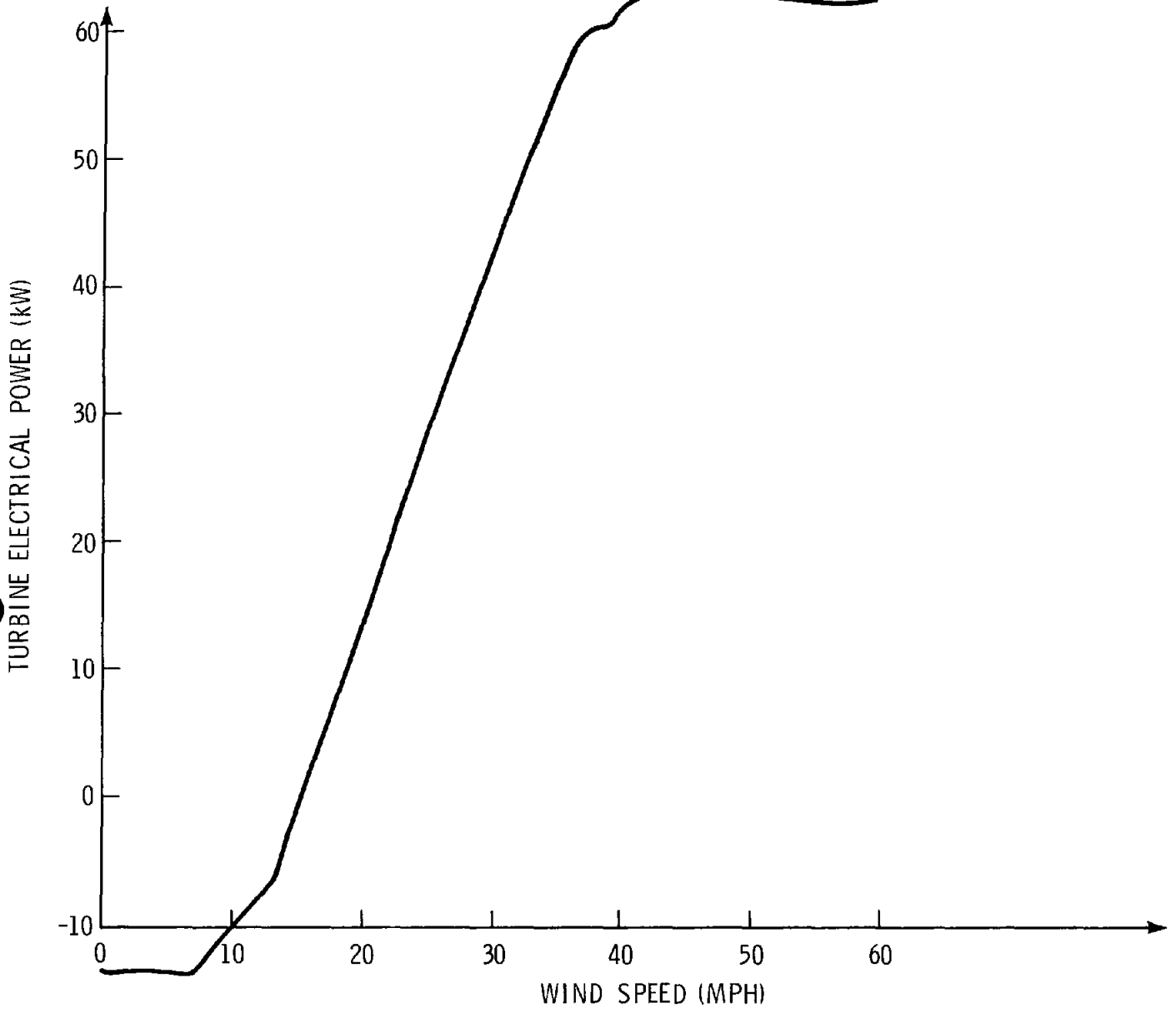


FIGURE 1

WIND TEST RECORD

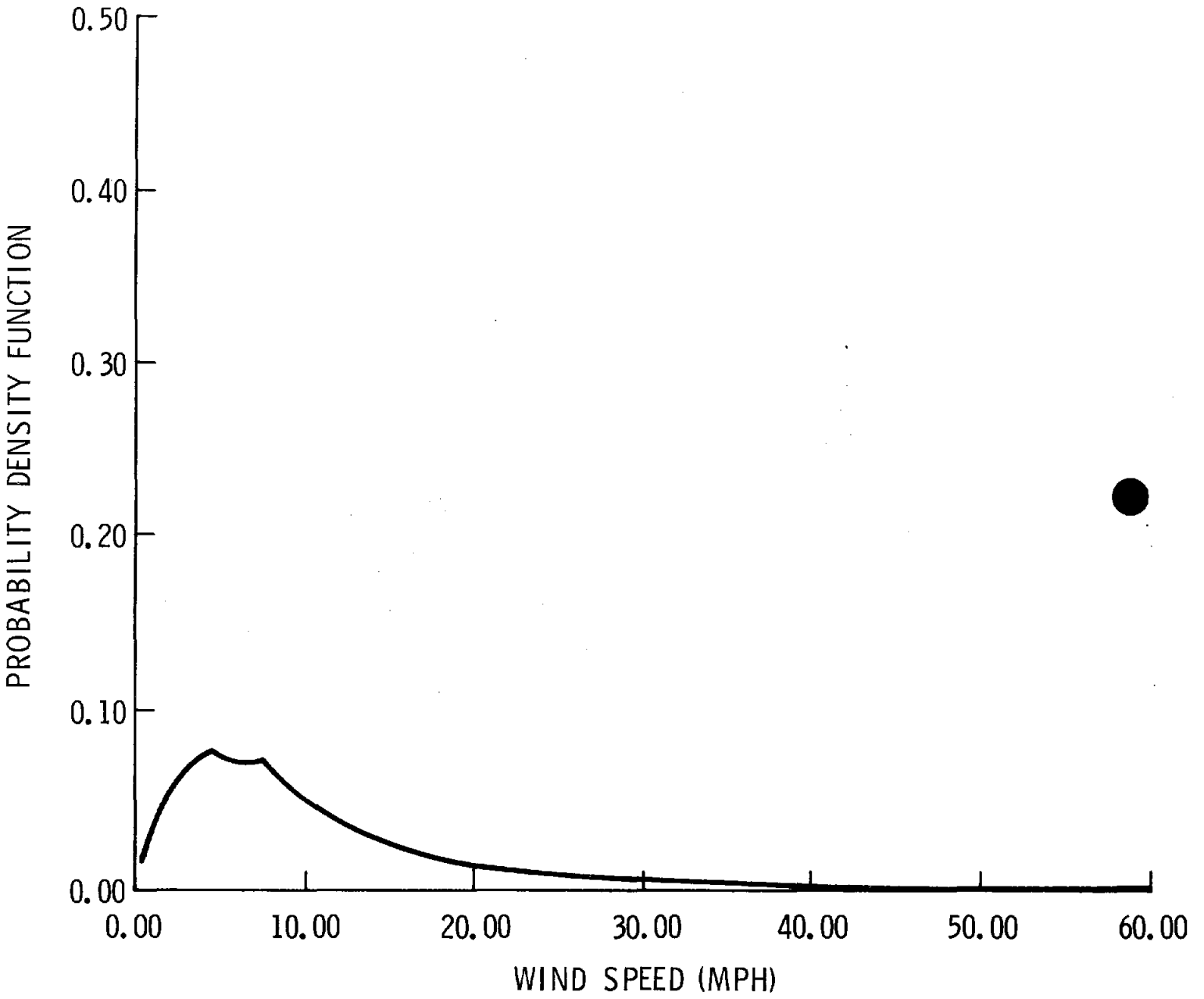


FIGURE 2

The actual computer model is a relatively simple FORTRAN program in which the electric power data are used to determine the power produced at every point of wind data, and the power produced is in turn integrated over the turbine "on" time to give energy generated.

The overall energy output that would be computed for a fixed set of power data depends on windspeed, turbine "on" time, and the number of starts. The number of starts is used by subtracting the number of starts multiplied by the energy consumed per start from the energy produced. The energy consumed per start has been measured to be approximately .6 kW-hr for the 17-m turbine.

The energy available is defined as the amount of energy that would be produced by the 17-m turbine at 50.6 rpm operating under an ideal algorithm, and is computed from the electric power data by integrating the power produced at every point of wind data over all time that the power is positive. The algorithm efficiency is then defined as the percent the energy produced is of the energy available.

Algorithm Types

Five different algorithms have been tested in parametric studies by the automatic control simulator. The first four algorithms have two parameters which are to be adjusted to find the optimal operating values. The two parameters are (1) the turn on threshold which is the minimum value required of average windspeed or average power before the turbine will be started, and (2) the test length which is the duration of the test period after which the turn on threshold is to be tested.

The five algorithms may be described as follows:

1. Discrete windspeed averages - At the end of each test length, the measured average is tested against the threshold. If the test fails, a new test is begun. If the test passes, the turbine is started. During turbine operation, the non-continuous averages are continued for turbine stop control. When the measured average is below the stop threshold, the turbine is stopped.

2. Moving windspeed averages - A new average is calculated over the test length if the turbine is on or off after every point of windspeed data. The computed average is then tested against the start threshold for a turbine start if the turbine is off or the stop threshold for a turbine stop if the turbine is on. After a start or stop, a 60 second blind period is introduced to simulate an actual start or stop.

3. Moving power averages - At each sample point of windspeed, a value of energy that would be produced by a running turbine during the sample interval is calculated using the electric power data. From this, a moving power average is computed and tested against the start threshold if the turbine is off or the stop threshold if the turbine is on, and the turbine is started or stopped accordingly.

4. Discrete, double power test - At the end of each test length, two power averages are calculated. One for the average over the entire test length, and second, for the last one-tenth of the test length. Both averages must be greater than the threshold value for a start to occur. Stops are based on a test of the average power over the entire test length.

5. Canadian coast algorithm - Certain Canadian VAWT systems have utilized a semi-mechanical control system with an overrunning clutch on the high speed shaft to permit the rotor to coast when below synchronous speed. This system could

conceivably reduce motoring losses in low wind conditions and simplifies the turn-off condition which can be based on a simple measurement of rotor rpm.

From a cold stop, one of the first four algorithms is used to decide if a start should be initiated by a starting motor which takes the turbine to some fraction of the synchronous rpm. The turbine is then allowed to coast until either synchronous speed is reached, at which time the generator engages, or 5 minutes has elapsed and the turbine rpm falls below a threshold value at which time the turbine is stopped. If synchronization is reached, when the torque at the high speed shaft becomes negative, the generator disengages and the turbine is allowed to coast until synchronization is attained or the threshold rpm is reached. Whenever the rotor is coasting, the system generator is assumed to motor without shaft load at synchronous speed. Windage losses in the generator are accumulated during the coast period.

Results and Conclusions

The results of the parametric computer runs are plotted in Figs. 3 through 7, and a synthesis of the results is plotted in Fig. 8. It is clear from the plots that for the first four algorithms, a best choice of test length and start threshold may be chosen to maximize the algorithm efficiency with the fewest number of starts. It is also clear that a bad choice of test length can greatly reduce the algorithm efficiency. It is possible that the optimized parameters will be somewhat site dependent.

The most efficient algorithm was found to be the Canadian coast algorithm with 93.7% efficiency with a stop threshold of 45 rpm while using the moving power algorithm with start threshold of 4 kilowatts and test length of 240 seconds for the cold

starts. The moving power algorithm was close to the Canadian coast algorithm with a maximum efficiency of 93.4% using a start threshold of 5 kilowatts, a stop threshold of zero kilowatts, and a test length of 360 seconds.

The least efficient algorithm was found to be the moving windspeed algorithm particularly at test lengths shorter than 240 seconds.

ALGORITHM #1 - DISCRETE WINDSPEED AVERAGES

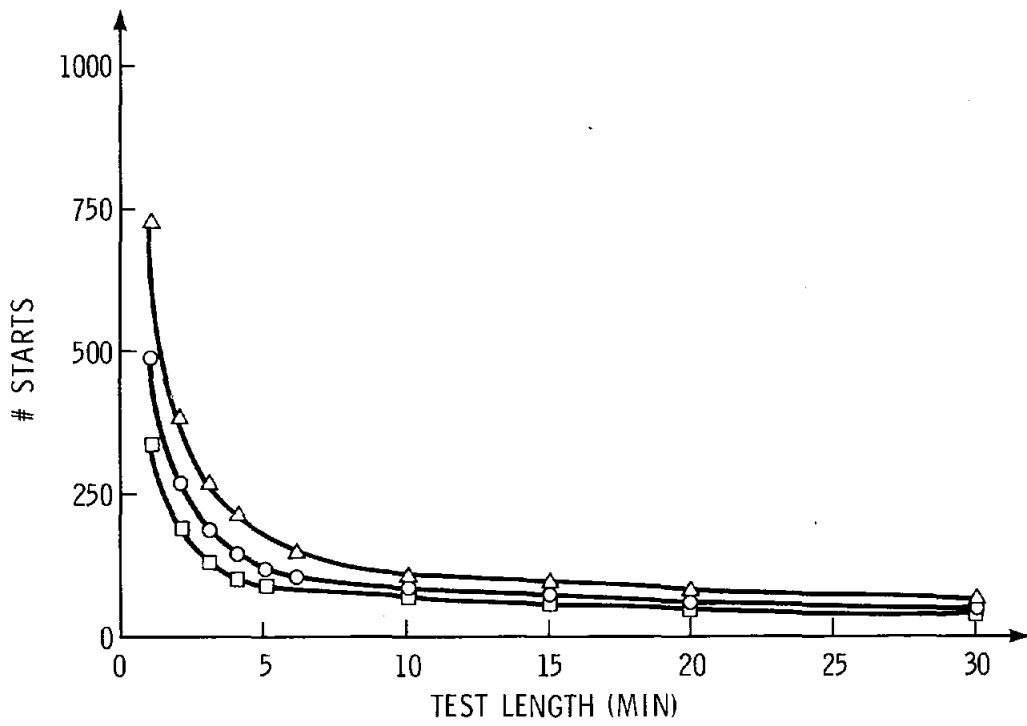
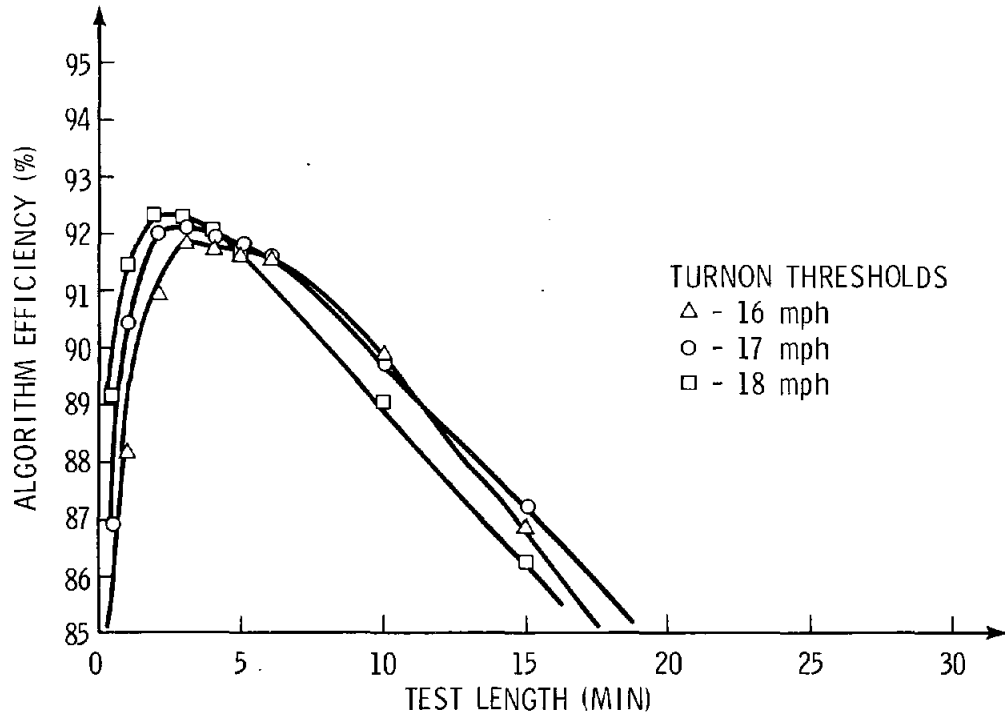


FIGURE 3

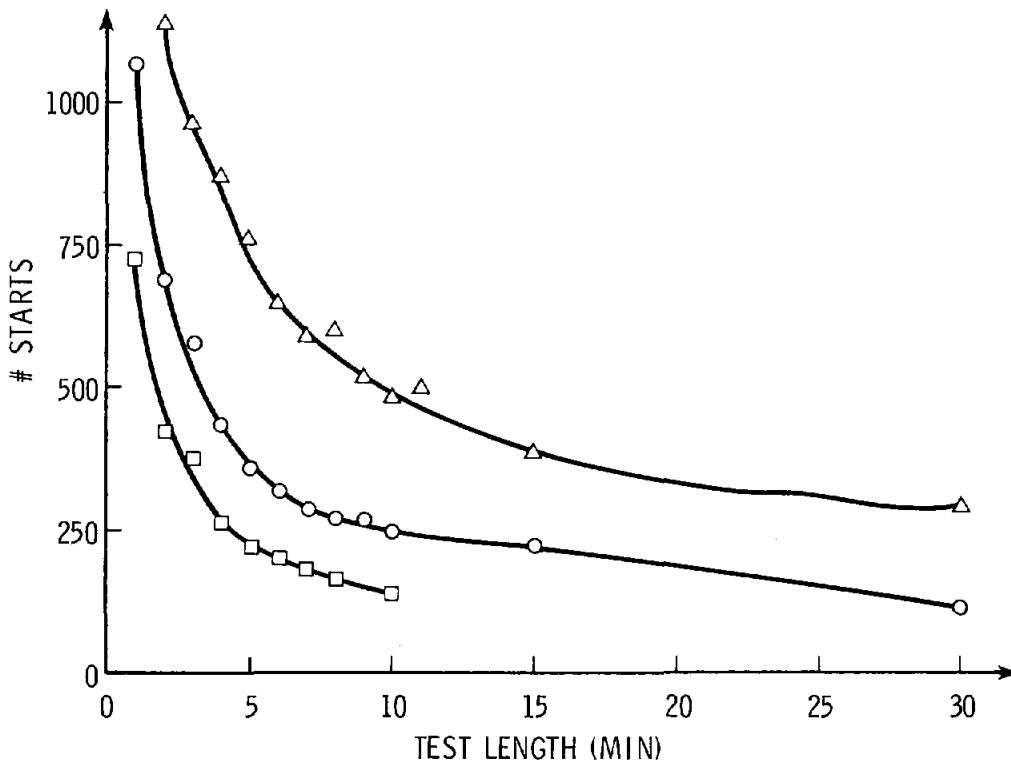
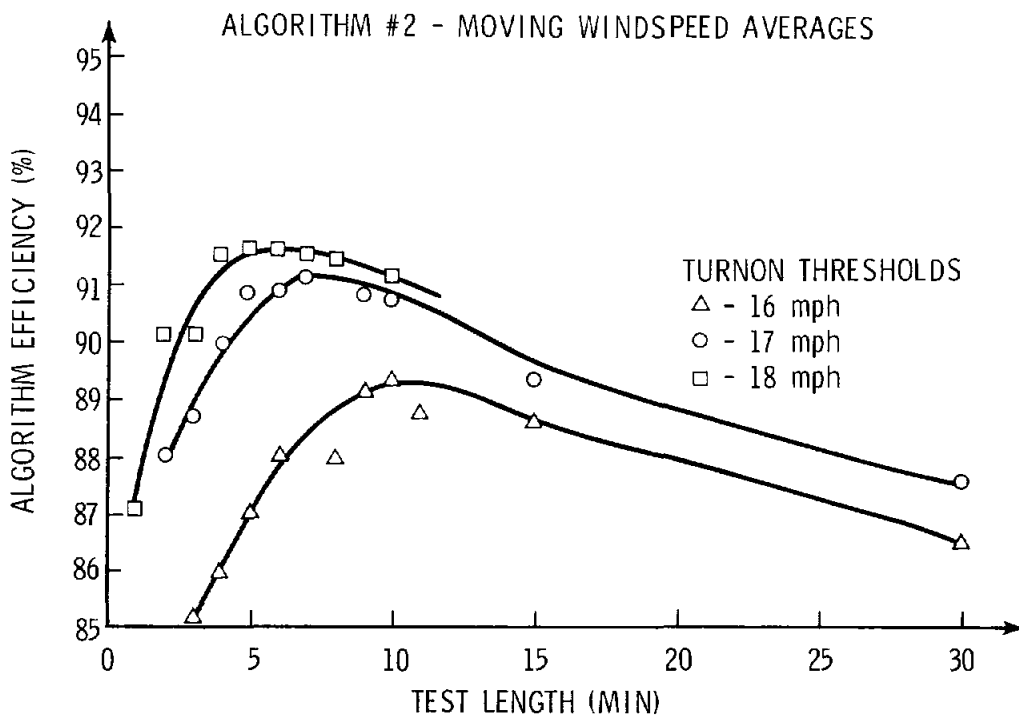


FIGURE 4

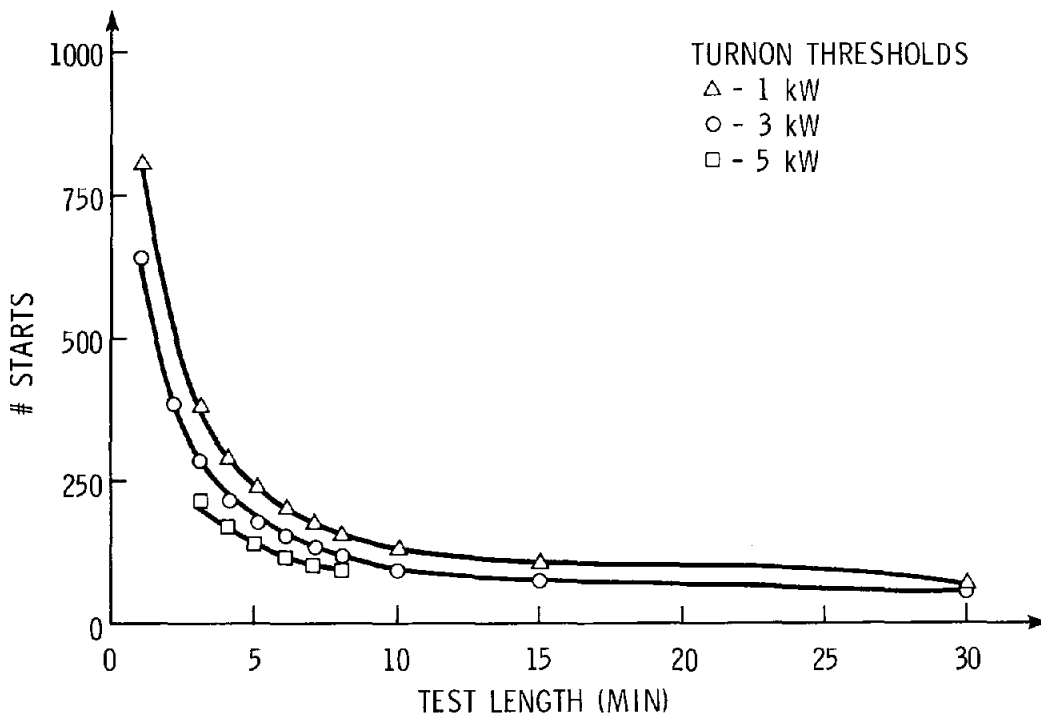
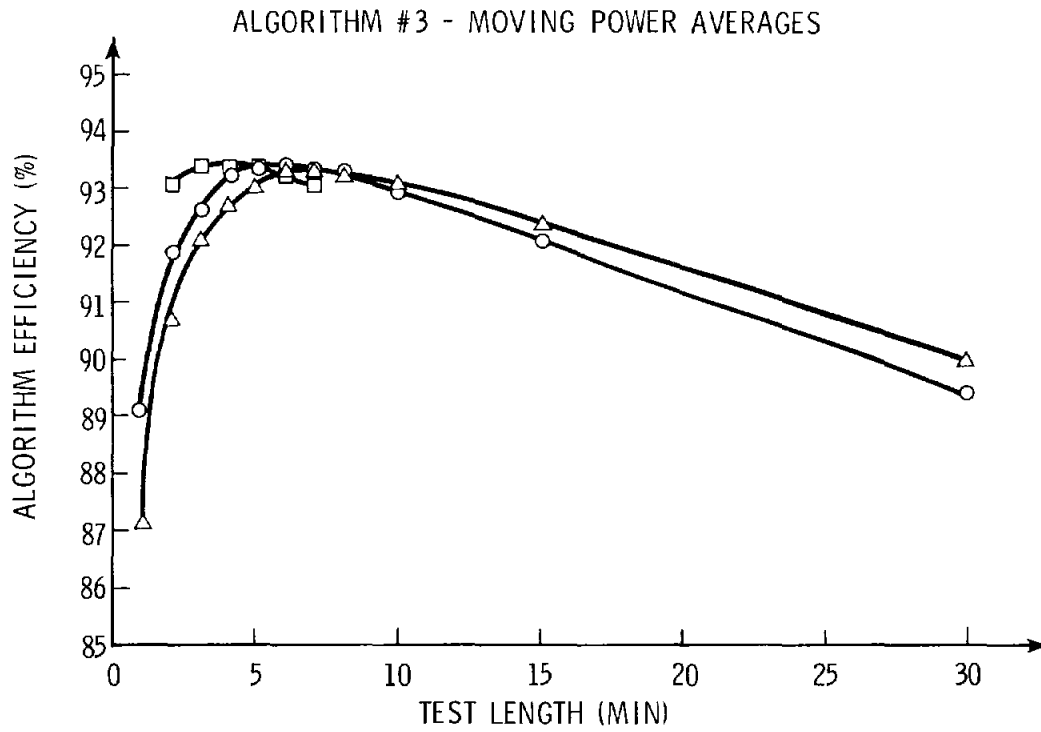


FIGURE 5

ALGORITHM #4 - DISCRETE, DOUBLE POWER TEST

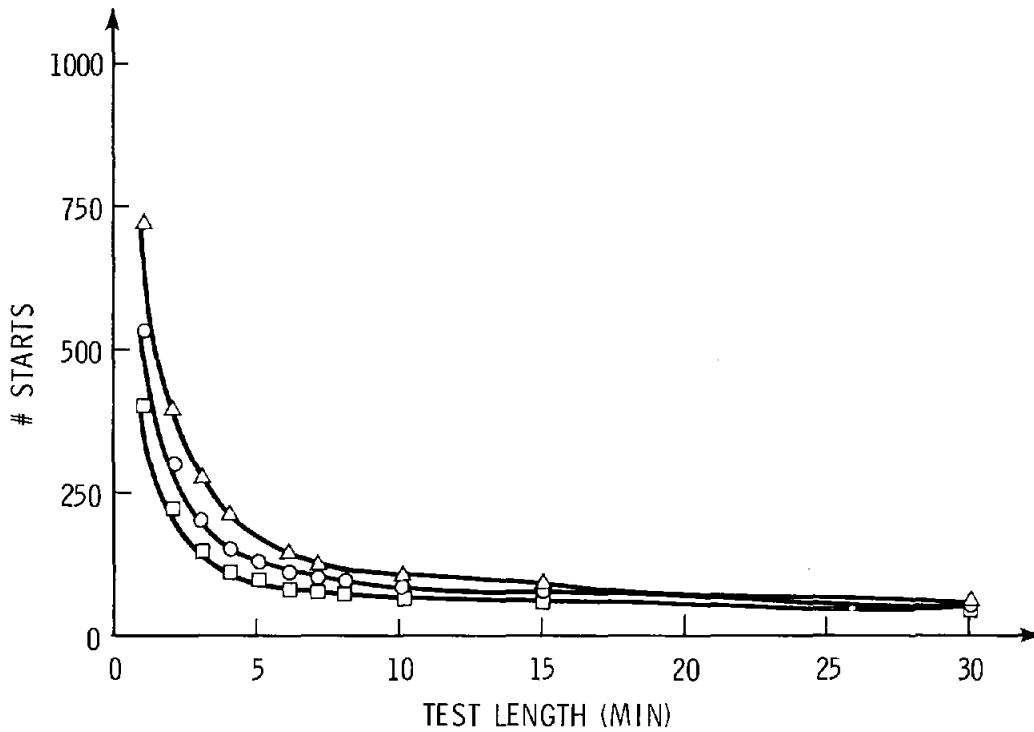
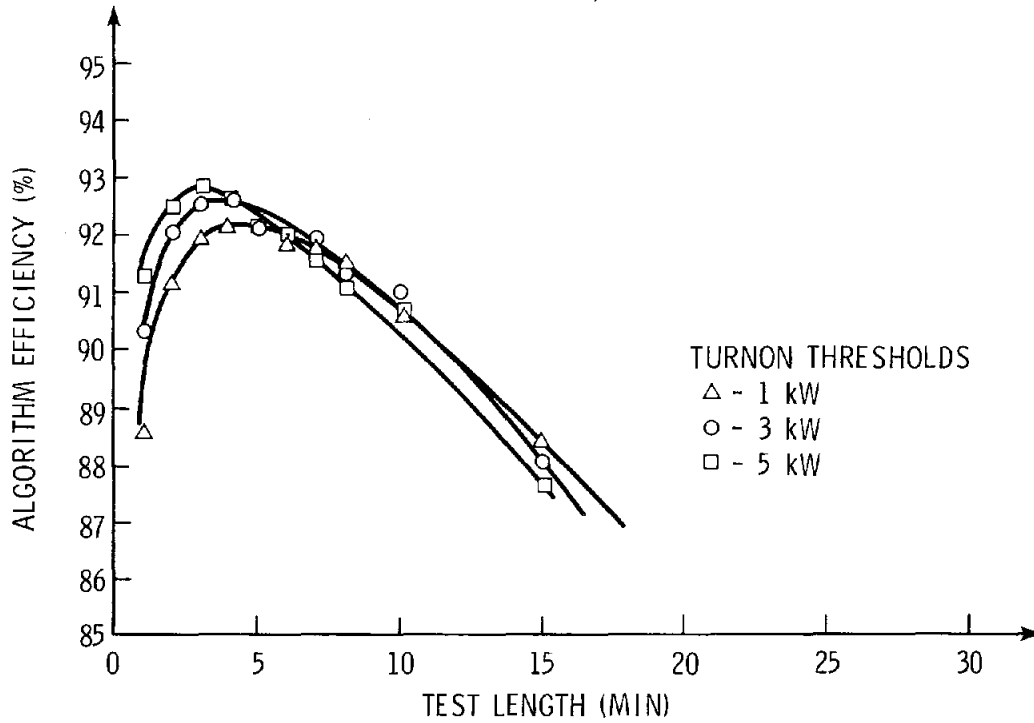


FIGURE 6

CANADIAN COAST ALGORITHM

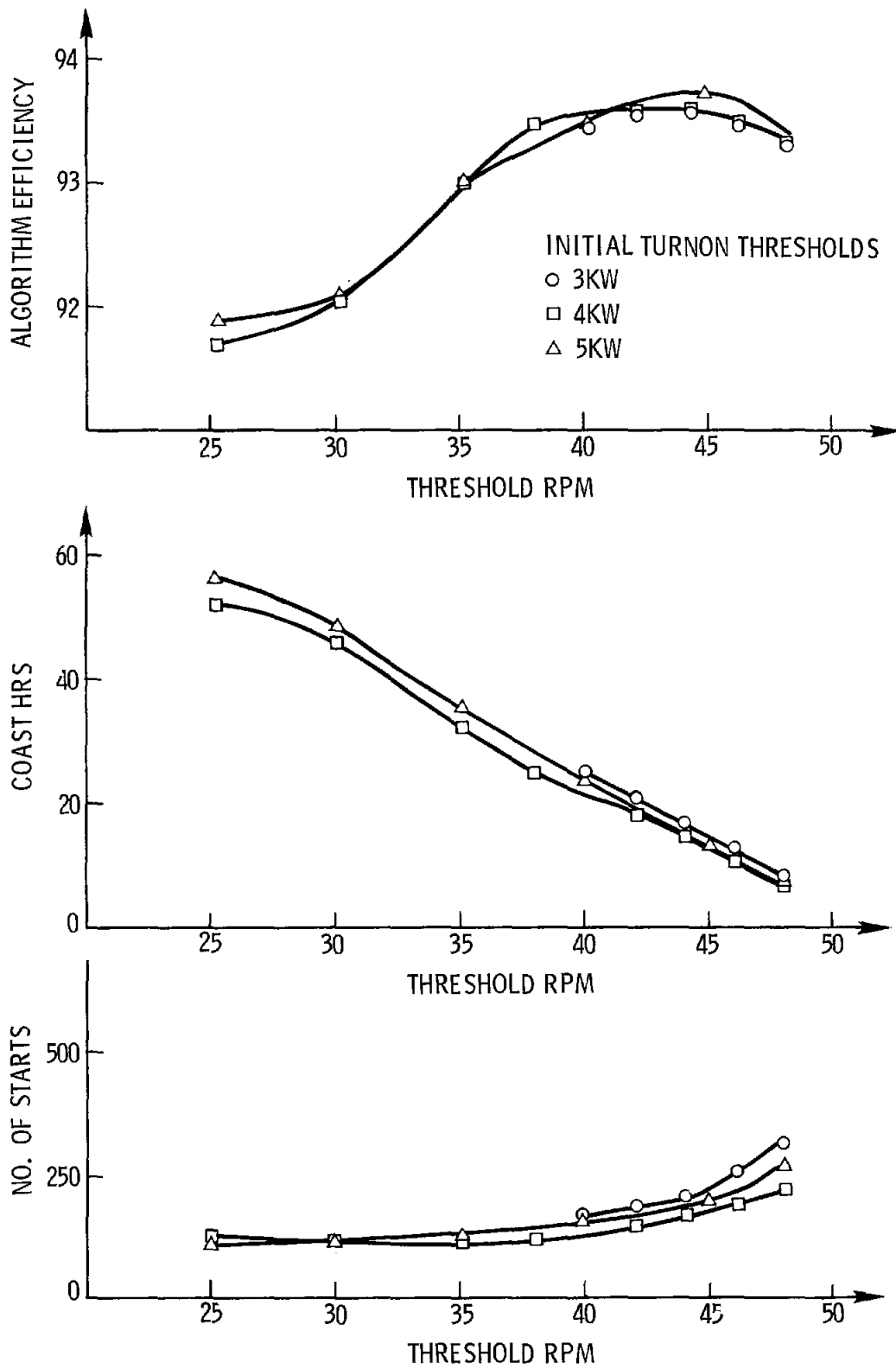


FIGURE 7

COMPARISON OF THE BEST CURVES
OF THE FIVE ALGORITHMS

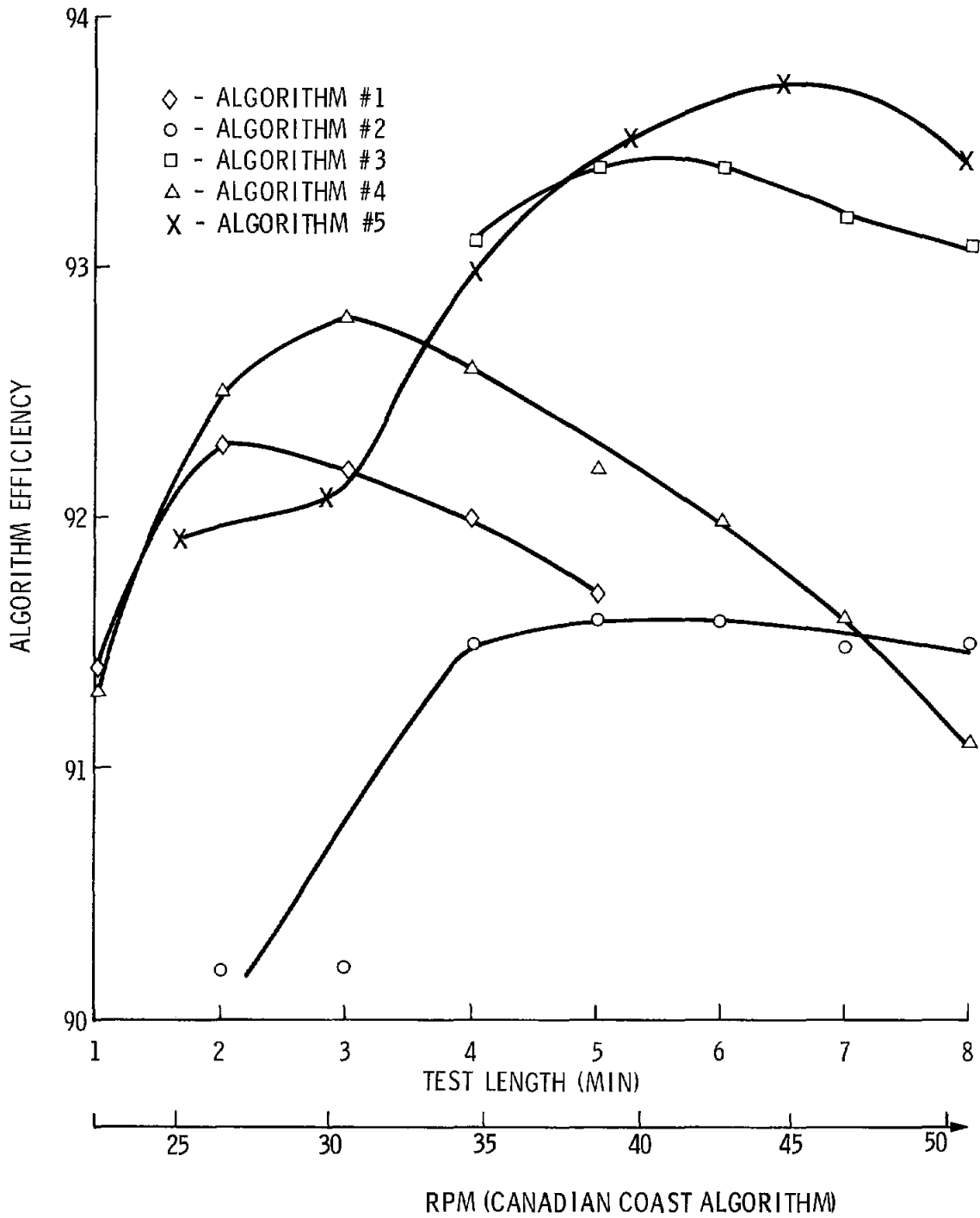


FIGURE 8

SECTION III
STRUCTURAL DESIGN OF VAWT SYSTEMS

OVERVIEW OF AVAILABLE TECHNIQUES FOR VAWT STRUCTURAL DESIGN ANALYSES

William N. Sullivan

The general problems facing the structural designer of a VAWT are fairly easy to state. The first problem is to assess the steady and vibratory stress levels throughout the system during normal, daily operations of the device. Through this assessment, the fatigue life of the proposed design may be established. The second problem involves establishing the survivability of the structure in unusually high winds or for special cases when the rotor is accidentally operated beyond its normal design envelope. A third problem is related to the first two -- the design tools should be flexible and accurate enough to permit an iterative approach toward an "optimized" (minimum cost) structure.

While the general design problems are easy to state, the solutions are much more complex. An "exact" solution to wind turbine structural design would require a coupled analysis including complete analytical understanding of rotating system structural dynamics, aeroelastic effects, aerodynamic load modeling, and meteorological statistics. The actual status of VAWT structural modeling is in an evolutionary state and falls short of completely representing all the aforementioned phenomena. Nonetheless, a set of approximate structural design procedures have been applied at Sandia for systems which have yielded excellent structural performance in the field. This paper will briefly summarize the current design procedures and discuss future plans for expanding and improving the analysis base.

The attempt to develop realistic design tools has been conducted in parallel with experimental measurements on actual VAWT systems. The primary source of these data is the DOE/Sandia 17 meter research turbine located in Albuquerque. Experimental data have provided an important basis for confirming and redirecting analyses. Throughout this seminar, discussion of specific structural analyses will refer to measurements made on the 17 meter rotor.

Basic Design Approach

With an admitted oversimplification of what is actually a varied set of design approaches, the current VAWT design practice follows a two-step procedure:

- (1) Establish the quasi-static stresses and deflections in a component subjected to the expected peak load. Mechanical design iterations follow if necessary to achieve statically acceptable stress and/or deflection levels.
- (2) Determine the resonant frequencies and possible dynamic instabilities of the statically-acceptable structure. Perturb the design if necessary to avoid dynamic amplifications in the response.

Note that in this procedure, design to static loads dominates the process, with dynamic considerations adjusted by design perturbations. This procedure has functioned adequately in the past because current generation VAWT systems have been designed to conservative static requirements. Also, the VAWT rotor tends to be a relatively stiff* system (lowest resonant frequencies above 3P), which enhances the validity of static analysis.

*This stiffness is a consequence of the relatively high solidity and low rpm of the rotor and the use of cable-supported (rather than cantilevered) towers.

The above process has the advantage of simplicity but it tends to encourage conservatism in establishing static performance levels. This is to protect from unaccounted-for dynamic stress amplifications which may occur in the structure. Considerable judgement and experience are required with the quasi-static approach to decide which resonances may be excited and, if so, how far the frequencies should be moved to avoid excessive excitation. The net effect of these shortcomings in the quasi-static approach will become more pronounced in next-generation VAWT hardware which should be designed less conservatively without significantly increasing the risk of structural failures. In anticipation of this trend, recent efforts at Sandia have emphasized the development of more comprehensive structural-dynamic design tools. These developmental tools are mentioned below along with the established tools used in the past and which will probably continue to be used in the future in conjunction with the more advanced developmental tools.

Specific Design Problems and Tools Utilized

This brief summary will list specific structural problems and indicate the tools used to solve these problems. Those tools which are in a developmental phase are indicated with an asterisk. In some cases, accompanying figures are indicated with example applications of design tools.

<u>Problems</u>	<u>Tools</u>
Quasi-static response of rotor blade to combined aerodynamic, centrifugal, and gravitational loads during operation; parked rotor survival in high winds	Non-linear finite element models (MARC); Figs. 1 and 2

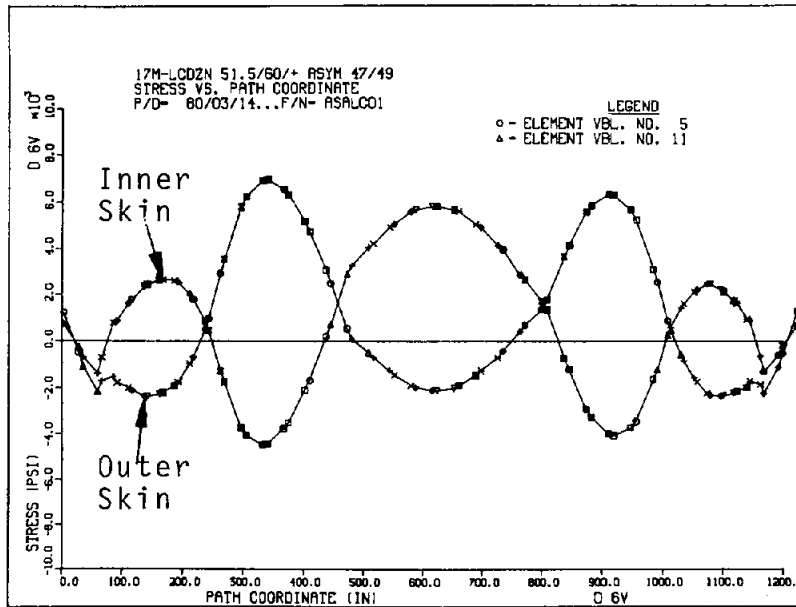


FIGURE 1. Flatwise Stress Distribution in the Alcoa Low-Cost 17-m Blade at 51.5 rpm in 60 mph Maximum Flatwise Load Which Occurs During Rotor Rotation

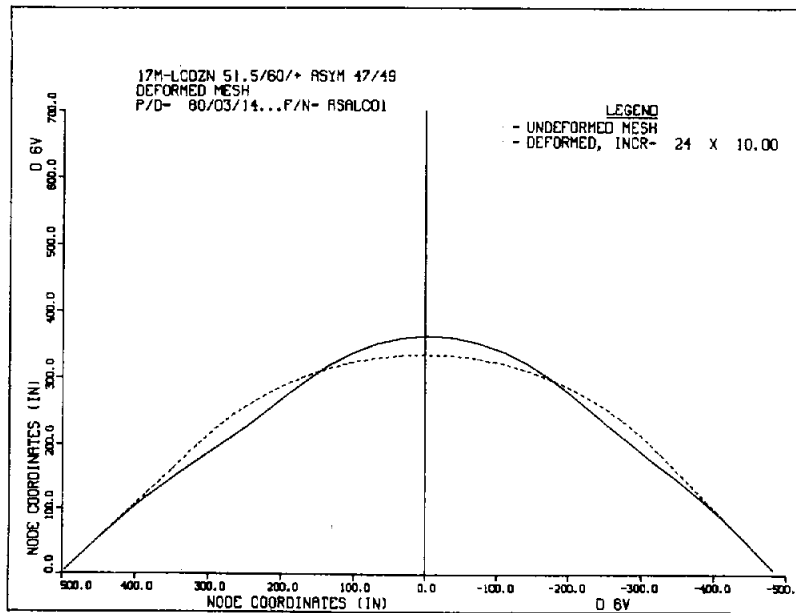


FIGURE 2. Deformed Mesh (10 x) for the Stress Distribution Shown in Fig. 1

Problems

Assessment of aerodynamic blade loads during operation

Determination of blade shape to minimize steady centrifugal and gravitational stresses

Tower buckling and bending response to axial and transverse loads

Attenuation of drive train torque ripple

Determination of system resonant frequencies and mode shapes

Forced system dynamic response, including rotating coordinate system effects

Determination of suitable tiedown cable design parameters

Avoidance of blade aeroelastic instabilities

Tools

Single streamtube aerodynamic model (FORCE), multiple streamtube^{*}, and vortex models^{*}; Fig. 3

Numerical determination of Troposkien curve (TROP); Fig. 4

Simple beam/column theory

Lumped mass dynamic response model

Finite element methods (SAP IV, NASTRAN^{*}, Hibbett and Karlsson^{*}); Fig. 5

Lumped mass models (VAWTDYN^{*}), finite element methods (NASTRAN)

Closed form solutions for cable response; experimental methods

Approximate methods to predict critical flutter speeds (Ham analysis); dimensional scaling from field test data^{*}; Hibbett and Karlsson finite element methods^{*}

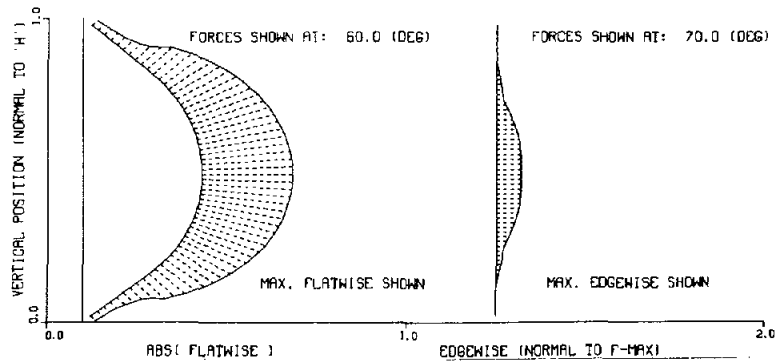


FIGURE 3. Flatwise and Edgewise Force Distributions Supplied by the Single Streamtube Model. The Blade Angle for these Distributions is the Azimuthal Angle Relative to the Ambient Wind Vector.

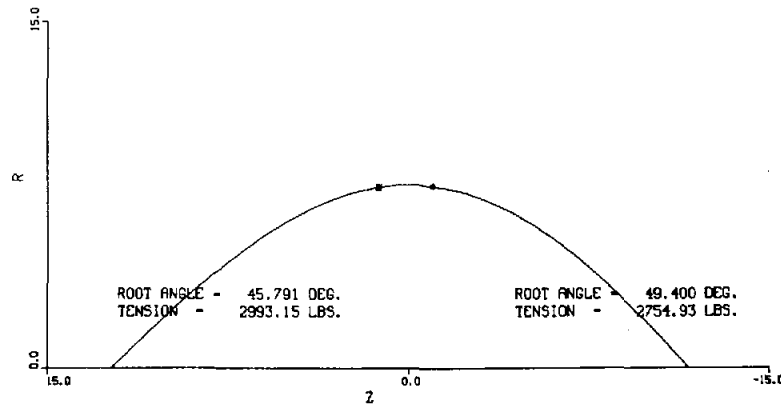


FIGURE 4. Troposkien (Spinning Rope) Shape for a 17-m Rotor Operating at Approximately 40 rpm. Gravity (Directed Left to Right) Distorts the Left-to-Right Symmetry of the Troposkien

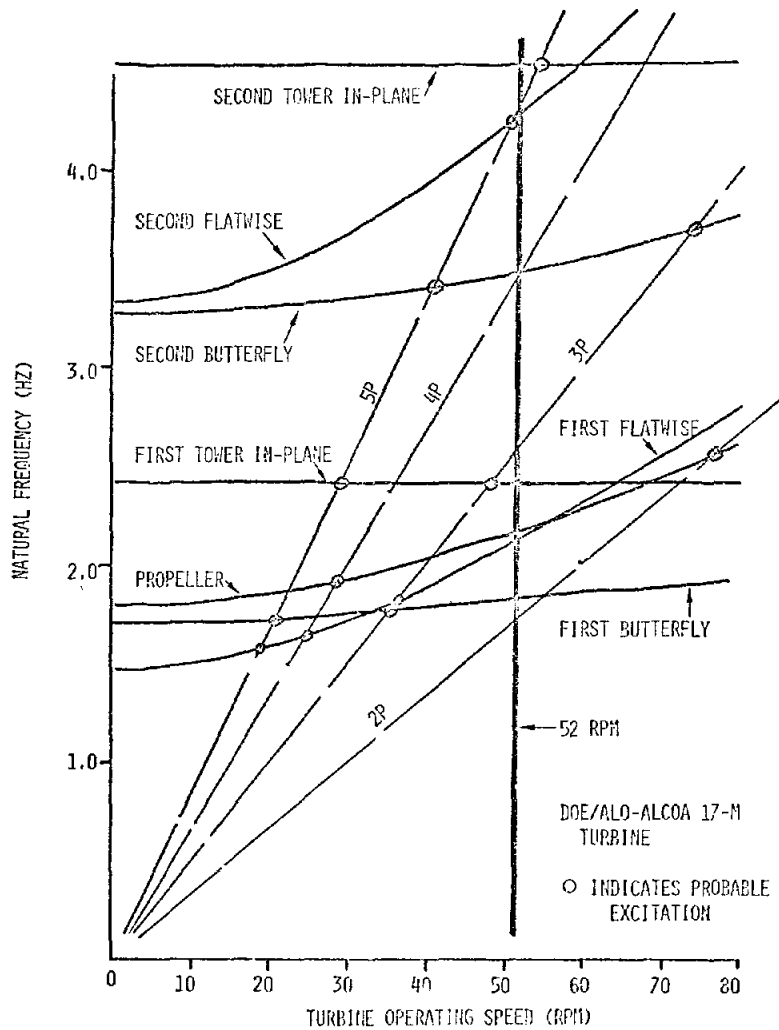


FIGURE 5. SAP IV Finite Element Predictions of Resonant Frequencies for the Low-Cost 17-m Rotor

The remaining talks in this session will address these design tools in more detail with examples of specific applications.

Concluding Remarks

The current status of VAWT structural analysis methods have been described as workable but immature. The workability is reflected by the fact that analysis tools exist to address all the known major VAWT structural design issues. And, these tools have been used to design structurally acceptable VAWT systems. The immaturity is reflected by the uncertain effects of the approximations built into the design tools which could lead to unforeseen structural problems in future systems. Because of this acknowledged immaturity in the design process, the programmatic efforts at Sandia will continue to emphasize a combined effort in prototype testing, structural measurements, and improved structural modeling techniques.

STATIC BLADE ANALYSIS OF THE DOE/ALCOA
LOW-COST 17 METER TURBINE

William N. Sullivan

Introduction

The DOE/Alcoa low-cost 17-m turbine is a new system designed and constructed by Alcoa under a DOE/Sandia contract. The hardware for this new machine is now being fabricated and the first unit is scheduled for installation at Rocky Flats this summer.

While the basic design of the low-cost 17-m was the responsibility of Alcoa, Sandia did conduct certain structural analyses of the blades on a consulting basis. In the interest of demonstrating the application of our static design tools, this paper will discuss the static blade analysis and the design changes which occurred as a result of this analysis.

The results presented here do not represent all of the structural analysis performed on the low-cost 17-m rotor. The complete effort, performed primarily by Alcoa, includes resonant frequency calculations and detailed analysis of all other critical structural components.

Structural Performance Goals

There were three performance goals that guided the blade static analysis:

- (1) Vibratory blade stresses below 6000 psi and peak stresses below 12,000 psi at a normal operating condition defined as 50 rpm in 60 mph winds.

- (2) Peak blade stresses below yield (approximately 25 ksi for the blade material) at an accidental overspeed condition of 75 rpm in 80 mph winds.
- (3) Peak blade stresses below yield in the upwind blade while parked (chordline normal) in a 150 mph wind.

In evaluating a blade design statically, only certain extreme aerodynamic conditions which occur as the blade rotates need be considered. The first of these is referred to as the C+A condition and corresponds to maximum flatwise loading of the downwind blade, where centrifugal and flatwise aerodynamic loads are in the same direction. This condition occurs simultaneously with maximum edgewise loading. The minimum flatwise loading occurs as the blade passes the upwind side and is referred to as the C-A condition since the aerodynamic and centrifugal loads are of opposite sense. The C-A condition also occurs simultaneously with maximum edgewise blade loading. The minimum edgewise load is assumed to be zero and to occur when the blade chord line is oriented either directly upwind or downwind. In calculating static vibratory stresses, flatwise vibratories are computed as half the difference between the C+A and C-A flatwise stress values; edgewise vibratories are computed as half the difference between the C+A edgewise stress and zero. Peak absolute stress values are taken from either the C+A or C-A solutions, whichever have the largest absolute values.

In general, it was found that conditions (1) and (3) dominated the static design. Note that these goals are evidently quite conservative. This degree of conservatism was felt to be appropriate in view of uncertain dynamic load amplifications or stress concentrations which could exist in the actual system.

Design Iterations

There were three major blade design changes effected by Alcoa which were motivated by results of the static analysis.

The first blade design consisted of the geometry shown in Fig. 1. This blade has a height-to-diameter ratio (H/D) of 1.5 and was assumed to be rigidly clamped to the tower. The blade section is the same as that now installed on the Sandia 17-m rotor, a NACA 0015 extrusion with a 24" chord. The initial static analysis of this section, summarized in Table 1, indicated that conditions 1 and 2 could be satisfied. The response of the blade to condition 3 was marginal because the flatwise blade stresses at the upper blade/tower clamp are about 27,000 psi (Fig. 2). Aside from this shortcoming in the first design, Alcoa found that the mechanical design of a truly rigid clamp at the blade ends was difficult due to the large flatwise and edgewise bending moments involved.

These difficulties led to a new blade/tower attachment scheme proposed by Alcoa. This consisted of a small, triangulated structure where the blade joins the tower. This is referred to as the "mini-strut" design (Fig. 3). The mini-strut was initially modeled for stress analysis as simply a zero blade displacement boundary condition where the blade and mini-strut intersect. Subsequent detailed modeling of the actual strut indicated that the boundary condition model was quite reasonable. The overall effect on blade performance is shown in Figs. 4 and 5. The mini-strut slightly reduced the flatwise and edgewise vibratory stresses and also reduced the peak blade stress in the 150 mph wind condition.

The final design perturbation was motivated by Alcoa's observation that gravity loads could conceivably produce significant peak tensile stresses in the lower mini-strut welds (Fig. 3). Because of the mechanical properties of the weld, a

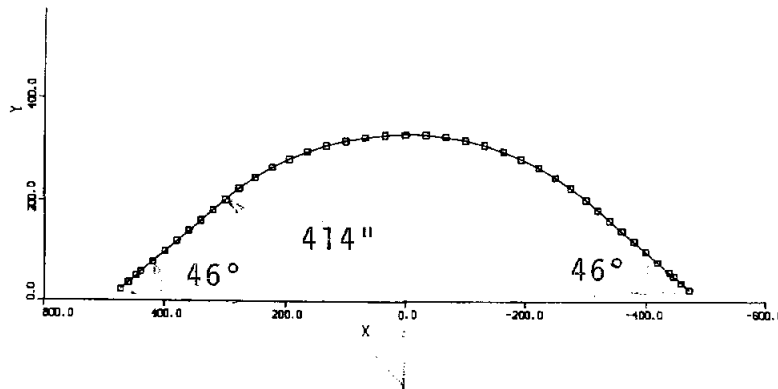


FIGURE 1. Initial Geometry and Finite Element Model of the Low-Cost 17-m Blade. Blade is Assumed to be Rigidly Clamped to the Tower

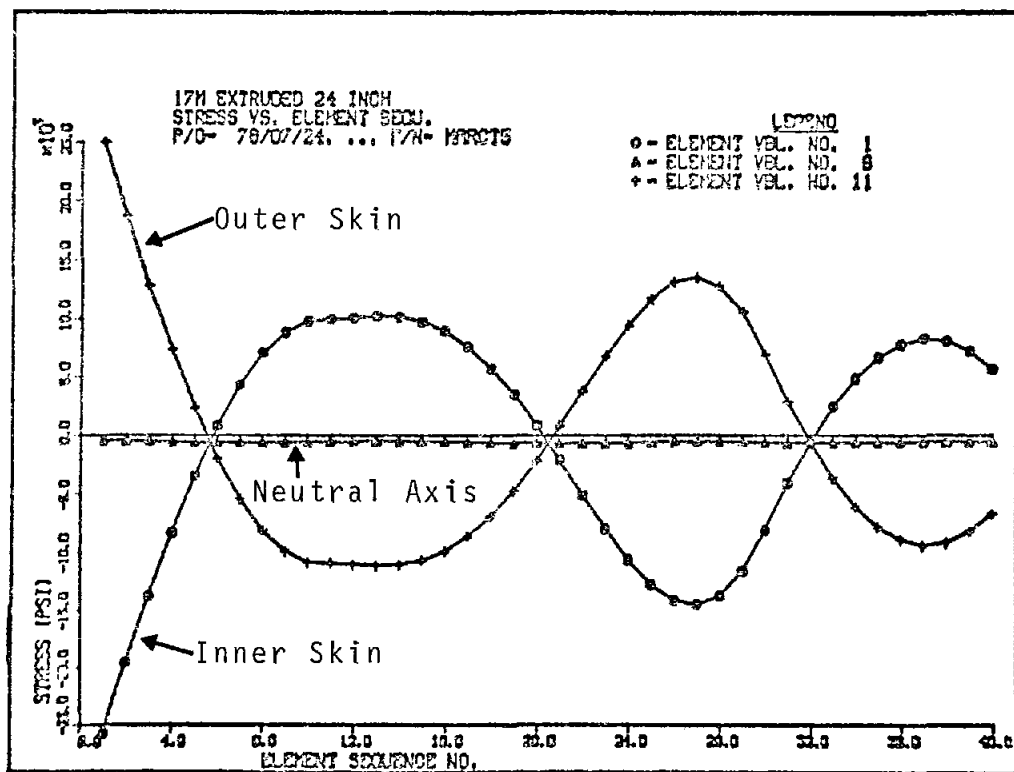


FIGURE 2. Response of the Early Blade Design to the 150 mph Wind. Stresses from Left to Right Run From the Upper to Lower Clamp, Respectively

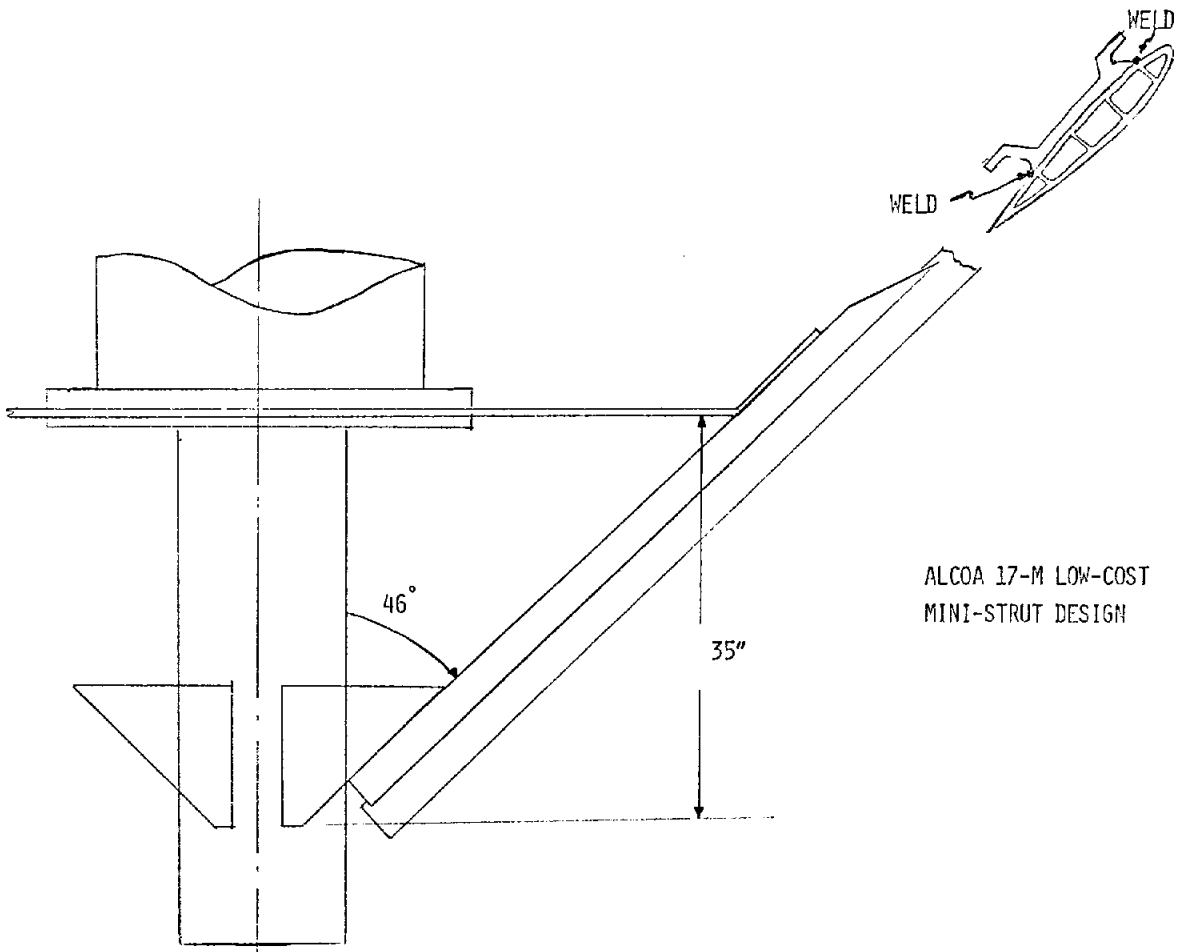


FIGURE 3. Mini-Strut Blade Clamp Designed by Alcoa

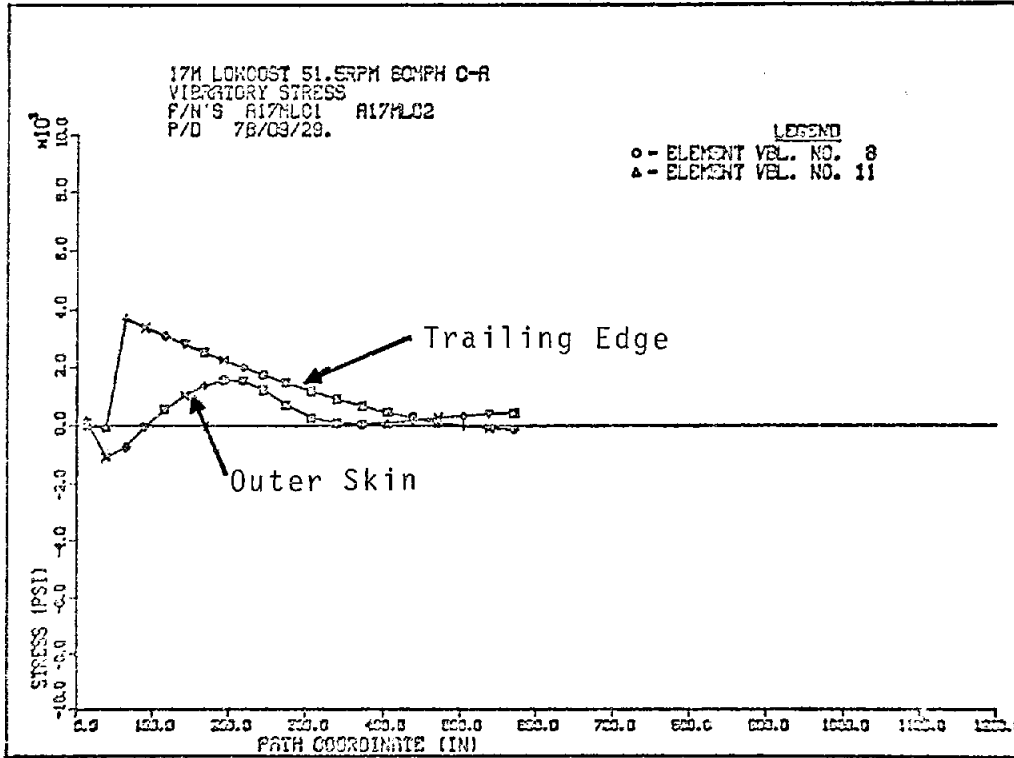


FIGURE 4. Vibratory Stresses for the Mini-Strut Blade Design on Flatwise (Outer Skin) and Edgewise (Trailing Edge) Portions of Blade. Only Upper Half of Blade Shown

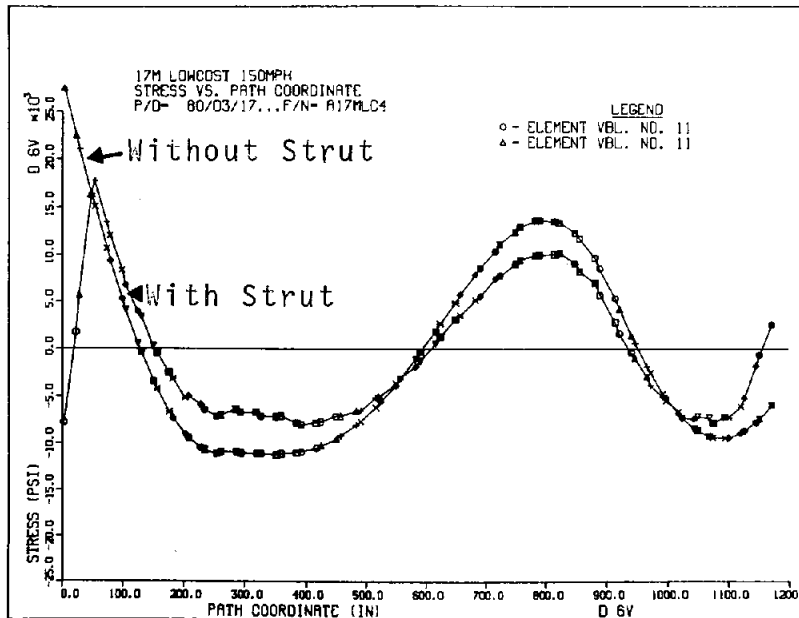


FIGURE 5. Improvement in Hurricane Load Outer Skin Flatwise Stresses Produced by the Mini-Strut

peak tensile stress as low as 6000 psi could conceivably damage the weld or at least reduce its fatigue life. A new finite element model was constructed which included gravity loads (gravity was not included in the analysis of the first two design iterations). The results of this model are shown in Fig. 6 for the C+A peak loading. The gravity loads do indeed lead to relatively high tensile loads in the vicinity of the lower strut welds.

A simple solution to this problem was found by changing the angle the blade root makes with the tower to more closely approximate the angle that would be assumed by the blade if it were freely pinned in the flatwise direction. This new geometry is shown in Fig. 7. The asymmetry in the geometry is due to gravity loads. The actual flatwise peak stresses in this new and final geometry are shown in Fig. 8, indicating a significant reduction in the peak tensile weld stresses. Figure 9 shows the response of the final design to the hurricane load condition.

Concluding Remarks

The final design of the low-cost 17-m blade has exceeded the structural performance goals set forth at the start of the contract.

The low-cost 17-m blade design is not a radical departure from earlier designs but is nonetheless innovative structurally. The mini-strut, asymmetric geometry, and H/D of 1.5 are new concepts which have not yet been thoroughly tested in a field installation. The prototype machine will be an important vehicle for monitoring the benefits of the innovations and the legitimacy of the analysis tools used for its design. As a result, the first unit will be instrumented and tested thoroughly.

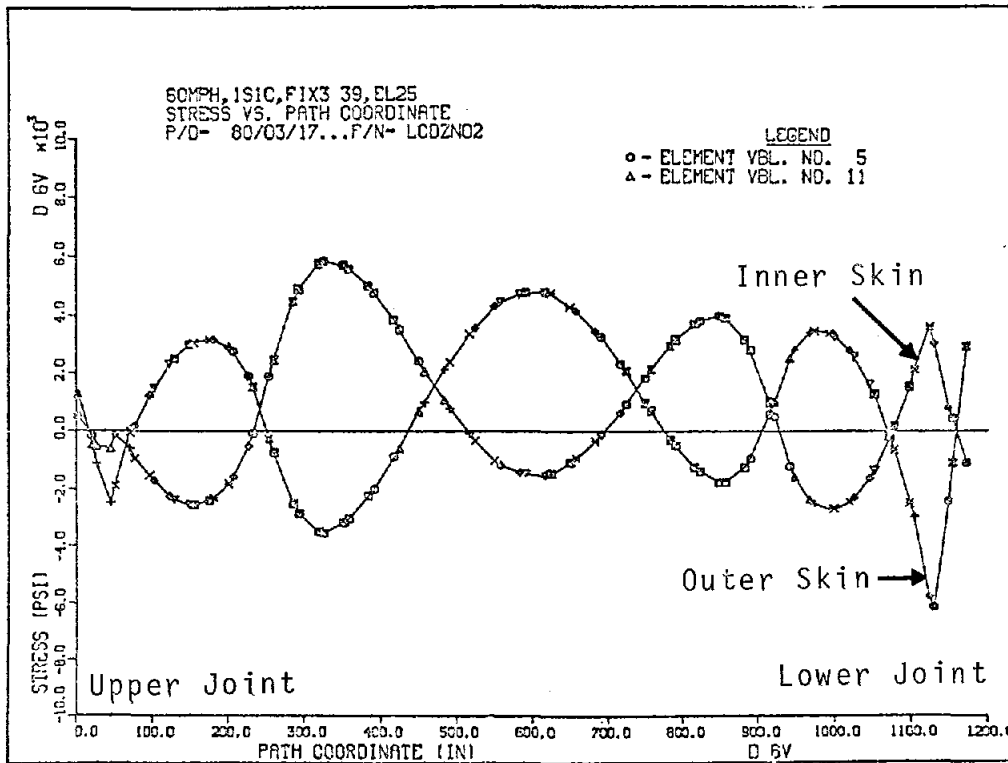


FIGURE 6. Flatwise Stress Distribution for the C+A Design Condition Indicating Relatively High Bending Stresses at the Lower Mini-Strut Attachment Point

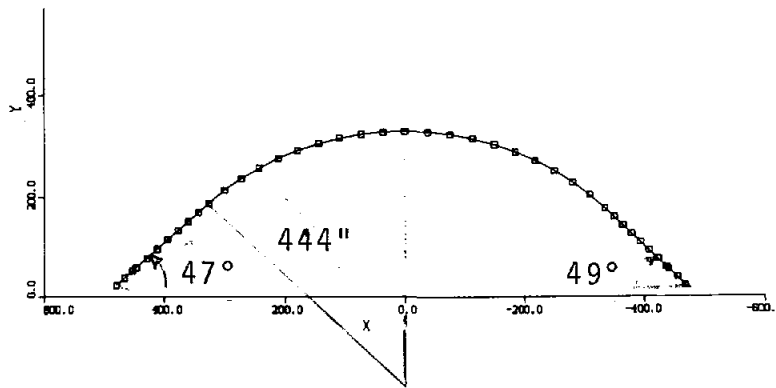


FIGURE 7. Revised Low-Cost 17-m Blade Geometry

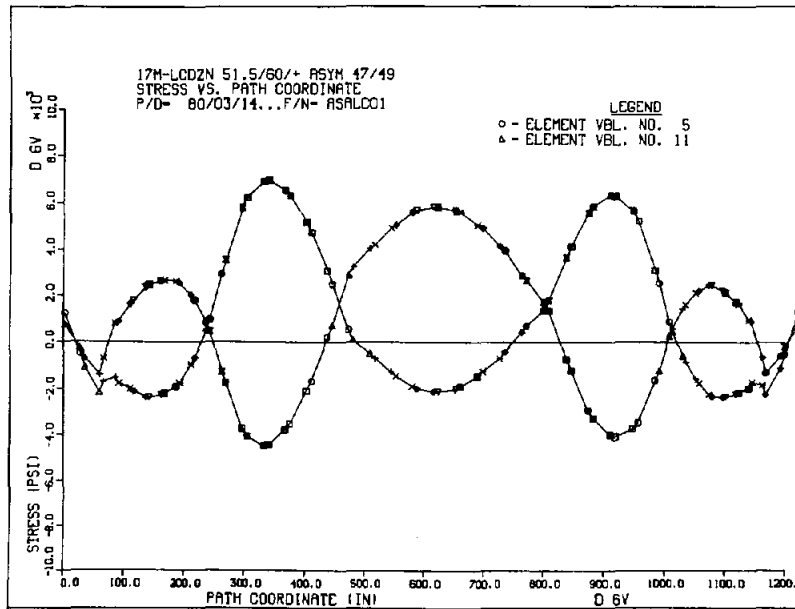


FIGURE 8. Flatwise Stress Distribution with the Revised Geometry Indicating Reduced Tensile Stresses at the Lower Mini-Strut Attachment Point

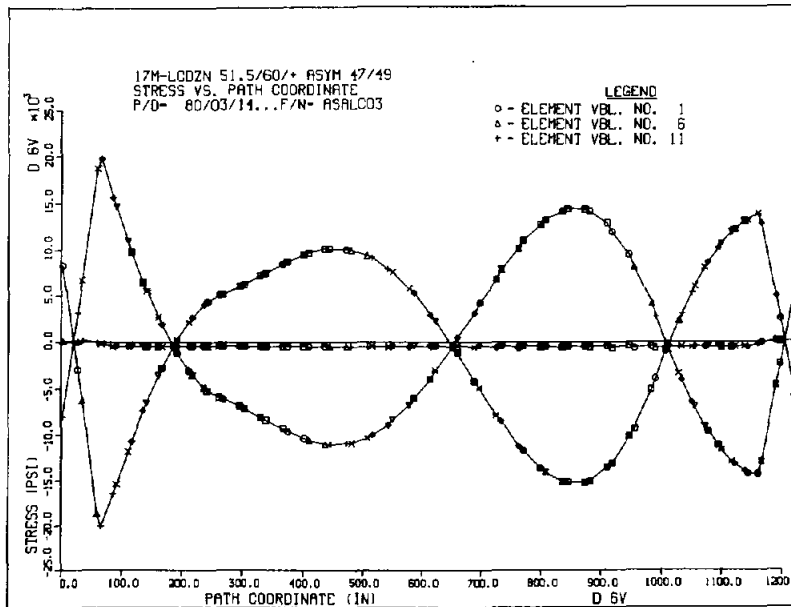


FIGURE 9. Parked Blade Hurricane Load Condition Flatwise Stress Distribution for the Revised Low-Cost Design

These data will be invaluable for identifying over- or under-conservatisms in the design and thereby impact the future of VAWT structural analysis procedures.

VAWT ROTOR STRUCTURAL DYNAMICS ANALYSIS METHODS

D. W. Lobitz

INTRODUCTION

Over the life of the VAWT program at Sandia, dynamic modeling has gone through an evolutionary process. Early on, essentially no dynamic modeling was performed except in accounting for centrifugal loading and time varying wind forces in quasi-static finite element analyses. Dynamic effects were designed out using relatively large factors of safety. Later, a capability was developed to identify natural modes and frequencies of the VAWT using finite element techniques, which accounts for frequency shifts due to centrifugal stiffening in the blades. This capability helped to identify modes which might be heavily excited during turbine operation, and in selecting operational frequencies which preclude excessive dynamic amplifications.

Recently, a transient dynamic analysis package (VAWTDYN) has been developed which includes gyroscopic effects. Using the finite element predictions of the frequencies to establish the stiffness and mass parameters in this model, several additional important dynamic effects have been noted. First, in the rotating turbine, modes which are independent in the stationary system become coupled. Consequently, excitation of any given mode in the rotating turbine can drive, through this "cross talk," other modes which could result in a more critical vibration. Secondly, it was found that, in addition to centrifugal stiffening, the gyroscopic effects also lead to significant frequency shifts. Thus, to get an accurate characterization of the natural frequencies of the rotating system these effects must be included.

More detailed discussions of the finite element modeling for identifying modes and frequencies and the VAWTDYN package for transient dynamics will be presented along with appropriate comparisons to experimental data gathered from the DOE/Sandia 17 m turbine.




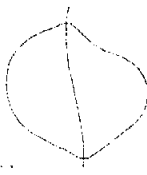

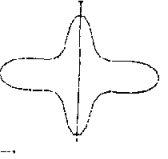
FINITE ELEMENT SPECTRAL ANALYSIS

The primary tool used in these analyses at Sandia is the SAPIV finite element code¹. Since this code is strictly a linear code, and therefore does not include nonlinear geometric effects, some modifications are necessary to accurately predict the frequency shifts resulting from centrifugal stiffening in the blades. Basically, these modifications involve adding terms to the stiffness matrix which account for changes in the bending stiffness due to a non zero tensile stress on the neutral axis of the blade caused by the centrifugal forces. Centrifugal stiffening is most prominent in flatwise bending (motion perpendicular to the chord of the blade) because the increase in stiffness is a much greater percentage of the total stiffness than in the edgewise case (motion parallel to the chord of the blade).

A number of finite element codes are available nationally which are capable of predicting modes and frequencies of VAWTs including these centrifugal stiffening effects. Codes which have been designed to handle large deformations automatically contain the nonlinear geometric effects and therefore do not require the modification mentioned above. Codes such as MARC, ADINA, ANSYS, ABAQUS, and NASTRAN fall into this category.

Finite element models used in SAPIV at Sandia generally consist of approximately 15 beam elements in the tower and 30 in each blade. The guy cables are represented by a linear spring at the top of the tower, with the transmission/generator assembly modeled by a torsional spring and a moment of inertia. These models have been qualified experimentally using spectral data obtained from the DOE/Sandia 17 m two-bladed turbine in a stationary configuration. In Table I, the predicted and measured frequencies are listed along with the predicted mode shapes. In all cases, the agreement is within 10%, and in many, within 5%. Although not shown in this table, the agreement is good for frequencies out to approximately 10 Hz. For future reference, note that the butterfly modes

TABLE 1 MODAL TEST RESULT SUMMARY
 17-M ROTOR, TWO EXTRUDED BLADES, NO STRUTS

<u>MODE IDENTIFIED FROM DATA</u>	<u>MEASURED FREQUENCY (HZ)</u>	<u>SAP IV PREDICTED (HZ)</u>	<u>THEORETICAL MODE SHAPE</u>
1ST FLATWISE	2.11	1.99	
PROPELLOR (BRAKE ON)	2.40	2.75	
1ST BUTTERFLY (EDGEWISE)	2.74	2.55	
1ST TOWER IN PLANE FLATWISE	2.93	2.88	
2ND BUTTERFLY (EDGEWISE)	4.36	4.30	
2ND FLATWISE	5.01	4.71	

are associated with both blades moving in the same direction, like butterfly wings flapping, whereas the in-plane modes involve motion in the plane of the blades.

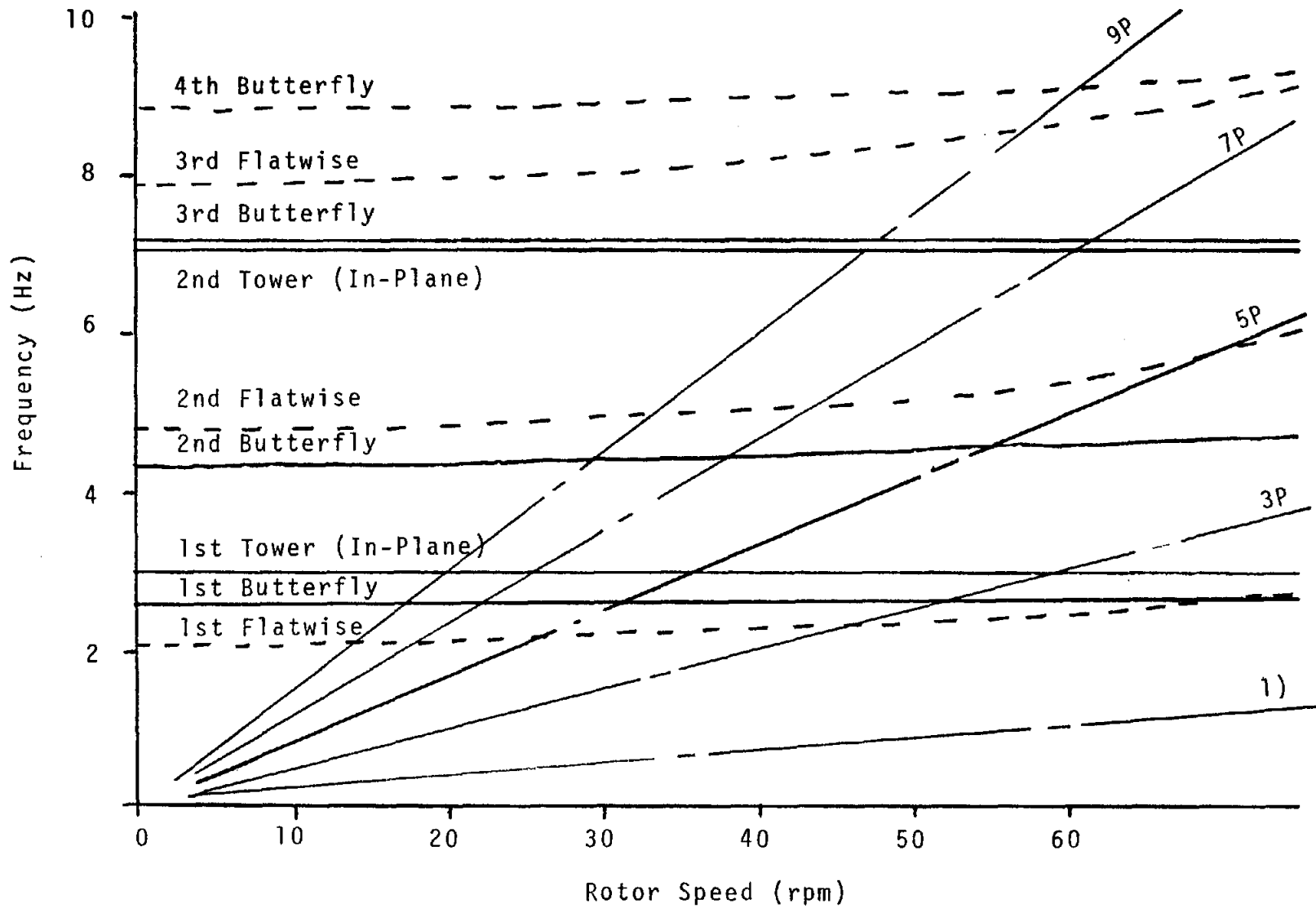
The variation of the frequencies with rpm, as predicted by SAPIV, is shown in the fan plot of Figure 1. In this plot, the modes represented by the dashed lines display significant centrifugal stiffening, while those depicted by the solid ones do not. The latter modes are those included in the VAWTDYN package which will be discussed. The broken lines denoted by 1P, 3P, etc., indicate the prominent per rev excitations. Crossing of the excitations with natural frequencies are noteworthy from a resonance standpoint, but may be erroneous due to additional frequency shifts caused by gyroscopic effects which are not included in the SAPIV model.

A model similar to that used with SAPIV is being developed for NASTRAN. The motivations for this duplication are that (1) NASTRAN is more accessible than SAPIV, (2) The pre-and-post processing options in NASTRAN are superior to those of SAPIV, and (3) using the differential stiffness capability of NASTRAN, centrifugal stiffening modifications are much easier to implement.

TRANSIENT DYNAMIC ANALYSIS

The numerical model developed at Sandia for transient dynamic analysis of two-bladed vertical axis wind turbines, VAWTDYN², is basically composed of a rotating network of rigid links interconnected by joints, springs, and dashpots, in which gyroscopic effects have been included. As shown in Fig. 2 the tower is represented by two rigid links joined together with a "U" joint. Torsional springs and dashpots are mounted in parallels across the joint to account for the bending stiffness and damping of the tower. Each blade is represented as a rigid body attached to the tower with ball joints (Fig. 3). The lead-lag stiffness and damping of each blade is modeled by appropriate springs and dashpots installed in parallel across these joints. The guy cables are modeled by

Fig 1 SAP IV Frequencies
17-m Rotor, Full Extruded Blades



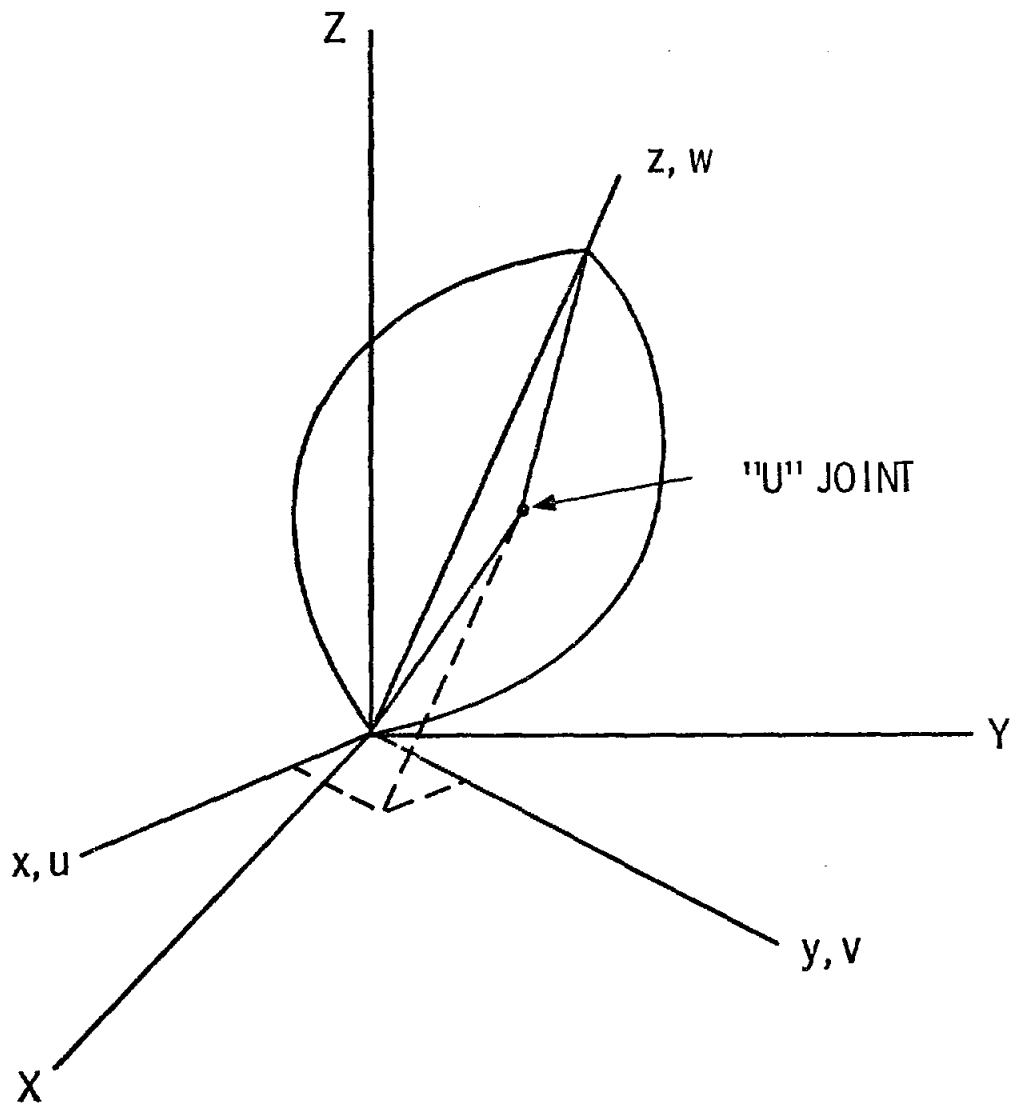


Figure 2: Tower Motions Included in the VAWTDYN Model.

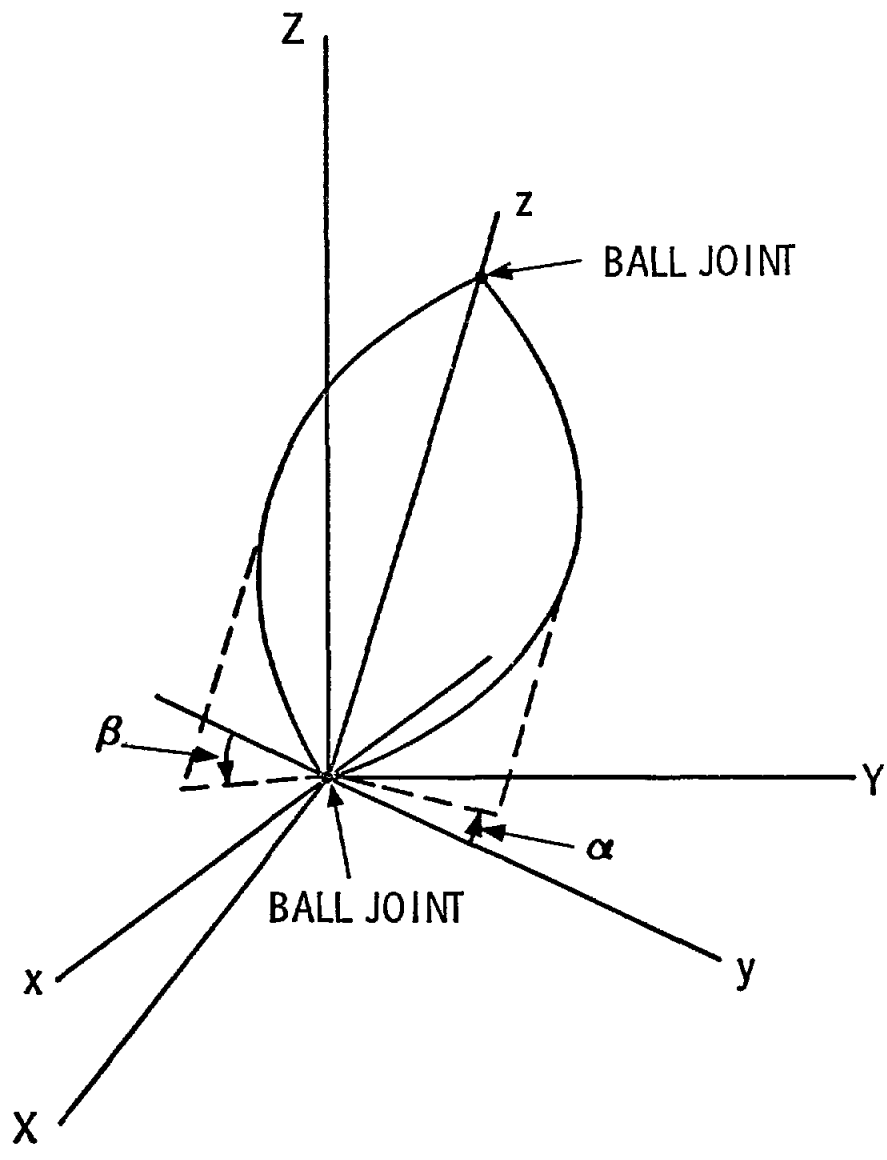


Figure 3: Blade Motions Included in the VAWTDYN Model.

horizontal linear springs and dashpots at the top of the tower and an axial force down the tower. At the base of the tower a torsional spring and dashpot represent the stiffness and damping in the drive train with the induction generator modeled by its torque versus rpm curve. Aerodynamic loads on the blades are computed using a single stream tube aerodynamic model³. The equations of motion developed for this system are solved numerically using an integrator designed for the integration of coupled sets of nonlinear ordinary differential equations associated with initial value problems.

VAWTDYN has been verified by exercising it on a number of problems with known closed-form solutions. It accurately predicts the natural frequencies of the turbine in a non-rotating configuration. With some slight modifications it has been used to predict the motion of symmetrical spinning tops. And finally, it accurately predicts frequency shifts and instabilities in whirling shafts.

Using VAWTDYN, a number of interesting observations have been made concerning wind turbine dynamics. For example, for the rotating turbine, a significant amount of modal cross-talk occurs. To demonstrate this, the spectrums shown in Figs. 4 and 5 indicate the natural frequencies embodied in the in-plane and butterfly response, respectively, for the non-rotating turbine. When the turbine is rotating at 50 rpm, the spectrum for the butterfly motion, displayed in Fig. 6, indicates that, in addition to the frequencies observed in the non-rotating case, two more are present. Careful examination reveals that these frequencies correspond to those of the in-plane motion which have been drawn into the butterfly response through modal cross-talk.

A second observation is that, in addition to frequency shifts caused by centrifugal stiffening, significant shifts also occur due to gyroscopic effects, reminiscent of those occurring in whirling shafts. The fan plot of Fig. 7 was created with VAWTDYN, adjusting the parameters so that the natural frequencies and modes correspond to those of the SAPIV model

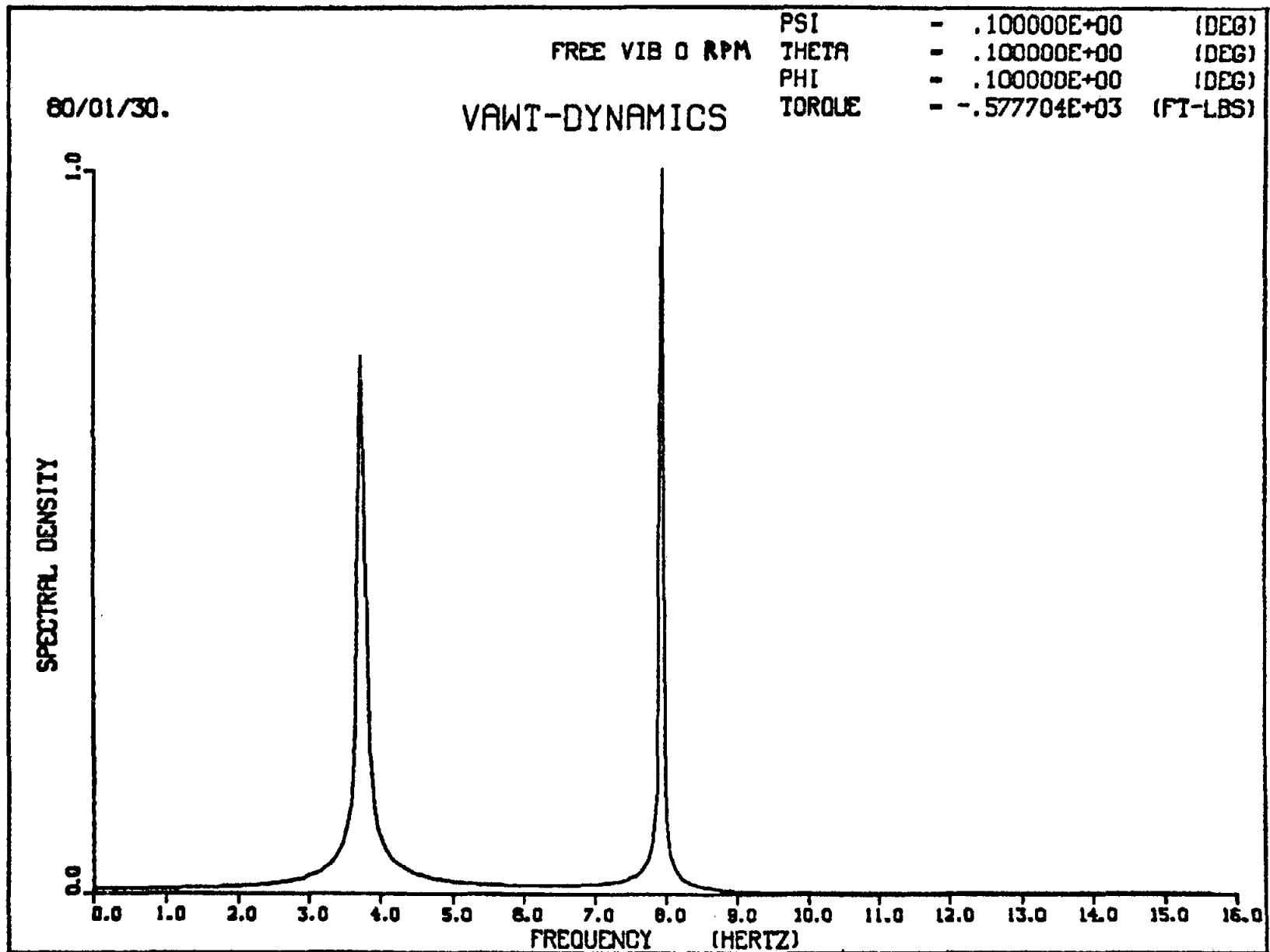


Figure 4: Spectrum of the Free Undamped In-Plane Motion, V , for the Midpoint of the Tower as Predicted by VAWTDYN for the Parked Configuration.

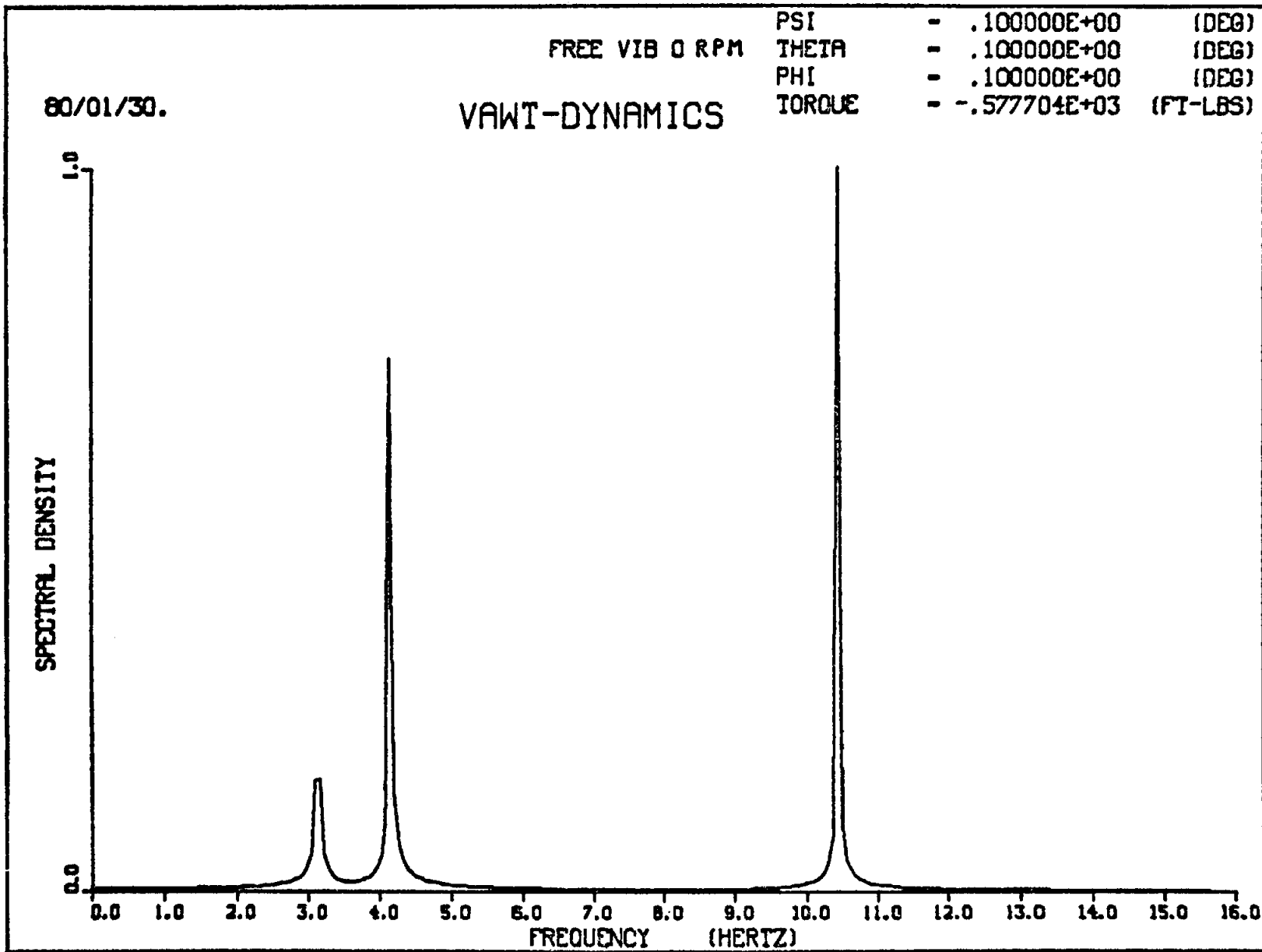


Figure 5: Spectrum of the Free Undamped Transverse Motion, U , for the Midpoint of the Tower as Predicted by VAWTDYN for the Parked Configuration.

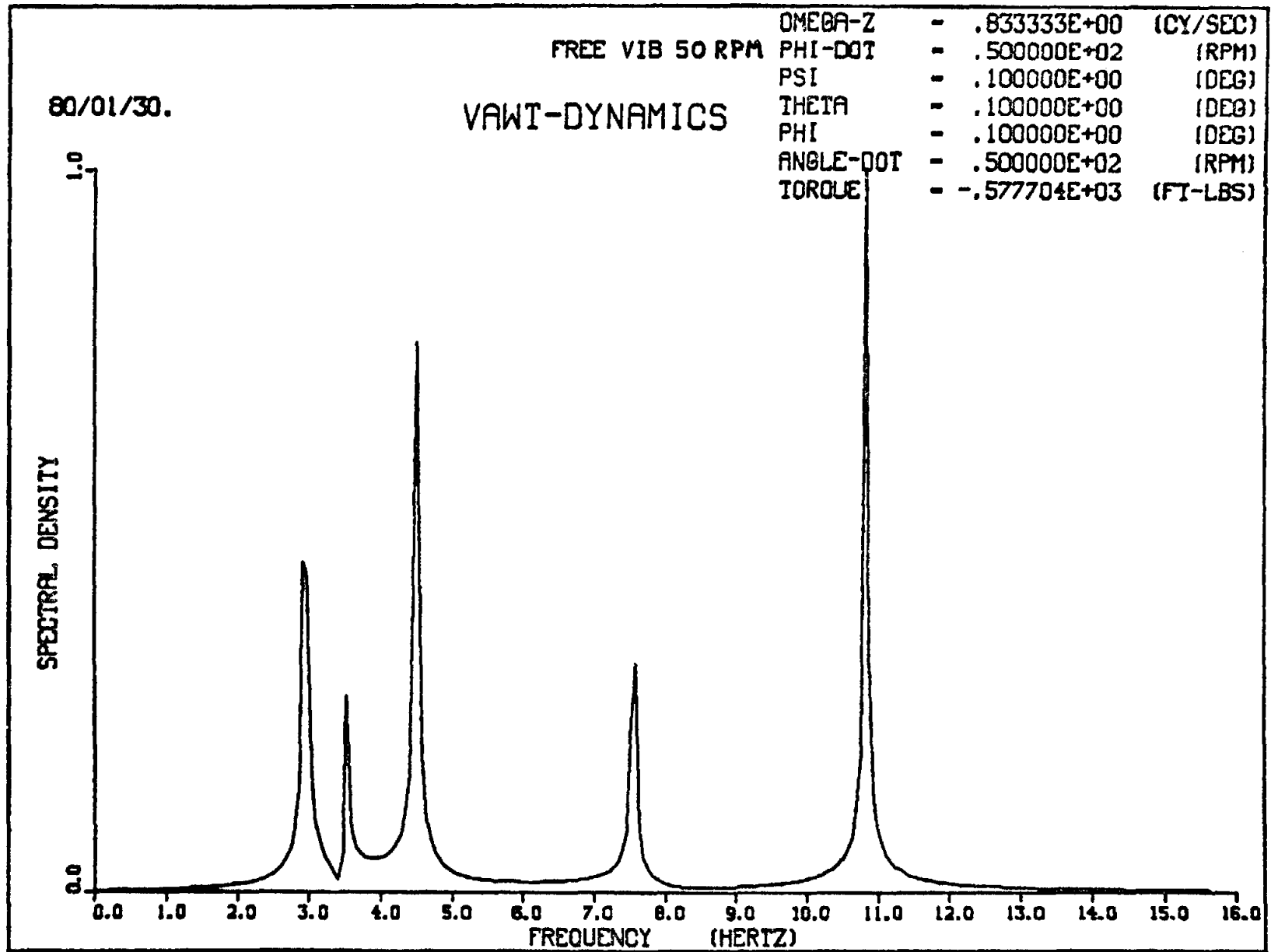
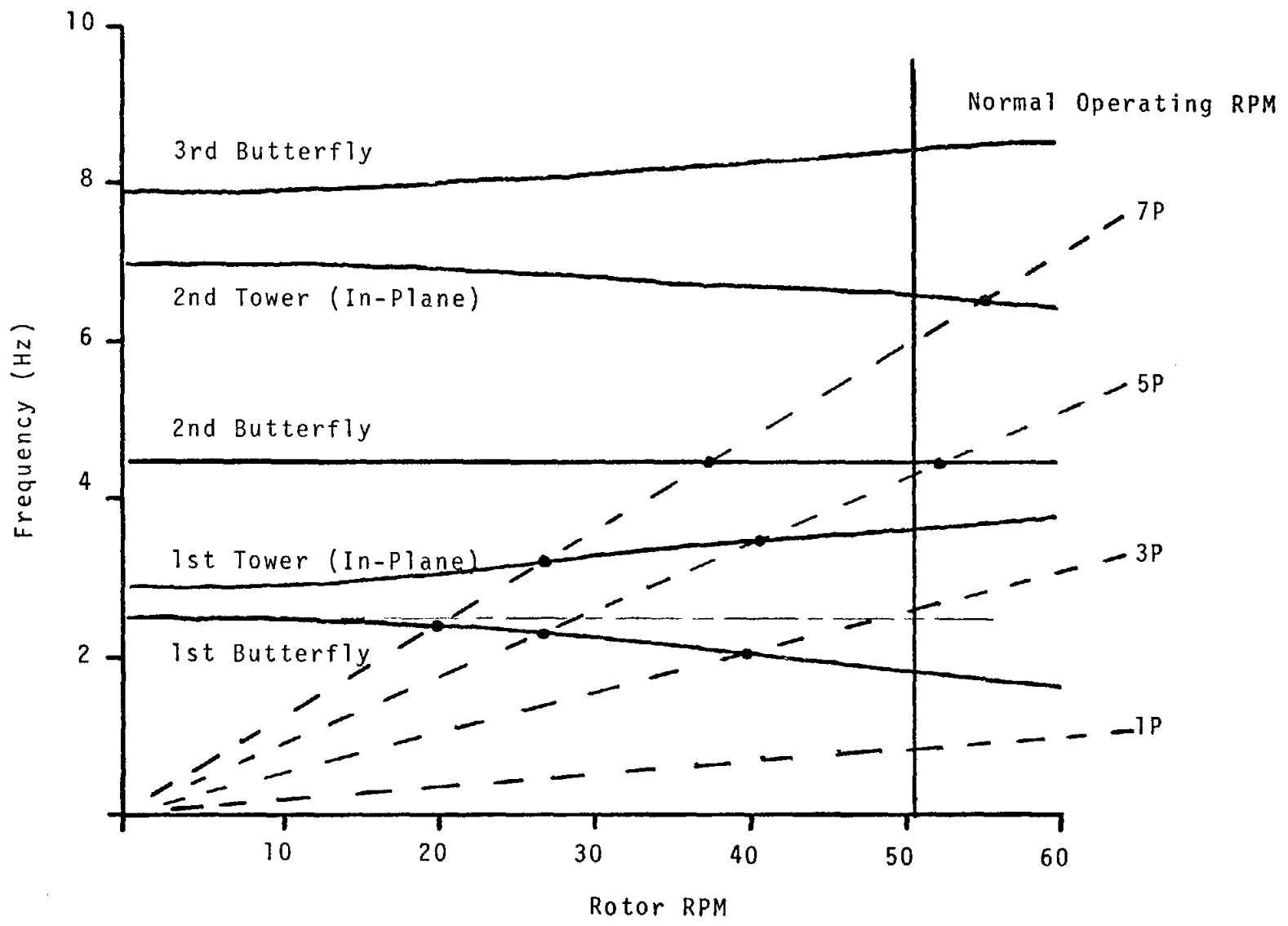


Figure 6: Spectrum of the Free Undamped Transverse Motion, U , for the Midpoint of the Tower as Predicted by VAWTDYN for the Turbine Rotating at 50 RPM.

Fig 7 VAWDYN Fan Plot
 17-m Rotor, Full Extruded Blades



rotating at 50.6 rpm, the operating speed of the DOE/Sandia 17 m turbine. Since the blades are rigid in the VAWTDYN model, no centrifugal stiffening can occur. Yet, as observed in the fan plot, significant frequency shifts are present. In fact, if these shifts were not taken into account, one might expect the 1st butterfly mode to resonate since the corresponding natural frequency, the operating rpm, and the 3P excitation all intersect at approximately the same point. However, with the shift, the 1st butterfly is clearly in no danger of resonating.

On the other hand, the fan plot does indicate that the 2nd butterfly mode may be driven by the 5/rev excitation, which corresponds to a frequency of 4.22 Hz for an operating speed of 50.6 rpm. To examine this possibility, VAWTDYN predictions of the spectral content of the butterfly response were obtained for the DOE/Sandia 17 m turbine at the above operating speed in a 40 mph wind, conditions where significant 5/rev excitation is present. A comparison of these predictions to the experimental data is shown in Fig. 8. The predominance of the 5/rev response is readily apparent. As the spectral density scale for the VAWTDYN predictions has been normalized, no absolute magnitude comparisons can be made. However, good agreement is demonstrated for the relative sizes of the various spikes in each curve. The time series from which these two spectrums were taken are shown in Fig. 9. Again, the vertical scales are not consistent, but the time scales are, except for a shift of 16 sec. Note the remarkable similarity of the signatures especially during the first 6 seconds of the records. If the wind speed is kept the same but the operating speed is moved to 46.7 rpm, away from the resonance, VAWTDYN predictions in the upper curve of Fig. 10 show a drastic reduction in the 5/rev response compared to the 1 and 3/rev responses. The experimental data presented in the lower curve also shows a significant reduction, although it is not as dramatic.

With regard to comparisons of predicted amplitudes to data, Fig. 11 displays the vibratory stress amplitudes at the root of the blade in the trailing edge versus windspeed, for the turbine operating at 50.6 rpm.

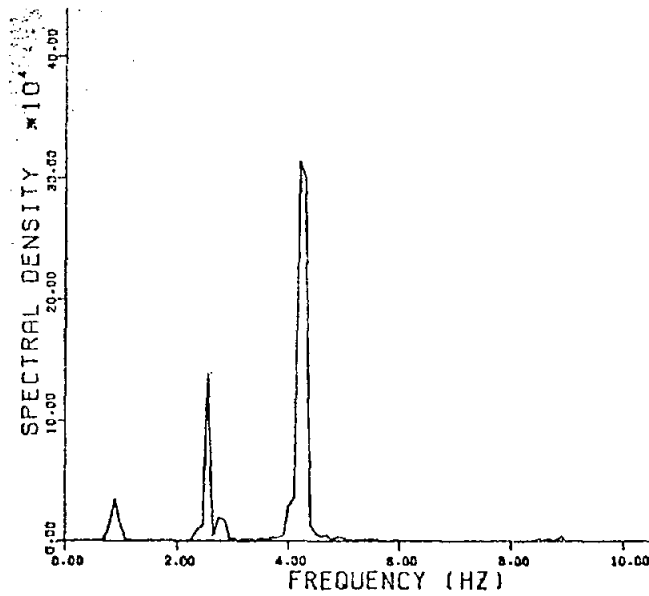
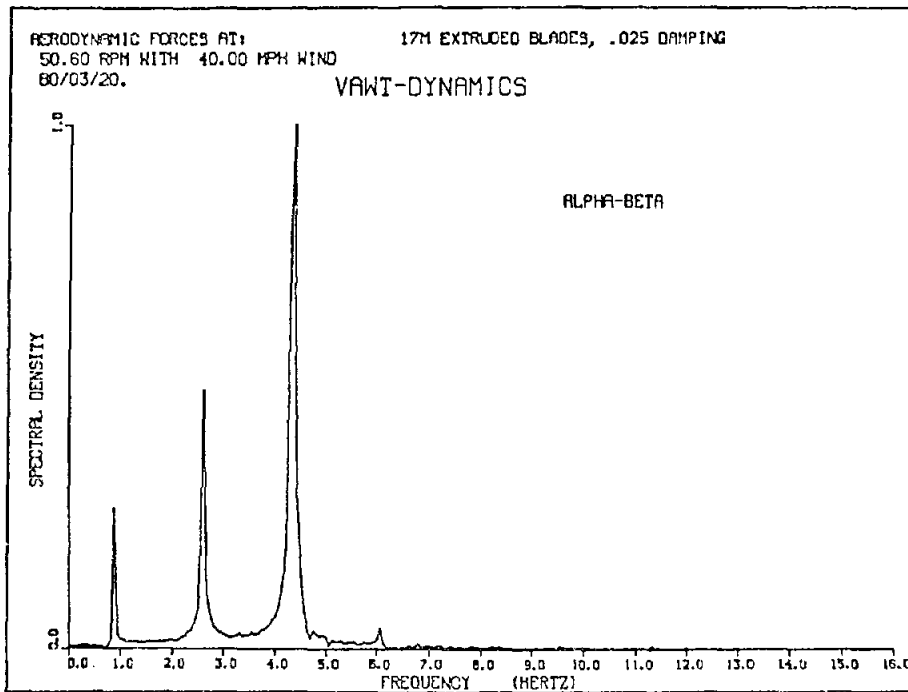


Figure 8: Comparison of the Spectral Content of the Butterfly Response, as Predicted by VAWTDYN, with Measured Data (50.6 rpm in a 40 mph Wind).

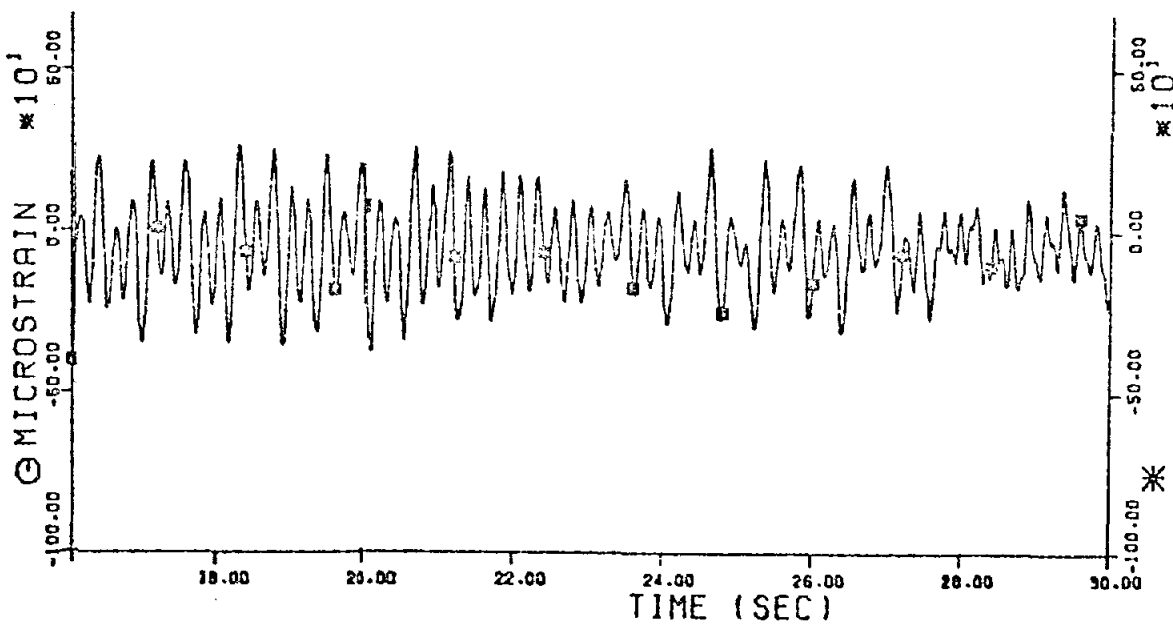
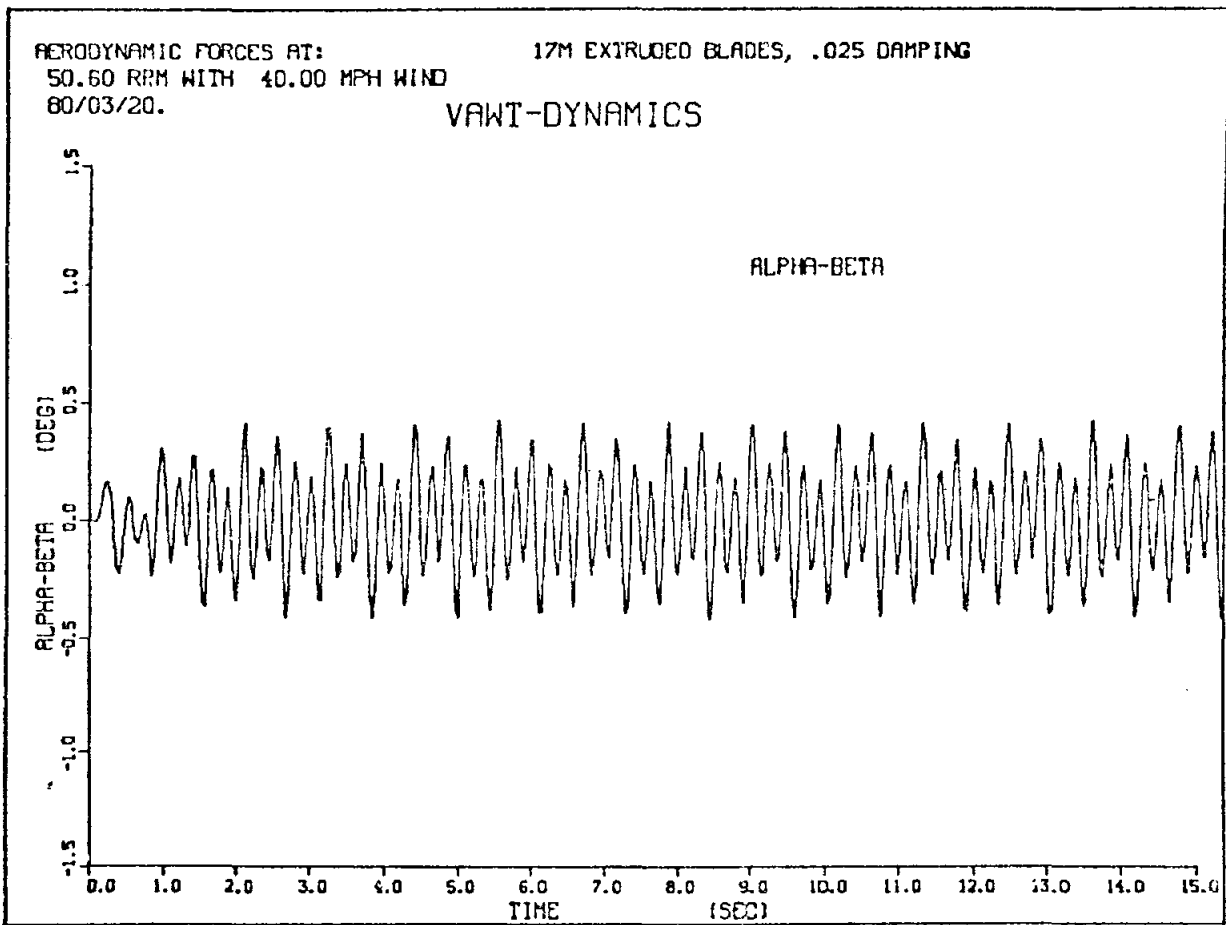


Figure 9: Comparison of the Time Series of the Butterfly Response, as Predicted by VAWTDYN, with Measured Data (50.6 rpm in a 40 mph Wind).

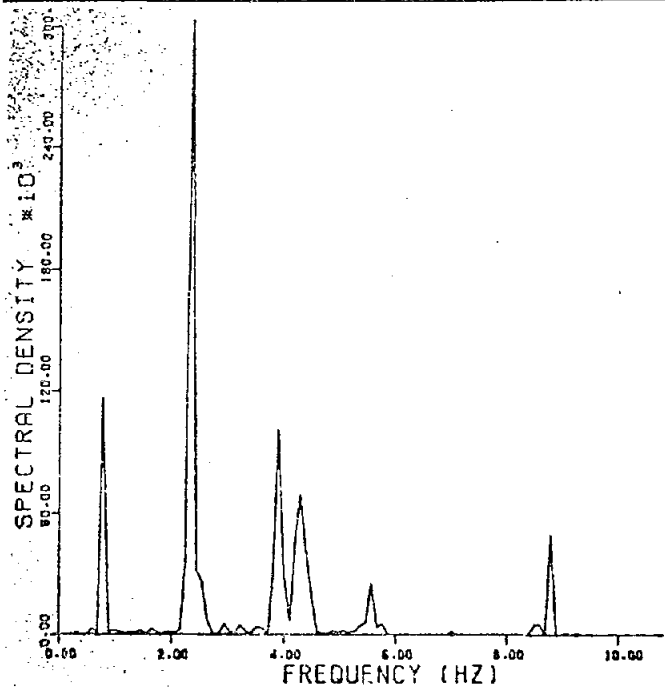
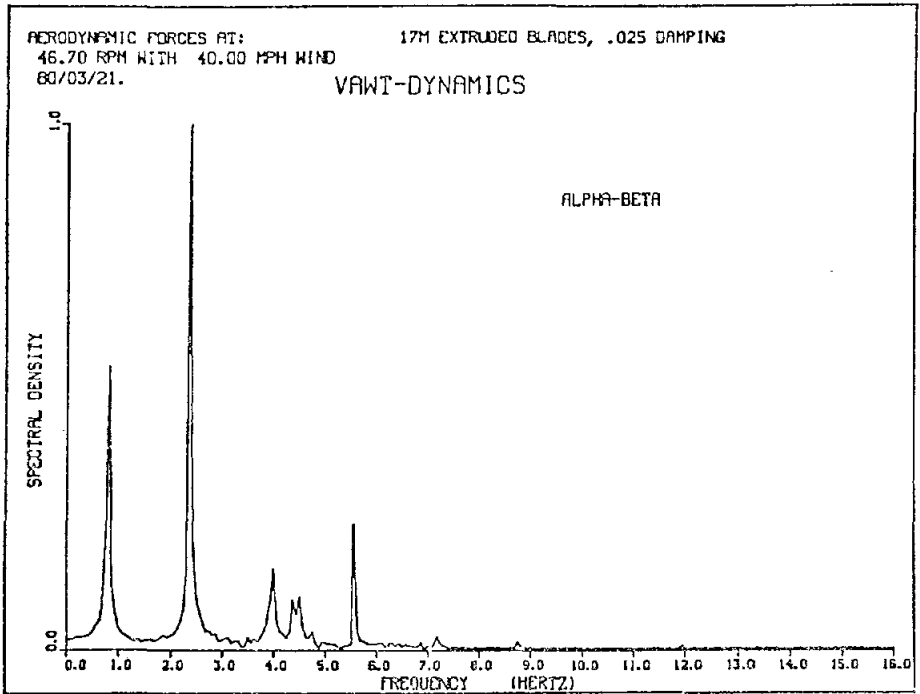


Figure 10: Comparison of the Spectral Content of the Butterfly Response, as Predicted by VAWTDYN, with Measured Data (46.7 rpm in a 40 mph Wind).

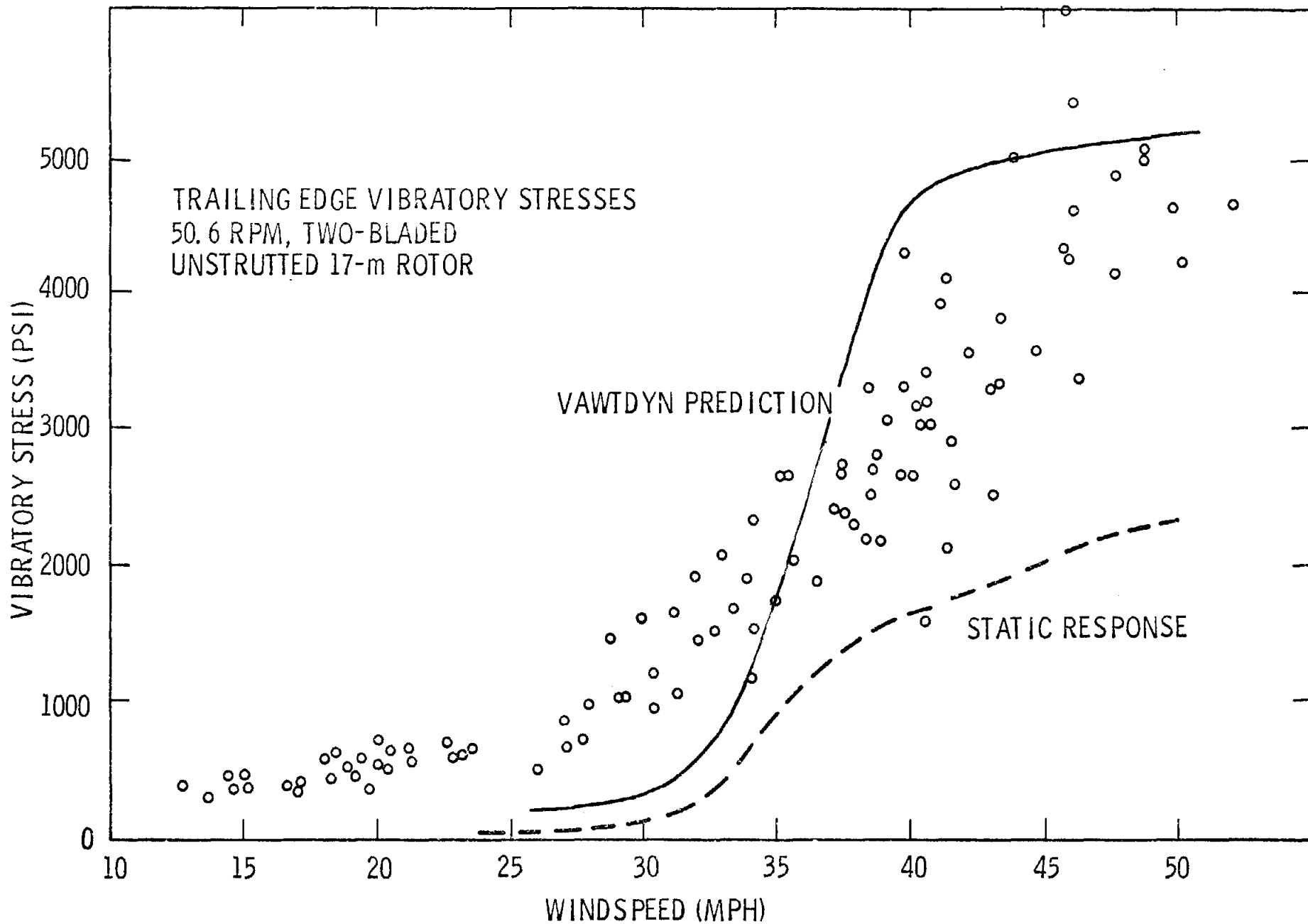


Figure 11: Comparison of VAWTDYN Predictions with Data for the Vibratory Stress Amplitudes at the Trailing Edge of the Blade Near the Root.

The solid curve is the VAWTDYN prediction with the open circles being experimental data. The prediction falls approximately within the scatter band of the data, but does not follow the mean in general. One possible cause for this is the inadequacy of single streamtube model in accurately defining the aerodynamic loads which are used by VAWTDYN for these predictions. In any case, as is evidenced by the dashed curve which represents the static response, significant dynamic amplification is present.

One last comparison of VAWTDYN predictions to data concerns turbine start-up in no wind. In Fig. 12 the torque in the low-speed shaft is plotted versus time as predicted by VAWTDYN with the corresponding measurements in Fig. 13. Although the agreement is generally good, VAWTDYN slightly under-predicts the time to start-up.

Even though experiences with VAWTDYN have been very encouraging and expectations are that it will be used regularly in the future as a design tool, it has several limitations. For instance, VAWTDYN is not a general purpose package for VAWT's and consequently, for different configurations, such as three bladed rotors, extensive modifications are necessary. The parameters in the model are difficult to determine, especially without a prior knowledge of the appropriate modes and frequencies of the turbine. And finally, VAWTDYN is not capable of modeling blade motions which deviate appreciably from rigid body motions about the tower. The consequences of this last limitation will be ascertained only after VAWTDYN has been tested with data from a variety of two-bladed systems.

One final activity being pursued in the dynamic analysis of VAWTs is in the area of blade flutter instability. Although this has not been a pressing problem with any of Sandia's research turbines, an accurate means of predicting this phenomenon is desirable when considering the variety of conceivable future machines. To this end Sandia has contracted with Hibbitt and Karlsson Inc. to provide a finite element capability for this purpose.

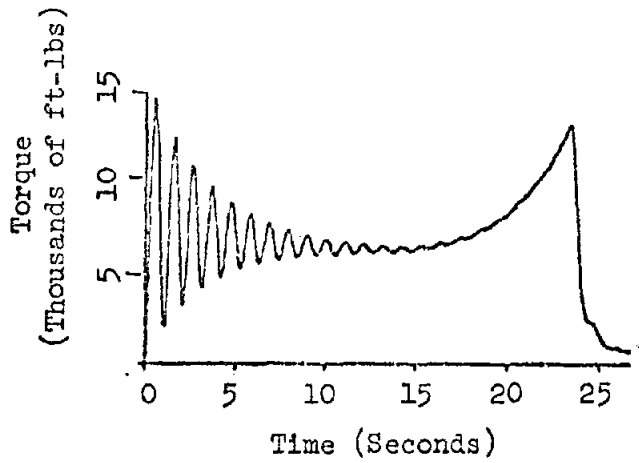


Figure 12: VAWTDYN Predictions of Low-Speed Shaft Torque Versus Time for Turbine Start-Up.

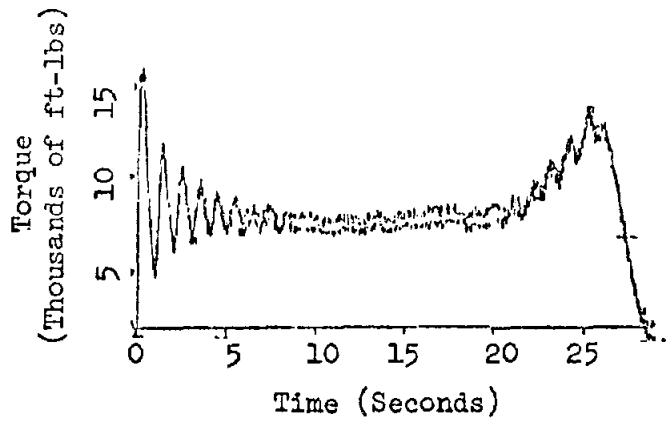


Figure 13: Experimental Low-Speed Shaft Torque Data for Start-Up,

CONCLUSIONS

Currently, it is felt at Sandia that dynamic analysis of vertical axis wind turbines can adequately be accomplished using a spectral analysis package which includes centrifugal stiffening effects along with transient dynamics package of the nature of VAWTDYN. With this combination, reasonably accurate fan plots for the lower modes of the system can be created and dynamic amplification factors can be estimated. However, extension of current methods and development of new ones for expanding predictive capabilities will definitely continue in the future. For example, development of VAWTDYN into a more general finite element capability has been discussed. This would effectively remove the previously indicated limitations. Also, consideration has been given to developing a spectral capability, possibly with NASTRAN, which includes the gyroscopic as well as the centrifugal stiffening effects. Progress in these and other development activities at Sandia related to dynamic modeling of VAWTs will be reported regularly.

REFERENCES

1. J. H. Biffle, "System Structural Response," Vertical Axis Wind Turbine Technology Workshop, May 17-20, 1976, SAND76-5586 (Albuquerque, NM: Sandia Laboratories, 1976).
2. D. W. Lobitz and W. N. Sullivan, VAWTDYN - A Numerical Package for the Dynamic Analysis of Vertical Axis Wind Turbines, SAND80-0085 (Albuquerque, NM: Sandia Laboratories, 1980).
3. J. H. Strickland, The Darrieus Turbine: A Performance Prediction Model Using Multiple Stream Tubes, SAND75-0431 (Albuquerque, NM: Sandia Laboratories, 1975).

DESIGN OF VAWT DRIVE TRAIN FOR TORQUE RIPPLE CONTROL

Robert C. Reuter, Jr.

ABSTRACT

Interaction between a steady wind and a rotating, Darrieus, vertical axis wind turbine produces time periodic aerodynamic loads which cause time dependent torque variations, referred to as torque ripple, to occur in drive train components. There is concern for the effect of torque ripple upon fatigue life of drive train components and upon power quality. Current capabilities for analyzing torque ripple are reviewed. Numerical results for torque ripple, determination of acceptable levels and methods of controlling it are presented and discussed.

INTRODUCTION

Power gathered from the wind by a vertical axis wind turbine (VAWT), operating synchronously, is in the form of mechanical torque at a specified rotational speed. Interaction of the rotating blades with the incident wind causes a time periodicity in the net torque acting on the turbine. This applied torque, obtained by integrating aerodynamic loads over all blades present, is transmitted through the turbine drive train components to the electric generator, and is called "torque ripple" by virtue of its intrinsic time dependence. Under the ideal conditions of a steady wind from a fixed direction, torque ripple may be visualized as a time dependent function oscillating, with a period related to the number of blades, about a mean torque value. Depending upon turbine operating conditions (such as wind speed and turbine RPM) and drive

train characteristics (such as component masses, torsional rigidities, gear ratios and generator slip), the magnitude of the oscillating portion of the applied torque, or the ripple, may be either amplified or attenuated at various locations along the drive train. Extended fatigue life requirements placed on the turbine and the need to generate high quality power, both suggest the desirability of keeping torque ripple to a minimum.

Recognition of the torque ripple problem and its consequences, and attempts to characterize it analytically and demonstrate control over it are not new^{1 2 3}. Two of the assumptions upon which early analytical work on torque ripple in VAWT systems^{1 2} was based are: (1) the wind is steady and from a fixed direction, and (2) the net applied torque is a simple harmonic function of time. Both assumptions aided in significantly reducing the analytical complexities of the problem; at the same time, however, they make correlation with data obtained in the field more difficult, principally because the wind is neither steady nor from a fixed direction. Models based on these assumptions captured the torque ripple behavior trends as parameters were changed¹, and permitted at least initial insight into understanding of the problem.

Recent aerodynamic models⁴, from which come the magnitude and time dependence of the net aerodynamic torque applied to the turbine, demonstrate that the assumption of a simple harmonic form for the applied torque is not always justified. This is because of asymmetries in the upwind and downwind aerodynamics⁴, and the large influence of stall at high wind speeds, a previously known result⁵. Even with a steady wind from a fixed direction, these non-simple-harmonic time dependencies of the problem can exist, and so it is logical that the next level of rigor in the torque ripple model be achieved by removing the assumption of simple harmonic behavior. This was

accomplished in the current model by using a general, Fourier expansion of the time dependent characteristics of the problem. The approach permits full representation of upwind and downwind asymmetries and multiple harmonics in the applied torque and drive train response which are prevalent at low tip speed ratios.

The purpose of the present paper is to review the current state of the analytical characterization of the torque ripple problem. Recent theory and experimental data correlation is presented, acceptable limits of torque ripple are discussed and methods of torque ripple control are considered.

THE TORQUE RIPPLE MODEL

A typical VAWT drive train consists of the following components: the turbine rotor (blades and rotating tower), various shafts and couplings which connect the rotor to the transmission, the transmission, more shafts and couplings which link the transmission to the generator, and the generator. Additional components may be present depending upon the specific turbine design, purpose and installation. For example, the DOE/Sandia 17-meter research turbine⁶ located in Albuquerque, NM, has a secondary gear ratio change capability in the form of interchangeable pulleys and a timing belt, located between the transmission (which has a fixed gear ratio) and the generator. This feature permits field evaluation of aerodynamic, structural and system performance in a synchronous mode under a variety of operating conditions. "Operating conditions" refers collectively to combinations of incident wind velocity and turbine operating speed. A popular parameter characterizing operating conditions is tip speed ratio, λ , which is equal to maximum blade speed, $R_{MAX}\Omega$, divided by incident wind speed, V . When $\lambda \geq 3.5$ the simple harmonic representation of applied torque and drive train response is justified^{1 5}, as seen in Fig. 1. However, when

$\lambda = 5.0$

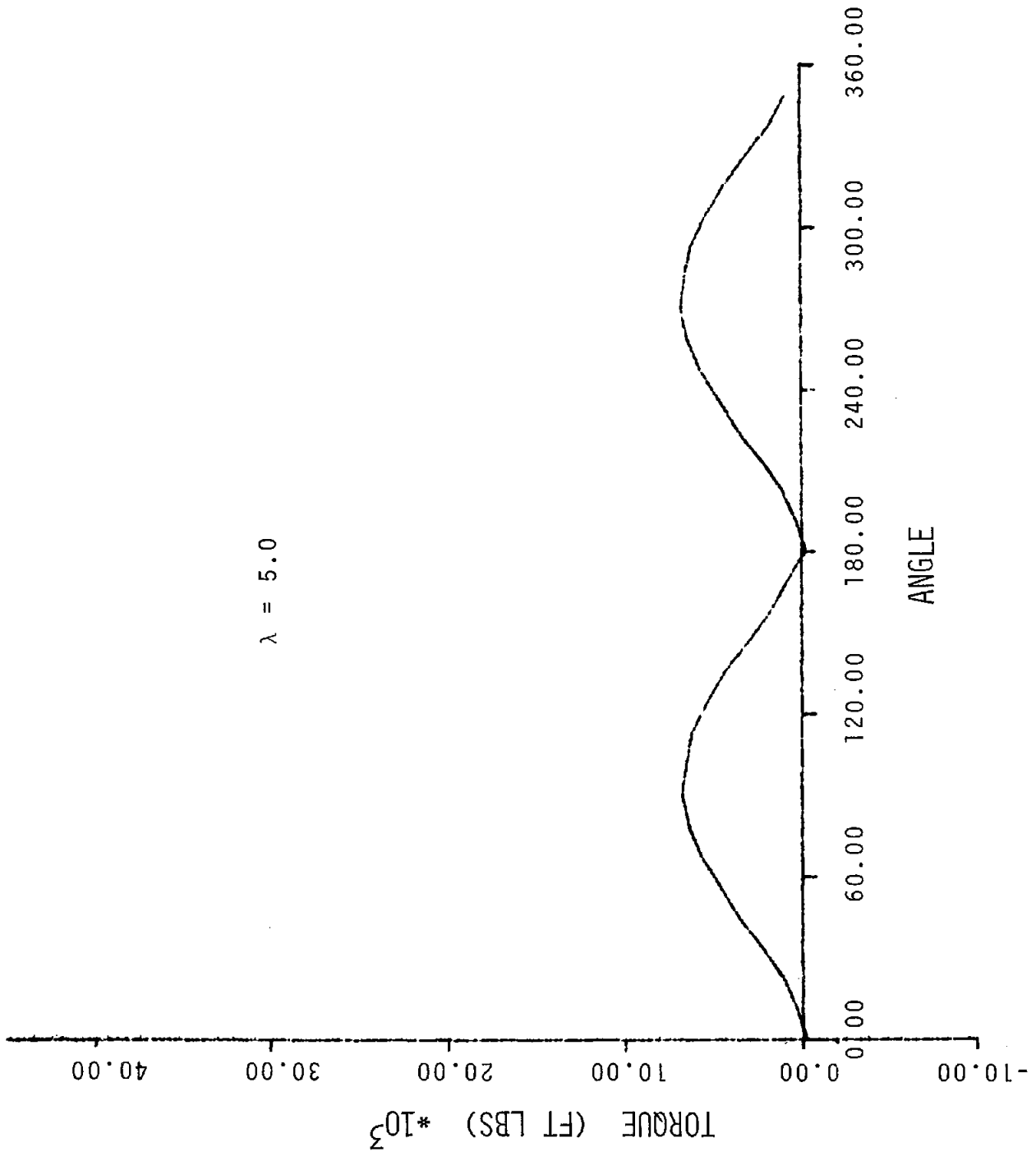


Figure 1. Applied torque versus azimuth position for one turbine revolution when $\lambda = 5.0$.

$\lambda \leq 3.5$, blade stall affects and upwind and downwind aerodynamic asymmetries become strong⁴, thus compelling a Fourier expansion of torque ripple time characteristics, see Fig. 2. Since peak turbine power and, therefore, peak mean torque occurs at a tip speed ratio in the range of 1.0 to 3.0⁶, it is essential that dynamic behavior of the turbine be well understood for low values of λ .

In order to study torque ripple, a model is developed which has three essential elements. The first is a mathematical representation of the physical characteristics of the entire drive train from which differential equations of motion can be written. The second is a representation of the functional dependence of the applied torque upon time. The third and final element of the model is the solution to the equations of motion subject to the applied loading, including numerical evaluation.

There are two versions of the first element. The original drive train model consists of four lumped masses connected in series to the generator by elastic, torsional springs [1]. This model captures three torsional modes which are reacted by torque in the drive train, the lowest two of which are the lowest corresponding modes of the turbine system. The third mode has a node close to the generator and tends to be quite high. A second model exists which combines pairs of the above masses and, thus, captures only the lowest torsional mode [2]. This model was developed in order to have a simpler analytical tool for numerical evaluation of torque ripple. A single expression was derived which allows calculation of torque ripple as a function of aerodynamic excitation parameters and drive train properties. Both the original four mass model and the two mass model represent solutions for simple harmonic excitation and are, therefore, limited to tip speed ratios greater than 3.5.

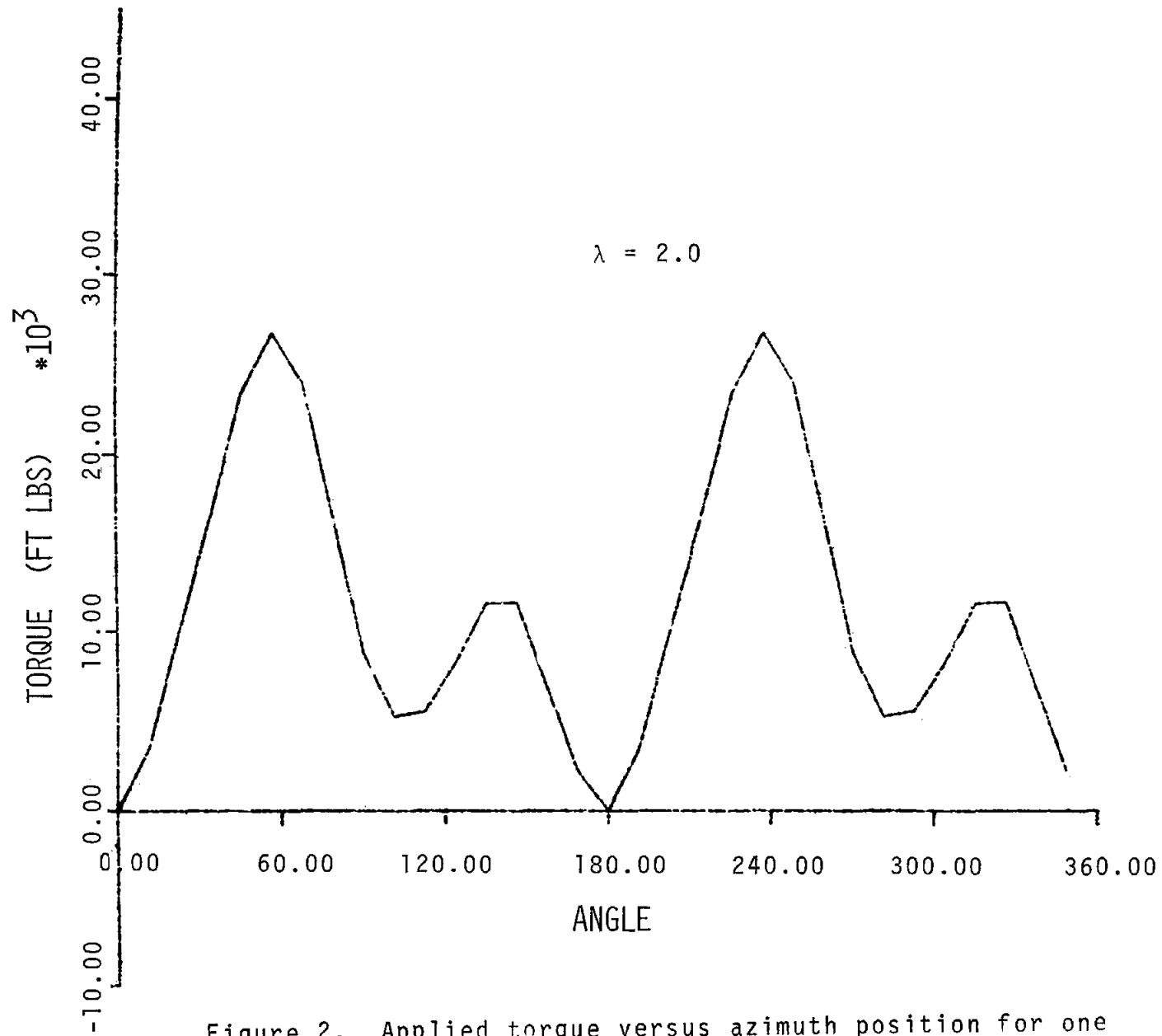


Figure 2. Applied torque versus azimuth position for one turbine revolution when $\lambda = 2.0$.

To expand torque ripple prediction capabilities to include low tip speed ratios, $\lambda \leq 3.5$, the present model with a Fourier expansion of time characteristics was developed. This model retains the four masses of the original model simply because higher torsional modes than the first may be excited as a result of design changes or higher harmonics in the applied torque. A schematic of the model appears in Fig. 3. J_B represents half of the total rotor inertia, and K_T is calculated so that the frequency associated with dumb-bell motion of the rotor matches that of the actual system. Other drive train properties may be either calculated or measured values.

The second element of the present torque ripple model consists of a decomposition⁷ of the functional dependence upon time of the applied aerodynamic torque as predicted by the vortex model⁴ for low tip speed ratios and stream tube models⁵ for high tip speed ratios. Changing from the vortex to the stream tube models is done to conserve computer time and cost. Applied torque is written in the form

$$T_A = T_0 + \sum_{i=1}^N T_i \cos \omega_i t + \sum_{i=1}^N \bar{T}_i \sin \omega_i t \quad (1)$$

where T_A can be applied fractionally to top and bottom of the rotor in order to account for wind shear, if desirable. Solutions are assumed to be of the form

$$\theta_j = A_0 + \sum_{i=1}^N A_i \cos \omega_i t + \sum_{i=1}^N \bar{A}_i \sin \omega_i t + \Omega_j t \quad (2)$$

TORQUE RIPPLE MODEL

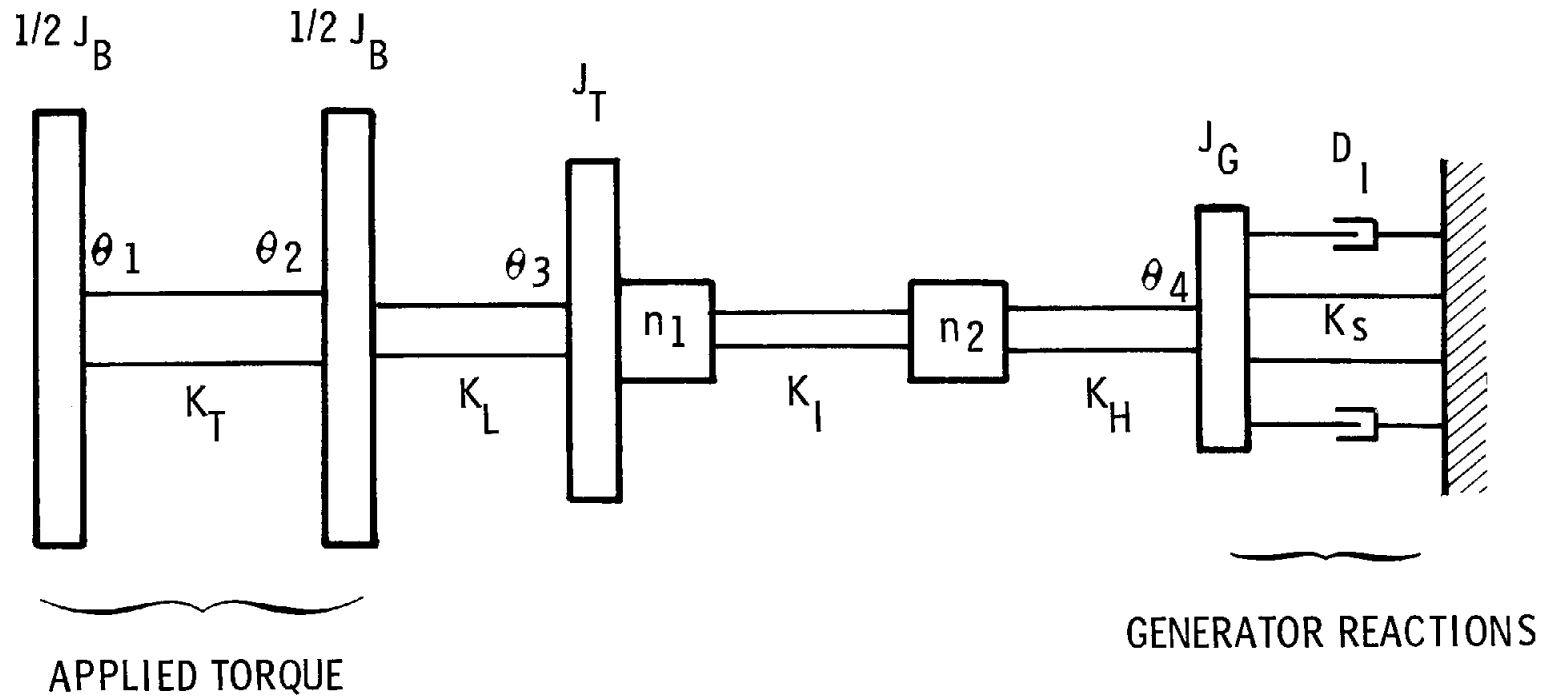


Figure 3. Schematic of turbine drive train components and nomenclature.

In (1) and (2), Ω_j is the drive train rotational frequency (speed), and $\omega_i = 2 i \Omega_j$ where j is an integer. The solution was obtained and a computer program, named FATE, was written to facilitate numerical evaluation.

NUMERICAL RESULTS/ALLOWABLE VALUES

Properties of the drive train of the present DOE/Sandia research turbine are:

$$\begin{aligned}
 J_B &= 1.92 \times 10^5 \text{ lb-sec}^2\text{-in} \\
 J_T &= 2.15 \times 10^3 \text{ lb-sec}^2\text{-in} \\
 J_M &= 27.1 \text{ lb-sec}^2\text{-in} \\
 D_I &= 824.0 \text{ lb-in-sec/rad} \\
 n_1 &= 35.6 \\
 K_T &= 1.46 \times 10^8 \text{ lb-in/rad} \\
 K_L &= 2.39 \times 10^6 \text{ lb-in/rad} \\
 K_I &= 1.25 \times 10^6 \text{ lb-in/rad} \\
 K_H &= 1.86 \times 10^4 \text{ lb-in/rad} \\
 n_2 &= \frac{1800}{n_1(\Omega)}
 \end{aligned}$$

where 1800 is the rotational speed of the generator and Ω is the rotational speed of the turbine, both in units of RPM. Torque ripple is defined in two ways. The first, labeled \tilde{T}_M , is the ratio of the mean-to-peak value and the mean value of torque, and is convenient when considering fatigue characteristics of the drive train. The second, labeled \tilde{T}_R , is the ratio of the mean-to-peak value and the turbine's rated torque, and is relatable to power quality. Thus,

$$\tilde{T}_M = \frac{T_{MAX} - T_{MIN}}{T_{MAX} + T_{MIN}} \quad (3)$$

$$\tilde{T}_R = \frac{T_{MAX} - T_{MIN}}{2 T_{RATED}} \quad (4)$$

Figure 4 shows both definitions of torque ripple in the low speed drive train components as a function of tip speed ratio for the DOE/Sandia research turbine operating at 50.6 rpm. Because of the rapid changes in \tilde{T} at low values of λ , numerical points are connected by straight lines. Three data points, based on the \tilde{T}_M definition, are shown in the figure and agree closely with predicted values of \tilde{T}_M . More data are not shown because of the difficulty in obtaining experimental information that is not influenced by the random nature of the wind. Notice that \tilde{T}_M increases with λ . This occurs because even though the oscillating portion of the torque is diminishing with λ , the mean value is diminishing faster, thus causing \tilde{T}_M to increase. \tilde{T}_R shows the change in only the oscillating portion of torque with λ (since it is normalized by a constant--the turbine rated torque), where it is seen to decrease.

To determine what level of torque ripple might be allowable from a fatigue or life expectancy standpoint, assume that drive train components follow the Goodman law for fatigue strength⁸. This law imposes a straight line relationship between fatigue strength for purely alternating stress (the dependent variable) and mean stress (the independent variable). Using this law and the above definition of torque ripple expressed as a % of mean torque, \tilde{T}_M , an expression for allowable \tilde{T}_M in terms of expected fatigue strength, σ_N , mean stress, σ_M , and ultimate strength, σ_u , of drive train components can be derived.

$$\tilde{T}_M \leq \left(\frac{\sigma_N}{\sigma_u} \right) \left(\frac{\sigma_u}{\sigma_M} - 1 \right) \quad (5)$$

Taking the fatigue limit as σ_N , a typical value for the ratio, (σ_N/σ_u) , for structural steels is 0.4. Using this value, Eq. 5 can be plotted versus the ratio (σ_u/σ_M) as in Fig. 5. Since (σ_u/σ_M) may be viewed as a safety factor for design of drive train components, whatever value is used can be located on the ordinate of Fig. 5, and as long as the \tilde{T}_M calculated from Eq. 3, falls on or below the corresponding \tilde{T}_M value in Fig. 5, infinite life can be expected. By taking the ratio, \tilde{T}_R/\tilde{T}_M , for specific values of λ (for example from Fig. 4), it can be seen that as λ increases, σ_M decreases. Thus, increasing λ corresponds to an increase in (σ_u/σ_M) and, therefore, an increase in acceptable levels of \tilde{T}_M . For the DOE/Sandia research turbine, a design safety factor of 2.0 was used for drive train components. Since maximum torque occurs at $\lambda \approx 1.5$, $(\sigma_u/\sigma_M) = 2.0$ on the abscissa in Fig. 5 corresponds to $\lambda = 1.5$. Using Fig. 4, it can be seen that $(\sigma_u/\sigma_M) \approx 3.0$ corresponds to $\lambda = 3.0$ $(\sigma_u/\sigma_M) \approx 4$ corresponds to $\lambda = 4.0$, and $(\sigma_u/\sigma_M) \approx 6.5$ corresponds to $\lambda = 6$. This demonstrates that the allowable values of \tilde{T}_M increase rapidly with λ . Examination of the values of \tilde{T}_M in Fig. 4 indicate that the DOE/Sandia research turbine does not have a fatigue problem.

Power companies have determined that power quality may be determined by the amount of "light flicker" that people can tolerate for extended periods of time. They have also determined that the "borderline of irritation" with 60 cycle power corresponds to a voltage variation of 0.5% of the line voltage. Since torque ripple in a generator is equivalent to current ripple in the line, acceptable torque ripple (expressed as a % of rated torque) can be related to voltage ripple. In the case of the DOE/Sandia research turbine, line impedance is approximately 4% of the load impedance. A maximum voltage

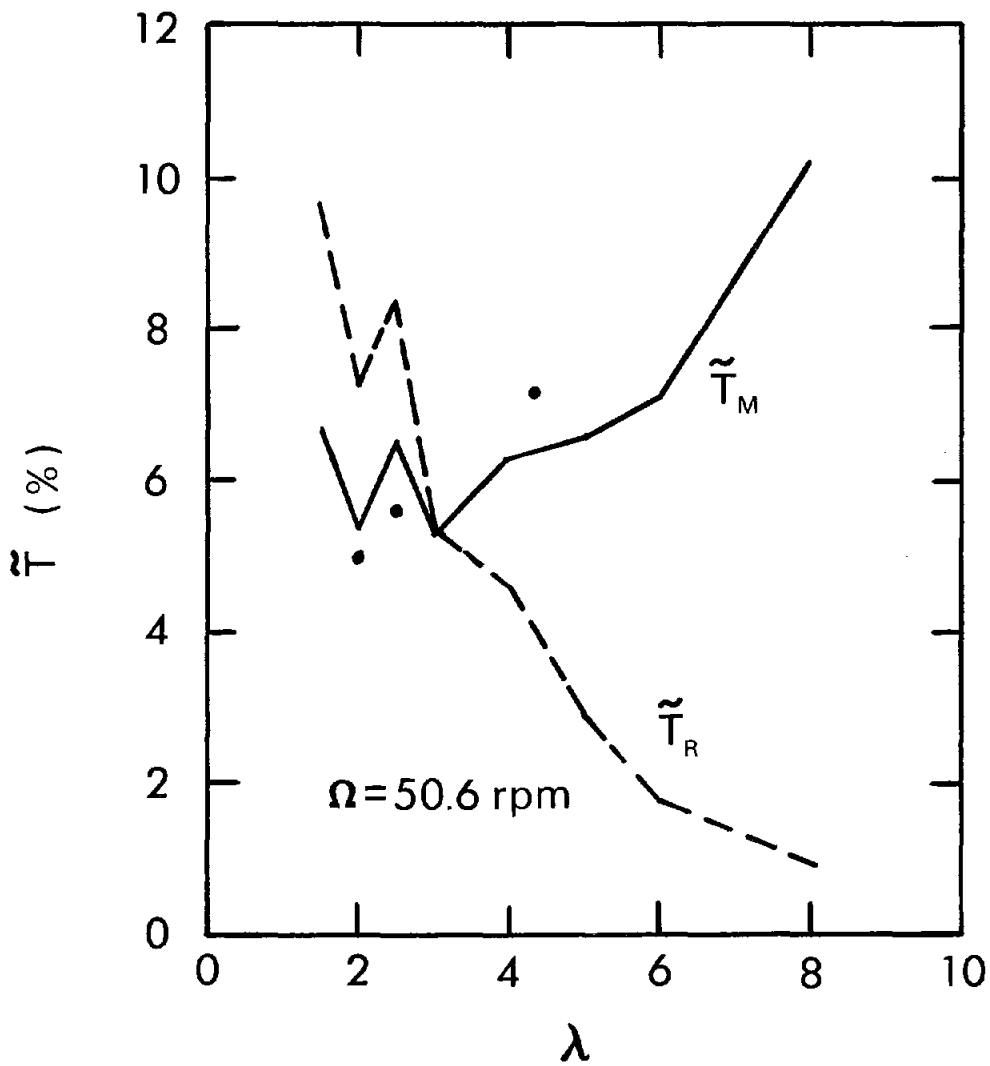


Figure 4. Torque ripple versus tip speed ratio for the DOE/Sandia research turbine operating at 50.6 RPM.

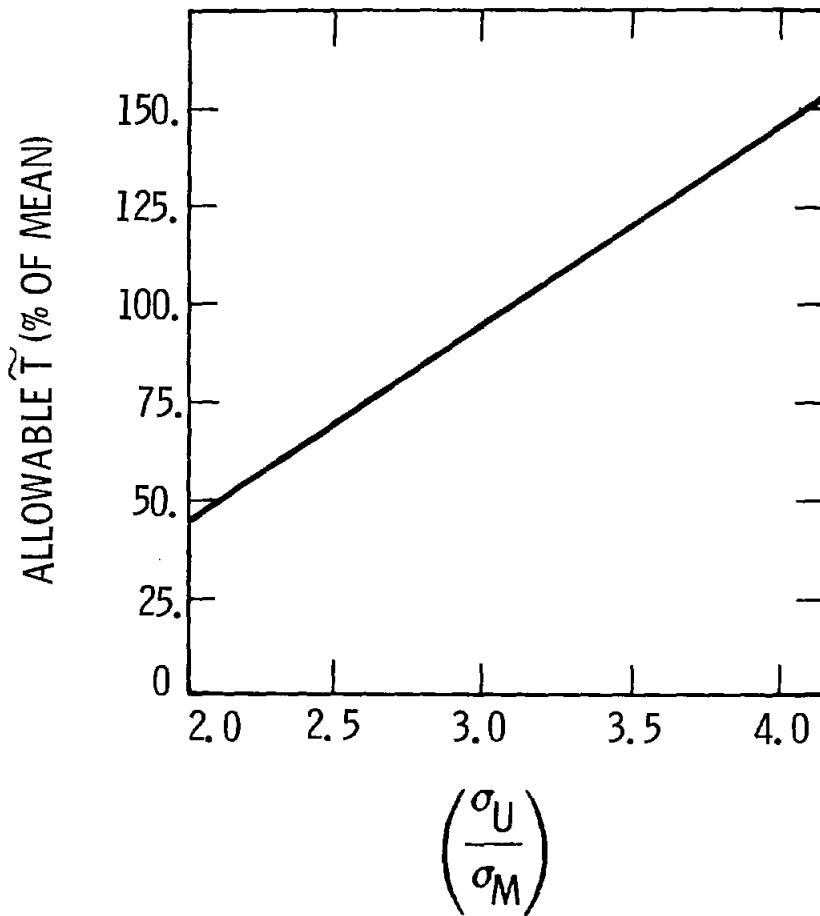


Figure 5. Allowable values of torque ripple (expressed as a % of mean torque) based on infinite life of drive train components.

ripple of 0.5%, therefore, corresponds to an allowable \tilde{T}_R of 12.5%. Results in Fig. 4 indicate that the research turbine does not have a power quality problem.

CONTROL OF TORQUE RIPPLE

Among the properties which characterize the torque ripple problem, the most readily and easily modified are drive train torsional rigidities and, perhaps, generator slip. Figure 6 shows numerical results for \tilde{T}_M versus λ for the research turbine and values which would have resulted from a doubling and a halving of the torsional rigidity of the low speed end of the drive train. While fatigue life does not appear to be reduced even with a doubling of the low speed stiffness, additional rigidity increases could cause problems. Since $\tilde{T}_R \approx \tilde{T}_M$ when $\lambda \approx 3$, doubling the stiffness of the low speed end could cause a noticeable reduction in power quality.

To see how a change in low speed torsional stiffness effects torque ripple, consider the results in Fig. 7, where \tilde{T}_M is plotted, for three low speed rigidities, as a function of turbine operating speed, Ω . Notice how the peak (which corresponds to the first critical drive train frequency) moves to the left with a reduction in low speed stiffness and to the right for an increase in drive train stiffness. The effect that this has on torque ripple at a specified operating speed is obvious. (This figure does not depict what occurs during start up. It provides torque ripple values in the drive train at specified operating speeds.) The behavior of \tilde{T}_R with Ω is similar to that shown for \tilde{T}_M in Fig. 7. Other methods of controlling torque ripple exist. An increase in generator slip tends to lower torque ripple values at moderate Ω , and increase them at higher Ω (above ~ 40 RPM). An increase in inertia properties tends to lower torque ripple at a given operating condition, but this may be costly. A reduction in gear ratio

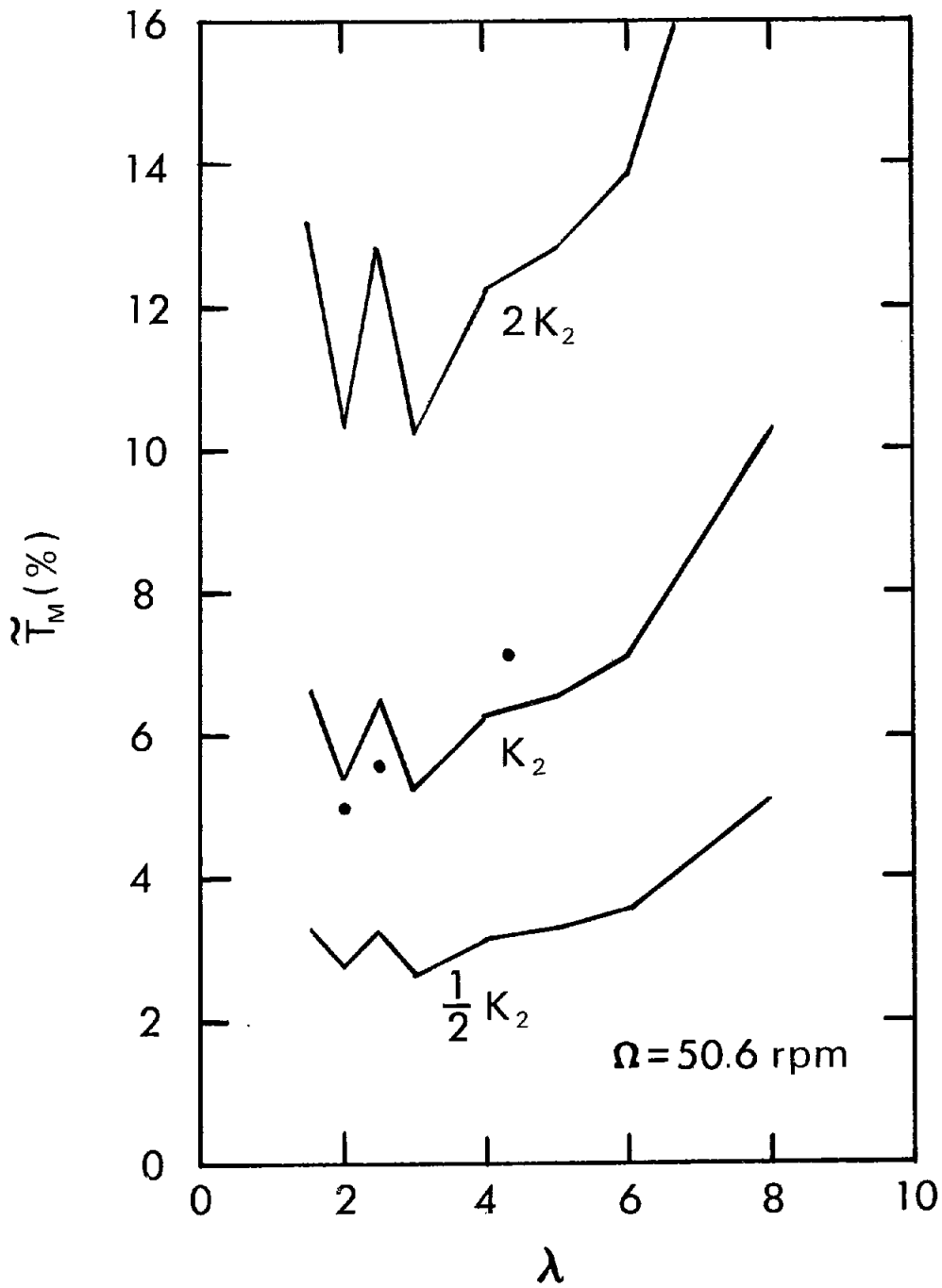


Figure 6. Torque ripple (expressed as a % of mean torque) versus tip speed ratio for various values of low speed drive train stiffness.

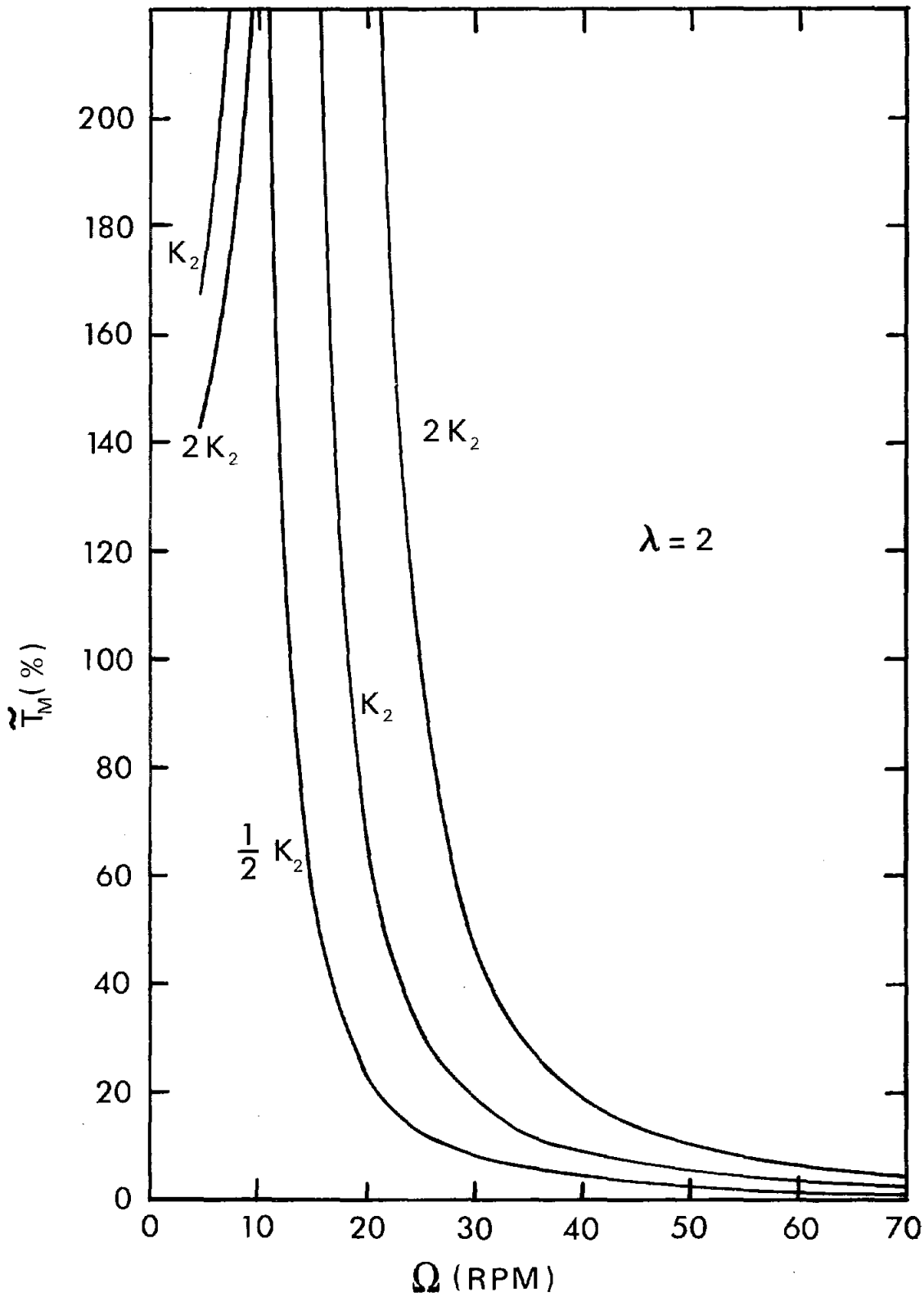


Figure 7. Torque ripple (expressed as a % of mean torque) versus turbine operating speed for various values of low speed drive train stiffness.

tends to lower apparent drive train rigidities and thus lower torque ripple. The most effective means of reducing torque ripple is, however, by reducing the low speed rigidity. This can be shown as follows.

Let K_1 represent either the low speed drive train (between the rotor and the transmission) stiffness or the high speed (between the transmission and the generator) stiffness, and let K_2 represent the other. Assume that the high speed stiffness has been corrected to the low speed end by multiplying it by the square of the gear ratio of the transmission. Let the entire drive train stiffness be represented by \bar{K} . Then

$$\bar{K} = \frac{K_1 K_2}{K_1 + K_2} \quad (6)$$

The change in \bar{K} can be expressed in terms of K_1 and K_2 and a change in either of these, say ΔK_1 .

$$\frac{\Delta \bar{K}}{\bar{K}} = \frac{\Delta K_1}{K_1} \left[\frac{K_2}{K_1 + K_2 + \Delta K_1} \right] \quad (7)$$

Now, let K_1 represent the high speed stiffness and recognize that $K_1 \gg K_2$. From Eq. 7

$$\lim \frac{\Delta \bar{K}}{\bar{K}} \rightarrow 0 \text{ as } \frac{K_2}{K_1} \rightarrow 0$$

which implies that, for a given change in the high speed stiffness, the net effect is nearly zero. Now let K_2 represent the high speed stiffness and recognize that $K_2 \gg K_1$. From Eq. 7

$$\lim \frac{\Delta \bar{K}}{\bar{K}} \rightarrow \frac{\Delta K_1}{K_1} \quad \text{as} \quad \frac{K_1}{K_2} \rightarrow 0$$

This implies that a change in the low speed stiffness will result in approximately an equivalent change in the overall drive train stiffness. Therefore, drive train stiffness changes are most effective when made at the low speed end. This result depends upon the high speed stiffness being much greater than the low speed stiffness, a condition which is most always true because of the effect that the gear ratio has on the high speed stiffness.

CONCLUSIONS AND RECOMMENDATIONS

Currently, the deterministic torque ripple problem is well understood. The source of torque ripple, its behavior with operating conditions, its response to property changes, and its allowable levels have been analytically predicted and experimentally verified¹. Torque ripple in two-bladed VAWT systems can be maintained at acceptable levels.

As mentioned earlier, collection of data for correlation with the deterministic solution is difficult. This is due to the stochastic nature of the wind which tends to increase torque ripple in the turbine drive train above values predicted by the deterministic model. As turbines increase in size, their natural frequencies are induced and their response times more nearly match the frequency content of the wind, thus aggravating the problem. Logically, the next step in torque

ripple modeling should deal with the stochastic nature of the wind, in terms of both its magnitude and its direction. It is this author's feeling, however, that this additional characterization will have to begin with a modification of the aerodynamic codes which predict the torque applied to the turbine.

ACKNOWLEDGMENT

The willing and frequent assistance of G. M. McNerney, New Mexico Engineering Research Institute, University of New Mexico, in providing the Fourier coefficients of the applied torque used in the numerical evaluation of torque ripple is gratefully acknowledged.

REFERENCES

1. R. C. Reuter, and M. H. Worstell, Torque Ripple in a Vertical Axis Wind Turbine, SAND78-0577 (Albuquerque, NM: Sandia National Laboratories, 1978).
2. P. J. Sutherland, unpublished work, (Albuquerque, NM: Sandia National Laboratories).
3. L. P. Mirandy, "Rotor/Generator Isolation for Wind Turbines," Journal of Energy, 1, No. 3 (May-June, 1977).
4. J. H. Strickland, B. T. Webster, and T. Nguyen, A Vortex Model of the Darrieus Turbine: An Analytical and Experimental Study, SAND79-7058 (Albuquerque, NM: Sandia National Laboratories, 1980).
5. P. C. Klimas, and R. E. Sheldahl, Four Aerodynamic Prediction Schemes for Vertical Axis Wind Turbines: A Compendium, SAND78-0014 (Albuquerque, NM: Sandia National Laboratories, 1978).
6. M. H. Worstell, Aerodynamic Performance of the 17-Meter-Diameter Darrieus Wind Turbine, SAND78-1737 (Albuquerque, NM: Sandia National Laboratories, 1979).
7. G. M. McNerney, Fourier Coefficients of Aerodynamic Torque Functions for the DOE/Sandia 17-M Vertical Axis Wind Turbine, SAND79-1508 (Albuquerque, NM: Sandia National Laboratories, 1980).
8. C. W. Richards, Engineering Materials Science (San Francisco: Wadsworth Publishing Company, Inc., 1961).

GUY CABLE AND FOUNDATION DESIGN TECHNIQUES

Thomas G. Carne

INTRODUCTION

On most vertical axis wind turbines support for the top of the tower is provided by guy cables. Cantilevered turbines or other means of support have been used; however, guy cable support appears to be the least expensive with most designs. For the guy cables to provide the support for the turbine, they must be designed to certain strength and stiffness requirements. Clearly they must be strong enough to hold the turbine in the highest winds which are specified for both parked and operating conditions. Also, the fatigue life of the cables, given the operating environment, must at least match that of the turbine. The stiffness requirement for the cables may be controlled by a number of aspects of the turbine design, such as the tolerances of the bearings at the base of the turbine or the natural frequency of a particular mode of vibration.

In addition to the cable strength and stiffness, there are a number of other consequences of the cable design which need to be considered. These include the cable sag, the blade/cable

clearance, the lateral vibrations of the cables, thermal expansion effects, the optimum number of guy cables, and the cable foundations. Each of these topics will be briefly discussed in this report with references to more detailed discussions and derivations.

CABLE STATICS

In this section we will examine static properties of the guy cables which include cable sag, cable stiffness, and the initial cable tension. Figure 1 displays the cable geometry and indicates some of the notation. The sag perpendicular to the cable can be approximated by the parabolic expression¹

$$d = \frac{w \cos^2 \alpha}{2T} s(C - s) , \quad (1)$$

where w is the weight per unit length, α is the cable elevation angle, T is the tension, C is the cable span, and s is the distance along the span from the top of the tower.

Note that the sag, d , is proportional to the weight per unit length or equivalently the cross-sectional area; also it is inversely proportional to the tension. Figure 2 shows the sag plotted as a function of the tension at the midpoint of the cable and at a point, $s = 0.13 C$, which is closer to the blades.

The axial stiffness of a guy cable has two components. One component is due to the elastic stretch of the cable, and the other is due to elongation of the span by pulling out the sag in the cable. When the sag is very small compared to the span, the axial stiffness can be approximately represented by²,

$$k = \left[\frac{C}{AE} + \frac{w^2 C^3 \cos^2 \alpha}{12 T^3} \right]^{-1} , \quad (2)$$

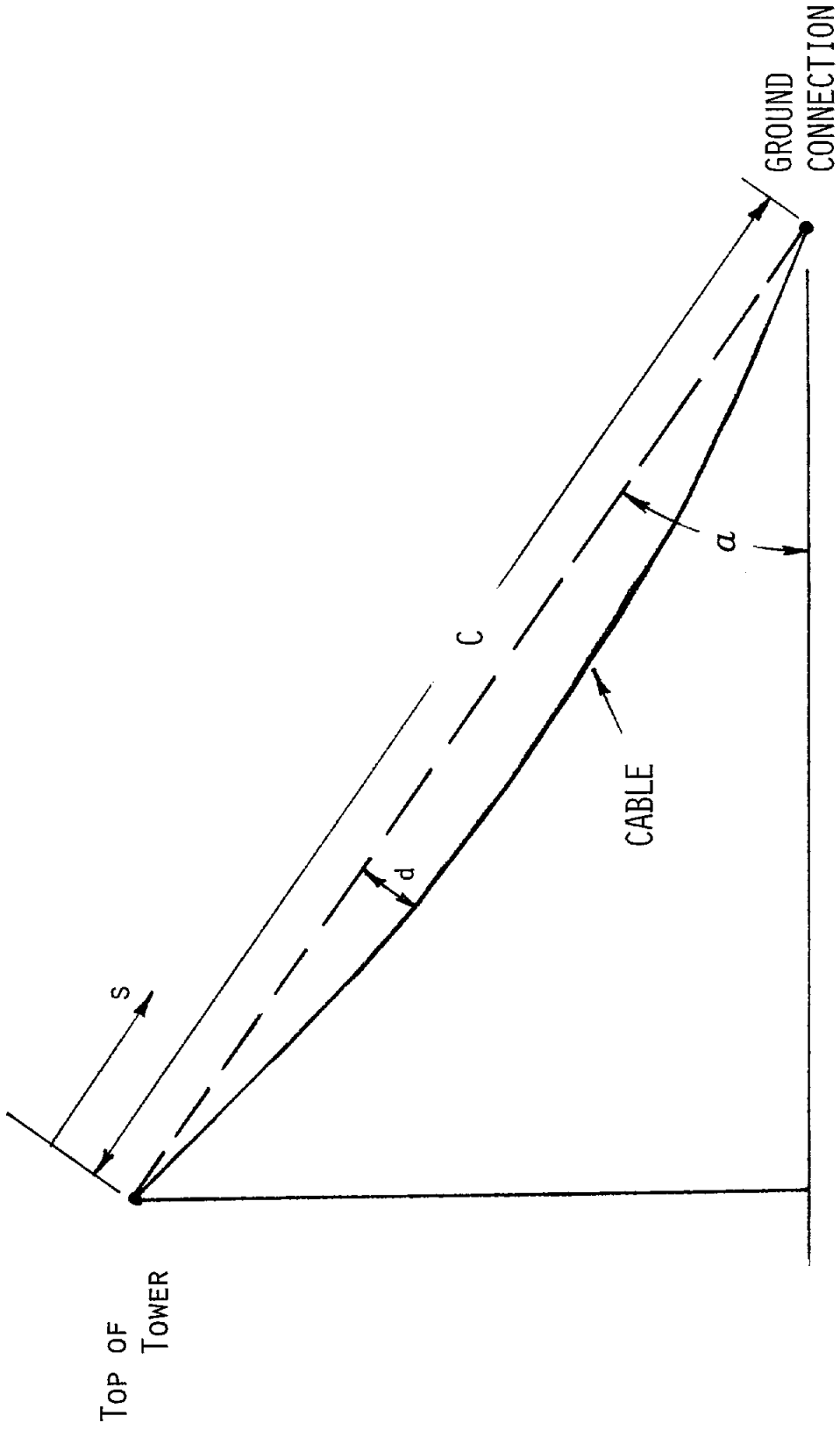


FIGURE I: CABLE GEOMETRY

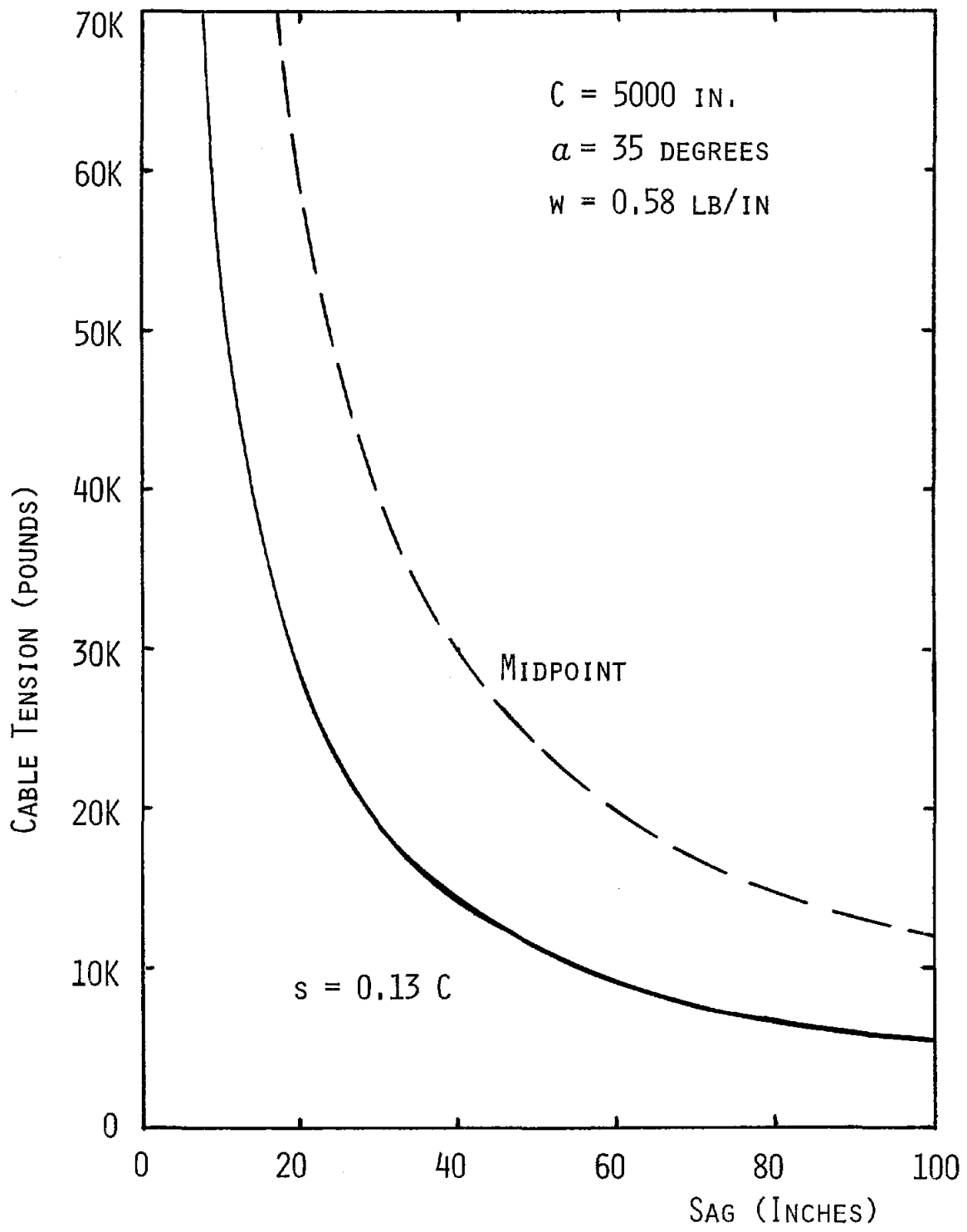


FIGURE 2: CABLE TENSION VERSUS CABLE SAG AT MIDPOINT AND $s = 0.13C$ FOR A MID-SIZE TURBINE

where A and E are the effective cross-section and modulus of the cable. The two components of the stiffness are clearly observed in this expression. Only for very taut cables can the first term alone, AE/C, be taken for the stiffness. To obtain the horizontal stiffness at the top of the tower, the cable axial stiffness is multiplied by $\cos^2 \alpha$. Figure 3 shows the cable stiffness plotted as a function of the tension. One can see from the figure how the stiffness approaches its asymptotic value. Figure 4 plots the stiffness as a function of the cross-sectional area A, keeping in mind that w is proportional to A through the density. Consequently, changes in the stiffness due to changes in the cross-sectional area are opposed by the two terms in the stiffness formula.

An important aspect of the cable stiffness is its nonlinear behavior. Since the tension (or force) appears in the stiffness formula (2), the stiffness is not constant with changes in the deflection. Consequently, as the top of the turbine deflects in the downwind direction, the stiffness contribution from each of the cables will change. In order to understand this nonlinear feature of the cables, let us rewrite (2) as

$$k = \frac{dT}{du} = \left[\frac{C}{AE} + \frac{w^2 C^3 \cos^2 \alpha}{12 T^3} \right]^{-1},$$

where u is the axial deflection. This equation can be integrated to obtain the displacement as a function of the tension. In this integration we can assume the span C is constant as long as the deflections are very small compared to the span, and this integration yields

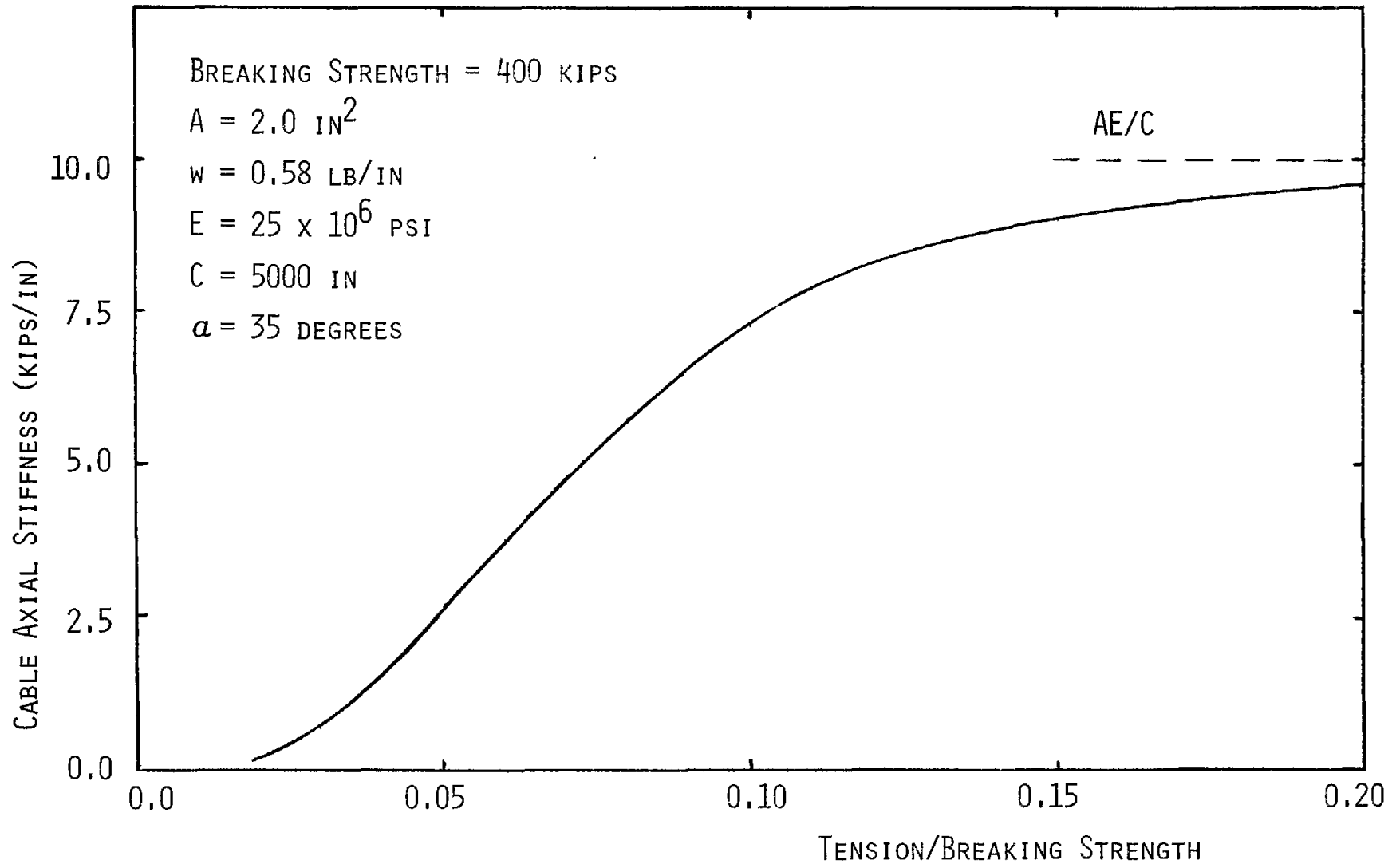


FIGURE 3: CABLE STIFFNESS VERSUS CABLE TENSION/BREAKING STRENGTH

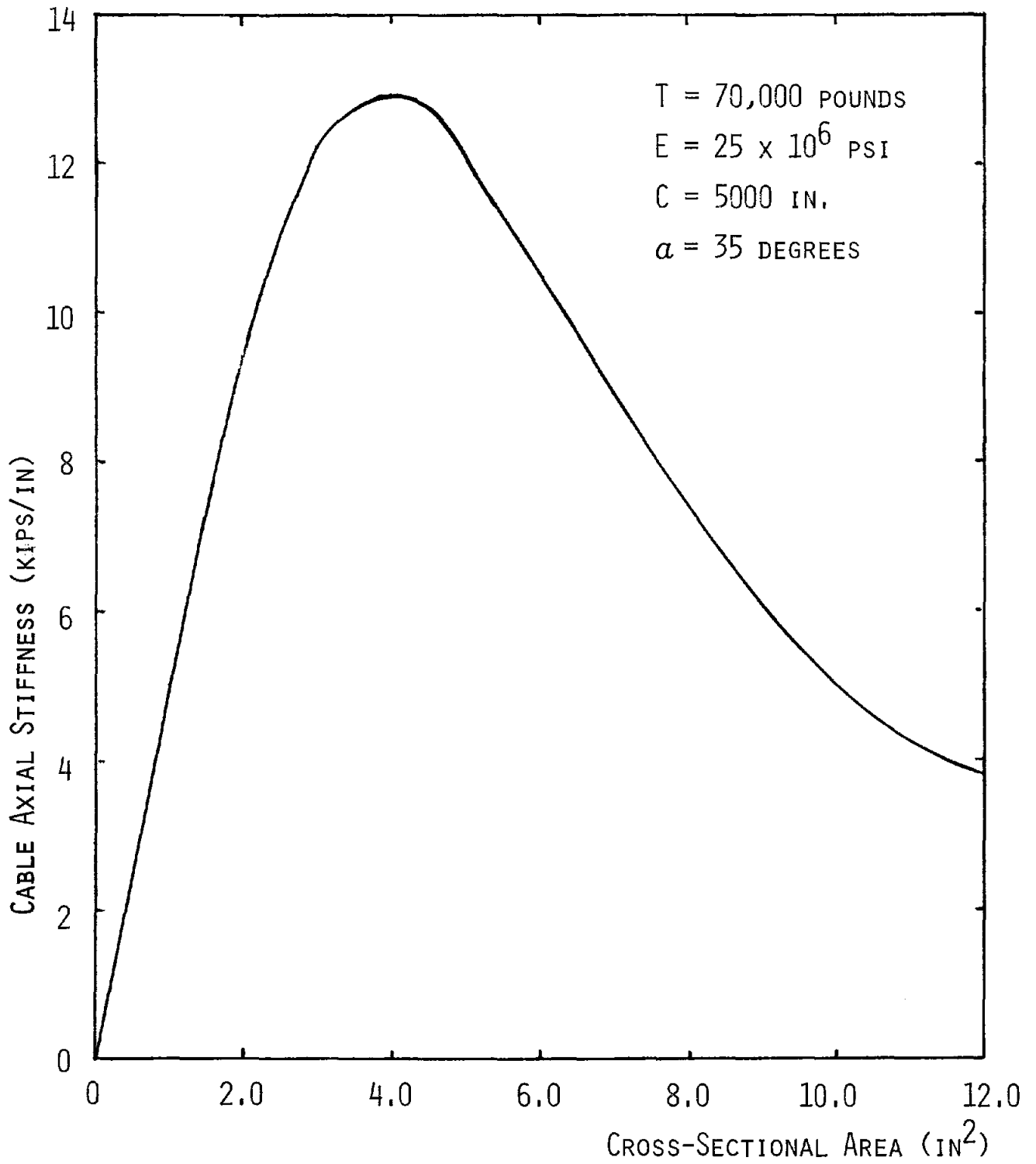


FIGURE 4: CABLE STIFFNESS VERSUS CABLE CROSS-SECTIONAL AREA

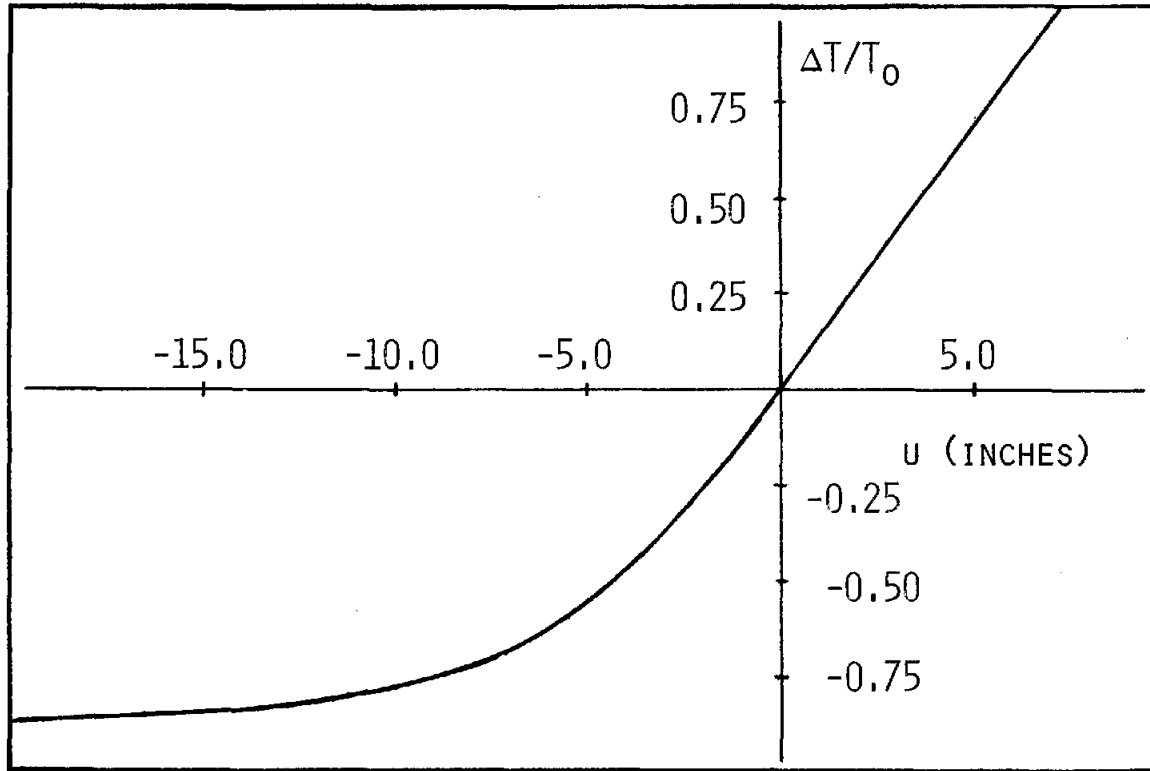
$$u = \left[\frac{C}{AE} + \frac{w^2 C^3 \cos^2 \alpha}{24} \frac{(2T_0 + \Delta T)}{T_0^2 (T_0 + \Delta T)^2} \right] \Delta T \quad (3)$$

where T_0 is the initial tension and ΔT is the change in tension. Figure 5 shows how the tension varies with the axial deflection. For high tensions it can be seen that the stiffness, $k = dT/du$, is constant and equal to AE/C ; for lower tensions the effect of the sag term becomes more important, and the stiffness is reduced dramatically. Figure 6 plots the stiffness versus the axial deflection.

Figure 5 is a useful design tool in two respects. First, it shows how quickly the tension in a cable can change when the top of the turbine moves. Secondly, it reveals the rate at which a cable must be tensioned as it is pulled to a cable anchor.

CABLE DYNAMICS

The only aspect of cable dynamics that has entered into current turbine design is the lateral vibrations of the cables. When the turbine is operating, the top of the turbine continuously moves as a result of the aerodynamic forces on the blades, with the net force resisted by the axial stiffness of the cables. This motion of the top of the turbine excites lateral vibrations in the cables. If a natural frequency of a guy cable is close to two per rev of the turbine (for a two-bladed turbine), then very large amplitude cable vibrations occur. Cable vibration causes concern due to the possibility of a blade strike and due to fatigue of the cable end fittings and attachments and the cable itself. The natural frequencies of vibration of a taut cable are



$T_0 = 70,000$ POUNDS
 $A = 2.0$ IN
 $w = 0.58$ LB/IN
 $E = 25 \times 10^6$ PSI
 $C = 5000$ IN
 $\alpha = 35$ DEGREES

FIGURE 5: THE CHANGE IN CABLE TENSION VERSUS CABLE AXIAL DISPLACEMENT

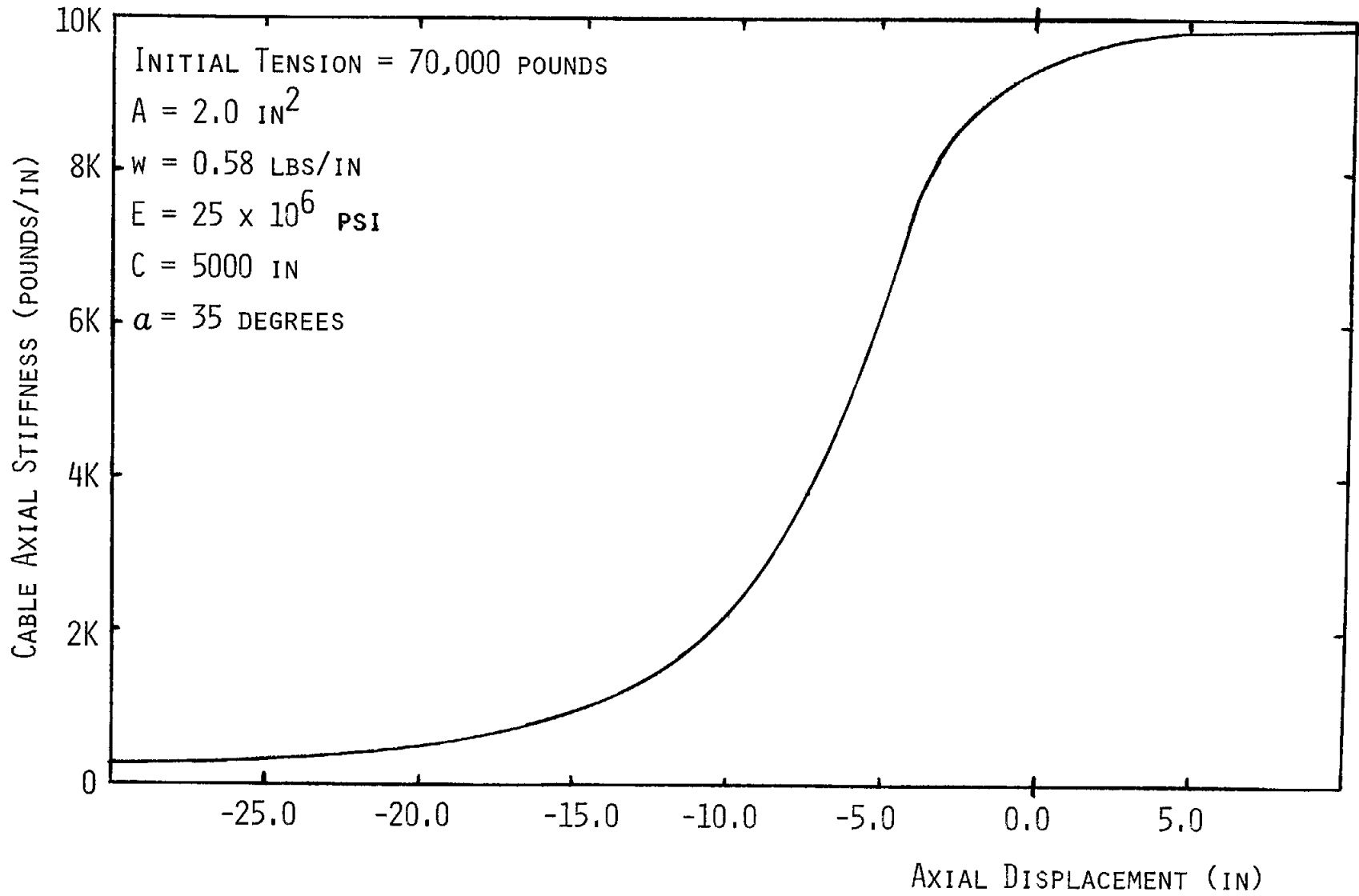


FIGURE 6: CABLE STIFFNESS VERSUS AXIAL DISPLACEMENT

$$f_n = \frac{n}{2C} \sqrt{\frac{T}{w/g}}, \quad (4)$$

where n is an integer and g is the gravitational acceleration. Experimental tests on the guy cables of the Sandia 17-Meter Research Turbine have verified the above expression and have yielded damping factors of two-tenths of one percent of critical, which are exceedingly low.

To insure that cable vibrations are not greatly excited, the cable tension must be so high that the lowest frequency in (4) is greater than two per rev (for a two-bladed turbine). However, this requirement is expensive for the turbine design as the prescribed cable tension impacts the requirements on the turbine and cable foundations, the bearings in the tower, and the buckling load of the tower. In order to reduce the tension below this requirement, some damping or constraint device will be necessary. A constraint on the cable, which drives up the natural frequencies above two per rev, or a damping device, which limits the dynamic amplification of the cable motion, would enable the tensions to be lowered below the vibration imposed limit. Setting the initial tension so that the cable frequencies lie between the excitation frequencies will probably not be sufficient since the results of the wind loading and thermal effects increase the prescribed initial tension into a fairly wide band of actual operating tensions.

CABLE/BLADE CLEARANCE

An important element in the guy cable design is the clearance distance between the cable and the blades, which has been discussed in detail^{3 4}. If we define the geometric

clearance as the distance between the blade and the cable, assuming that the cable is straight rather than sagging; then the geometric clearance must be sufficient for cable sag, cable vibration, and the motion of the blades, with an appropriate safety factor. For ease in design the clearance specification has been defined for a single point on the blades called the strike point. For most Darrieus turbine designs this point is the junction of the straight and curved sections of the blade.

The minimum requirement for the geometric clearance is the sum of a vibration requirement and a sag requirement. The blade motion has been assumed to be very small compared to potential cable vibrations and consequently is neglected. The vibration requirement is

$$\text{Vib} = 0.015 C, \quad (5)$$

and the sag requirement for a cable elevation angle of thirty-five degrees is

$$\text{Sag} = 0.038 w C^2/T. \quad (6)$$

Thus, the geometric clearance must equal or exceed Sag plus Vib. The sag requirement should be evaluated with the lowest conceivable tension that can result during operation and include thermal effects which will be discussed later. Also, the sag requirement will depend on the elevation angle of the cable. One should note that Sag is proportional to C^2 while Vib is only proportional to C , so Sag will grow faster than Vib with larger turbines. However, Sag will not exceed Vib until the turbine is very large.

The cable elevation angle of thirty-five degrees is the angle which produces a maximum horizontal stiffness for a given tension and cross-sectional area⁵. Other angles definitely can be considered in order to reduce the axial load on the tower, reduce the land area spanned by the cables, or other considerations. An elevation angle of thirty-five degrees or less does ease the design since it increases the geometric clearance. Another method to obtain a larger geometric clearance is to include some sort of cable outrigger on the top of the tower. However, outriggers have not proven to be economically or structurally efficient in most designs.

THERMAL EFFECTS

Because of thermal expansion in the tower and the cables, daily and seasonal temperature changes cause the tension in the cables to vary⁵. Experimental studies performed on the Sandia 17-Meter Turbine⁶, show that during daylight the temperature of a white tower exceeds the ambient temperature by as much as ten degrees. Also the temperature of the cables is generally greater than that of the tower. Defining β by $\Delta T_c = \beta \Delta T_t$, where ΔT_c and ΔT_t are the temperature changes of the cables and the tower occurring during one day; then the largest factor, β , measured in Albuquerque was 1.12. Given a certain change in temperature of the tower, then the change in cable tension, ΔP , was shown⁵ to be

$$\Delta P = \frac{k_t k_c (\eta_t \sin^2 \alpha - \eta_c \beta) C \Delta T_t}{k_t + 4k_c \sin^2 \alpha}, \quad (7)$$

where C is the cable length, k_t and k_c are the stiffnesses of the tower and a cable, α is the cable elevation angle, and η_t and η_c are the tower and cable thermal expansion

coefficients. Using k_c to represent the axial stiffness of the cable in equation (7) is slightly more general than equation (23)⁵ in that k_c could represent the cable stiffness even in the nonlinear region.

Equation (7) can be simplified if k_c is much less than k_t , and then we have

$$\Delta P = k_c (\eta_t \sin^2 \alpha - \eta_c \beta) C \Delta T_t . \quad (8)$$

This equation is easy to understand physically as it equates the change in tension to the product of a difference of thermal expansion coefficients, the cable length, the change in temperature, and the cable axial stiffness. Figure 7 shows the change in cable tension as a function of the temperature change in the tower for various values of β for the 17-Meter Turbine. The figure shows that a forty degree change in tower temperature with a $\beta = 1.12$ causes a reduction in the cable tension of three thousand pounds, which is about twenty percent of the initial tension.

NUMBER OF CABLES

The number of cables required to support the turbine is obviously at least three; however, the optimum number of cables is an open question. There are two aspects of this question--the structural response quantities and the cost. Examining first the structural quantities, let us compare two different cable designs, one with N equally spaced cables and the other with M equally spaced cables, with M greater than N . Size the M cables so that the cross-sectional areas and the tensions are N/M times that of the N cable design. We leave

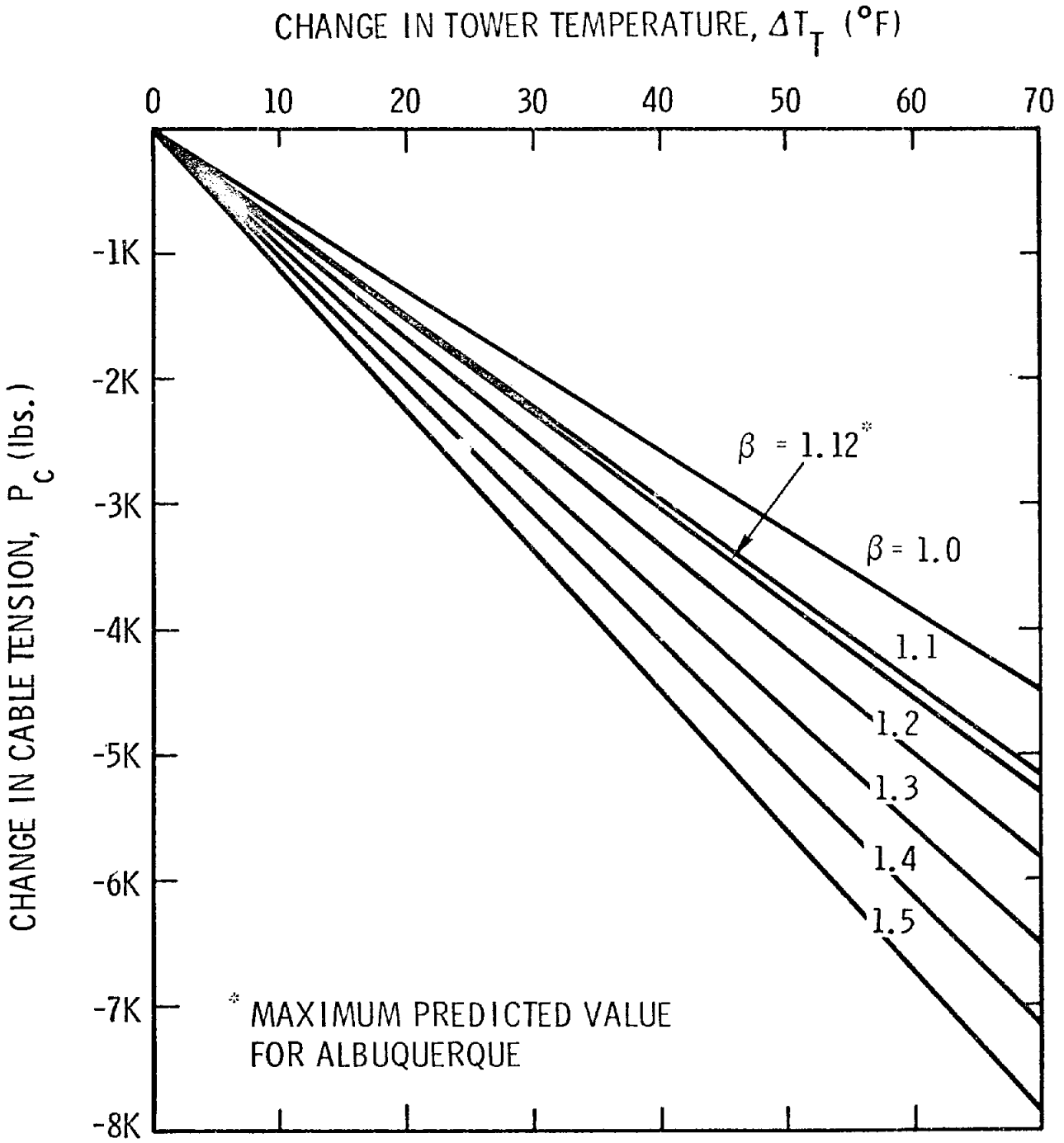


FIGURE 7: THE CHANGE IN CABLE TENSION VERSUS THE CHANGE IN TOWER TEMPERATURE

the cable elevation angle and the cable length the same. These two different designs are identical in the following structural characteristics: (1) the axial cable stiffness including the nonlinear term; (2) the cable sag distance; (3) the total axial load imposed on the tower; (4) the total weight of all the cables; (5) the lateral frequencies of the cables; (6) the stress in the cables; and (7) the loss in tension due to thermal expansion. In fact, the two designs are identical in their physical behavior with the following minor qualification. The equivalence holds to the degree that the cable response remains linear during operation when the tensions of the cables vary due to the aerodynamic loads. For the cable designs currently considered, this qualification can be ignored. More discussion and derivation of these above statements are available.⁷

We return now to the cost considerations since the structural features of the two designs are identical for all practical purposes. As the total volume of material of the two cable designs are the same, the cost considerations would include: (1) the cost per unit weight of different size cables; (2) the cost of M smaller anchors as compared to N larger ones; (3) the cost in handling different size cables; (4) the cost of cable tension adjusters; (5) the cost of a device for pulling the cables to the anchors; plus other fabrication or assembly costs. Also, the factor of safety on the anchors could conceivably be reduced if the cable system was redundant (five or more cables).

GUY CABLE FOUNDATIONS

In this section on the foundations or anchors for the cables, very little detail will be included since there are two very complete references which also include design information for the turbine foundation^{8 9}. To briefly summarize, there

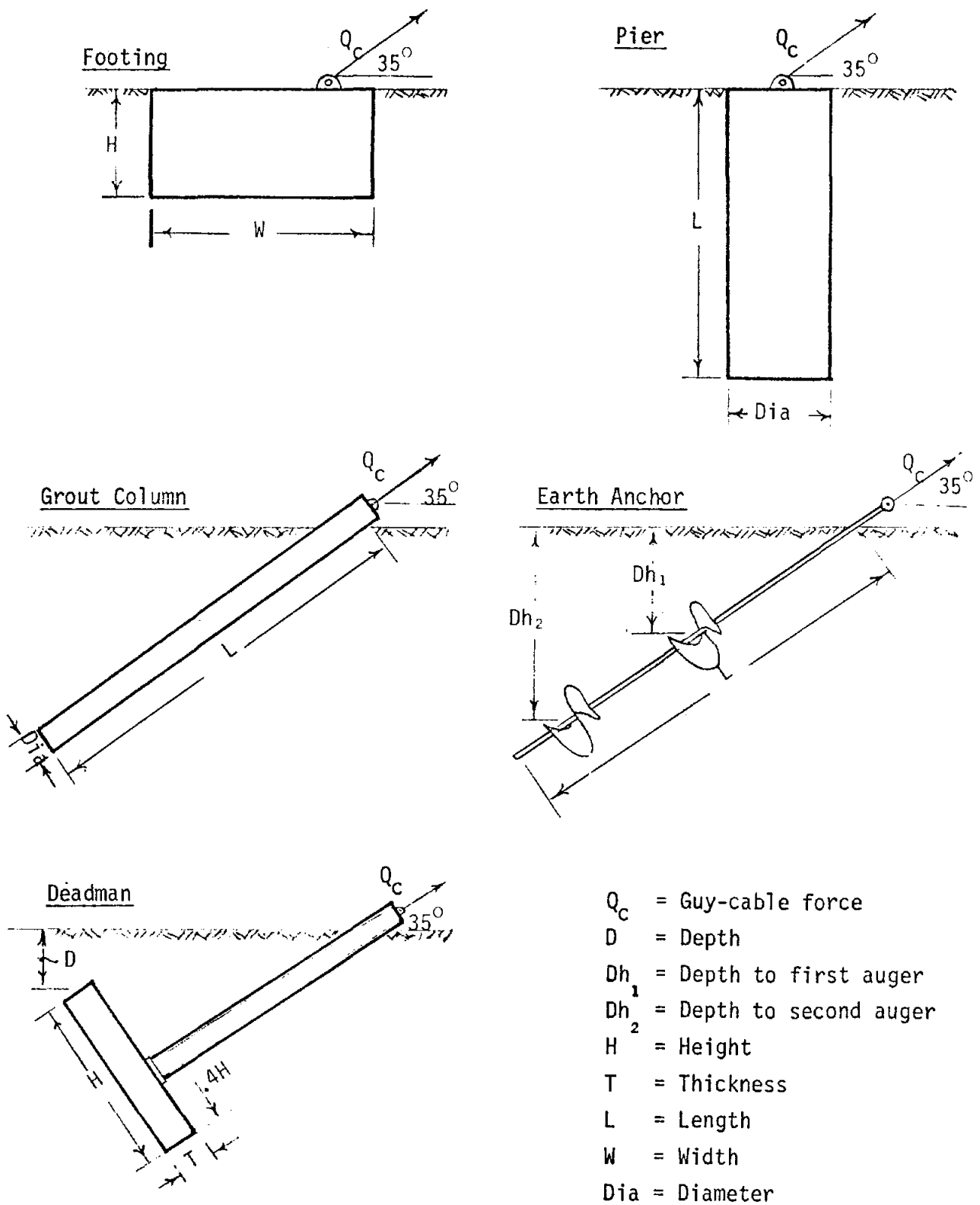


Figure 8. Guy-Cable Anchor Types

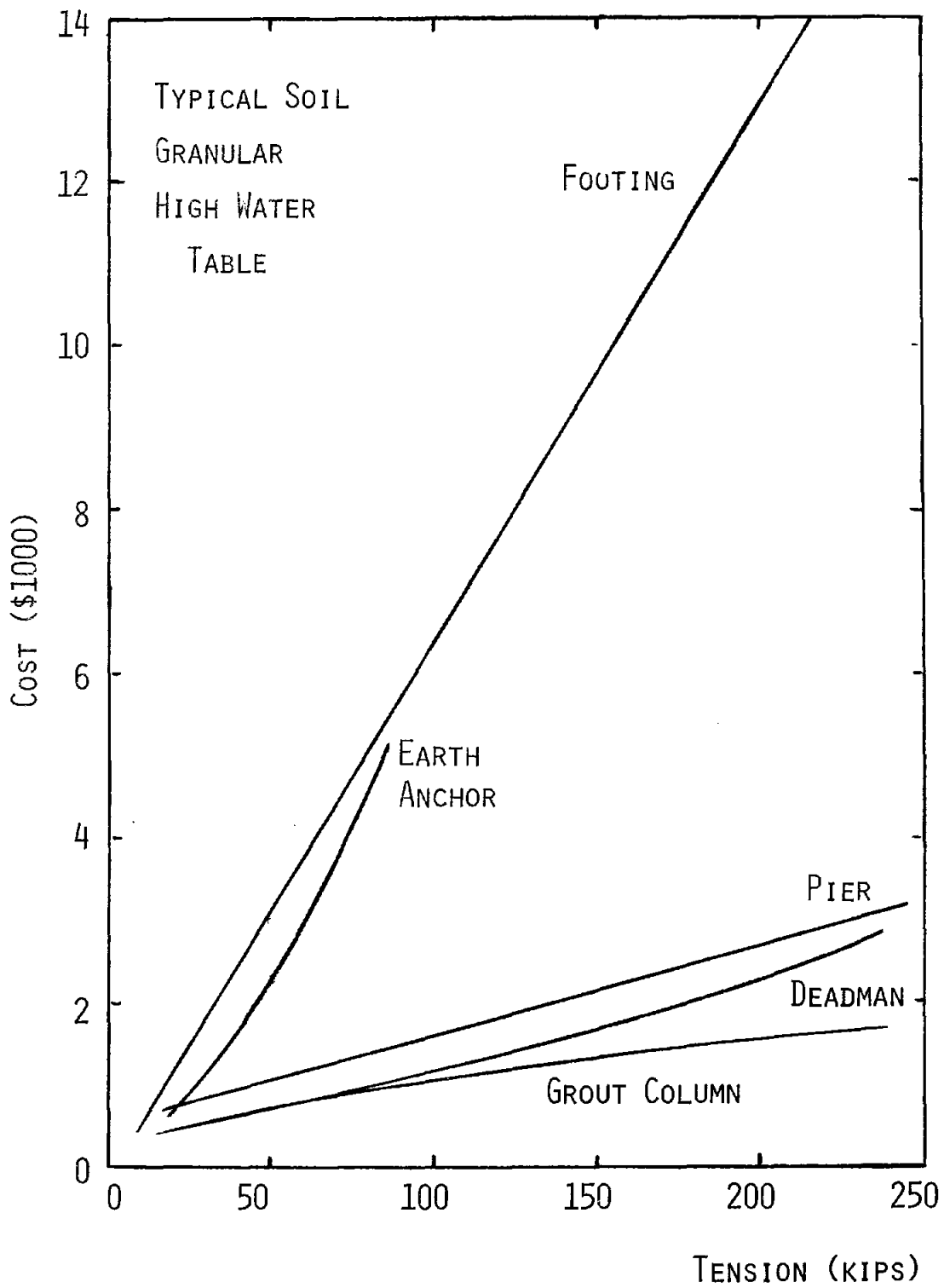


FIGURE 9: CABLE ANCHOR COST VERSUS TENSION

are five basic kinds of cable anchors, and they are diagrammed in Figure 8⁸. The best or least expensive anchor for a particular turbine will depend on the guy tension, the soil conditions, the movement tolerances on the foundation, and local building practice. Figure 9 plots the cost of a foundation versus the cable tension for these five foundation types⁸. The figure is for a typical soil which is granular with a high water table. However, these data can look far different for other soil conditions, so this figure should not be assumed to be typical. Complete data is available^{8 9} on other soil conditions and on the movement tolerances for the foundations.

REFERENCES

1. R. C. Reuter, Jr., Tie-Down Cable Selection and Initial Tensioning for the Sandia 17-Meter Vertical Axis Wind Turbine, SAND 76-0616 (Albuquerque, NM: Sandia National Laboratories, 1977).
2. M. Shears, Static and Dynamic Behavior of Guyed Masts, Report No. 68-6, Berkeley, CA: University of California, Structures and Materials Research Dept. of Civil Engineering, 1968.
3. Carne, T. G., Internal Memorandum, Sandia National Laboratories, Albuquerque, NM, September 26, 1979.
4. Carne, T. G., Internal Memorandum, Sandia National Laboratories, Albuquerque, NM, February 27, 1980.
5. R. C. Reuter, Jr., Vertical Axis Wind Turbine Tie-Down Design with an Example, SAND 77-1919 (Albuquerque, NM: Sandia National Laboratories, 1977).
6. A. Ortega, Internal Memorandum, Sandia National Laboratories, Albuquerque, NM, May 17, 1977.
7. Carne, T. G., Internal Memorandum, Sandia National Laboratories, Albuquerque, NM, to be published.
8. H. E. Auld, and P. F. Lodde, A Study of Foundation/Anchor Requirements for Prototype Vertical-Axis Wind Turbines, SAND 78-7046 (Albuquerque, NM: Sandia National Laboratories, 1979).
9. P. F. Lodde, Wind Turbine Foundation Parameter Study, SAND80-7015 (Albuquerque, NM: Sandia National Laboratories, 1980).

SECTION IV
AERODYNAMIC PERFORMANCE OF VAWT SYSTEMS

VERTICAL AXIS WIND TURBINE AERODYNAMIC
PERFORMANCE PREDICTION METHODS

Paul C. Klimas

Nomenclature

A_s	Turbine swept area
c	Blade chord
C_ℓ	Blade airfoil section lift coefficient = $\ell / (1/2) \rho_\infty V_\infty^2 c$
C_d	Blade airfoil section drag coefficient = $d / (1/2) \rho_\infty V_\infty^2 c$
C_p	Power coefficient, $Q\omega / (1/2) \rho_\infty V_\infty^3 A_s$
d	Blade airfoil section aerodynamic drag
K_p	Power coefficient, $Q\omega / (1/2) \rho_\infty A_s (R\omega)^3 = C_p / X^3$
L	Blade length
ℓ	Blade airfoil section aerodynamic lift
N	Number of blades
Q	Turbine torque
R	Turbine maximum radius
Re_c	Chord Reynolds number, $\rho_\infty R\omega c / \mu_\infty$
V_∞	Freestream velocity
X	Turbine tip speed ratio, $R\omega / V_\infty$
α	Blade section angle-of-attack
μ_∞	Freestream viscosity
ρ_∞	Freestream density
ω	Turbine rotational speed
σ	Solidity, NcL / A_s

I. Introduction

A large collection of models exist which predict aerodynamic performance of vertical axis wind turbines (VAWTs). These models range from the relative simplicity of calculations based upon a combination of empirical information and conservation of momentum principles to those using rather complex vortex filament representations and may or may not include unsteady effects. Reference 1 lists and briefly describes many of the quasi-steady approaches while Ref. 2 discusses some of the dynamic treatments. Sandia Laboratories uses three basic computer schemes when making VAWT aerodynamic performance calculations. The specific choice depends upon the relative needs of modeling accuracy and computational speed. This paper describes each of the three schemes and gives examples of their capabilities. Since each model requires access to turbine blade aerodynamic section data, some attention is also given to the origins of the data used at Sandia Laboratories.

II. Aerodynamic Performance Models

A. DARTER (Darrieus Turbine, Elemental Reynolds Number)

DARTER³ is an essentially analytical model which has its physical basis in the conservation-of-momentum principle and is quasi-steady. The assumptions made and descriptive equations are reminiscent of the classical actuator-disc model of propeller aerodynamics. DARTER uses a multiple streamtube system, i.e., the turbine swept area is modeled by an arbitrary number of adjacent and aerodynamically independent areas over which the conservation-of-momentum principle is applied. A typical streamtube is shown in Fig. 1. A detailed description of the mathematical development is given in Ref. 4 and is

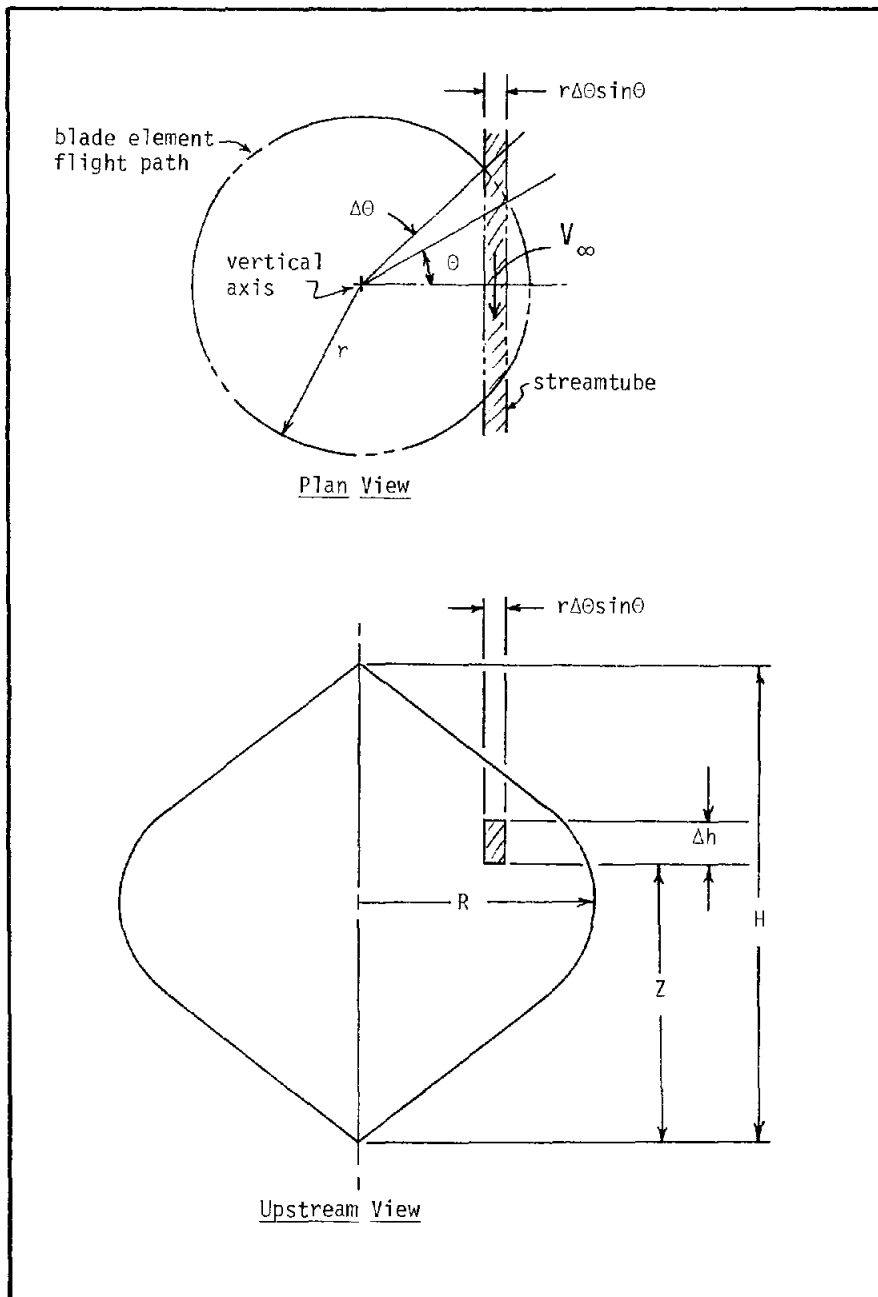


FIGURE 1. Typical Streamtube

summarized as follows. Since energy is extracted by the turbine blade elements as they pass through any streamtube, the rotor streamtube velocity is less than the ambient airstream velocity. A time averaged streamwise momentum equation can be used along with the Bernoulli equation to relate the streamwise force exerted by the blade elements to both the rotor streamtube and ambient airstream velocities. The streamwise force may be resolved into components normal and tangential to the blade element. The latter, of course, contributes to the rotor torque. These two force components may be non-dimensionalized and related through a simple rotational transformation to the blade section aerodynamic coefficients, C_l and C_d , and the blade element angle-of-attack, α . The ultimate expression of the streamwise conservation-of-momentum is a transcendental equation in one unknown, the rotor streamtube velocity. This equation is iteratively solved with each iteration involving access to blade section characteristics data. Convergence is nominally quite rapid. Reference 4 states that computer (CDC 6600) processing time averages 4×10^{-3} seconds per streamtube with a convergence error of less than 1×10^{-3} on the ratio of streamtube-to-ambient velocity. Rotor power, torque, and drag are obtained by averaging the contributions from each streamtube.

The blade section airfoil characteristics used at Sandia Laboratories are tabulated as C_l and C_d vs. α for a number of values of Reynolds number. A two-way interpolation is performed in the DARTER conservation-of-momentum equation iteration. This allows for the use of accurate section data values when considering variations in circumferential and spanwise blade relative velocities. Included in the latter are effects due to ambient windstream shear.

Blade planform geometries treated by DARTER include straight, parabolic, and straight line-circular arc-straight line troposkien approximation. Figure 2 is a comparison between

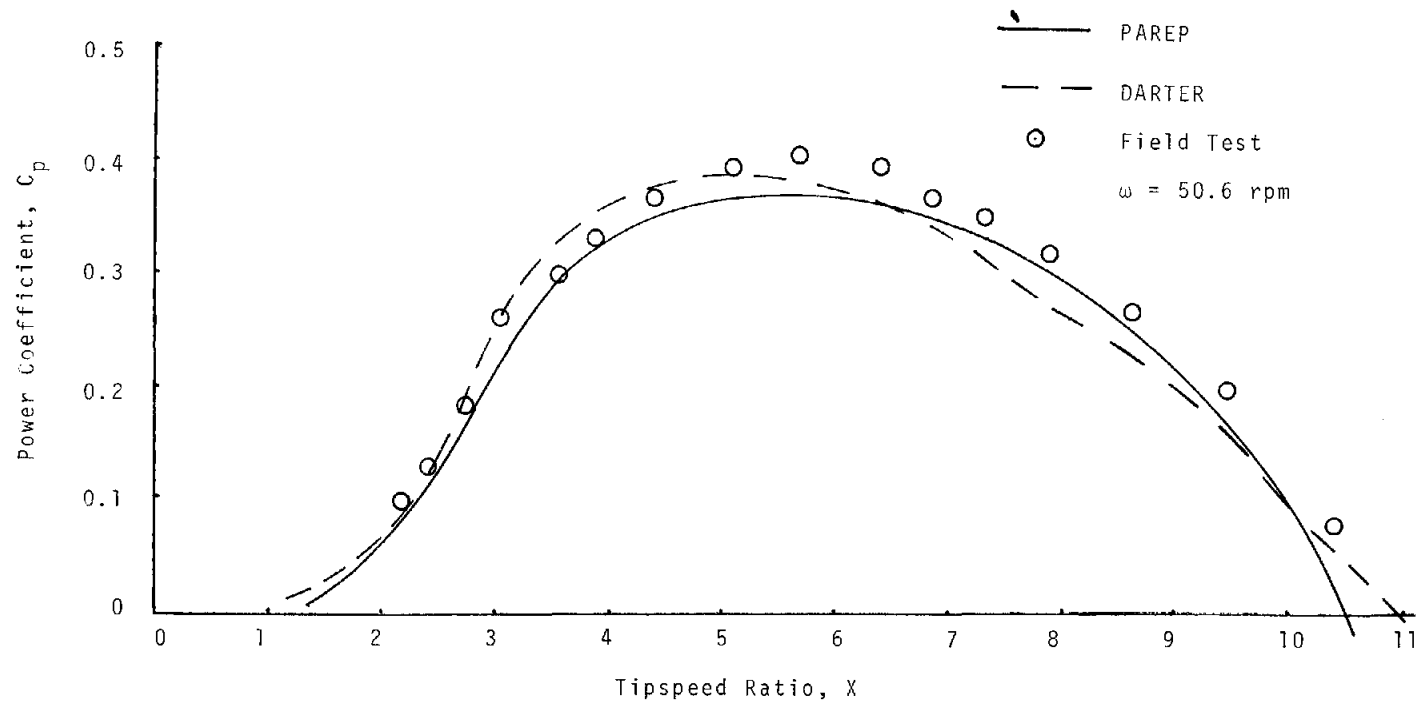


FIGURE 2. C_p vs. X , Sandia 17-m-D, $H/D = 1.0$, Two NACA 0015 24" c bladed Darrieus

DARTER predicted and actual measured performance on the Sandia 17-m-D, H/D = 1 two NACA 0015 bladed turbine. The planform here is the troposkien approximation.

B. PAREP (Parametric Representation)

PAREP⁵ falls more into the category of a design tool than that of a mathematical model. DARTER does a reasonable job of predicting maximum power coefficients (C_p 's and K_p 's) and the tipspeed/ambient windspeed ratios at which they occur. However, for high blade loadings and high solidities, there is often considerable discrepancy between theory and experiment away from the maximum power coefficients. PAREP is a sequence which combines theory with results of wind tunnel testing to better represent overall aerodynamic performance. Specifically, PAREP operates by first referencing curve fits of relevant output from DARTER for a given turbine design. This is due to the fact that, over a reasonable range of blade Reynolds number and turbine solidity, C_{pmax} , $X @ C_{pmax}$, K_{pmax} , and $X @ K_{pmax}$ can be expressed as simple functions of Re and σ . Next, 2-m wind tunnel test results are used to provide the value of X at "runaway" (high speed ratio at which zero aerodynamic torque is produced). After the user chooses some low value of the zero aerodynamic torque-speed ratio (between one and two, as the final results are relatively insensitive to a choice in this range), a curve is fit between the two zero-power speed-ratio points which passes through the two power coefficient maxima. The shape of this curve is predicted from the 2-m wind tunnel test results.

The basic advantage in using PAREP is that it is extremely fast working. Its primary function is to provide aerodynamic performance inputs to system economic evaluation parametric studies. The basic disadvantage is that the fundamental curves were fit to turbines whose design parameters and operating conditions fall into a relatively narrow range.

Figure 2 shows a typical PAREP power coefficient prediction.

C. VDART (Vortex Darrieus Turbine)

The momentum based models, while able to treat a wide range of design and operating conditions, intrinsically suffer from two major deficiencies. Firstly, since the streamtubes are aerodynamically independent, no consideration is given to the aerodynamic influence of any one blade upon the flowfield through which any other one is passing. Secondly, each streamtube calculation simultaneously treats both traverses of each blade through the streamtube. The effects of the pass through the upwind half of the streamtube are not dealt with in calculating the contributions of the blade element pass through the downwind half of the streamtube. These shortcomings are not seriously felt at low tip speed ratios where blade element wakes are relatively quickly swept downstream. However, they become more apparent as both X and the blade wake spatial density increases. The inability of the momentum models to treat these two types of blade interference led to the synthesis of a more sophisticated model, VDART,⁶ based upon a vortex filament representation of the turbine blades and their wakes.

Briefly, VDART is a vortex/lifting line representation of the turbine blades and the wake they generate. The blades are divided into segments, each of which is modeled by a single "bound" vortex which remains attached to the blade segment and a pair of "trailing" vortices at each of the segment's two extremities (see Fig. 3). These trailing vortices account for spanwise lift variations and are convected into the turbine wake. Also carried downstream of each segment are "shed" vortices which model timewise variations in the bound vorticity. The sum of velocities induced by the totality of the bound, trailing, and shed vortex systems plus that of the ambient stream define the aerodynamic flowfield. Once this is established at a given operating condition, the lift and drag of the

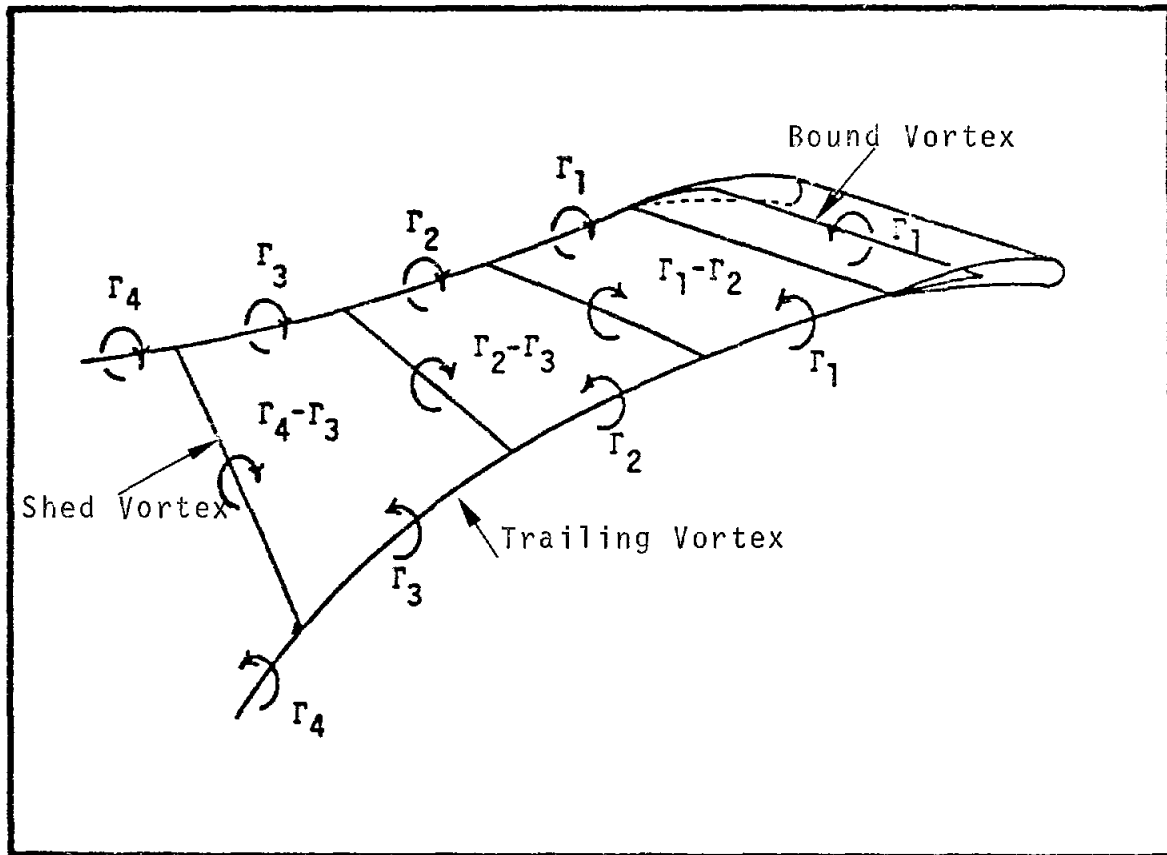


FIGURE 3. Vortex System for a Single Blade Element

blade segment is obtained using airfoil section data. Reference 6 gives a full discussion of VDART as well as a listing of the code. Also given is a two-dimensional version.

The basic mathematical representation in VDART is quite viable. Shortly after it was obtained by Sandia, VDART was modified to allow both a Reynolds number and angle-of-attack interpolation on blade airfoil section data and an ambient wind shear capability. Figure 4 illustrates a VDART power coefficient prediction as compared to field measurements on the Sandia 5-m Darrieus. Multiple turbine arrays may also be treated. Figure 5 presents some effects on aerodynamic performance of two identical Sandia 17-m turbines whose line of centers is coincident with the ambient wind direction for a single separation distance. This distance is small enough so that the neglected effects of freestream turbulence on wake decay may be considered small. Blade element dynamic stall effects have been included. Sandia experience with high Reynolds number operation of NACA 0015 section blades indicated that there was some lift curve (C_l vs. α) hysteresis as the blades passed in and out of aerodynamic stall as they traversed their circumferential paths at low tip speed ratios. Figure 6 compares the two-bladed torque measured on the Sandia 17-m turbine with that calculated by VDART modified by a simple dynamic stall model given in Ref. 7. Also shown are the unmodified, quasi-steady VDART values for the same set of conditions. Another deficiency of the momentum models is their lack of ability to model blades whose sections are unsymmetrical. This comes from the fact that the upwind and downwind traverse of each streamtube is not considered separately. The deficiency has become relevant in the light of recent efforts to bring about cost of energy reductions through aerodynamic design. The treatment of blade sections with camber or pre-set fixed pitch is quite simple with the vortex models. Figure 7 summarizes the effects of pre-set pitch on performance as given by the two-dimensional version of VDART. This 2D version was

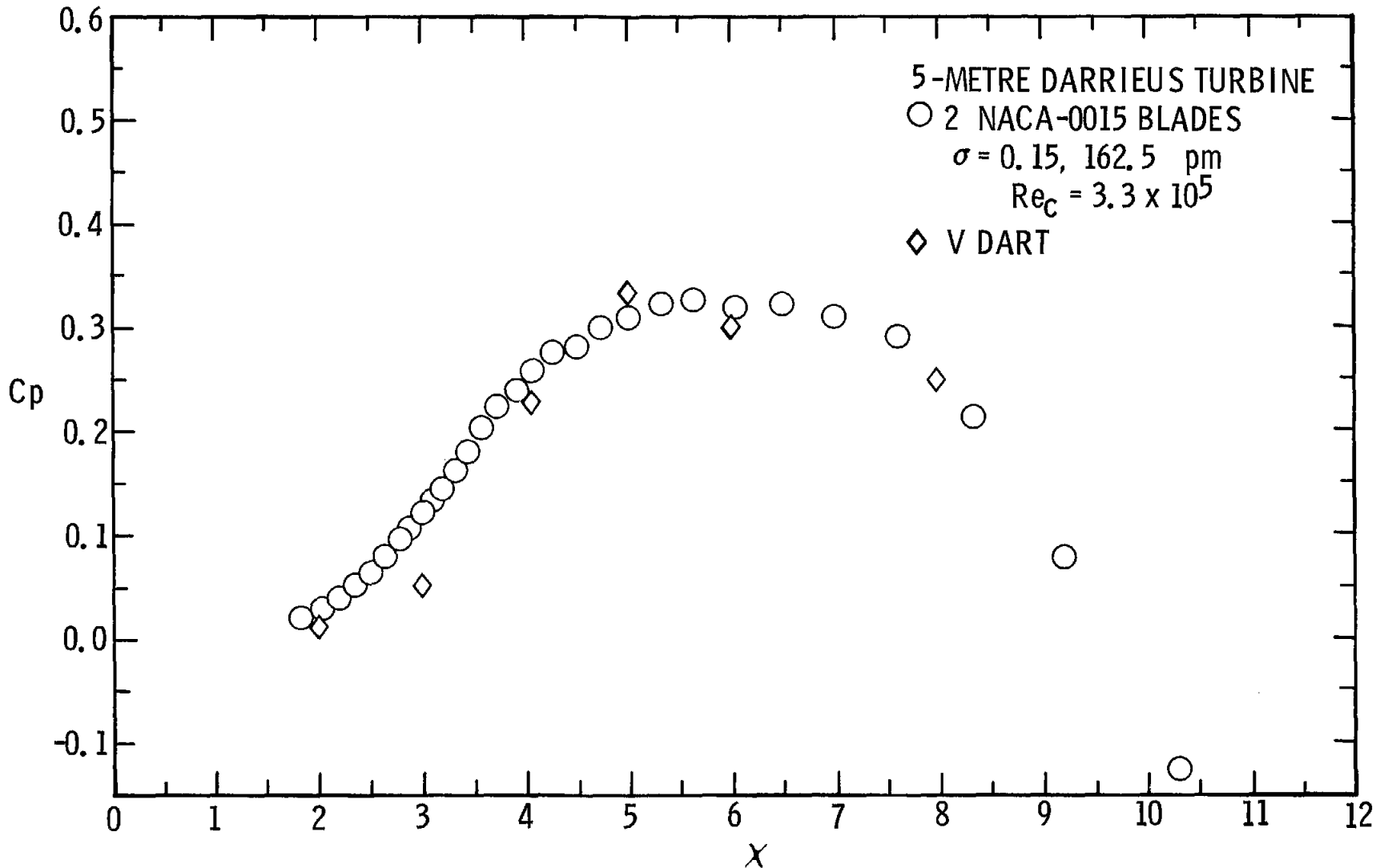


FIGURE 4. A Comparison of the Two Bladed 5-m Turbine Performance Data with the VDART Computer Program at 162.5 rpm

TURBINE-TURBINE INTERFERENCE

50.6 RPM $H / R = 2.0$
 NB = 2 $c/R = 0.073$
 R = 8.5 m

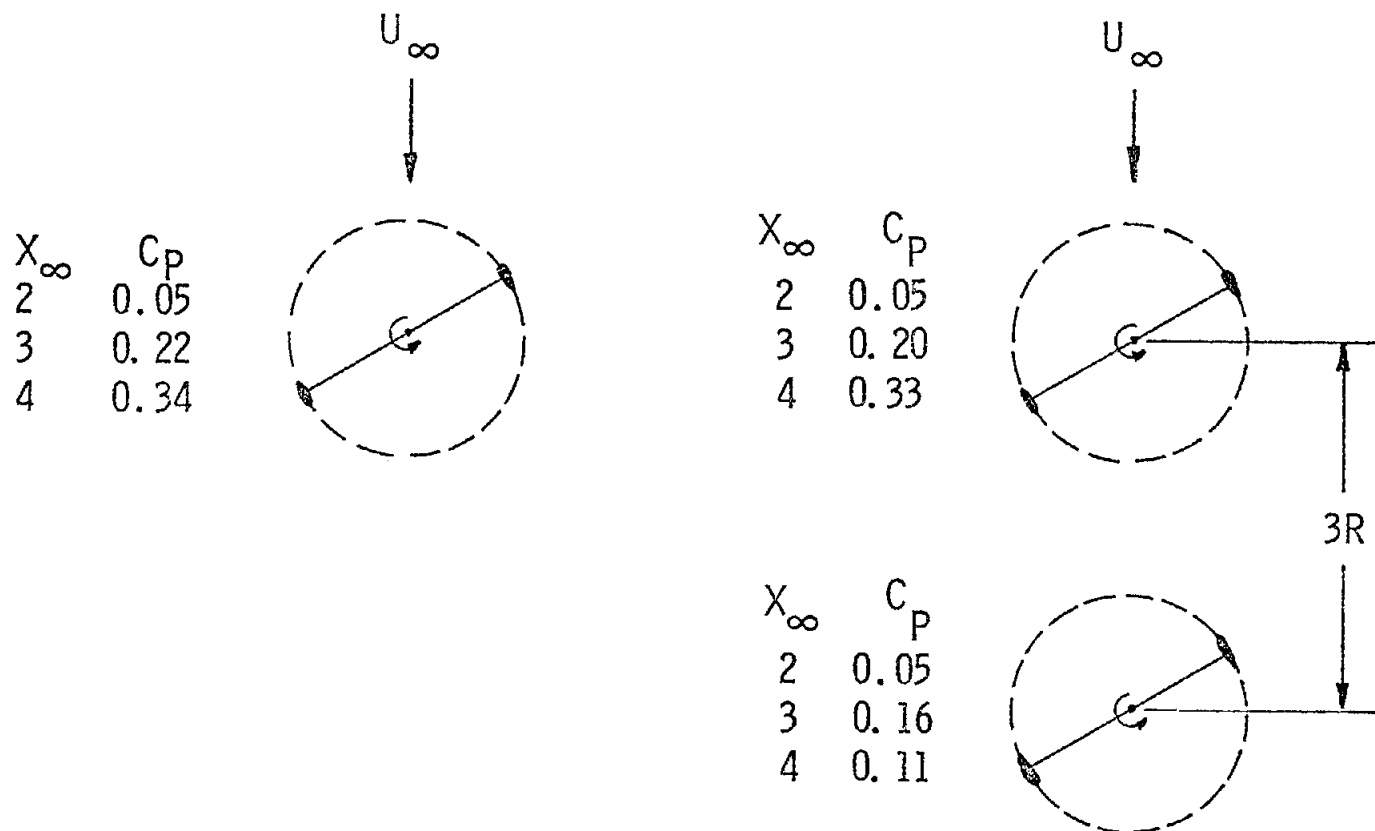


FIGURE 5. VDART Calculated Performance, 2 Sandia 17-m-D Turbines Operating in Proximity

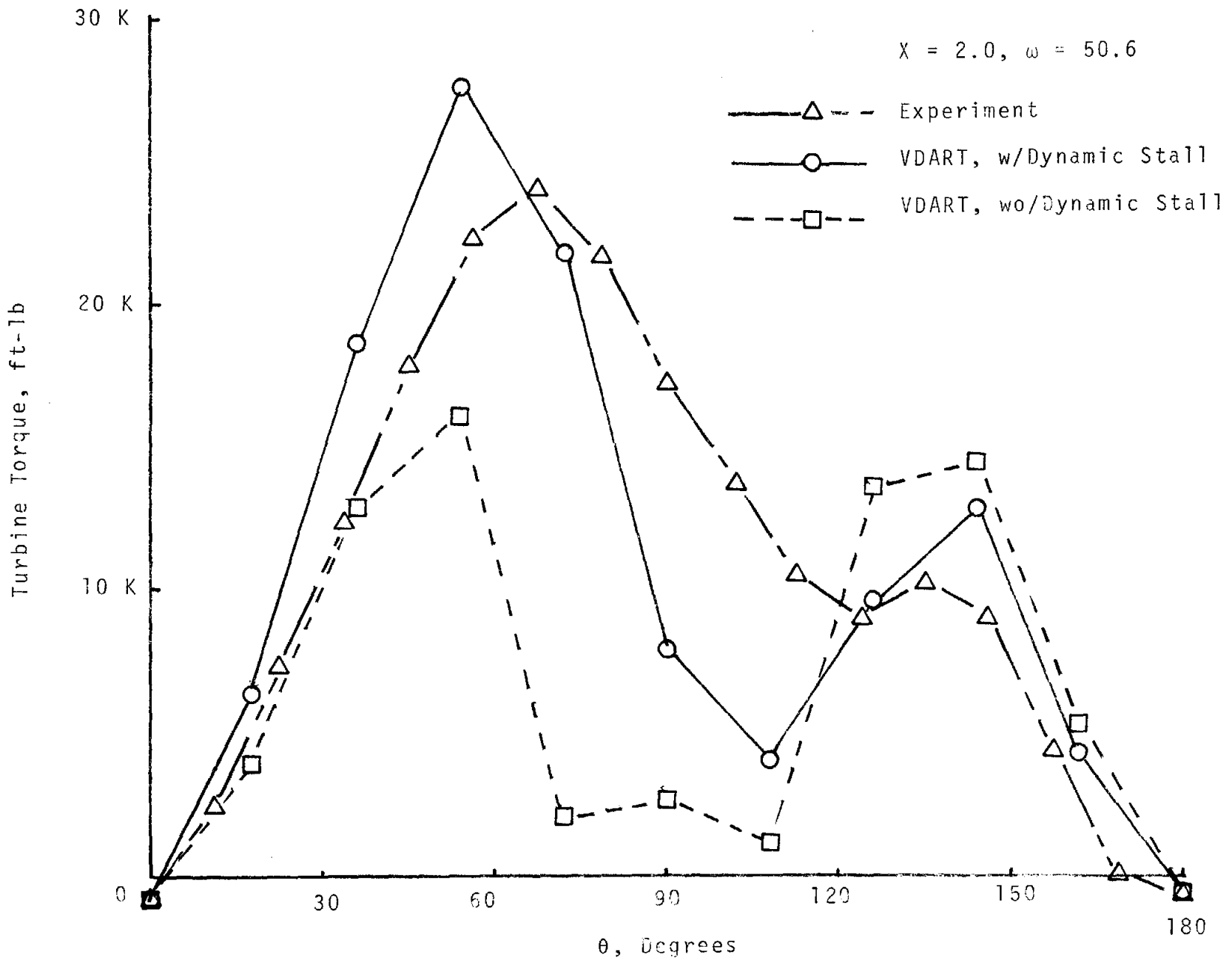


FIGURE 6. Two-Bladed Torque, Sandia 17-m Turbine, 2 NACA 0015 Blades

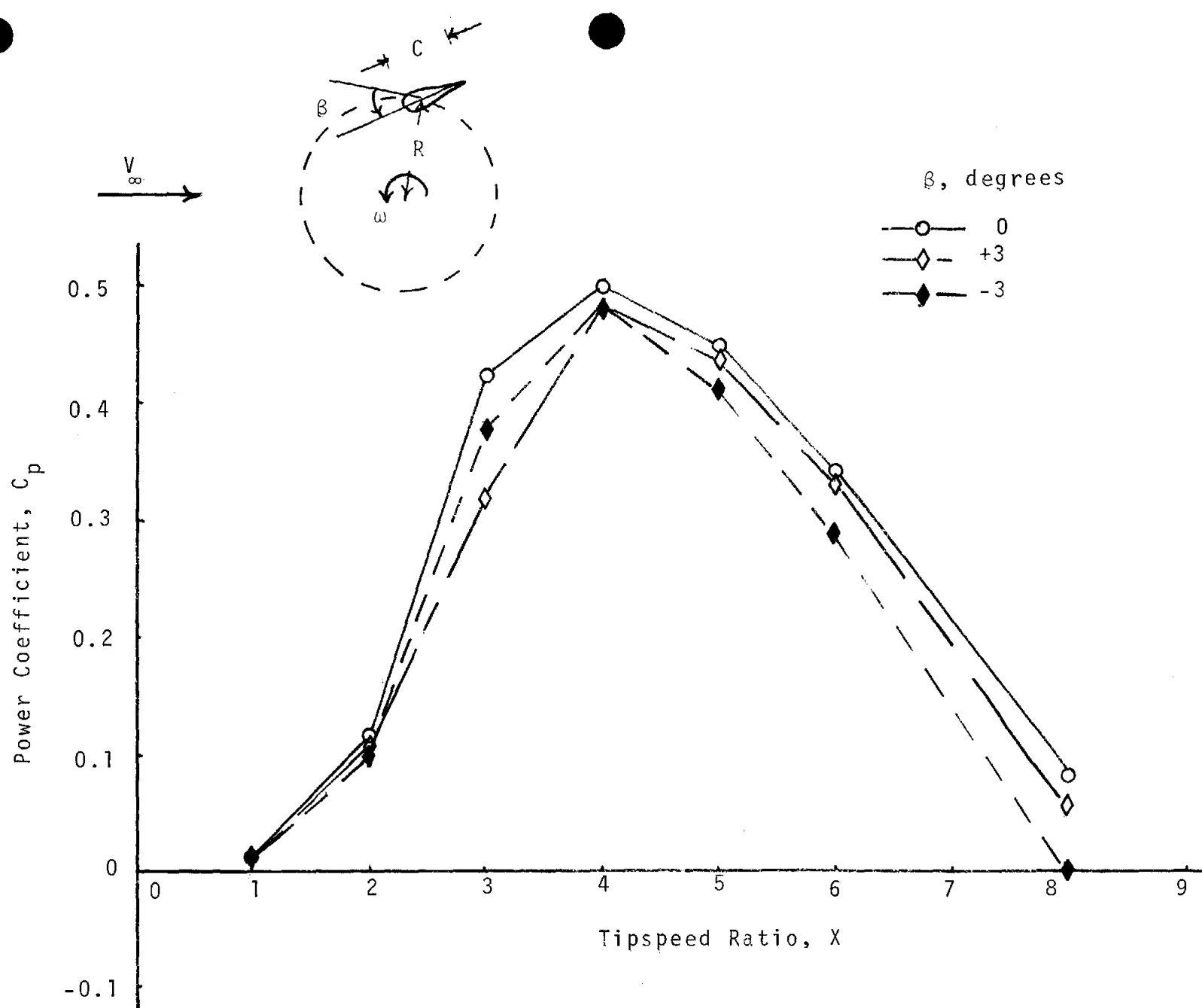


FIGURE 7. VDART2 Prediction, Power Coefficient, C_p vs. Tip Speed Ratio, X , Two-Dimensional Darrieus, 2 NACA 0015 Blades, $C/R = 0.1$, $Re = 1 \times 10^6$

used to estimate the effects on performance of increasing rotating tower size. As the Fig. 8 schematic shows, the tower was modeled by a semi-infinite Rankine body whose wake velocity was related to tower drag. Figure 9 summarizes the results.

VDART, and all other discrete filament models, have two shortcomings. The first of these are their large computer processing times. Efforts are currently underway to reduce these by a number of means. Secondly, convergence at high values of X (≥ 8) and high solidities has not been demonstrated.

III. Blade Section Characteristics

Blade airfoil section data suitable for use in Darrieus turbine applications is not nearly as readily available as it is for most other uses. Typical aeronautical situations involve section operation in the linear portion of the lift curve and at Reynolds numbers in the $10^6 - 10^7$ range. It is section characteristics for these conditions which are commonly accessible. This is not generally true when VAWT aerodynamics are considered. Depending upon blade element local radius and circumferential location relative to the ambient wind direction, the element may be either operating in the linear C_l vs. α region or in deep stall and at Reynolds numbers which are many orders of magnitude lower than the 10^6 value. Conducting a wind tunnel test series each time information is needed on a particular section is undesirable from both the economic and time requirements point of view. In order to quickly generate required blade section aerodynamic information, Sandia has chosen to adopt a hybrid procedure. In this scheme the linear and early stall characteristics are computed using a NASA/LRC provided airfoil synthesizer code.⁸ Late and post stall C_l , C_d vs. α behavior is taken from a Sandia entry into the Wichita State University Low Speed Tunnel where a number

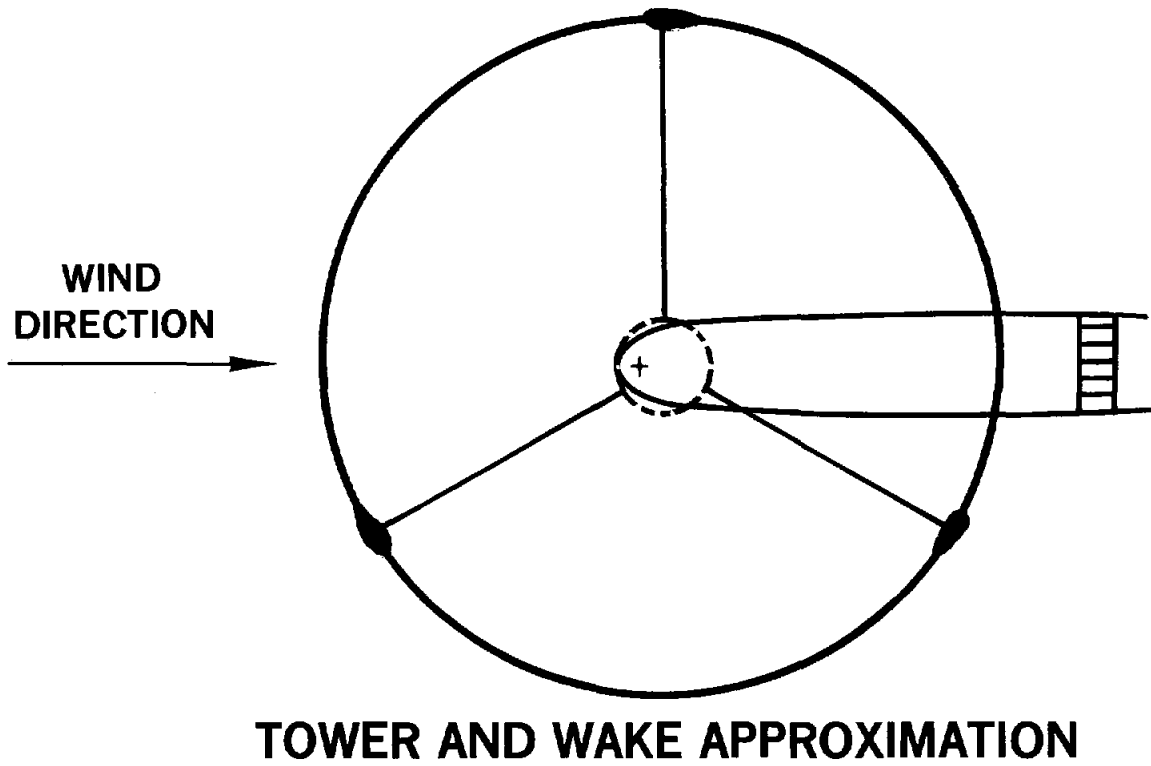
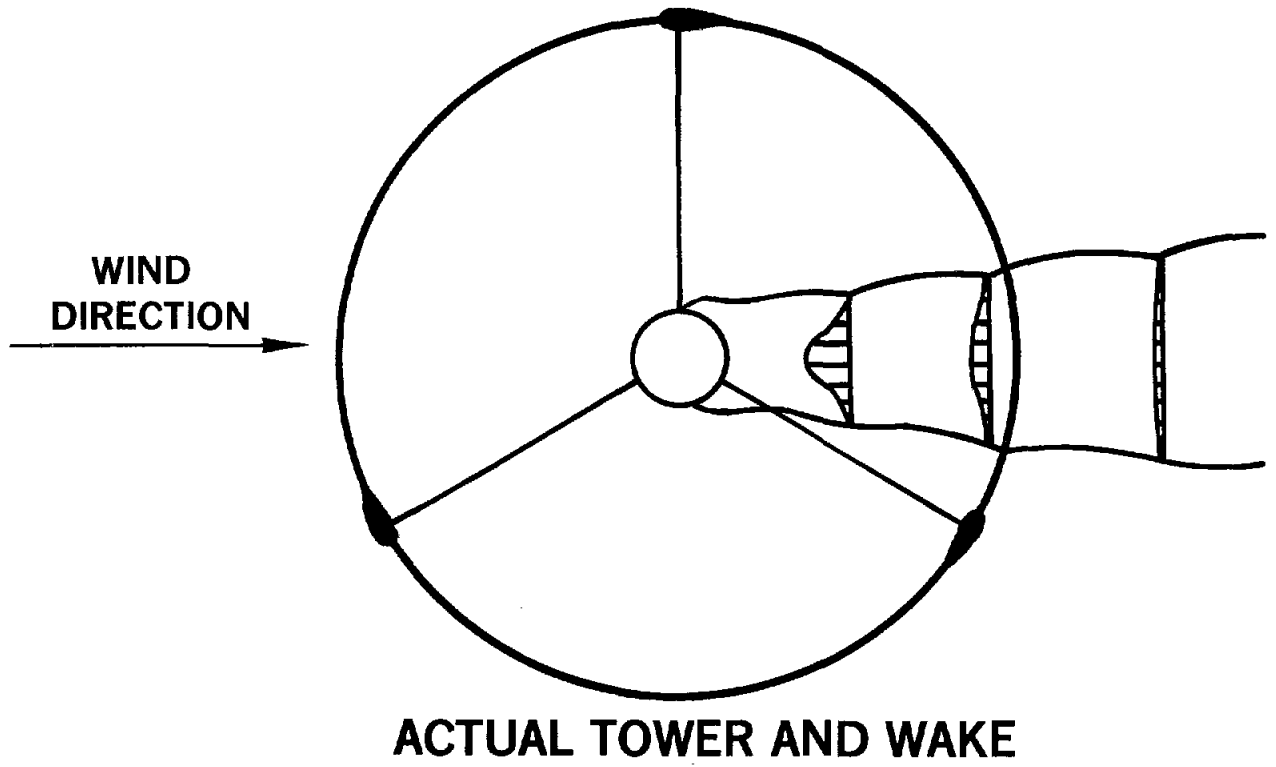


FIGURE 8. Schematic of Tower Wake Model

PREDICTED EFFECT OF TOWER SIZE ON PERFORMANCE

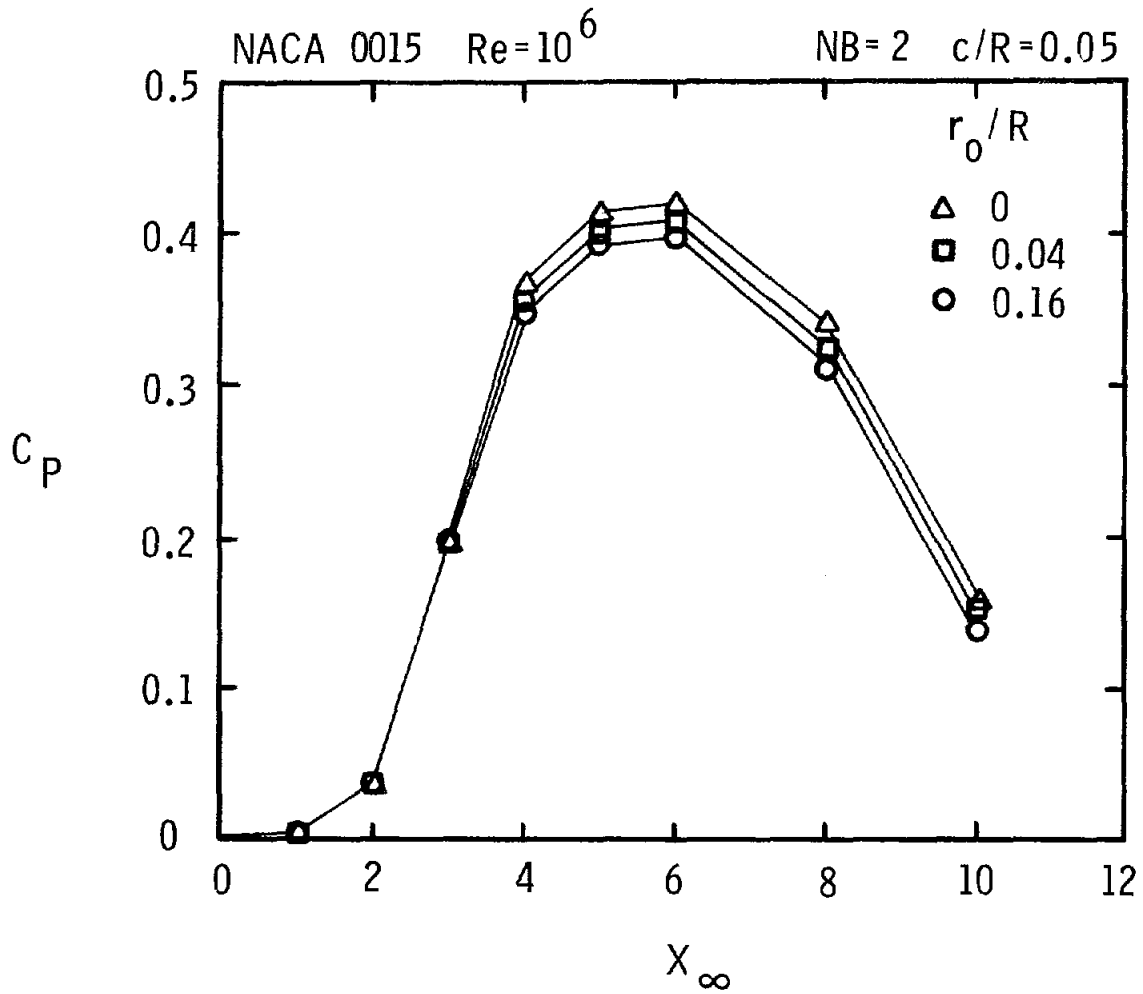


FIGURE 9. VDART2 Prediction, C_p vs. X , Two-Dimensional Darrieus, Varying Rotating Tower Size

of symmetrical profiles were tested over an angle-of-attack range from 0 to 180° at Reynolds numbers between 3 and 7×10^5 . At high values of α the results were found to be essentially independent of profile geometry and Reynolds number, allowing these data to be used for arbitrary sections and Re's. The merge points between calculated and measured values were determined through performance matching; i.e., the C_ℓ , C_d vs. α tabulations (when used with DARTER) which gave the best agreement with measured Sandia 17-m turbine performance were those chosen.

IV. Summary

Three basic approaches to calculating Darrieus wind turbine aerodynamic performance are described. The origins and capabilities of each are discussed along with their relative advantages and disadvantages. The procedure used at Sandia Laboratories for obtaining blade airfoil section characteristics, required for two of the three performance calculation models, is outlined.

References

1. B. F. Blackwell, W. N. Sullivan, R. C. Reuter, and J. F. Banas, "Engineering Development Status of the Darrieus Wind Turbine," Journal of Energy 1, No. 1 (1977), 50-64.
2. H. Ashley, "Some Contributions to Aerodynamic Theory for Vertical Axis Wind Turbines," ibid., Vol. 2, No. 2 (1978), 113-119.
3. Users Manual for DARTER, Sandia Laboratories (to be published).
4. J. H. Strickland, The Darrieus Turbine: A Performance Prediction Model Using Multiple Streamtubes, SAND75-0431 (Albuquerque, NM: Sandia Laboratories, 1975).
5. T. M. Leonard, A User's Manual for the Computer Code PAREP, SAND79-0431 (Albuquerque, NM: Sandia Laboratories, 1979).
6. J. H. Strickland, B. T. Webster, and T. Nguyen, A Vortex Model of the Darrieus Turbine: An Analytical and Experimental Study, SAND79-7058 (Albuquerque, NM: Sandia Laboratories, 1980).
7. R. E. Gormont, A Mathematical Model of Unsteady Aerodynamics and Radial Flow for Application to Helicopter Rotors, USAAMRDL TR 72-67 (Fort Eustis, Virginia: U.S. Army Air Mobility Research and Development Laboratory, 1973).
8. R. Eppler, "Turbulent Airfoils for General Aviation," Journal of Aircraft 15, No. 2 (1978), 93-99.

MEASURED AERODYNAMIC AND SYSTEM PERFORMANCE OF THE 17-M RESEARCH MACHINE

Mark H. Worstell

Since starting operation in March 1977, the DOE/Sandia 17-m wind turbine has provided a wealth of performance data. Performance, in the context of this paper, is broken down into two distinct areas:

1. Aerodynamic power output of the turbine rotor.
2. Drive train power losses.

Total system performance is the combination of the two.

To date, there have been three rotor configurations used in aerodynamic performance testing. In relation to the drive train, two transmissions of different construction have been tested. A summary of the performance data taken will be presented along with the observed trends. Basic descriptions of the turbine, operation, and data collection and reduction will be included so as to provide a good base of comprehension.

Turbine Description

Figure 1 shows the 17-m turbine in its present test configuration. The basic turbine layout and general specifications can be seen in Figs. 2 and 3, respectively. There have been a total of three rotor configurations tested to date: 2 and 3 strutted blades, and 2 unstrutted blades. The strutted 3 blade configuration is shown in Fig. 4. The blades of the strutted configurations are of a composite structure utilizing aluminum extrusions, honeycomb, and fiberglass material. The struts, those blade sections forming an X shape from the center of the rotor, are identical in construction to the outer blade

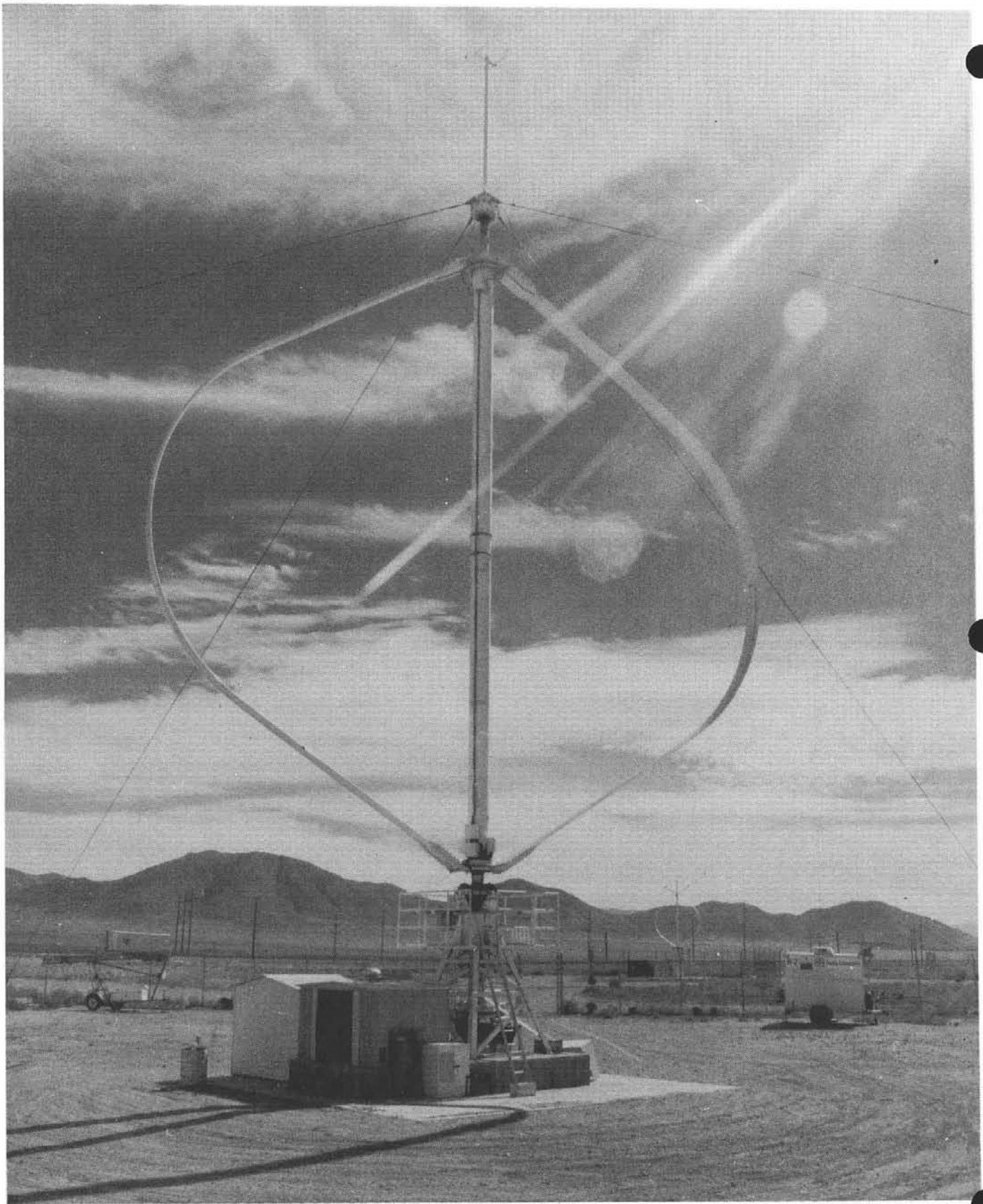
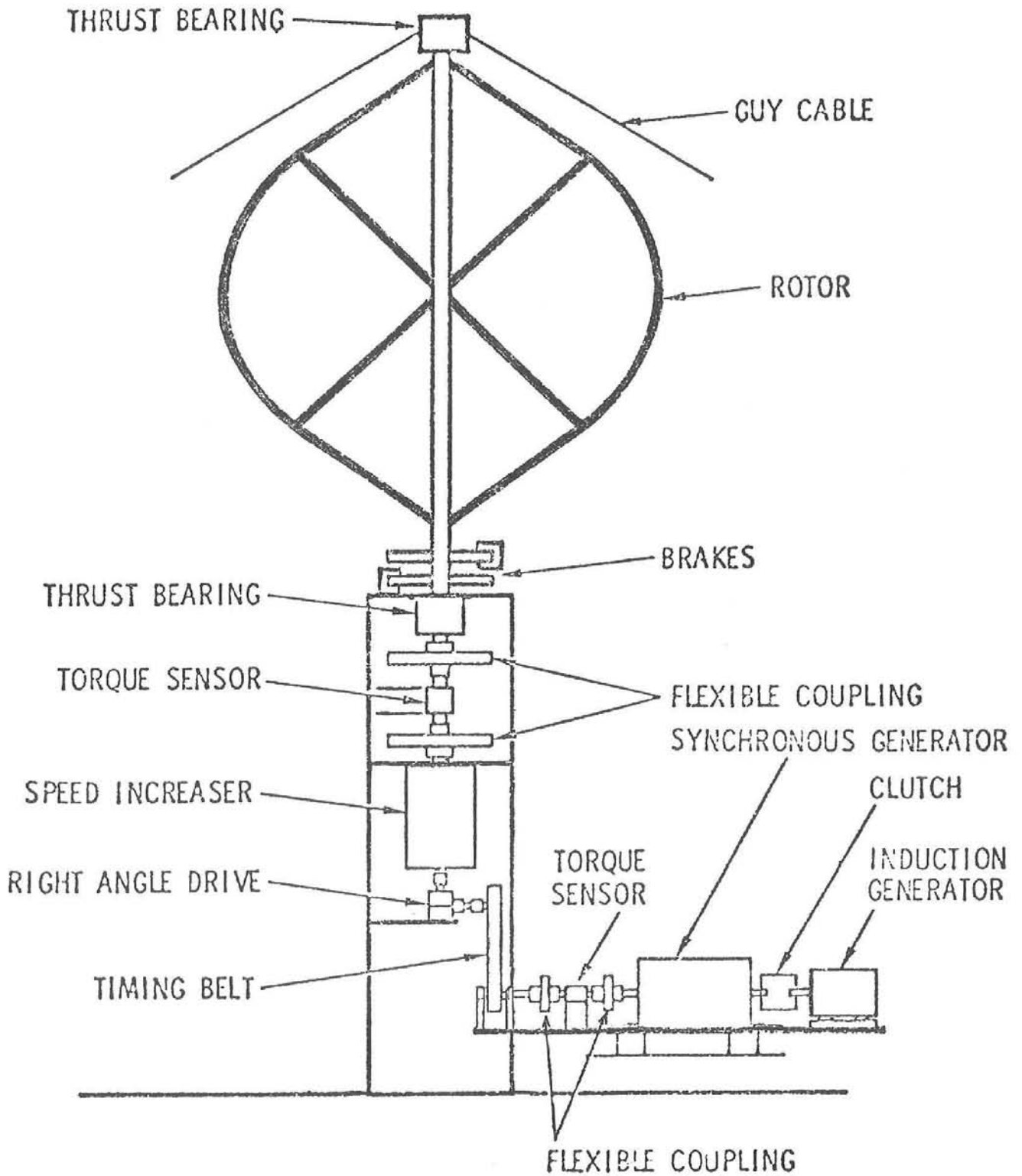


FIGURE 1. DOE/Sandia 17-m Wind Turbine, 2 Unstrutted Blades



17 Meter Drive Train Schematic

FIGURE 2

17 Meter Test Turbine Specifications

	<u>Original Spec</u>	<u>Present Spec (If Different)</u>
Rotor Diameter	54.9 ft	
Rotor Height	55.8 ft	
Swept Area	2014 ft ²	
Ground Clearance	16.0 ft	
Overall Height	110 ft	94 ft
Operating Speed	29.6-52.5 rpm	29.8-54.8 rpm
Number of Blades	2 or 3	
Rotor Solidity	0.14 0.21	0.16 0.24
Blade Manufacturer	Kaman	Alcoa
Blade Material	Fiberglass/ Honeycomb/ Aluminum Extrusion	Aluminum Extrusion
Airfoil Section	NACA 0012	NACA 0015
Chord Length	21.0 in	24.0 in
Use of Struts	Yes	No
Blade Length	79 ft	
Blade Shape	Straight- Circular- Straight	
Blade Joints	Pinned	Rigid
Blade Weight (ea)	713 lbm	1370 lbm
Strut Weight (per blade)	446 lbm	0 lbm
Speed Increaser	3-Stage Planetary	3-Stage Parallel Shaft
Manufacturer	Crichton	Philadelphia Gear
Rating	135 hp	172 hp
Speed Increaser Ratio	42.9:1	35.58:1
Belt Drive Ratio to Motor	1.42:1 to 0.8:1	1.7:1 to 0.92:1
Motor/Generator (Induction) (Synchronous)	75 hp Squirrel Cage 75 hp	
Brake	Dual Independ- ent 30" Disc	
Brake Torque Capacity (ea)	53,000 ft-lb	
Tower OD	20 in	
Tower ID	18 in	

FIGURE 3 (Continued on Next Page)

FIGURE 3 (Continued)

Number of Guy Cables	4
Cable Angle (to Horizontal)	35°
Cable Diameter	1 in
Cable Pretension	12,000-18,000 lb
Cable Length	129 ft

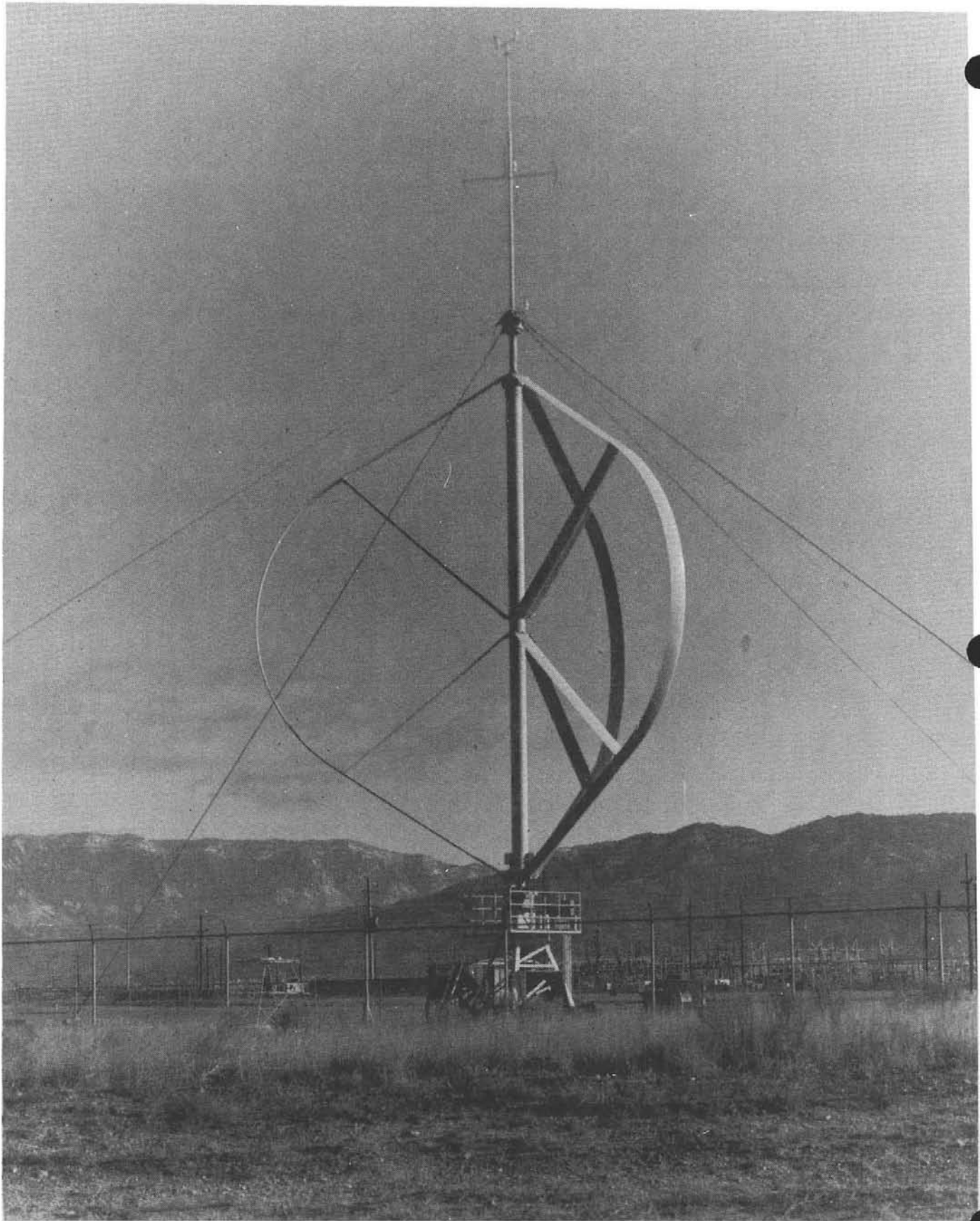


FIGURE 4. DOE/Sandia 17-m Wind Turbine, 3 Struttled Blades

sections which form the rotor shape. The struts are intended only for structural support and ideally do not affect rotor performance. The 2 unstrutted blades are of a one piece aluminum extrusion whose outer rotor dimensions are identical to that of the strutted blades. The airfoil section and chord (length measured from leading to trailing edge of blade) is changed from that of the strutted blades. One may think of the extruded blade being "fatter" and "longer" than that of the composite. By its process of manufacture and lack of need of struts, the extruded blade represents a significant cost reduction over the original composite blade.

The drive train as depicted in Fig. 2 illustrates those components which will represent some degree of power loss. These include thrust bearings, speed increaser (or transmission), timing belt, shaft bearings, and electrical generators. Two transmissions have been tested to date which gave discernable differences in power loss. During the 2 and 3 strutted blade testing, a planetary transmission was used in conjunction with a right angle drive. When the unstrutted blades were mounted in March 1979, this setup was replaced by a parallel shaft gearbox with a built-in right angle drive. This change was not performed due to damage of the original transmission (of which there was none discernable) but rather to test the parallel shaft gearbox.

As observed in Fig. 2, there are two electrical generators either of which may be utilized in testing. The synchronous generator is a device whose operating speed is a precise 1800 rpm and is the type typically used in utility power plants due to its favorable power characteristics. The induction generator, which also serves as a starting motor for the 17-m, varies slightly from 1800 rpm during operation though not enough to affect the outcome of performance testing results. The induction generator represents a cost reduction over the synchronous along with its associated controls, but exhibits

less favorable power characteristics than the synchronous. In this paper, all of the test results were taken using the induction generator exclusively. As can be noted in Fig. 2, although the synchronous generator is uncoupled electrically from the utility line, its armature is still turning during turbine operation.

Operation

The DOE/Sandia 17-m Darrieus wind turbine is essentially a constant speed machine, that is, the rotational speed of the rotor remains constant during operation even though the windspeed varies. This is accomplished by using the electrical generator (which is coupled directly to the utility line and hence constant speed) as the speed controller. By selecting a generator whose power capacity is equal to or greater than that of the wind turbine, an essentially constant, or synchronous rotational speed is realized. This is due to the inherent nature of a constant speed Darrieus wind turbine to level off in power output regardless of windspeed.

To provide a means of testing the 17-m at a number of rotor speeds, various sizes of pulleys are used with the timing belt (Fig. 2), thus altering the overall drive train gear ratio. Typical rotor speeds tested have been between 29.6 to 52.5 rpm. Again, for the purposes of this paper, the rotational speed of the turbine rotor can be considered as constant regardless of windspeed.

Data Collection and Presentation

It is the desire to assimilate data that will illustrate the performance characteristics of the 17-m in order to be used in conjunction with ongoing analytical studies addressing Darrieus wind turbine performance. These data typically take the form of what is known as a C_p , or performance curve. The C_p curve is simply a measure of the pure aerodynamic efficiency of the turbine rotor. It does not include any drive train loss.

The C_p curve is an almost universally accepted measure of turbine performance. The power present in undisturbed wind is equal to $1/2\rho_\infty A V_\infty^3$ where

ρ_∞ = undisturbed air density

A = area normal to wind

V_∞ = undisturbed windspeed

Quite notable here is the V_∞^3 term. C_p is defined as the ratio of turbine power output to the original power present in that wind intercepted by the turbine rotor. The area used is the swept rotor area which on a qualitative basis, for this machine, would appear as a disc with a diameter of 17-m. C_p then is the aerodynamic efficiency of the turbine rotor. The theoretical maximum (C_{pmax}) of any wind machine is approximately 0.60; all real life machines are below this, typically around 0.30 to 0.42. C_p is always expressed as a function of tip speed ratio, X . X is defined to be equal to $R\omega/V_\infty$ where:

R = maximum turbine rotor radius

ω = rotational speed of rotor

The data collection process employed with the DOE/Sandia 17-m wind turbine in its most basic terms entails simultaneously sampling undisturbed windspeed, the torque sensors, and the power transducer of the generator at a sample rate of typically four per second and then averaging these readings with previous ones for the same windspeed measured to within 0.5 mph. The sampled power outputs are then corrected to a standard day in Albuquerque corresponding to an air density of 0.0625 lbm/ft^3 so as to provide a uniform basis of data compilation and comparison. This data reduction technique is known as "Bins"¹ and has provided a repeatable means of free air testing of wind turbines. The end result is a listing of windspeed increments from 0 to 60 mph, the number of data samples collected in each windspeed bin, and the average of the transducer readings. The C_p curves and drive train power

loss curves follow directly from this.

Information concerning aerodynamic rotor output is taken from the torque sensor immediately below the bottom rotor thrust bearing as in Fig. 2. The losses of the thrust bearings are added to the measured values so that the resulting data reflect the pure aerodynamic performance of the rotor. Mechanical losses of the drive train are found by comparing the outputs of both torque sensors, and the losses of the generator can be determined by subtracting the generator power output from that of the torque sensor immediately in front of it.

The end result of the data sampling and reduction is a compilation of the rotor output as a function of undisturbed windspeed (C_p curves directly follow) and the losses present in the drive train which includes the induction generator.

Aerodynamic Performance

The first rotor configuration to be tested was that of 2 strutted blades. This was initiated in March 1977 and covered a period of 10 months. A summary of the test data can be seen in Fig. 5. Breakeven windspeed is defined as that windspeed where the rotor actually begins to produce power. Noticeable in Fig. 5 are several basic trends:

1. Breakeven windspeed increases with turbine rotational speed.
2. C_{pmax} tends to reach its highest level at 37 to 42 rpm.
3. Peak turbine power output, P_{max} , increases with turbine speed, occurring at progressively higher windspeeds.

One noticeable discrepancy is C_{pmax} for 45.5 rpm. This is most likely due to some form of error in the instrumentation or data acquisition. A complete presentation of test results for this configuration is available in Ref. 2.

17 Meter Aerodynamic Performance Test Summary
 Test Site Elevation 5440 Feet
 30' Reference Height

2 Blades with Struts

<u>RPM</u>	<u>Breakeven V</u> <u>(mph)</u>	<u>C_{Pmax}</u> <u>@ X</u>	<u>P_{max}</u> <u>@ V</u> <u>(kW) (mph)</u>
29.6	8.2	.342 @ 5.04	7.4 @ 15.9
33.6	8.2	.361 @ 5.27	12.3 @ 17.8
37.0	8.2	.376 @ 5.37	18.5 @ 22.6
42.0	9.1	.370 @ 5.67	28.9 @ 25.5
45.5	10.1	.303 @ 4.57	37.0 @ 27.4
48.4	10.1	.341 @ 6.12	47.9 @ 30.3
52.5	10.1	.340 @ 5.02	57.3* @ 31.3

FIGURE 5

*Higher winds are needed here to ascertain peak value.

A third strutted composite structure blade identical to the original two was added in January 1978. The effect of adding a third blade was to increase the rotor solidity from 0.14 to 0.21. Rotor solidity, σ , is the ratio of the apparent blade area (chord x blade length x number of blades) to rotor swept area. The performance characteristics of a wind turbine vary with rotor solidity which in the case of large utility wind turbines will typically be in the range of 0.14 to 0.16.

Figure 6 presents a summary of test results for the strutted 3 blade configuration. Noticeable in these results are trends 1. and 3. of the strutted 2 bladed mode. C_{pmax} , however, appears not to have a strong dependence on turbine speed. In comparing the 2 and 3 strutted blade results, for the same turbine speed, the visible trends are:

1. Breakeven windspeed for 3 blades is slightly higher than for 2.
2. C_{pmax} appears to be on the same order, but occurs at a lower tip speed ratio (higher windspeed) for 3 blades than 2.
3. The peak turbine output for 3 blades was higher than for 2.

1. and 3. tend to suggest that the C_p curve for 3 blades is shifted towards lower tip speed ratio relative to 2 blades. Figure 7 illustrates this for 37.0 and 52.5 rpm. The essence of this figure is that the 17-m turbine is more efficient in higher winds with 3 blades, but less so in lower winds than with 2 blades. This is a significant trend where desirability will, of course, depend upon the wind frequency distribution of the geographic area of application. Reference 3 gives further details of the strutted 3 bladed aerodynamic performance.

In March 1979, the 17-m turbine was fitted with 2 unstrutted extruded aluminum blades. During this changeover, the planetary gearbox was replaced by the parallel shaft gearbox

17 Meter Aerodynamic Performance Test Summary
 Test Site Elevation 5440 Feet
 30' Reference Height

3 Blades with Struts

<u>RPM</u>	<u>Breakeven V</u> <u>(mph)</u>	<u>C_p</u> @ X <u>P_{max}</u>	<u>P_{max}</u> @ V <u>(kw) (mph)</u>
37.0	9.1	.368 @ 5.00	24.7 @ 22.6
42.2	9.1	.323 @ 4.45	39.7 @ 27.4
45.5	10.1	.340 @ 4.57	54.8 @ 30.3
48.4	11.1	.352 @ 4.41	61.8 @ 30.3
52.5	12.5	.346 @ 4.38	81.4*@ 33.2

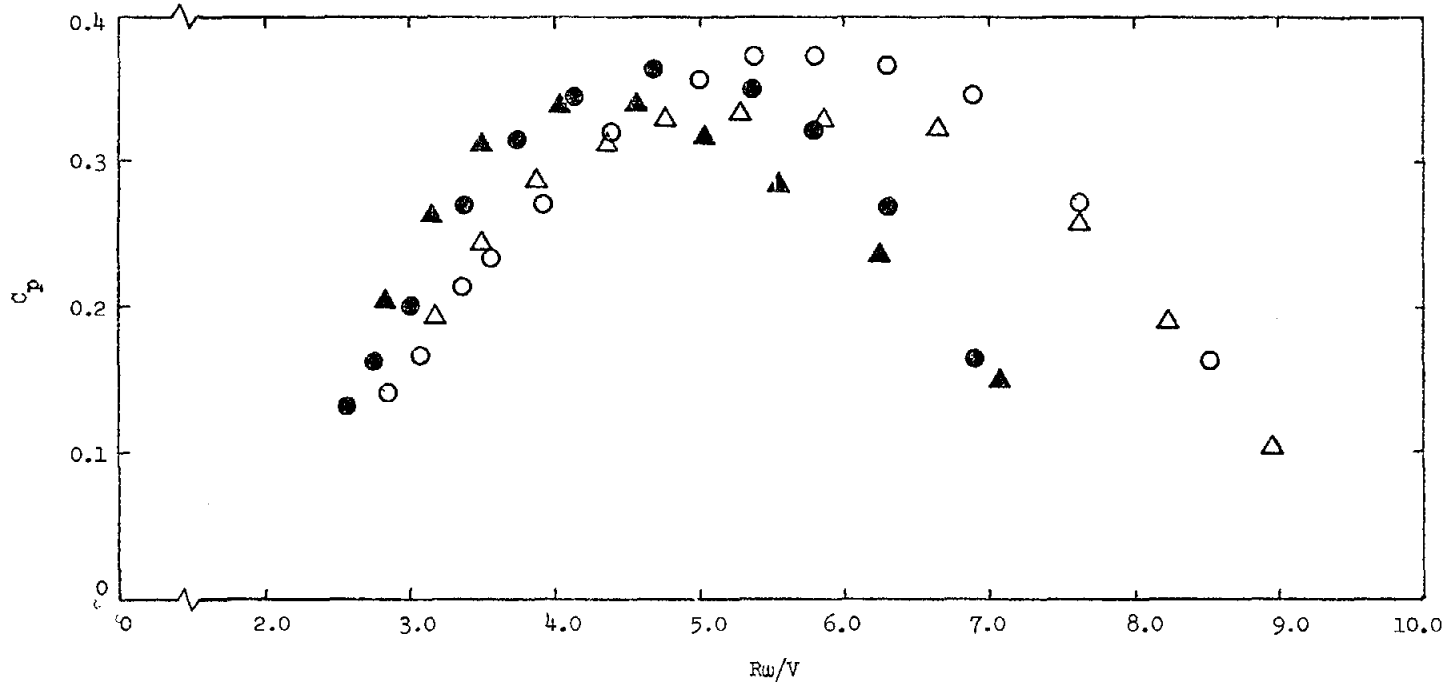
FIGURE 6

*Higher winds are needed to ascertain peak value.

17 Meter Turbine

rpm
37.0 52.5

- ▲ 3 Blades, $\sigma = 0.21$
- △ 2 Blades, $\sigma = 0.14$



C_p as a Function of Tip Speed Ratio

FIGURE 7

which, because of its different gear ratio, constrained the turbine to operate at moderately different rotational speeds than earlier. Figure 8 depicts a summary of the results obtained to date with this configuration. This figure may be subject to change due to further data assimilation and should not be taken as final although any subsequent changes will most probably be minor.

The extruded blades demonstrated the same basic trends as described for the 2 strutted blades with the exception that C_{pmax} occurred for 33.7 and 38.7 rpm. In comparing the 2 extruded blades to the 2 strutted composite blades, the following impressions come to light:

1. Breakeven windspeed for the unstrutted blades is lower than for the strutted.
2. C_{pmax} for the unstrutted blades is significantly higher.
3. The unstrutted blades produce a higher peak power output.

To provide insight into these trends, Figs. 9 through 12 are presented. These comparisons were performed at essentially the same rotational speeds of the turbine.

Figures 9 and 10 indicate that the extruded blades provide a higher C_p at all tip speed ratios tested for the rotational speeds presented. The direct implication of this is perhaps better shown in Figs. 11 and 12 which plot turbine rotor power output as a function of windspeed for the above conditions. Quite noticeable is the higher power output of the extruded blades in moderate to high winds. Another distinct difference is that the windspeed for power regulation (that windspeed where the turbine output begins to level off) is moderately higher for the extruded blades.

17 Meter Aerodynamic Performance
 Test Site Elevation 5440 Feet
 30' Reference Height

2 Unstrutted Extruded Blades

<u>RPM</u>	<u>Breakeven V (mph)</u>	<u>C_p_{max} @ X</u>	<u>P_{max} @ V (kW) (mph)</u>
33.7	6.3	.453 @ 5.74	18.2 @ 19.7
38.7	6.3	.454 @ 6.07	27.6 @ 23.6
42.2	8.2	.407 @ 5.33	39.3 @ 26.5
46.7	9.2	.409 @ 5.54	Incomplete
50.6	9.2	.409 @ 5.66	Incomplete

Note: This figure may be subject to modification following further data assimilation.

FIGURE 8

Two-Bladed Rotor Efficiency
vs Tip Speed Ratio

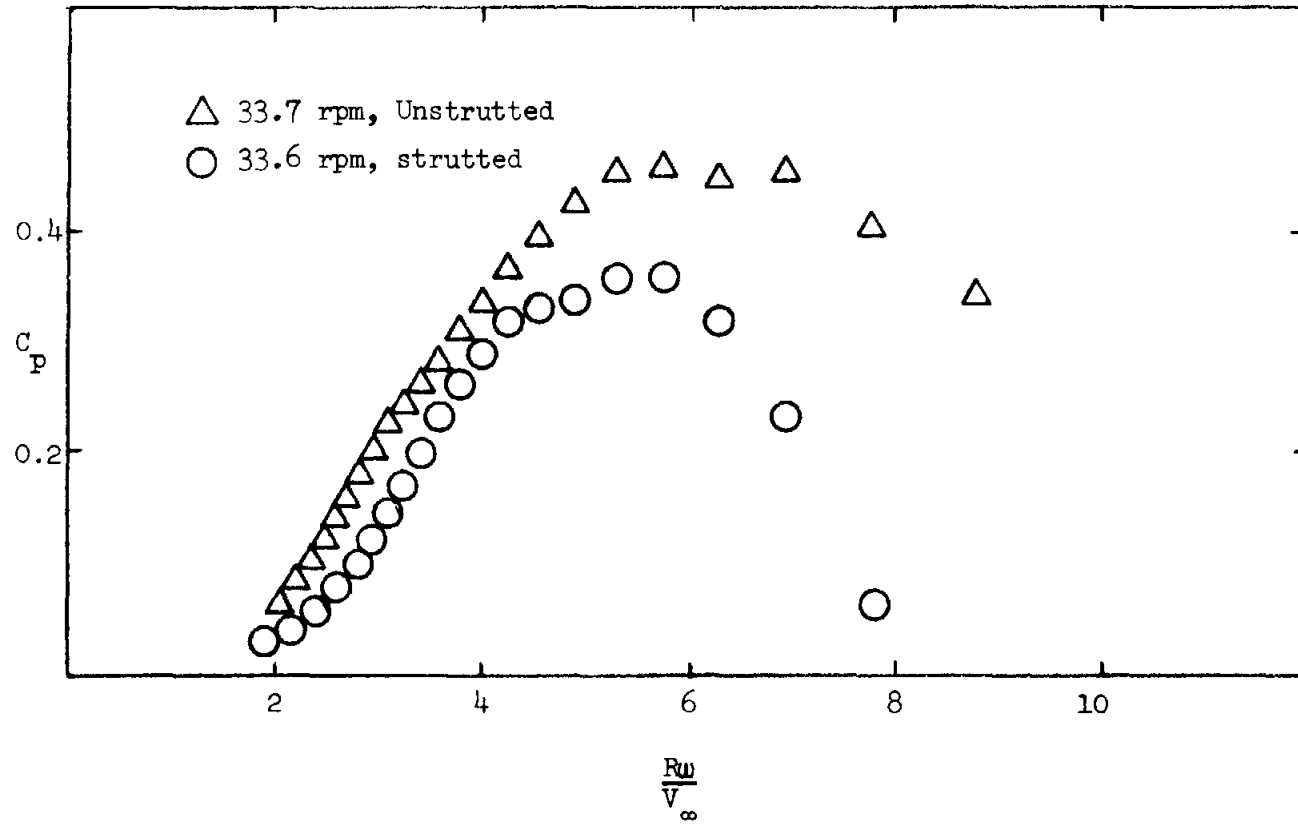


FIGURE 9

Two-Bladed Rotor Efficiency
vs Tip Speed Ratio

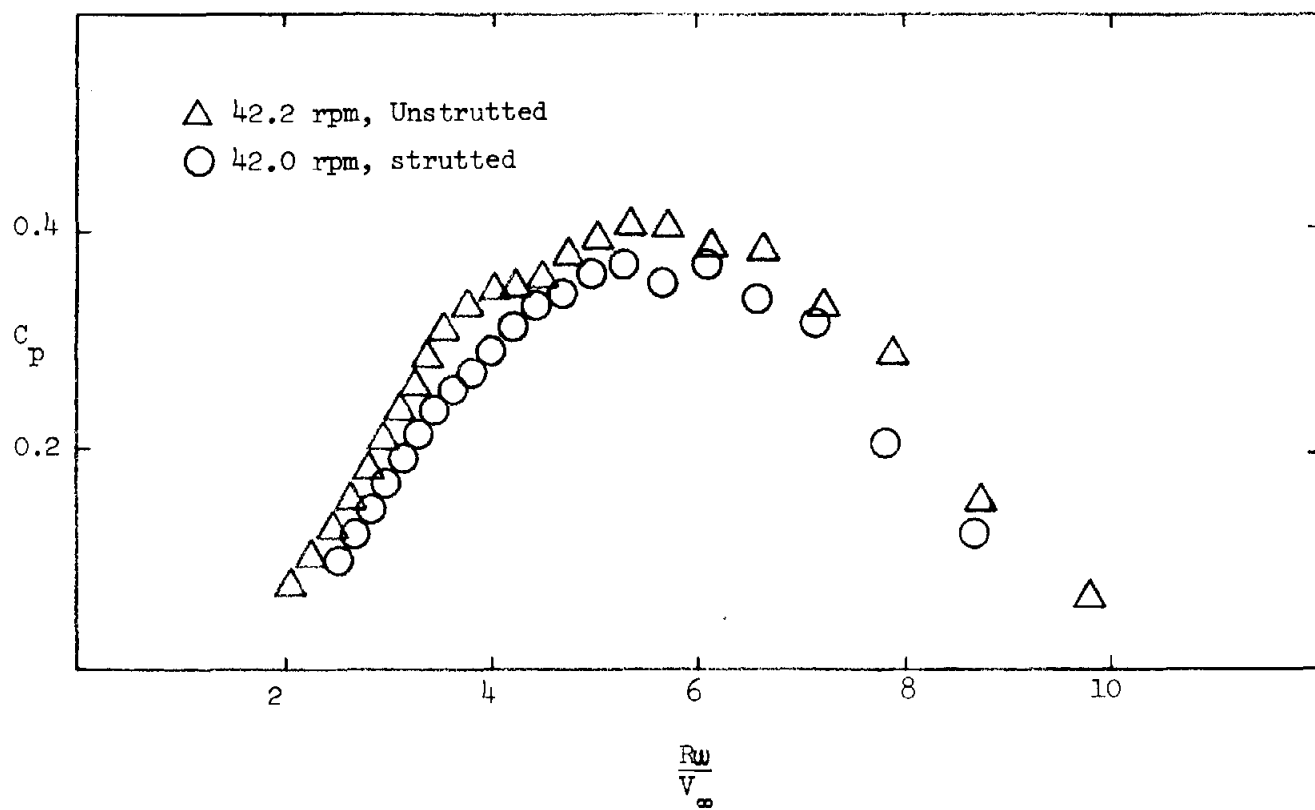


FIGURE 10

Rotor Output vs Centerline Windspeed
2 Blades

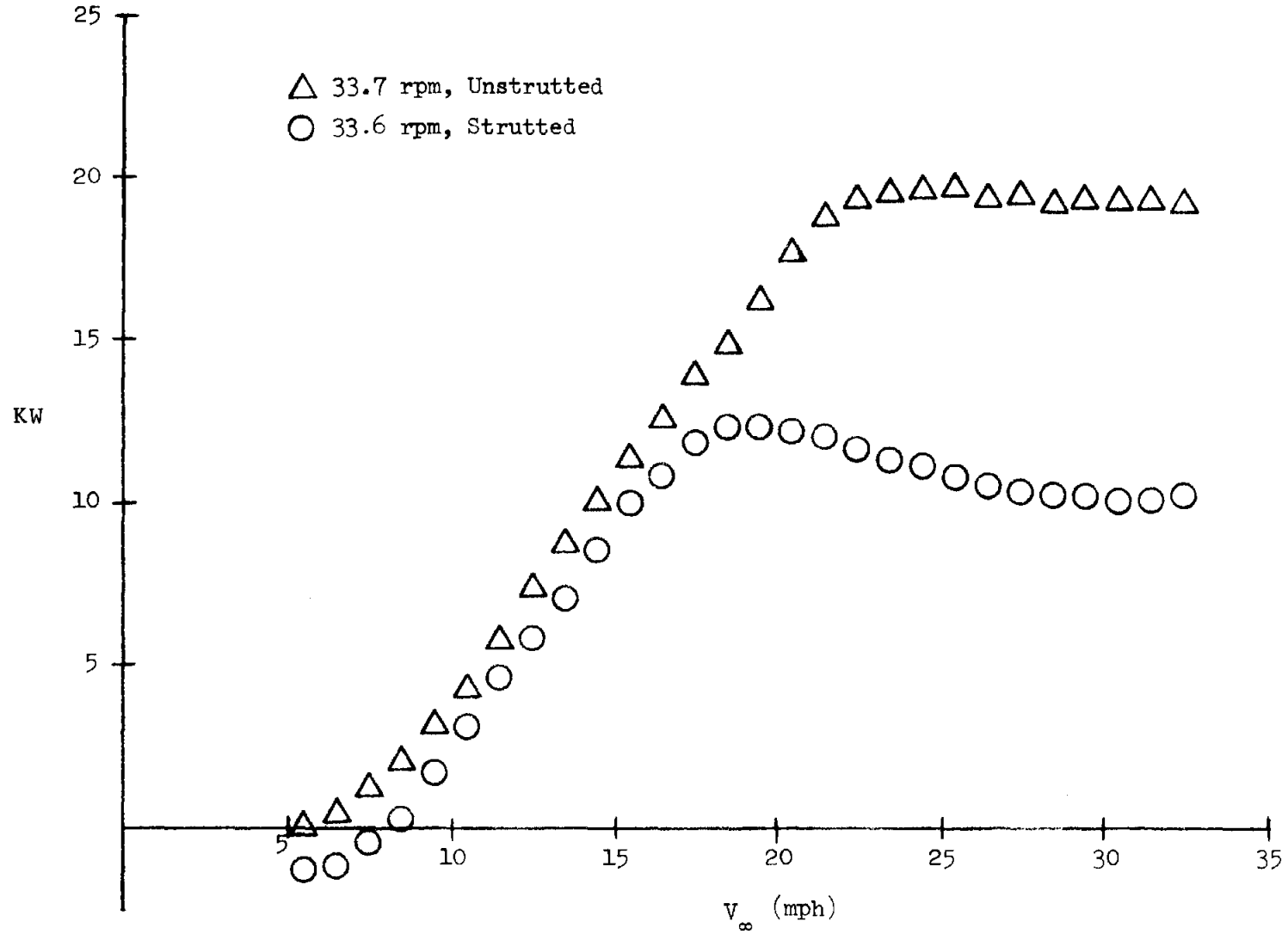


FIGURE 11

Rotor Output vs Centerline Windspeed

2 Blades

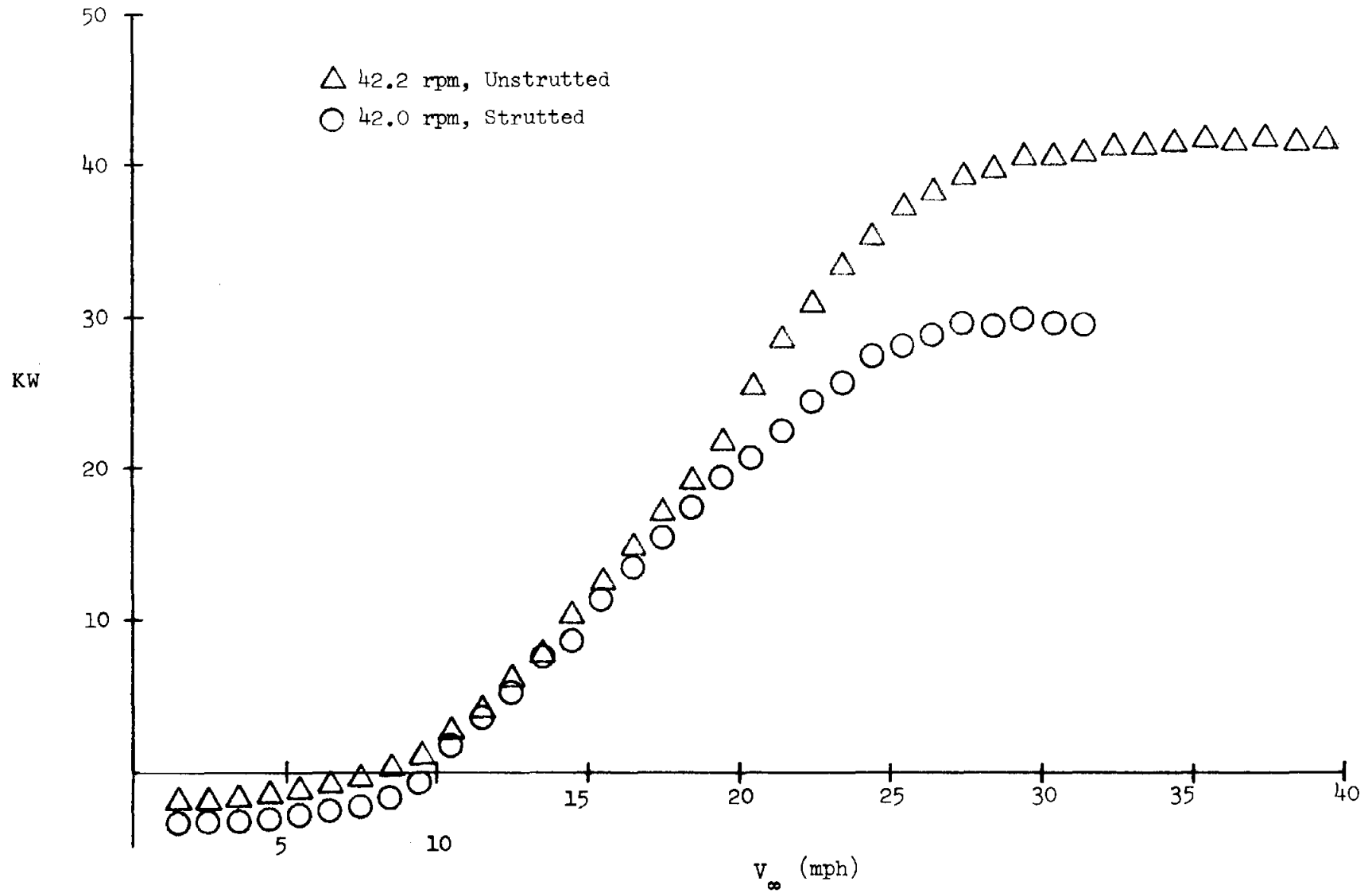


FIGURE 12

The differences exhibited between the strutted composite blades and the unstrutted extruded blades can be attributed to several reasons. First of all, the struts themselves operate in the wake of those blade sections extracting the major portion of power and may literally become drag devices. The performance of the Darrieus wind turbine, like the majority of WECS (wind energy conversion systems), is quite adversely affected by the presence of drag. This would account for the overall increase in performance of the unstrutted blades compared to the strutted.

A second possible cause is the airfoil sections themselves. The extruded blades utilized a NACA 0015 as compared to the original NACA 0012. This introduces a change in the airfoil lifting characteristics that when coupled with the longer chord length of the extruded blades could account for the power output regulation point moving towards higher windspeeds and peak output output being higher for the extruded blades.

Overall, the performance of the unstrutted extruded blades is quite encouraging particularly since extrusions represent a viable low-cost means of blade construction for the Darrieus wind turbine.

Drive Train Power Loss

In conjunction with aerodynamic performance testing of the 17-m, the drive train losses were also investigated. These losses are a combination of tare torque of the rotor thrust bearings, gearbox, timing belt, and generator losses along with the associated drive shaft bearings.

Tare torque losses of the 17-m have been measured and found to be equal to 287 ft-lb_F which is independent of the turbine rotational speeds tested. This tare torque represents a power loss of 2.06 kW @ 50.6 rpm which varies linearly with rotor speed. It should be stated that the rotor thrust

bearings are deliberately oversized and represent a loss more than what would be considered normal.

A very interesting area of drive train losses has been that of the gearbox and timing belt. As stated earlier, there have been two gearboxes used with the 17-m turbine with the same timing belt. The performance of these units was determined by comparing the two torque sensors present in the drive train. The losses in this portion of the drive train can be broken down into three basic categories:

1. Gear mesh losses.
2. Bearing losses.
3. Windage and oil churning losses.

Literature available on gearbox losses suggests that 1. accounts for the majority of loss with 2. and 3. for well designed gearboxes, being quite low or negligible, respectively, as when compared to the total. Gear mesh losses typically occur as a sliding function of rolling resistance of gear teeth, shearing of the oil film, and other not fully understood mechanisms. Both Refs. 4 and 5 categorize gear mesh losses as being a constant percentage loss of input power. In other words, the efficiency of gear meshing is constant. It is stated, however, gear mesh efficiency will vary for operating speed and oil viscosity. Reference 4 does suggest adding 25% to gear mesh losses to account for bearing losses.

The drive train of the 17-m turbine exhibited the losses as seen in Fig. 13. This figure depicts all losses except that loss due to the tare torque of the turbine rotor thrust bearings as previously described. A constant 5 kW loss attributable to the induction generator and all spinning hardware between it and the torque sensor immediately in front of the synchronous generator is also included. The trends observed in Fig. 13 are:

DRIVE TRAIN LOSS VS INPUT POWER

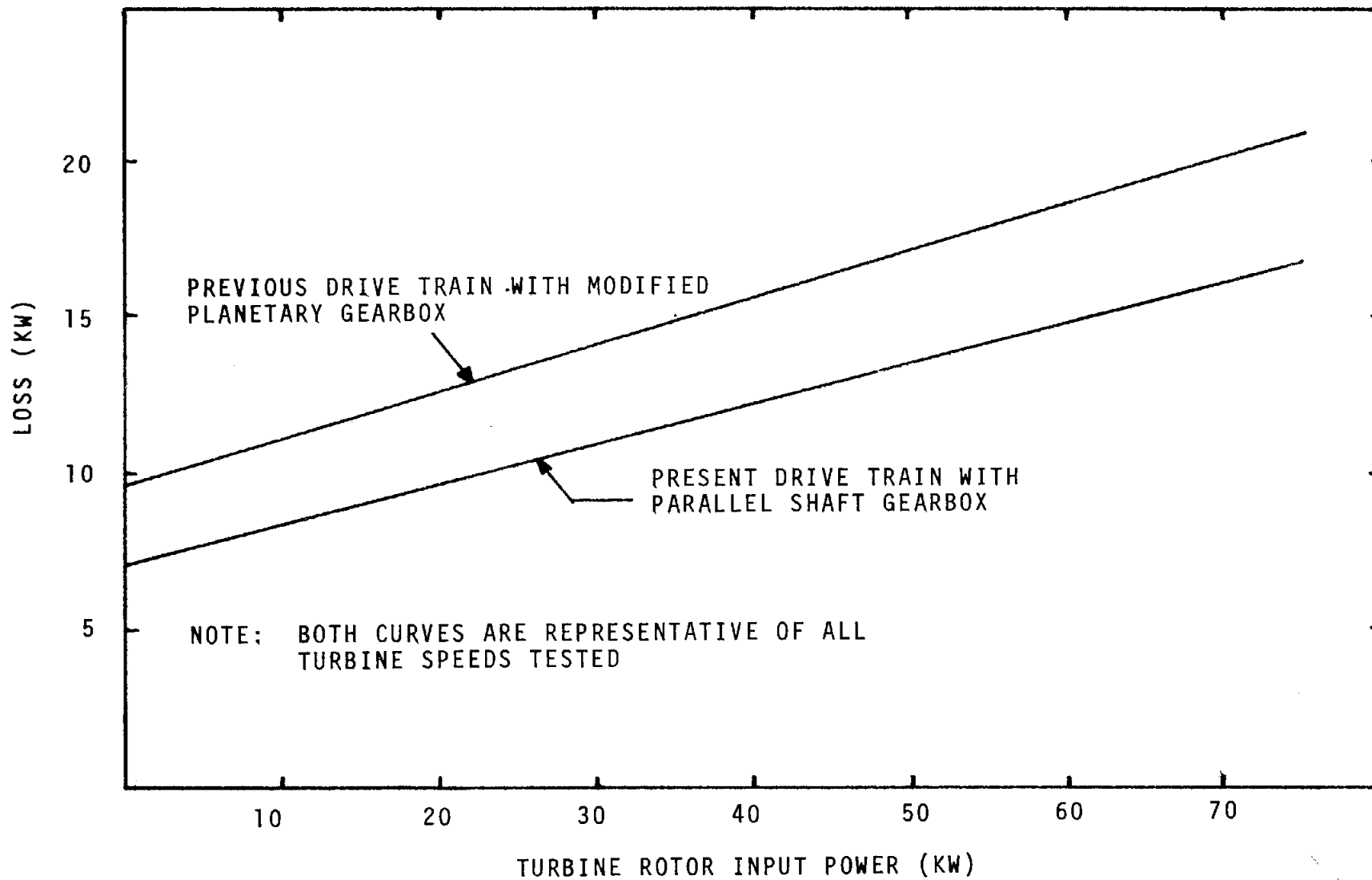


FIGURE 13

1. The parallel shaft gearbox is more efficient than the original planetary.
2. For both gearboxes, the power loss was not dependent on turbine rotational speed which indicates that viscous and oil churning losses are minimal.
3. The total losses are high when considering the power output of the DOE/Sandia 17-m wind turbine.

Of these trends, 3. is the most significant in light of drive train losses representing a parasitic affect upon overall turbine performance. As stated earlier, however, because of the DOE/Sandia 17-m wind turbine being essentially a research and development machine, over-design has been intentionally incorporated in many areas, the drive train being one. For example, the gearbox ratings, and accordingly losses, are a good deal more than what is absolutely necessary.

The fact that the parallel shaft gearbox was more efficient than the planetary, although the planetary gearbox has a lower rating, is of interest, too. Due to its nature of construction, the planetary gearbox has considerably more moving parts and specifically, gear meshes. Apparently, these additional gear meshes along with associated bearings manifested themselves as increased power loss. This tends to lend an argument towards simplicity in gearbox design.

The last area of the drive train under investigation is that of the induction generator. These devices are typically of high efficiency, on the order of 90% from half to full load. In the case of the 17-m turbine, the data, though somewhat scattered, indicated an almost constant loss of 5 kW occurring between the torque sensor mounted on the high speed generator shaft (next to synchronous generator) and the output terminals of the induction generator. This figure is in keeping with known efficiencies of induction generators, but the tendency of the data to suggest an almost constant

value regardless of turbine power input is somewhat surprising.

One possible explanation for this trend is that windage, a significant loss in electrical generators, is constant -- the generator armature is turning at a constant speed. Coupled with this, because of the drive train arrangement, windage of the clutch and synchronous generator armature are also included in this value. The total affect of this is to "mask" the other losses in the induction generator, such as resistance heating, that will vary with power input.

Overall, the drive train losses exhibited generally well defined and explainable trends. Again, it is stated that because of intentional over-design, these losses are indeed high for a wind turbine of the power output of the 17-m.

Conclusion

The DOE/Sandia 17-m wind turbine will continue performance testing and these results will be made known to the technical community as they are properly processed. The information gained to date has been of a most illuminating nature with regards to both the various hardware tested and analytical modeling techniques.

References

1. R. E. Akins, Performance Evaluation of Wind Energy Conversion Systems Using the Method of Bins - Current Status, SAND77-1375 (Albuquerque, NM: Sandia Laboratories, 1978).
2. M. H. Worstell, Aerodynamic Performance of the 17 Meter Diameter Darrieus Wind Turbine, SAND78-1737 (Albuquerque, NM: Sandia Laboratories, 1979).
3. M. H. Worstell, Aerodynamic Performance of the 17 Meter Diameter Darrieus Wind Turbine in the Three-Bladed Configuration: An Addendum, SAND79-1753 (Albuquerque, NM: Sandia Laboratories, 1980).
4. H. E. Merritt, Gear Engineering (New York, Toronto, and London: Pitman Publishing Co., 1971).
5. D. W. Dudley, Gear Handbook (New York: McGraw-Hill, 1962).

POSSIBLE AERODYNAMIC IMPROVEMENTS FOR FUTURE VAWT SYSTEMS

Paul C. Klimas

I. Introduction

In general, current lift-type vertical axis wind turbines use blades whose section profiles are symmetrical (NACA 0012, 0015 and 0018, for example). These sections are also mounted such that their chords are normal to the local radius vector from the rotating tower axis. There is no reason to believe that this is an optimum design from the cost of energy (COE) point of view. The following paragraphs illustrate how system COE is affected by specific changes in the C_p vs X aerodynamic performance curve. The dependence of these changes upon blade section aerodynamic characteristics is discussed. The dependence is illustrated through the results of some field tests of the Sandia 5-m Darrieus turbine.

II. Effects on COE of Changing Certain Performance Curve Parameters

One version of the Sandia VAWT economic optimization code¹ allows the user to assess the effects on COE brought about by changes in turbine aerodynamic performance characteristics. Three changes identified in this manner as decreasing COE are (1) increase maximum power coefficient (C_{pmax}), (2) move the tip speed ratio at stall regulation ($X @ K_{pmax}$) closer to $X @ C_{pmax}$, and (3) increase the X 's of all points on the C_p vs X curve. The Alcoa/DOE 17-m diameter turbine may be used to illustrate how specific changes in these parameters quantitatively

change COE. Table 1 gives the predicted decreases in COE associated with each individual performance modification and the combined impact of simultaneously making all three. The reference condition is taken as operation at sea level in a 6.7 m/s (15 mph) median windspeed. The aerodynamic performance evaluation is made by the code PAREP.² The magnitudes of the indicated COE improvements suggest that their pursuit may be worthwhile.

III. Dominant Blade Section Aerodynamic Parameters Governing the C_p vs X Performance Curve

The previous section showed how system COE responded to changes in various turbine aerodynamic performance parameters. This section discusses how these performance parameters are in turn influenced by blade airfoil section characteristics.

- A. C_{pmax} : The measure of turbine maximum efficiency, C_{pmax} , is proportional to a form of the standard measure of airfoil efficiency, lift-to-drag (l/d). The particular form is the maximum average value found when the average is taken over one complete turbine blade(s) revolution. This average ratio, $(\overline{l/d})_{max}$, is a function of section Reynolds number, Re , section camber, section thickness/chord (t/c), blade pre-set pitch or incidence, ϵ , and turbine solidity, σ . Generally, increases in Re lead to increases in $(\overline{l/d})_{max}$ while the ratio typically drops with increasing t/c . Non-zero values of ϵ reduce $(\overline{l/d})_{max}$. Higher cambers give higher $(\overline{l/d})_{max}$ at positive angles-of-attack, α , but reduce the ratio when $\alpha < 0$. Increasing turbine solidity has been shown to lead to larger values of C_{pmax} . This is postulated to be the result of a more favorable incident windstream angularity developing as the incident streamline divergence increases with σ .

TABLE 1
 Anticipated Reductions in Cost of Energy to
 Alcoa/DOE 17-m Diameter System Through Aerodynamics

	<u>Change</u>	<u>Reference</u>	<u>New</u>	<u>COE Decrease (%)</u>
1.	C_{pmax}	0.39	0.41	5.0
2.	$\frac{X @ K_{pmax}}{X @ C_{pmax}}$	0.55	0.70	8.0
3.	X	range	1.25 x range	2.5
4.	1,2,3 above simultaneously			14.0

- B. K_{pmax} : The non-dimensional measure of turbine maximum power, K_{pmax} , varies qualitatively with blade section maximum lift coefficient, C_{lmax} . In particular, the variation is with the maximum average value taken over a complete revolution. C_{lmax} depends upon Re , t/c , camber, ϵ , and section pitch rate, $\dot{\alpha} = d\alpha/dt$. For symmetrical profiles increasing Re and t/c bring about higher C_{lmax} values. As was the case with $(\overline{\ell/d})_{max}$, greater camber increases C_{lmax} for $\alpha > 0$ and reduces it when $\alpha < 0$. Non-zero ϵ will always reduce C_{lmax} . If the section pitch rate is sufficiently high, certain dynamic effects are felt. Depending upon turbine rotational velocity, ω , these dynamic stall effects tend to postpone the onset of, or the recovery from, blade aerodynamic stall. The net effect for blades using symmetrical profiles is to increase C_{lmax} .
- C. X : Only four specific values of tip speed ratio really need to be addressed as the entire C_p vs X curve may be reasonably approximated using these four points. These four are X_{cutoff} , $X @ K_{pmax}$, $X @ C_{pmax}$, and X at zero aerodynamic power. For a given turbine rotational speed, ω , the cutoff ambient windspeed value directly gives X_{cutoff} . The sign of $d(X @ K_{pmax})/dK_{pmax}$ may be positive or negative depending upon the mechanism changing K_{pmax} . The same may be said for $X @ C_{pmax}$. The $X @ C_p = 0$ involves the value of ambient windspeed below which no power will be generated. In this condition the blade sections operate at average α 's which are typically on the order of a few degrees or so. Then $X @ C_p = 0$ depends upon the average value of section drag coefficient, $\overline{C_{d0}}$, found in the range $-4^\circ \lesssim \alpha \lesssim 4^\circ$ or so. Increases in this tip speed ratio go along with decreases in $\overline{C_{d0}}$. This quantity increases with

increasing t/c , camber and $|\epsilon|$, but in general decreases with increasing Re . An exception here is for values of Re near Re_{crit} , the point at which the boundary layer transitions from laminar to turbulent. For typical symmetrical blade profiles $5 \times 10^5 < Re_{crit} < 1 \times 10^6$.³

In considering all of the above comments, it should be noted that they are qualitative and do not treat mutual effects. It should also be realized that certain sectors of the blade circumferential traverse impact performance more than others. For example, the upwind half of the traverse is more strongly felt than the downwind portion and advancing trajectories tend to be more dominant than retreating in either the down or upwind halves.

IV. Comparison of Performance Characteristics of Sandia 5 Meter Darrieus Using Symmetrical and Cambered Blade Sections

As mentioned above, blade section cambering is one of the candidate means of altering a C_p vs X curve. Sandia Laboratories has tested a variant of its 6" chord NACA 0015 aluminum blades on its 5-m turbine. The variant was extruded with a 1% camber located at mid-chord. The airfoil is therefore designated NACA 1515. Table 2 summarizes the preliminary results of testing at 175 rpm for both the cambered and uncambered 15% t/c , 6" chord sections on the Sandia 2 bladed 5-m Darrieus.

The motivation for choosing the 1515 section was to investigate the premise that a symmetrical profile traversing a curvilinear flowfield was equivalent to a cambered profile traversing a rectilinear flowfield.³ The 1515 was the section which, when operating at $X = \infty$ (no wind) at the turbine equator could be considered the equivalent of the 0015 under the above postulate.

Following the stated premise, the comparisons listed in Table 2 and detailed in Figs. 1 through 4 may be best understood if the actual 0015 blade is thought of as an unsymmetrical profile cambered with the concave side outward and the actual 1515 blade as a symmetrical profile. Figure 5 gives the equivalences and Fig. 6 is a schematic of the drag polars for the two sections. The solid polar was characteristic of results obtained with straight planform blades of symmetrical cross-section in a curvilinear flowfield in experiments conducted at West Virginia University.⁴

- A. $X @ C_p = 0$: The higher $X @ C_p = 0$ for the 1515 blades follows from Fig. 6; the lower C_d in the $-4^\circ \lesssim \alpha \lesssim 4^\circ$ range substantiates this conclusion.
- B. C_{pmax} : The lower C_d 's over the α range centered near zero account for the 1515's higher C_{pmax} .
- C. $X @ C_{pmax}$: As in (B), finding $(\bar{r}/d)_{max}$ at lower $|\alpha|$ implies a higher tip speed ratio.
- D. K_{pmax} : The 1515 blades will stall at lower geometric angles-of-attack (α_g) when on the upwind advancing traverse and at higher α_g 's on the upwind retreating traverse than the 0015. Since the advancing traverse dominates due to the higher relative air speeds, the net effect is a lower K_{pmax} for the 1515. The downwind half of the circuit does not contribute nearly as much as the upwind due to the large amount of energy having been extracted by the blades on the upwind traverse. Note the more gradual transition to regulation with the 1515 blades.
- E. $X @ K_{pmax}$: It does not appear possible to simply explain the 1515's lower $X @ K_{pmax}$. Apparently the net effect of changing the α_g 's over the entire circular blade path is such that the average value

TABLE 2
Preliminary Performance Comparison Between Cambered
at 175 rpm and Symmetrical Blade Section Operation of
Sandia 5-m Darrieus

<u>Characteristic</u>	Blade	
	<u>0015</u>	<u>1515</u>
C_{pmax}	0.328	0.378
K_{pmax}	0.0060	0.0055
X @ C_{pmax}	5.5	5.7
X @ K_{pmax}	3.2	2.9
X @ $C_p = 0$	9.7	10.2

REC ID	TURBINE	RPM	ANEM DESIGN	CUR RECS
	5.	175.0	2	YES
252621.				
252921.				
260222.				
260722.				
261622.				
262222.				
270222.				
270622.				
270922.				
271422.				

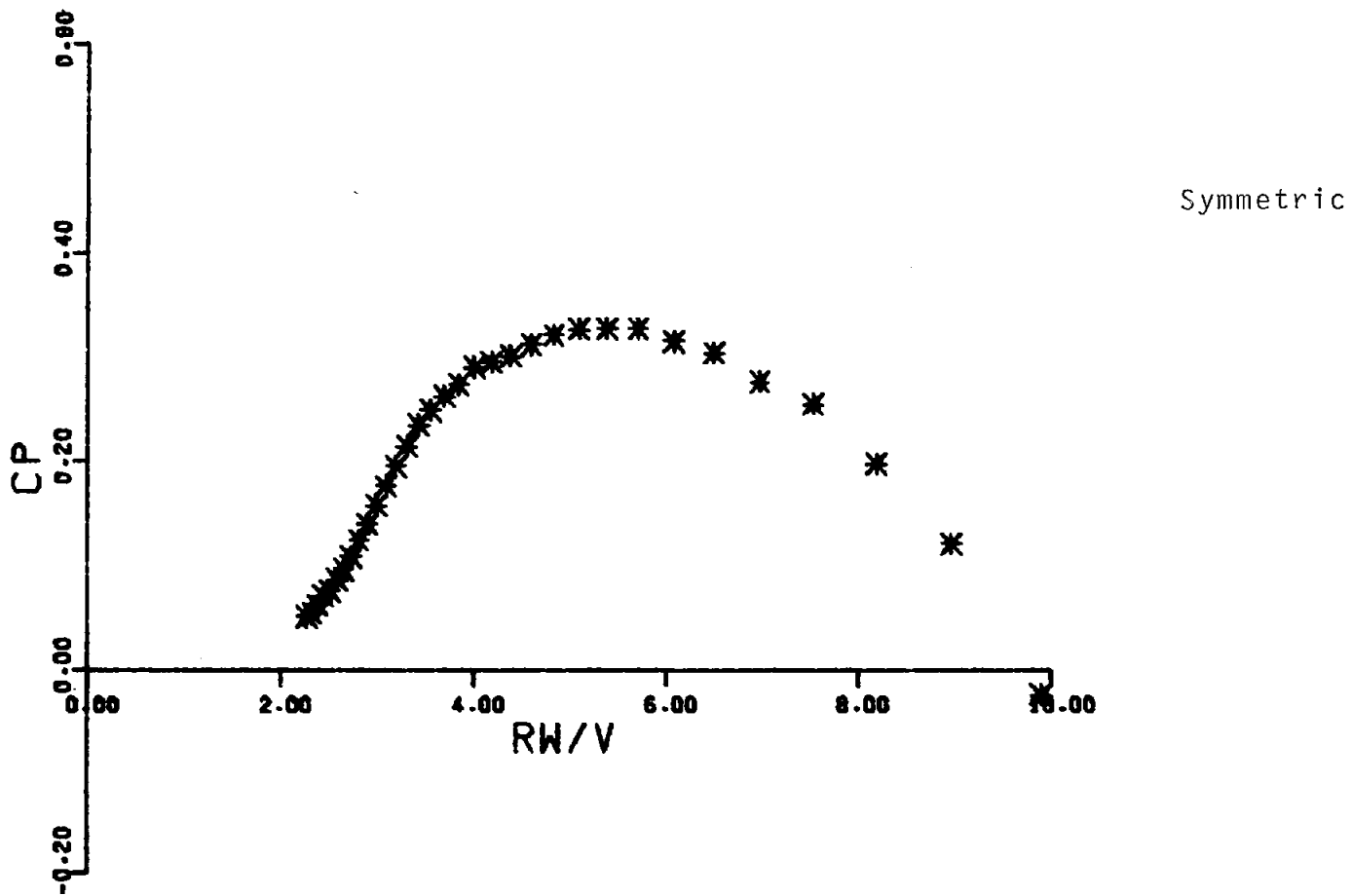


FIGURE 1. C_p vs X , Sandia 5-m 2-bladed Darrieus, NACA 0015 Section

REC ID	TURBINE	RPM	ANEM DESIGN	CUP RECS
	5.	175.0	1	YES
390621.				
390712.				
390711.				
390713.				
391022.				
391111.				
391112.				
391211.				

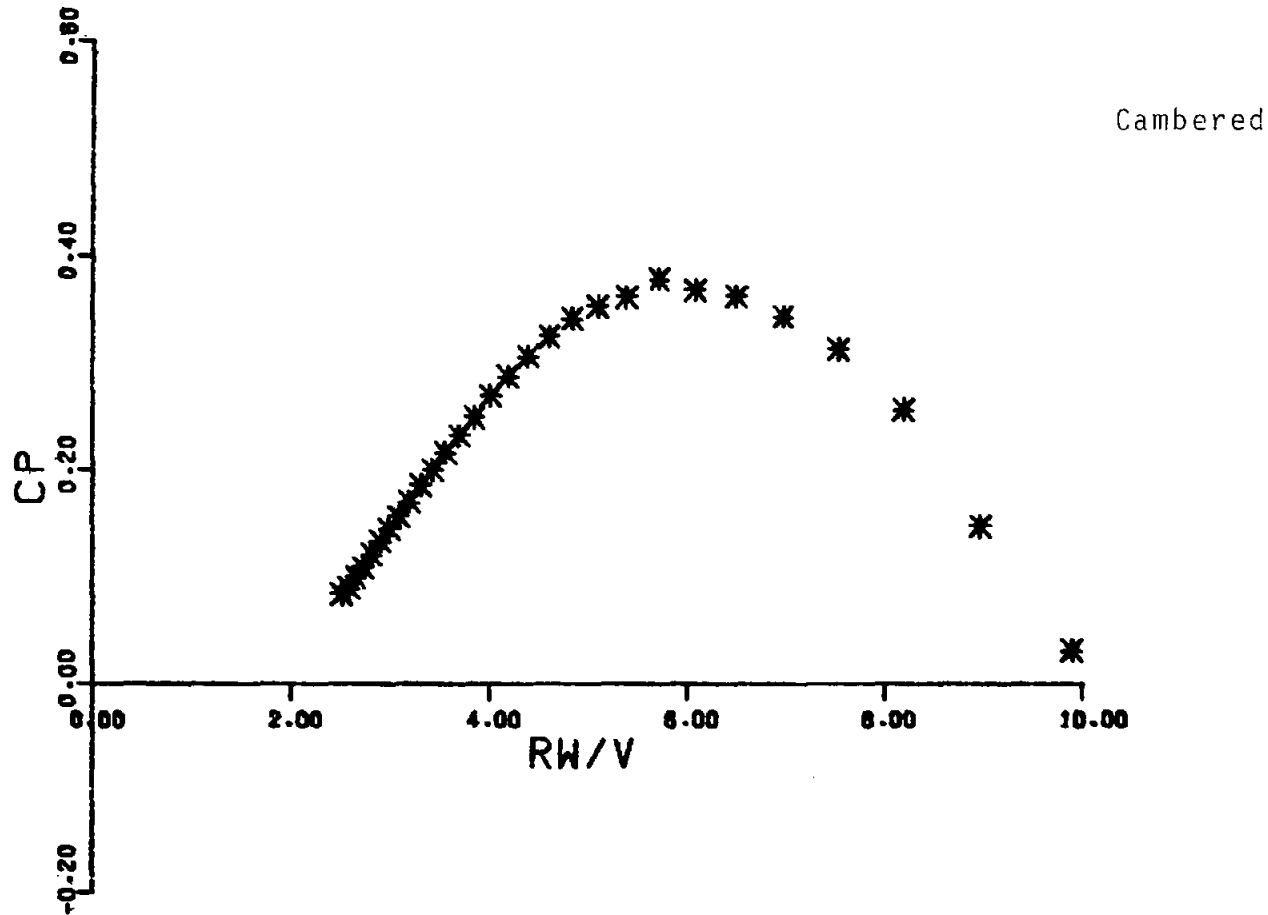


FIGURE 2. C_p vs X , Sandia 5-m 2 bladed Darrieus, NACA 1515 Section

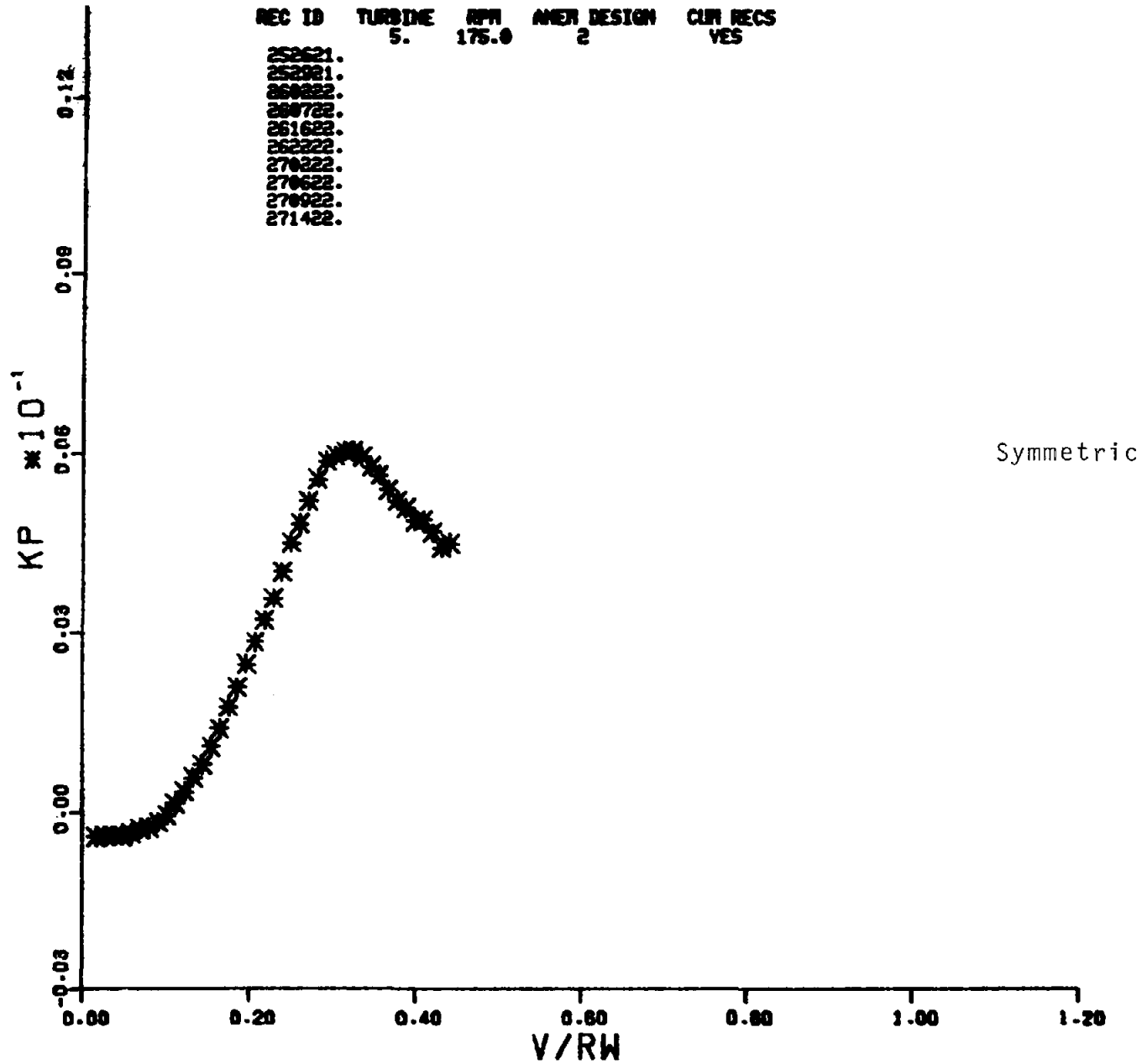


FIGURE 3. K_p vs X , Sandia 5-m 2 bladed Darrieus, NACA 0015 Section

REC ID	TURBINE	RPM	ANEM DESIGN	CUR RECS
390621.	5.	175.0	1	YES
390712.				
390711.				
390713.				
391022.				
391111.				
391112.				
391211.				

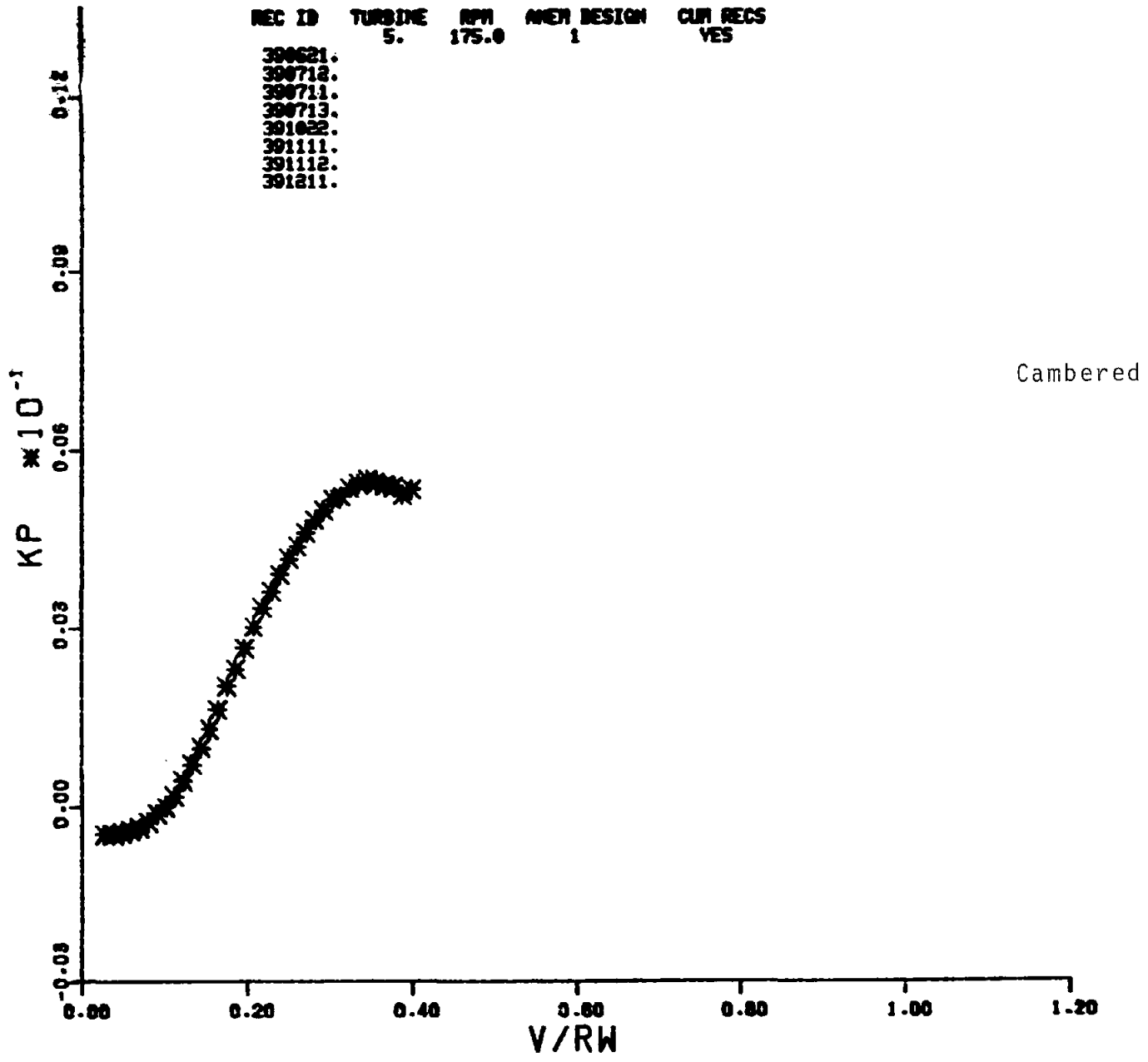


FIGURE 4. K_p vs X , Sandia 5-m 2 bladed Darrieus, NACA 1515 Section

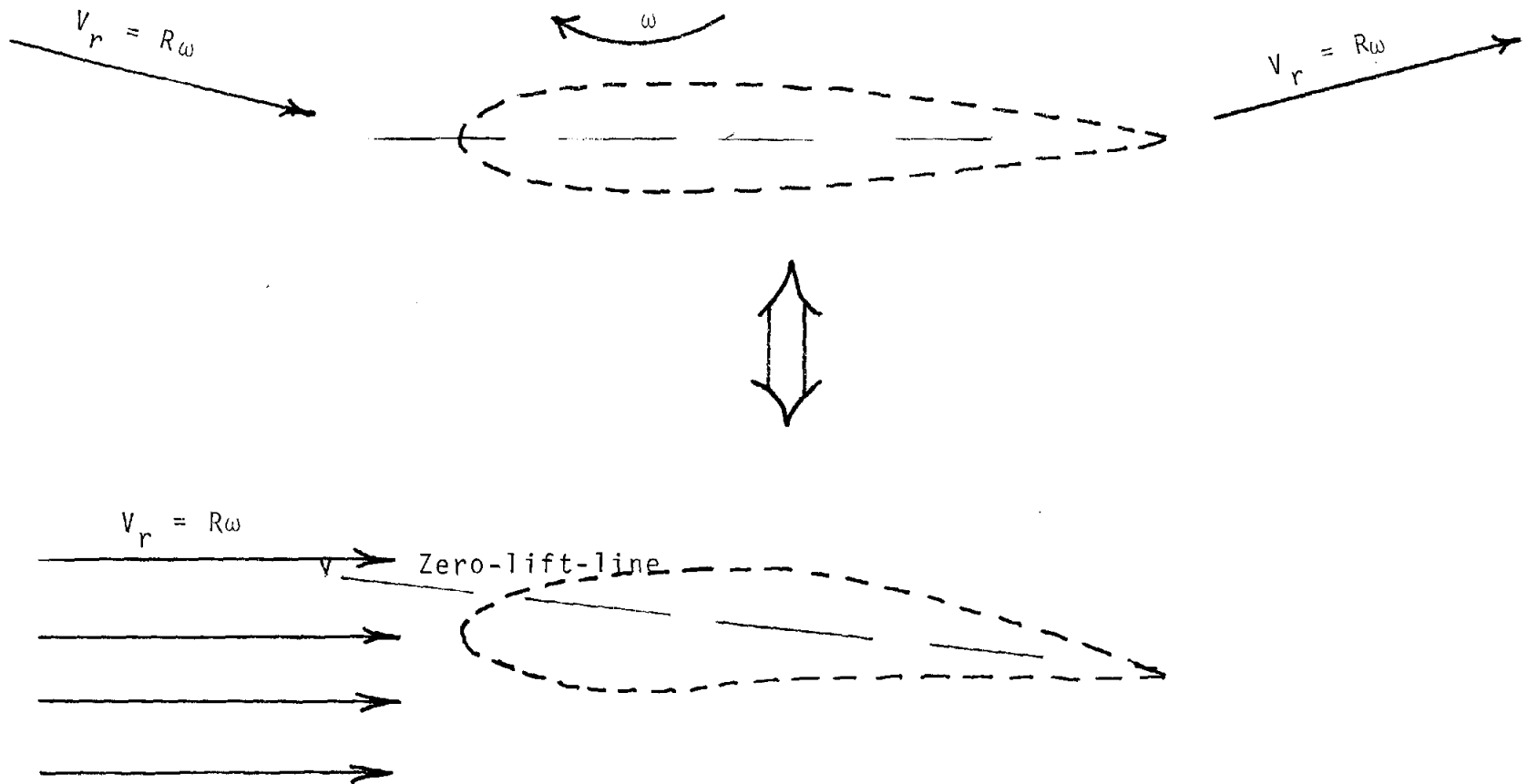


FIGURE 5. Geometric Airfoils in Curvilinear Flow Transform to Equivalent Virtual Airfoils in Rectilinear Flow

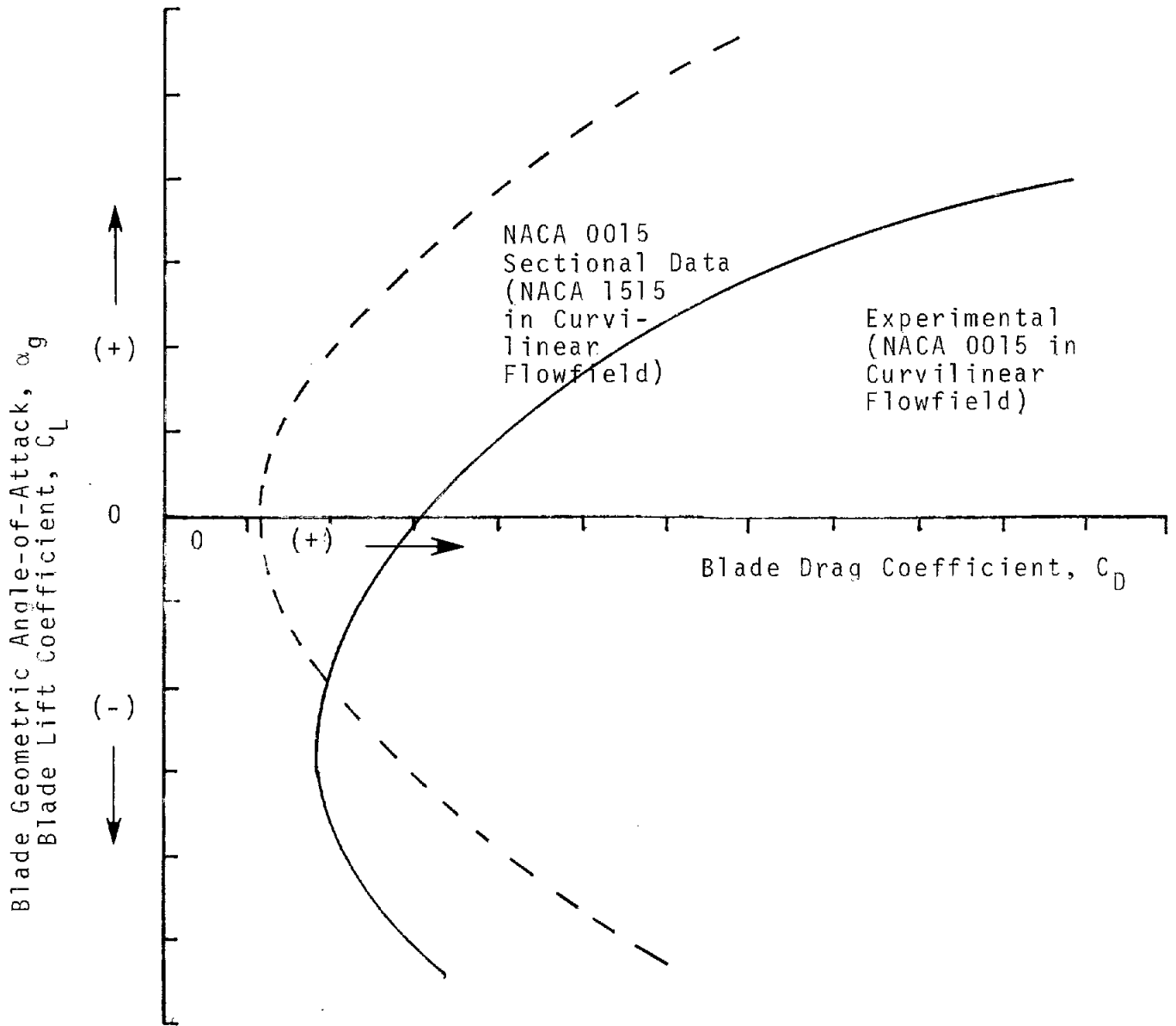


FIGURE 6. Measured and Postulated Curvilinear Flowfield Drag Polars

for sufficient stall to achieve regulation is higher for the 1515 section blades than the 0015's.

V. Summary

Effects upon Darrieus turbine costs of energy of changing certain aerodynamic performance characteristics are noted. The dependence of those performance parameters upon airfoil section properties is discussed. Examples of this dependence are given in terms of experimental results using blades of cambered airfoil sections.

References

1. W. N. Sullivan, Economic Analysis of Darrieus Vertical Axis Wind Turbine Systems for the Generation of Utility Grid Electrical Power, Volume II - The Economic Optimization Model, SAND78-0962 (Albuquerque, NM: Sandia Laboratories, 1979).
2. T. M. Leonard, A User's Manual for the Computer Code PAREP, SAND79-0431 (Albuquerque, NM: Sandia Laboratories, 1979).
3. R. E. Walters, P. G. Migliore, and W. P. Wolfe, "Innovative Straight-Bladed Vertical Axis Wind Turbine," Proceedings of the Wind Energy Innovative Systems Conference (Golden, CO: SERI, 1979).
4. P. G. Migliore and W. P. Wolfe, Vertical Axis Wind Turbine Experiments and Analysis, Volume III: Some Effects of Flow Curvature on the Aerodynamics of Darrieus Wind Turbines (Golden, CO: SERI, forthcoming).

SECTION V
SYSTEM ENGINEERING AND ECONOMICS

SUMMARY OF VAWT ECONOMIC STUDIES AND OPTIMIZATION TECHNIQUES

Robert O. Nellums

Introduction

This paper surveys the economic analysis which has been conducted at Sandia on first-generation VAWTs. Economic methods discussed are the parametric optimization model and the consultant cost study. Results are summarized for energy cost and sensitivity to changes in study ground rules and system configuration. Much of the information for this paper has been drawn from the economic study published in August of 1979 by Sandia.¹

Methodology

Ground Rules

The information summarized in this paper must be qualified according to ground rules which were established for the economic study. Table 1 lists the ground rules which were

ECONOMIC STUDY SCOPE GROUND RULES

1. DESIGNS ARE BASED UPON DEMONSTRATED MANUFACTURING TECHNOLOGIES
2. ROTOR OPERATES AT CONSTANT RPM, DRIVING AN INDUCTION MOTOR/GENERATOR CONNECTED TO A UTILITY GRID
3. BLADES ARE ATTACHED TO A TOWER OF TUBULAR CROSS SECTION, SUPPORTED AT THE TOP BY THREE GUY CABLES
4. TWO AND THREE BLADED OPTIONS ARE CONSIDERED, CONSTRUCTED OF CONSTANT CROSS SECTION NACA 0015 HOLLOW ALUMINUM EXTRUSION
5. ROTOR DIAMETERS RANGE FROM 18 TO 150 FEET

Table 1

laid in order to limit the investigation to a realistic scope. These assumptions have been based upon demonstrated applications to increase confidence in study results. These rules are likely to be modified by future developments in VAWT design. For instance, blade profile modification is currently under study. Table 2 lists the driving structural criteria which

ECONOMIC STUDY
STRUCTURAL GROUND RULES

1. STRUCTURAL COMPONENTS ARE DESIGNED TO A 6000 PSI VIBRATORY STRESS CRITERIA FOR OPERATION IN 60 MPH ROTOR CENTERLINE WINDSPEEDS
2. STRUCTURAL COMPONENTS ARE DESIGNED FOR PARKED SURVIVAL IN 150 MPH ROTOR CENTERLINE WINDSPEEDS
3. GUY CABLE STIFFNESS CRITERIA ARE BASED UPON SCALED CHARACTERISTICS OF THE SANDIA 17-M VAWT TEST BED

Table 2

represent a simplified approach to an extensive and incompletely understood problem. Structural assumptions also have been partially verified using experimental data. Table 3 lists the

ECONOMIC STUDY
ECONOMIC GROUND RULES

1. DESIGN OPTIMIZATION IS BASED UPON MINIMIZING CAPITAL COST PER UNIT OF ANNUAL ENERGY ASSUMING A 15 MPH MEAN WINDSPEED DISTRIBUTION REFERENCED TO 30 FEET
2. ANNUAL WINDSPEED DURATION CURVES ARE DERIVED FROM FORMER NASA STUDIES
3. WINDSPEEDS REFERENCED TO 30 FEET ARE CORRECTED TO ROTOR CENTERLINE HEIGHT USING A .17 WIND SHEAR EXPONENT
4. COST OF ENERGY IS CALCULATED:

$$(\$/KWH) = \frac{18 \times (\text{CAPITAL COST, \$}) + 200 \times (\text{ANNUAL O\&M, \$})}{.9 \times (\text{ANNUAL ENERGY OUTPUT, KWH})}$$

Table 3

final set of ground rules which were planned to make the analysis at Sandia comparable with windspeed^{2,3} and cost of energy⁴ assumptions of other studies. However, comparability between studies continues to be a problem and a careful description of economic methods is the best means at present of allowing comparison.

The Economic Optimization Model

The economic optimization model is actually many models representing successive iterations leading up to the most advanced first-generation model, VERS16. An outline of the model appears in Fig. 1. This model was developed to study the rela-

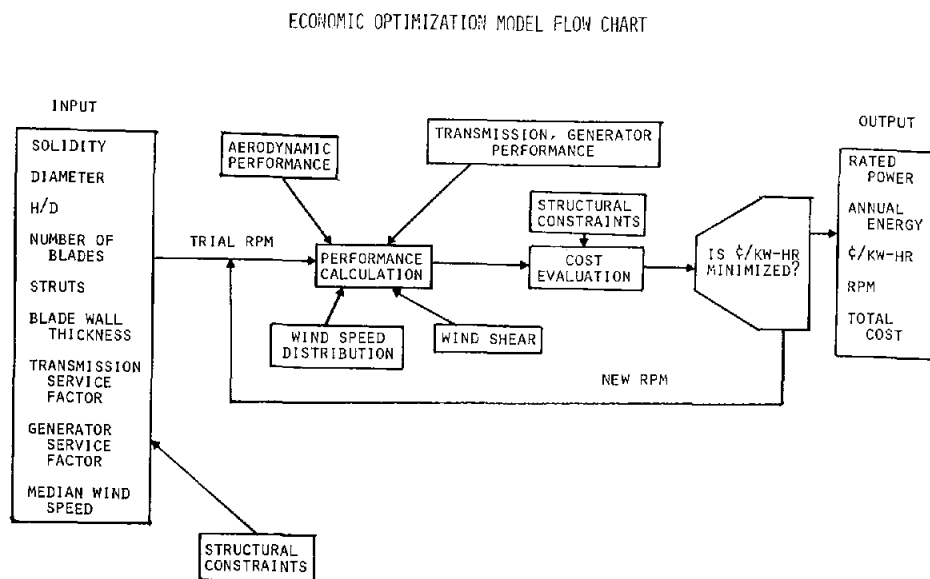


Figure 1

tive cost and benefits resulting from changes in system specification. VERS16 is believed to perform such relative analysis reliably. However, business related costs, operating costs, and many minor item costs have been neglected from VERS16 making it desirable to use other means of estimating absolute energy costs.

The Consultants' Point Design Economic Studies

Two consultants, A. T. Kearney and Alcoa Laboratories, were contracted to independently estimate the price at which Sandia wind turbine designs could profitably be fabricated, sold, and installed. Six point designs were specified in detail for this study. Cost quotes from industrial component manufacturers and field contractors were compiled by each consultant to be combined with the labor, overhead, and profit

requirements of a hypothetical wind turbine company. The scenario for the company included production rates of 10 and 100 megawatts of total VAWT capacity per year and a market assumption of concentrated customers within a 500 mile radius. The scenario for business organization was left to each consultant to decide and Kearney adopted a low investment, low value added business structure where all parts and labor were contracted out while Alcoa adopted a highly capitalized, vertically integrated company scenario.

Results

Optimized Designs and Costs

The results described here are based upon ground rules which, if changed, could substantially modify these conclusions. Characteristic properties for a system optimized using VERS16 are shown in Table 4. In general, the cost of energy is rela-

ECONOMIC STUDY <u>CONCLUSIONS</u>	
ROTOR	H/D = 1.5, TWO BLADES, UNSTRUTTED (STRUTS MAY BE DESIRABLE FOR DIAMETERS ABOVE 150 FEET)
SOLIDITY	RANGES BETWEEN .12 AND .14 DEPENDING UPON ROTOR DIAMETER
RPM	CONSISTENT WITH A WINDSPEED RATING OF 30 MPH, CUT-IN SPEED OF 10-12 MPH, AND PLANT FACTOR OF 20-25%
GROUND CLEARANCE	GENERALLY AS LOW AS POSSIBLE
SIZE	SMALL BUT SIGNIFICANT ECONOMIES OBSERVED FROM 50-150 FEET ROTOR DIAMETER, OPTIMUM SIZE > 150 FEET FOR MINIMUM COST OF ENERGY
COST OF ENERGY	4-6¢/KWH FOR 15 MPH MEAN ANNUAL WINDSPEED

Table 4

tively insensitive to small ($\pm 10\%$) deviations from the design parameters shown in Table 4. Tables 5 and 6 provide design and capital cost estimates for the six point designs as analyzed by the consultants, while Fig. 2 plots the cost of energy for these designs including automatic operation controls and annual operating and maintenance costs.

POINT DESIGN SPECIFICATIONS FROM ECONOMIC OPTIMIZATION MODEL

NOMINAL RATING (KW)	10	30	120	200	500	1600
ACTUAL RATING (KW)	8	26	116	226	531	1330
DIAMETER x HEIGHT (FT)	18 x 27	30 x 45	55 x 83	75 x 113	100 x 150	150 x 225
ANNUAL ENERGY COLLECTION, 15 MPH MEDIAN (MW-HR/YR)	13.7	51.6	244	484	1070	2950
ROTOR RPM	163	95.0	52.0	40.1	31.1	21.0
RATED WIND SPEED (MPH)	34	32	31	30	31	30
PLANT FACTOR (%)	19.3	22.3	24.0	24.4	22.6	24.9
BLADE CHORD (IN)	6	11	24	29	43	64

Table 5

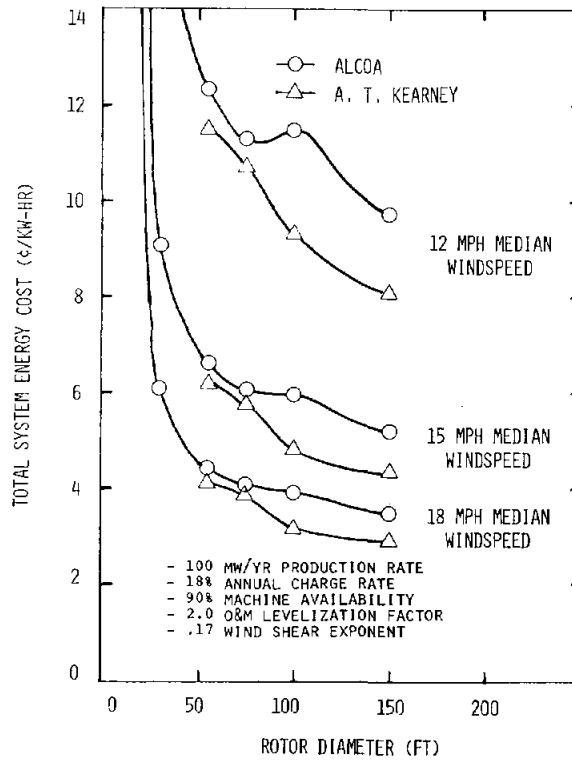


Figure 2

REVISED COMPONENT COST SUMMARY
100 MW/YR PRODUCTION (K \$)

NOMINAL SYSTEM SIZE	SOURCE	BLADES	TOWER	DRIVE	TIEDOWN	ELECTRICAL	DELIVERED SALES PRICE	FOUNDATION	ERECTION	TOTAL
10 kW	Alcoa	.7	1.9	2.6	.6	1.4	7.0	.9	1.1	9.0
30 kW	Alcoa	1.8	2.5	4.3	1.3	1.4	10.6	2.1	1.4	14.1
120 kW	Kearney	7.7	11.0	14.0	4.1	12.7	49.5	10.1	9.7	69.3
	Alcoa	9.4	4.5	18.5	2.5	12.7	47.6	16.0	14.0	77.6
200 kW	Kearney	13.5	18.8	30.5	9.8	29.6	102.2	10.1	12.4	124.7
	Alcoa	16.7	13.5	28.3	6.1	19.3	83.9	24.5	20.5	128.9
500 kW	Kearney	26.4	37.1	65.2	19.7	37.7	186.1	12.8	27.0	225.9
	Alcoa	34.1	41.0	64.1	14.9	52.3	206.4	45.0	37.0	288.4
1600 kW	Kearney	92.7	89.4	178.1	64.7	52.3	477.2	30.6	45.0	552.8
	Alcoa	130.7	121.6	176.8	42.2	47.7	519.0	133.0	67.0	719.0

Table 6

Cost Sensitivities

Rotor Diameter - The sensitivity of energy cost to rotor diameter is shown in Fig. 2 to be gradually decreasing through the largest size studied. Additional development work on the larger systems is warranted to verify this trend. Since turbine weight per unit of output increases with size, the trend in energy cost with size is expected to have a minimum. VERS16 indicates (Fig. 3) a minimum in the curve occurring near 100 ft

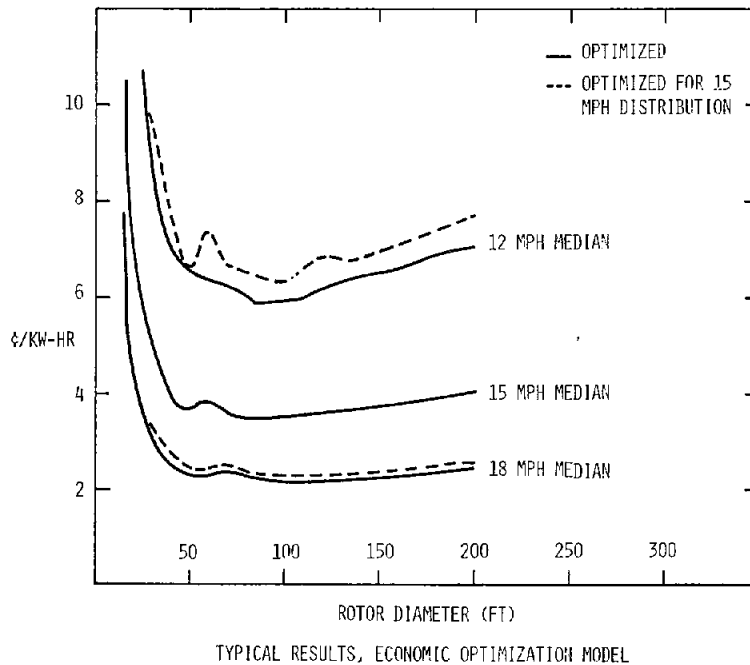
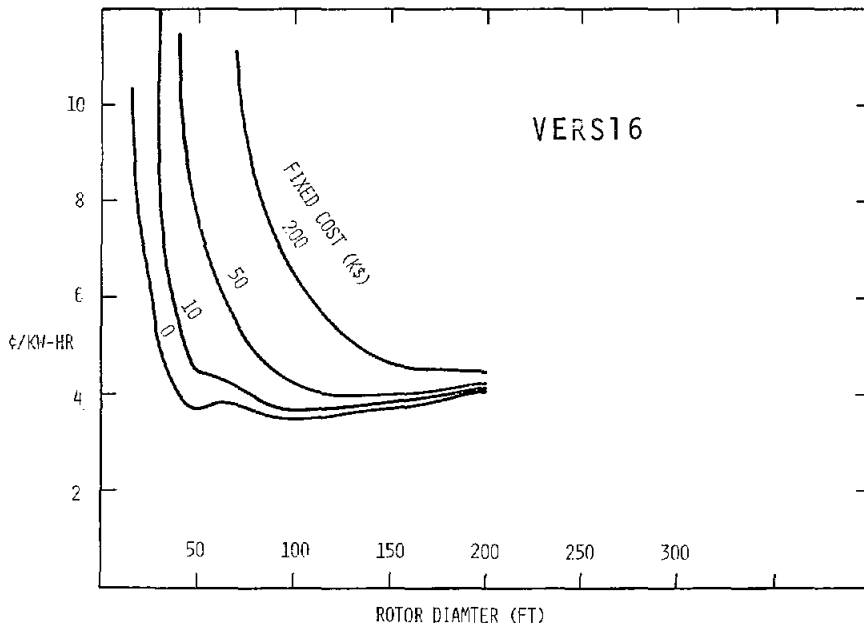


Figure 3

diameters* and if the consultants' study were to be extended to diameters above 150 ft, a minimum in the curve might be expected to occur shortly. The location of the minimum is quite sensitive to assumptions relating to fixed costs (Fig. 4) and wind shear (Fig. 5).

*VERS16 does not include the cost of automatic controls or annual O&M which both tend to have large fixed components such as would shift the optimum toward larger sizes.



EFFECT OF FIXED COSTS ON SYSTEM COST OF ENERGY

Figure 4

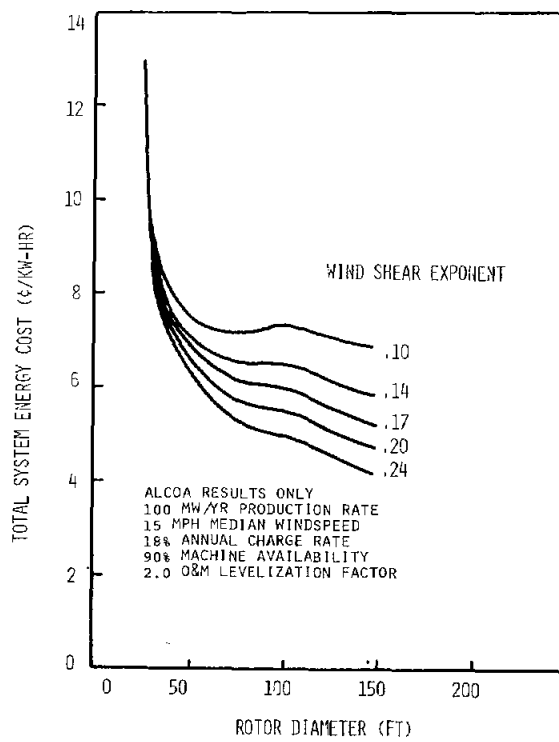


Figure 5

Windspeed Average - The cost of energy is quite sensitive to median annual windspeed as indicated by Fig. 2. Figure 3 shows the effect of optimizing turbine design rpm at average windspeeds other than 15 mph as stated in the ground rules.

Wind Shear - The energy produced by large systems is heavily impacted by the assumption of wind shear magnitude. Figure 5 shows the relative costs of energy given wind shear exponents other than the .17 appearing in the ground rules.

Operating Speed - Figure 6 shows the effect of operating

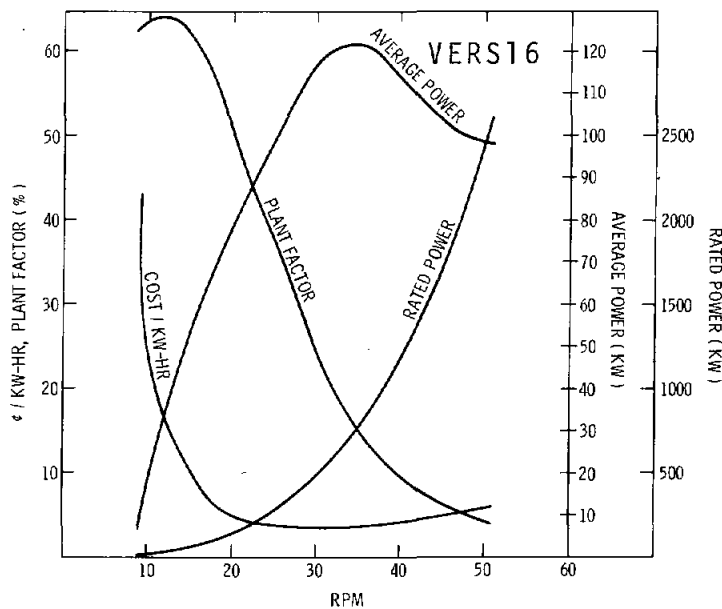


FIGURE 6. 500 kW Point Design

rpm on turbine characteristics. The optimization of energy cost involves balancing two effects which vary with rpm; average power and drive train capacity. Plant factor, the ratio of average to rated power, may be of qualitative importance, but was not considered in the optimization.

Rotor Solidity, Blade Number - Solidity refers to the blade chord length in relation to rotor size. Figure 7 indicates the sensitivity of energy cost to solidity and blade number. An increase in blade solidity tends to increase

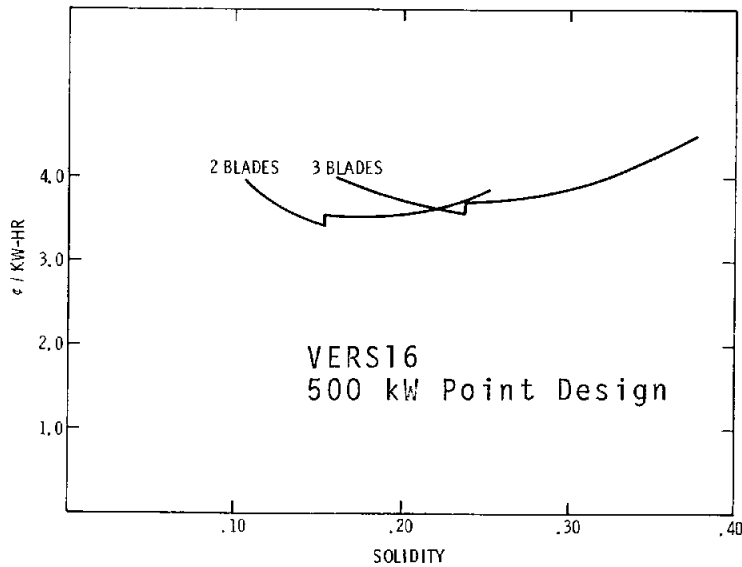


Figure 7

aerodynamic efficiency and improve structural properties in the blade. These benefits must be balanced against the costs for greater blade material and increased transmission torque capacity resulting from the lower rpm accompanying higher solidities. Three blades are shown to be slightly less cost-effective than two; however, the choice of two or three blades may be heavily dependent upon unquantified cost potential relating to torque ripple in the two bladed case and vibrational dynamics in the three bladed configuration.

Height-to-Diameter Ratio - Figure 8 shows the effect of

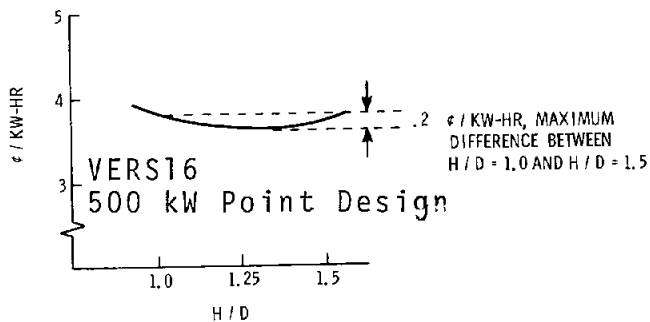


Figure 8

H/D on energy costs. For a given swept area, increasing H/D tends to increase rpm for reduced transmission cost and also utilize wind shear to a greater degree. Counteracting this effect are increased tower and tiedown costs and decreased aerodynamic efficiency at H/D greater than 1.0. The decision to use H/D of 1.5 on the point designs was primarily motivated by a desire for a steep blade angle at the guy cable attachment to minimize potential for blade/cable interference.

Annual Charge Rate on Capital and Fixed Charges - Figure 9 indicates the effect on energy costs of annual charge rates

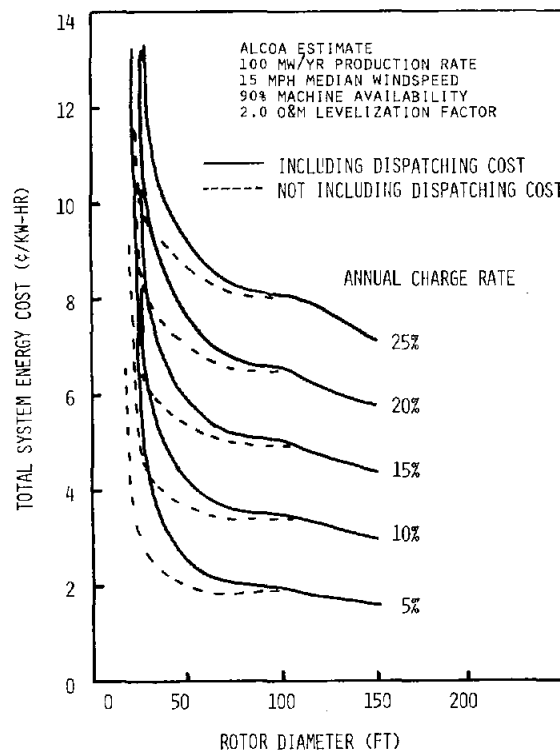


Figure 9

other than the 18% rate which was stated in the ground rules. Also indicated is the magnitude of the effect of a \$433 annual dispatching cost which was assumed to occur for the monitoring of each machine regardless of size. Smaller size machines are

seen to be heavily penalized by costs such as the \$433 which do not scale according to size. Another major cost which did not scale proportionally was the automatic control system. Smaller machines may appear more attractive than is indicated by this study in applications where labor for operation is available at low cost.

New Directions

The concepts costed and optimized in the first-generation economic study are currently being translated into hardware. In September of 1980, the first of four DOE/Sandia 17-m VAWTs being built under contract by Alcoa Laboratories is scheduled to be operational. Cost performance for these machines is expected to compare favorably with the consultants' study considering that only four units are to be built. Figure 10 shows

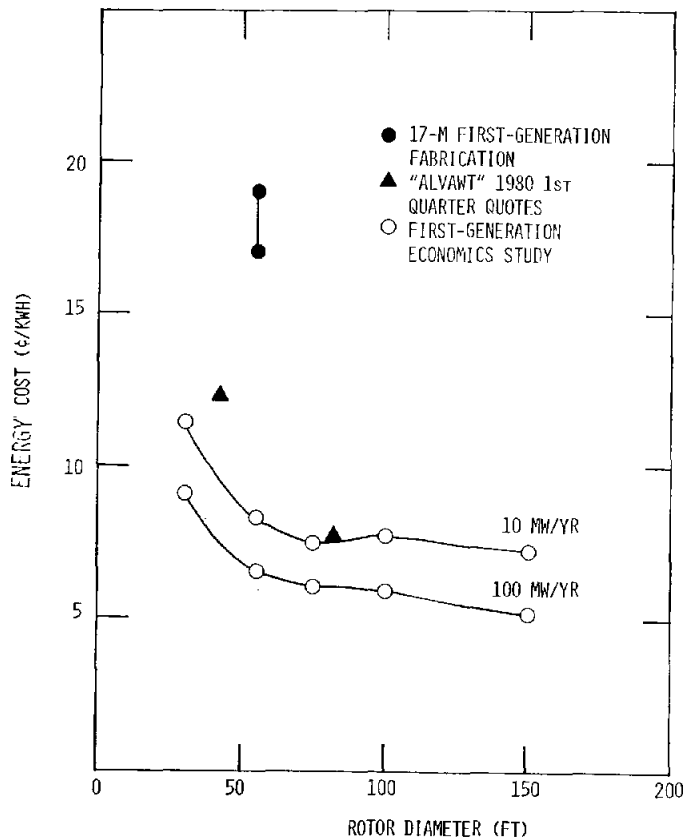


Figure 10

the budgeted fabrication and erection cost* for the 17-m and for Alcoa's internally developed prototypes using O&M and performance estimates from the economic study.

Currently, economic analysis is being conducted at Sandia Laboratories as part of the general effort toward the development of a second-generation design. The methodologies summarized in this paper are being modified to study revised cost, structural, and performance relationships.

*17-m costs as shown do not include engineering or bid and proposal costs for the contractor.

References

1. Economic Analysis of Darrieus Vertical Axis Wind Turbine Systems for the Generation of Utility Grid Electrical Power -- Vol. 1: W. N. Sullivan, Executive Summary; Vol. 2: idem, The Economic Optimization Model; Vol. 3: R. D. Grover and E. G. Kadlec, Point Designs; and Vol. 4: W. N. Sullivan and R. O. Nellums, Summary and Analysis of A. T. Kearney and Alcoa Laboratories Point Design Economic Studies, SAND78-0962 (Albuquerque, NM, Sandia Laboratories, 1979).
2. General Electric Co., Valley Forge Space Center, Design Study of Wind Turbines, 50 kW to 3000 kW for Electrical Utility Applications - Volume II, Analysis and Design, ERDA/NASA/9403-76/2, NASA CR-134935 (Cleveland: NASA Lewis Research Center, 1976).
3. Kaman Aerospace Corp., Design Study of Wind Turbines, 50 kW to 3000 kW for Electric Utility Applications - Analysis and Design, DOE/NASA/9404-76/2, NASA CR-134937 (Washington, DC: U.S. Department of Energy, 1976).
4. J. R. Ramler, R. M. Donovan, Wind Turbines for Electric Utilities: Development Status and Economics, DOE/NASA/1028-79/23, NASA TM-79170 (Washington, DC: U.S. Department of Energy, 1979).

POSSIBLE IMPROVEMENTS IN VAWT ECONOMICS

Emil G. Kadlec

In my previous paper entitled "Current and Future Design Characteristics of Vertical Axis Wind Turbines," the impact of future design characteristics and goals on weight was assessed. The impact on system cost and the cost of energy will be discussed in this presentation.

Review of Changes in Characteristics, Design Philosophies, and Goals from Current to Future Designs

Rather than reiterate all the material presented earlier, only the changes will be highlighted in this presentation.

Specification

Future designs will be required to operate to about 40 mph instead of 60 mph and will be required to withstand 120 mph in the parked condition versus 150 mph.

Design Philosophy

Thinner wall, non-constant cross section blades will be used in the future when consistent with structural requirements and low-cost fabrication techniques.

Lower cable tensions will be used in future designs.

Changes in the aerodynamic performance will be attempted. These include both increasing the power coefficient (C_p) and changing the shape of the C_p curve so that stall regulation occurs earlier.^{1,2}

Conservatism

The buckling safety factor of 10 will be reduced to 5 for the tower design.

General Features

Better matching of speed increaser capabilities and system requirements will be attempted as well as improved speed increaser design and shared function components.

Lower cost installation designs and procedures will be incorporated.

Impact of Goals

In order to assess the impact of some of these potential changes or goals, a study of weights and costs was made of an intermediate class Darrieus wind turbine. This study used the system model VERS16¹ and its derivative ECON16. A fixed geometry and size were chosen so that no optimization was permitted on size, solidity, and height-to-diameter ratio. A 14 mph median windspeed Weibull distribution was chosen. Optimization was allowed on tip speed and rating.

The effects of reduced specification changed design philosophy desired and already achieved aerodynamic characteristics were estimated. The changes affecting structure were to reduce the design windspeed as discussed earlier, cable tension, buckling safety factor, and the blade wall thickness ratio by 50%.

The aerodynamic characteristics examined were the increase of the C_{pmax} from 0.39 to 0.41 (already demonstrated on the 17-m research turbine) and the effect of moving the tip speed ratio (λ) at stall (regulation) closer to the tip speed ratio at the maximum power coefficient (C_{pmax}). The value chosen was

$\frac{\lambda_{reg}}{\lambda_{cpm}} = 0.7$. The current value is between 0.5 - 0.55.

The effects of the structural type changes were as follows:

	<u>Weight Reduction</u>	<u>Cost Reduction</u>
Blades	50%	41%
Tower and Bearings	53%	54%
Tiedowns	45%	45%
Speed Increaser	10%	6%
Generator	10%	5%
Foundation	---	40%
Assembly and Installation	---	30%
Overall System	43%	36%

The total energy was reduced by about 2% and the system rating was reduced by 10%. The cost of energy was reduced by 35%, which is consistent with the 36% reduction in total system costs and the relatively unchanged total annual energy.

When the aerodynamic effects were added to the above changes and the system was reoptimized, the blade, tower, and tiedown weights were not affected, the transmission weight was reduced an additional 6% to a 16% reduction, and the generator weight was increased by 7% to a 3% reduction. The system rating increased to 97% of the original and the total energy increased 13% to 11% over the original and the COE was reduced 43%.

These effects on system weight and cost are tabulated below:

	<u>Weight Reduction</u>	<u>Cost Reduction</u>
Blades	50%	41%
Tower and Bearings	53%	54%
Tiedowns	45%	45%
Speed Increaser	16%	13%

(Continued on Following Page)

	<u>Weight Reduction</u>	<u>Cost Reduction</u>
Generator	3%	2%
Foundation	---	40%
Assembly and Installation	---	30%
Overall System	44%	37%

The reduction in estimated costs for foundations, assembly, and installation is due to the reduced load and handling requirements of the lighter system.

A foundation and tiedown anchor study³ conducted since the construction of the models VERS16 and ECON16 indicates that substantially lower cost anchors and foundations are feasible.

By applying all the previously discussed cost reductions due to structural considerations, improved aerodynamics, and foundation costs to the point design¹ cost estimates, the cost goals for the second-generation are calculated and presented in Fig. 1.

Achievement of these goals will require continued technology development. However, achievement or near achievement of these goals does seem reasonable.

SECOND-GENERATION VAWT ENERGY COST GOALS

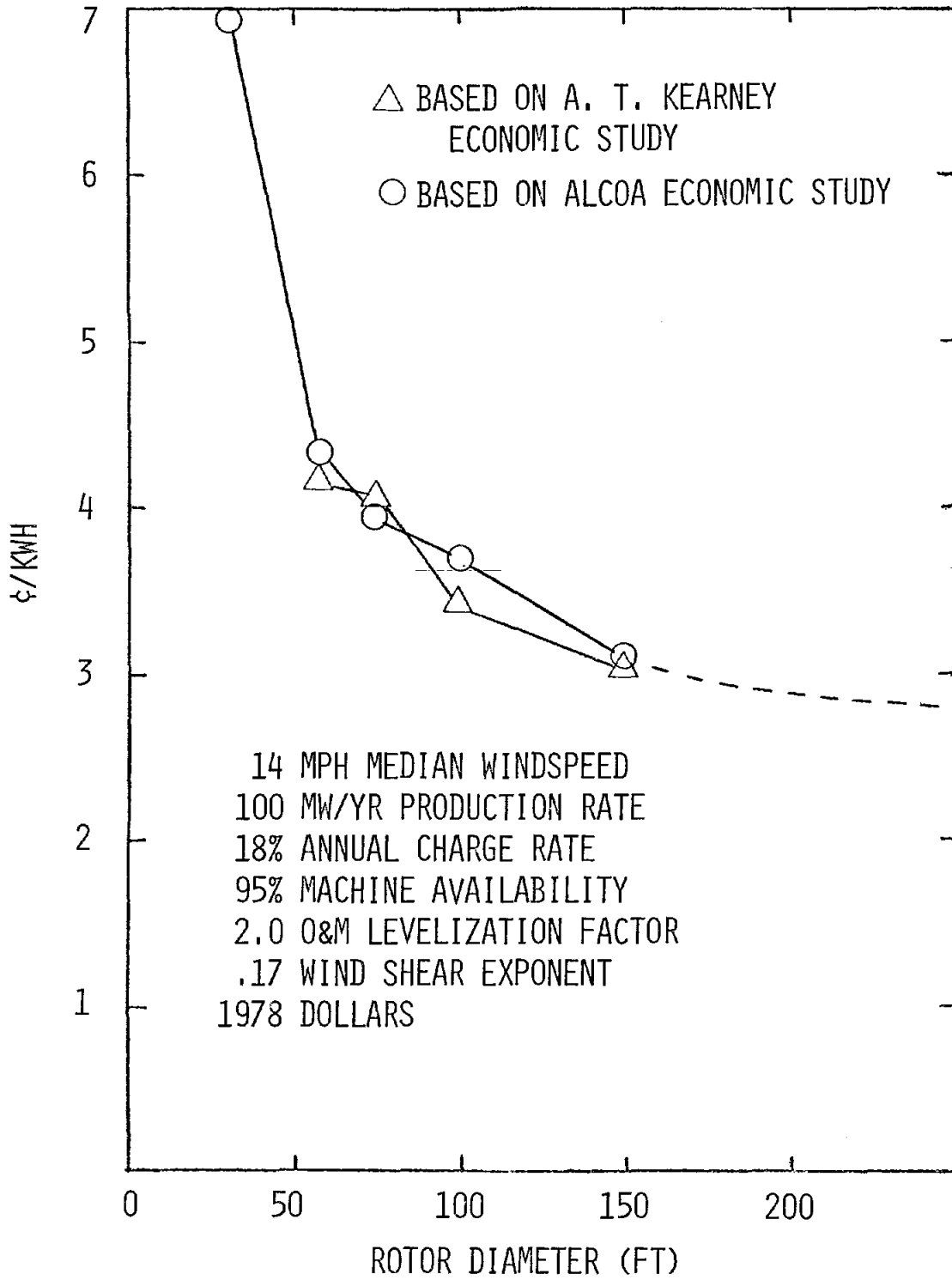


FIGURE 1

References

1. Economic Analysis of Darrieus Vertical Axis Wind Turbine Systems for the Generation of Utility Grid Electrical Power -- Vol. 1: W. N. Sullivan, Executive Summary; Vol. 2: idem, The Economic Optimization Model; Vol. 3: R. D. Grover and E. G. Kadlec, Point Designs; and Vol. 4: W. N. Sullivan and R. O. Nellums, Summary and Analysis of A. T. Kearney and Alcoa Laboratories Point Design Economic Studies, SAND78-0962 (Albuquerque, NM: Sandia Laboratories, 1979).
2. E. G. Kadlec, Characteristics of Future Vertical Axis Wind Turbines, SAND79-1068 (Albuquerque, NM: Sandia Laboratories, 1978).
3. H. E. Auld and P. F. Lodde, A Study of Foundation/Anchor Requirements for Prototype Vertical Axis Wind Turbines, SAND78-7046 (Albuquerque, NM: Sandia Laboratories, 1979).

SECTION VI
EXPERIMENTAL MEASUREMENTS

INSTRUMENTATION OF THE 17 METER RESEARCH TURBINE

M. T. Mattison

The 17 meter vertical axis research wind turbine is the third in a series of Darrieus machines designed and operated by Sandia National Laboratories for the Department of Energy.

These machines are located at the wind turbine test site on Kirtland Air Force Base near Albuquerque, New Mexico. The test site, approximately 1/2 mile east of the main Sandia Laboratories technical area, includes Building 899; a meteorological tower; and the 2, 5, and 17 meter research turbines. The area is typical arid mesa land, free of other structures. Although the average annual wind velocity is relatively low, storm winds are frequent, especially in the spring, when westerly dust storms are a daily occurrence. At other times, winds may be funneled into the area through Tijeras Canyon, in the nearby Sandia Mountains. There are also violent summer thunderstorms, typical of desert regions, which provide strong, but brief, frontal winds. All in all, a lively regime for testing, but poor for power production.

Building 899 houses all control and data processing equipment at the test site. Power is derived from a 480/208 V, 3-phase transformer just south of the control building, which contains the switchgear for control and distribution.

The 17 meter VAWT is 437 feet west of the control building, and is enclosed in a plant-protection fence, 180 feet on a side, just outside the four downguy anchor pads. Fencing is necessitated by the fact that the test site is open to the public, subject to access restrictions on the base as a whole.

Physical security is enhanced by an alarm system on the control building, and by roving Sandia Laboratories guard force patrols.

Instrumentation

The 17 meter turbine at Sandia is clearly configured for research; as an example, the present blade-mounting flanges can accept either 2 or 3 blades, as desired.

Each blade is heavily instrumented with strain gauges bonded to the aluminum surfaces. Such gauges are resistively variable with elongation along a single axis, and are the active elements in a temperature-compensated four-element bridge network. Thus, a strain in the substrate material's surface causes a proportional change in the bridge's resistive symmetry. If a regulated supply voltage is applied to one pair of the bridge terminals, a voltage proportional to the lack of resistive symmetry appears across the opposite pair. For typical resistive strain gauges, this imbalance signal is of the order of a millivolt for one microstrain (microinches of strain per inch of gauge length).

To resolve such small signals, amplification is needed. Also, if the gauge wiring is very long, a considerable amount of noise may be introduced into the measurement. Normal practice, therefore, is to "signal condition" the output of each strain gauge bridge with a low-pass filter and a differential voltage amplifier.

PCM System

A frequently used technique for connecting electrical signals between stationary and rotating parts is that of slip rings, in which a fixed set of brushes continuously wipe a rotating conductive collar. Even if slip rings introduced no electrical noise on contact potentials, the sheer number of individual circuits would prohibit their use for such an

extensive strain gauge layout. Instead, the signal conditioning filter/amplifiers are placed on the rotating structure, and some form of signal multiplexing must be used.

A multiplexing system which has gained favor since digital circuits became cheap and reliable is PCM time-division multiplexing, in which samples of each signal to be transmitted are taken in turn.

Repetitive sequential sampling is called "commutation", from the use, in early analog telemetry systems, of an actual segmented commutator similar to that on a DC motor.

If sequential samples are commutated by a solid-state multiplexer, and are then converted to digital values, we have the basis for a PCM system ("PCM" stands for pulse code modulation, which is clearly a reference to radio telemetry). In such a system, the individual digital sample "words" are clocked out of a storage register in a serial bit-stream; the start of the series of samples is marked by a fixed pattern of one or more "sync words."

This periodic pattern of the sync words is recognized by coincidence logic in the receiving system as the start of a frame; a tracking oscillator can then be made to "lock" on the repetition rate, and subsequent data words can be identified by counting bits. The data words are stored in registers, awaiting further processing.

Figure 1 is a block diagram of a packaged PCM signal-conditioner/encoder like that used on the rotor of the 17 meter VAWT. This commercially-procured system includes plug-in modules for strain gauge signal conditioning, and has 25 Hz filters for each data channel. Such filters are needed to avoid errors due to aliasing at the sampling rate of 50 per second. The current system has 65 available channels, of which 36 are used for blade strain gauges (48 channels, with three

TO STRAIN GAUGE BRIDGE

POWER OUTPUT

SIGNAL CONDITIONER/PCM ENCODER

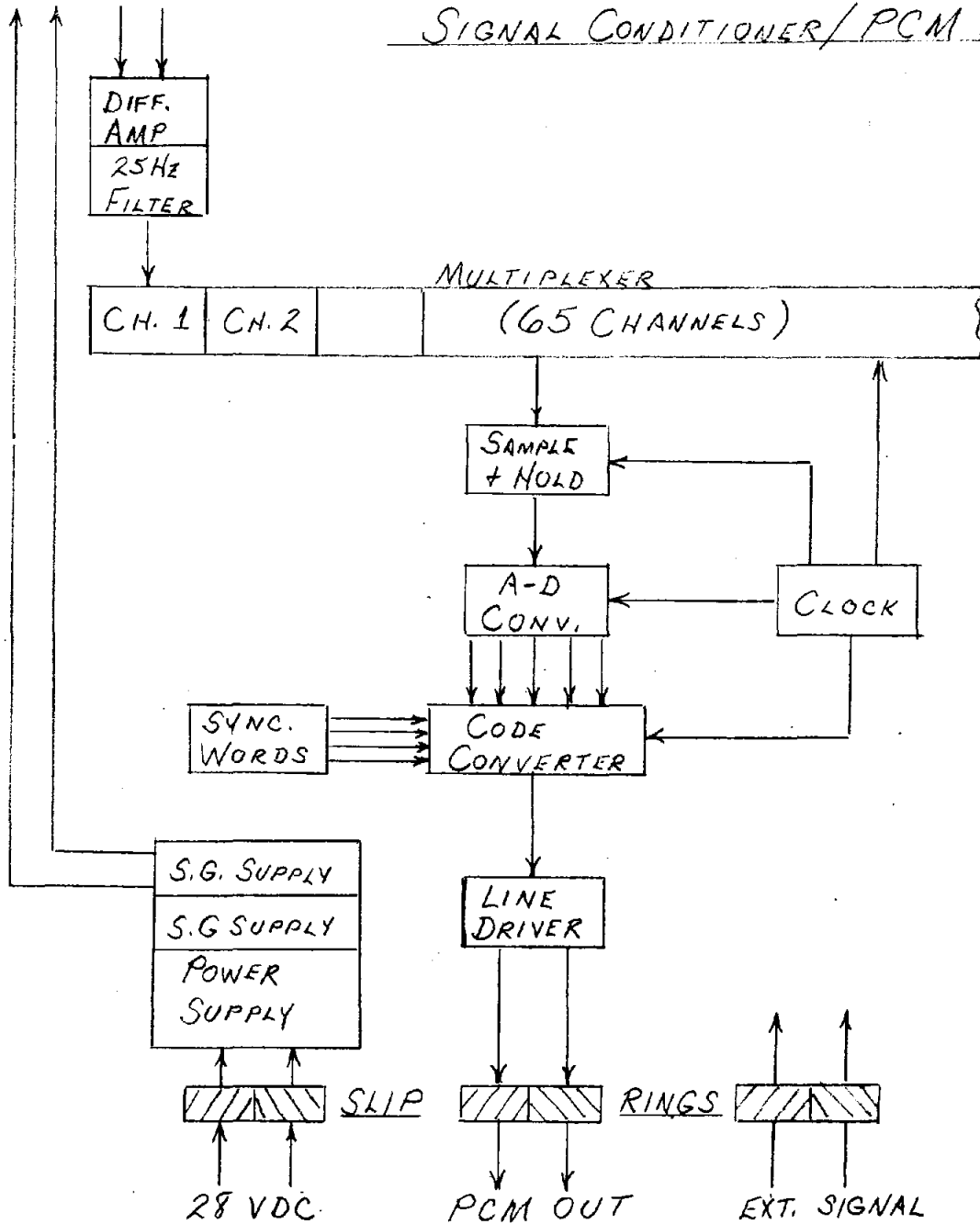


FIGURE 1

blades). Four additional channels carry data from non-rotor instrumentation, passed up through slip ring pairs, for convenience in data analysis. Since it is relatively simple to connect data pairs to unused channels, extra rotor instrumentation is straightforward, if not always easy. At present, we have two accelerometer pairs on the rotor tower, and two points were recently removed from the blades, upon completion of an aerodynamics experiment.

A-D System

Most non-rotor data either originate, or are signal-conditioned, in the control building; an HP2313B multiplexer/A-D converter is used to acquire data from all three wind turbines. At present, 32 channels of high level (± 10.12 V) data plus 16 channels of millivolt-level data, with programmable amplification, can be sequentially or selectively sampled under program control. The system can be expanded by addition of plug-in multiplexers and slight modifications to software. Sampling rates, for most of our data acquisition routines, are operator-selectable. The data are quantized to 12 binary bits, with a measured accuracy of ± 1 bit, or ± 5 mV.

Environmental Measurements

Since wind energy conversion is the fundamental purpose of the wind turbine test site, a large number of anemometers and wind direction indicators are used. The meteorological tower, currently being re-erected and re-instrumented, will have anemometers at 3, 10, 17-1/4, and 30 meters, with direction indicators at 3 and 30 meters. Two anemometers and a wind direction indicator are mounted at 30 meters, on a jackstaff above the 17 meter turbine. One of the two available portable towers is now sited to the west of the 17 meter turbine, providing data at 44 feet. Four other anemometers are located on the test site.

The re-instrumented meteorological tower will have temperature sensors at 3 and 30 meters. Currently, a weather station hutch contains a temperature sensor and a barometric pressure sensor, both with readout instruments in Building 899. These data are used for calculation of air density, for aerodynamic efficiency determinations.

Performance and Control Measurements

The 17 meter turbine is primarily a research machine, with actual production of electrical energy a poor third in the schedule of priorities. It does, however, include both a Kato 75 kVA, 480 V, 3-phase, 4-pole synchronous generator, and on the same shaft, a Lincoln 75 HP, 460 V, 3-phase, 4-pole squirrel cage induction motor. An electrically operated clutch/brake connects the two.

Due to the poor starting characteristics of synchronous generators, turbine starting is usually done with the induction motor, with or without the aid of a timed reduced-voltage starter. A synchronometer is available for changeover to the synchronous generator, but since most testing is done with mechanical parameters in mind, the induction motor is normally left on line to serve as a speed-regulating load, which fortuitously becomes a generator when driven above its synchronous speed of 1800 rpm.

Power demanded and generated by these machines is measured by means of Hall-effect transducers which, with the aid of instrument-grade current and potential transformers, take the instantaneous vector product of current and voltage, to yield a bipolar analog of electrical power. Similar transducers are used to measure rms current and voltage.

Combination torque/speed transducers which use strain gauges for torque measurement and a geartooth/pickup arrangement to measure shaft speed, are installed on both the high

and low speed shafts. Output from these transducers is transmitted by modulated carriers to demodulator units in the control building. These units contain circuitry to provide a digital readout of both speed, torque, and shaft power. Shaft power is presented in terms of kilowatts, positive when the turbine rotor is being driven and negative (by our convention) when the turbine rotor is delivering energy to the generator. Analog signals, suitably scaled, are available for data recording purposes from these commercially available systems.

The turbine brakes are a dual, disc/caliper system in which normal stops are effected by a remotely controlled proportional valve. Pressure is generated by a commercial Vickers pump, with reservoir. This pressure is telemetered to the control building by a commercial transducer. The emergency/parking system is fed by a hydraulic reservoir of the air-bladder type, charged remotely by means of a balance valve from the hydraulic pump. A spring-loaded solenoid valve in this system provides for remote control, with automatic motor disconnect, and for automatic application of the emergency brake in the event of electrical power failure. Available reservoir pressure is also telemetered and displayed at the control console.

Brake disc temperature and transmission lubrication pressure are similarly remotely displayed at the console, while the control rack contains displays of rotor speeds and torques for all three turbines, a selectable anemometer and wind-direction display, and a selectable guy tension display for the four 17 meter downguys.

Data Processing System

The Sandia wind turbine test site data system is structured around a Hewlett-Packard 2112 minicomputer. This is a 16-bit machine, with 32,768 words of core memory. The operating system and programs are stored on the fixed platter of an

HP7905 disc drive; data are stored on removable cartridge discs used with the same drive.

The operating console is a Tektronix 4014 graphics terminal, with a Tektronix 4631 hardcopy unit for permanent records of displayed data. Graphics capability is heavily used, since most analytical work is output in plot form.

Other major peripherals include the PCM decommutator, the HP2112B A-D subsystem, an HP7970E 9-track digital tape unit, an HP1540A multiprogrammer, a paper-tape reader/punch, and a card reader.

The organization of the input-output system in the HP2112 computer allows very convenient interfacing; standard plug-in relay cards are used for automatic control of turbine functions, and a utility interface card is used to read the output of a Datal digital cartridge-tape portable data acquisition unit. Until recently, this unit was used at the crest of Sandia Peak, collecting wind data at 11,000 feet.

Programming

The minicomputer system runs under a relatively primitive, but effective, operating system: Hewlett-Packard's DOS III. Virtually all programming is done in FORTRAN IV, using calls to a few Sandia-written machine language routines and to the system handlers to accomplish input-output tasks. All analysis is performed on a post-test basis, it being more vital to get test data stored on disc than to have real-time presentations. However, all data taken at the site have been catalogued on the fixed disc, so that past tests having parameters within a specified range are selectable by data disc and test number. Most of the data analysis is performed on the same computer system; a rather complete set of specialized analytical and mathematical routines is available.

Automatic Control

Control of the 17 meter turbine was originally done entirely from manually operated switches on the control console in Building 899. Since that time, significant controls have been duplicated with relays operable under program control from the computer, with interlocks to prevent catastrophies. Although most testing is still controlled manually, automatic control is fully operational, with capability for unattended data collection, selectable operating parameters, and a reasonably elaborate set of safety criteria.

The Future

Performance testing of the current 2-bladed configuration of the 17 meter turbine is reasonable complete. Testing of a 3-bladed configuration, using the old fiberglass blades, was done long ago, but the third aluminum blade will probably be installed this year. A redesign to a 1.5:1 configuration is well underway, and this should permit some serious rework of existing instrumentation, as well as control systems. A study of cable damping is now in progress, and results of aerodynamic tests with cambered blades on the 5 meter turbine appear promising.

At the moment, instrumentation effort is concentrated on preparations for acceptance testing the commercially designed 17 meter low-cost VAWT. A similar effort, extending well into the future, appears likely for larger, more powerful systems. The future looks very busy; we welcome it.

INSTRUMENTATION FOR THE 17 METER LOW-COST VAWT

M. T. Mattison

As part of the Department of Energy's program to encourage commercial development of vertical axis wind turbines for the production of electrical energy, the Aluminum Company of America (Alcoa) has contracted to design, fabricate, and install four low-cost 17 meter VAWTs.

In addition to design consultation and other project functions, Advanced Energy Projects Division of Sandia National Laboratories has been tasked by the DOE with acceptance testing of each turbine. To perform this function, special instrumentation is required, over and above that required for turbine operation. A trailer-based data acquisition facility is being prepared for support of this activity.

Turbine Characteristics

The Alcoa 17 meter low-cost VAWT, as currently defined, has a rotor height-to-diameter ratio of 1.5:1, and has two three-piece extruded aluminum blades attached to the central rotor tube, or column, by welded strongbacks, and supported by ministruts. The rotor is supported by three downguys at the top bearing, and by a short tower structure at the lower bearing. A short torque-buffer shaft is attached by flexible couplings to the central column and to the speed-increaser transmission. The high speed shaft drives, or is driven by, a 150 Hp, 3-phase, 480 V induction motor, which serves both as the starting motor and the electrical generator.

A single anemometer on a self-supporting crank-up tower at approximately the radius of the downguy anchor pads, serves

as the primary control instrument. A pulse tachometer on the high speed shaft provides a measurement of turbine speed. Two hydraulic brake systems (service and emergency/parking) are provided on the high speed shaft.

An Intel 8748 microprocessor, with subsequent relay logic, is used to control the turbine. Pushbutton controls at the microprocessor enclosure select either manual or automatic operation. Operating characteristics of the turbine can be set into the control box by means of digital switches. These characteristics are:

- Minimum Operating Windspeed (MPH)
- Integration Time for Minimum Windspeed (SEC)
- Maximum Operating Windspeed (MPH)
- Integration Time for Maximum Windspeed (SEC)
- Maximum Turbine Speed (RPM)
- Maximum Time to Accelerate to Rated RPM (SEC)

In addition to restrictions on operation imposed by these settings, the system may be inhibited by other conditions. These are:

- Microprocessor Failure
- Tachometer Failure
- Excessive Vibration
- Generator (or Ground) Fault
- Power Interruption
- Extreme Cold

Failure to operate for reasons other than low or high winds will enable an alarm circuit, and will require manual resetting of the control system. A set of labeled L.E.D.'s is available for help in trouble diagnosis.

An additional control function was added to the system at Sandia's request: an external link is provided in the "Extreme Cold" leg of the relay logic. Opening this circuit will inhibit

turbine operation by application of the emergency/parking brake. This emergency function will be operable either manually or under program control from the instrumentation trailer.

Test Instrumentation

An effort has been made to avoid any possible interference with normal turbine operation. Only four control functions are to be monitored by the acceptance-test instrumentation:

- Anemometer Pulse Rate
- Tachometer Pulse Rate
- Vibration Switch Closure
- Parking/Emergency Brake Release

Outputs from the anemometer and tachometer are TTL-level pulse trains, which will be isolated from the control circuitry by unused segments of an existing hex inverter module. A line-driver card will be added to the microprocessor enclosure to transmit these signals to the test data trailer, where they will be regenerated, clipped, and integrated to provide analog voltage levels suitable for further processing.

The vibration switch and brake release indicators are "dry" relay contacts, unconnected to the turbine circuitry, whose continuity will be monitored at the trailer. The brake release indicator will be used for data acquisition program scheduling, to warn that the turbine is about to start or stop.

A set of Hall-effect transducers, with their associated current and potential transformers, will be added to the switch-gear enclosure to monitor electrical power (both utilized and generated), and rms current and voltage.

The turbine rotor will be instrumented with 24 strain gauges, as shown in Fig. 1, for verification of calculated stress levels and vibrational characteristics of the rotating structure. An additional strain gauge pair will be installed

STRAIN GAUGE LOCATIONS - 17M LOW COST

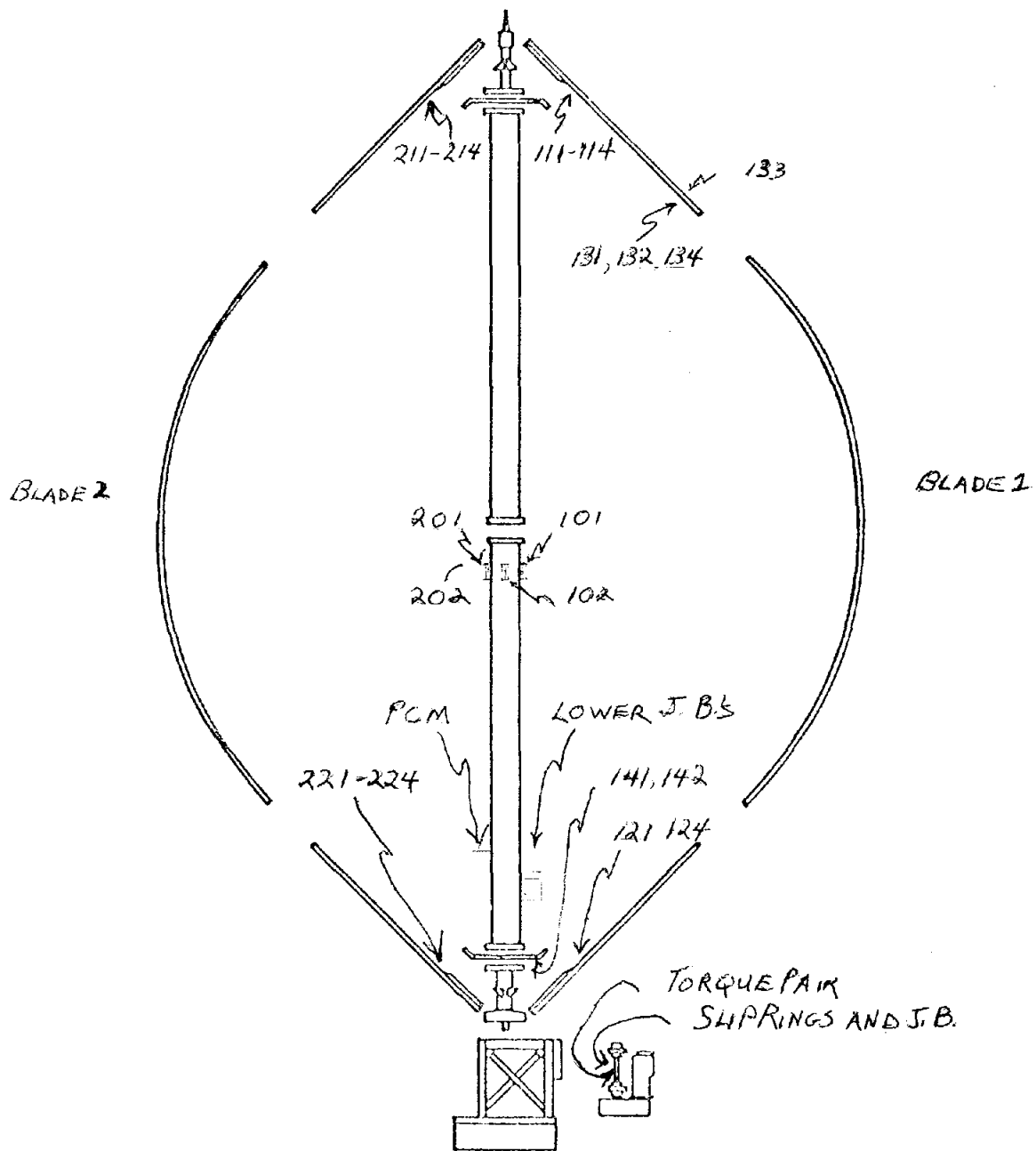


FIGURE 1

on the low speed torque shaft to serve as a torquemeter. The temperature-compensating bridge completion units, required for each strain gauge, will be mounted near the rotor column on which a set of junction boxes will be mounted for interconnection to multiconductor signal cables. These cables will be dressed along the rotor column to a final pair of junction boxes just above one of the ministruts. The cable to the torque pair will run through a clearance hole in the rotor column, down through the center in the lower bearing, around the torque shaft's upper Falk coupling, and terminate in a junction box at the inner slip ring mounting.

Data Acquisition

To facilitate collection of torque and strain gauge data from the turbine rotor, an EMR 600-series data acquisition package will be mounted on the center column approximately four feet above one of the lower ministruts. It is powered by 28 volts DC, supplied from the instrumentation trailer through segments of a 24-pair slip ring set mounted near the top of the torque-buffer shaft.

This data acquisition package includes signal conditioning (strain gauge power supplies, pre-filters, and differential amplifiers) for 32 analog data channels. It also includes a pulse-code modulation (PCM) system, whose serial pulse-train output will then be carried through a slip ring pair to the instrumentation trailer.

Each analog signal is sampled in sequence 50 times per second, and is converted into a 10-bit offset binary number (-5.12 v = zero counts, 0 v = 256 counts, and +5.11 v = 1023 counts). For the strain gauge signals, one bit (10 millivolts) will be equivalent to about 7 microstrains (microinches per inch of gauge length).

The complete PCM format is shown in Fig. 2. Note that seven channels are derived from off-rotor transducers. These signals are included in the PCM frame for convenience in data storage and analysis. They will be passed up to the PCM system through slip ring pairs after signal conditioning.

Environmental Data

As a check on the performance of the Alcoa anemometer, a separate anemometer and wind direction indicator will be mounted on a pipe mast at the instrumentation trailer. A small instrument shed outside the trailer will contain sensors for measurement of ambient temperature and barometric pressure, needed for aerodynamic efficiency calculations.

Instrumentation Trailer

A commercial Bakertrail semi-trailer, 25 feet long by approximately 7-1/2 feet wide, is being modified to house the mobile instrumentation facility. Operable from either 480 V or 208 V, 3-phase electrical power, it will provide shelter and work space for a maximum crew of three. Extra insulation, a heating and air conditioning system, and a fair amount of under-trailer storage space have been provided to permit independent operations at environmentally severe remote locations. Three 6-foot equipment racks, plus an operator's console position, occupy the forward end. A small workbench, storage cabinets, and rudimentary facilities for food storage and preparation occupy the rear end. Two tinted glass windows at the sides of the operator's console are intended to serve as escape hatches and to provide a view of the wind turbine under test. Tiedown rings are provided to stabilize the trailer under high wind conditions.

PCM Layout - 17 Meter Low-Cost

<u>CH#</u>	<u>Strain Gauge</u>	<u>Blade</u>	<u>Location</u>
1	111	1	Upper Attachment-Leading Edge
2	112	1	Upper Attachment-Fwd Strongback Edge
3	113	1	Upper Attachment-Aft Strongback Edge
4	114	1	Upper Attachment-Trailing Edge
5	211	2	Upper Attachment-Leading Edge
6	212	2	Upper Attachment-Fwd Strongback Edge
7	213	2	Upper Attachment-Aft Strongback Edge
8	214	2	Upper Attachment-Trailing Edge
9	121	1	Lower Attachment-Leading Edge
10	122	1	Lower Attachment-Fwd Strongback Edge
11	123	1	Lower Attachment-Aft Strongback Edge
12	124	1	Lower Attachment-Trailing Edge
13	221	2	Lower Attachment-Leading Edge
14	222	2	Lower Attachment-Fwd Strongback Edge
15	223	2	Lower Attachment-Aft Strongback Edge
16	224	2	Lower Attachment-Trailing Edge
17	131	1	Upper Joint-Leading Edge
18	132	1	Upper Joint-Maximum Thickness, Inside
19	133	1	Upper Joint-Maximum Thickness, Outside
20	134	1	Upper Joint-Trailing Edge
21	141	1	Lower Strut-At Fwd Notch, Underside
22	142	1	Lower Strut-At Aft Notch, Underside
23	101*	Tower	In Blade Plane, Below Joint, Toward Blade 1
24	102**	Tower	90° Trailing, Below Joint
25	Torque Pair		
26	H.S. Shaft Speed (Alcoa)		
27	Windspeed (Alcoa)		
28	Windspeed (Sandia)		
29	Wind Direction (Sandia)		
30	Generator Power		
31	Generator Current		
32	Generator Voltage		

* May be in series with 201 (in plane, toward blade 2)

** May be in series with 202 (270° trailing)

FIGURE 2

Data Analysis and Storage

A Hewlett-Packard 2112M digital computer, similar to the one used at the wind turbine test site at Sandia, is the nucleus for data processing. An HP7906 disc drive, with one fixed and one cartridge disc, provides program and data storage. The operator's console is an HP2648 graphics terminal, with a Tektronix 4631 video hardcopy machine for desired permanent records of displayed data.

An EMR 2746 PCM decommutator, with plug-in peripherals and a custom-built computer interface, provides program-selectable access to any or all of the data words in the PCM format. An octal display of any selected channel is available on the front panel.

A separate data acquisition system, the HP2313B A-D converter/multiplexer, provides sampled digital data for any or all of 48 channels of analog data, 32 of which are high-level (± 10.12 V), differential input, and 16 of which may be low-level differential signals, amplified under program control. The system is expandable by addition of plug-in multiplexer/amplifier cards. Resolution is 12 binary bits (± 1 part in 4095) which provides adequate accuracy and dynamic range.

A tentative format for data inputs to the HP2313B A-D system is shown in Fig. 3. This format follows the channel assignments now in use at Sandia; its adoption would allow use of some specialized analysis programs without modification.

Programming

The data acquisition routines that will be used for testing the low-cost VAWTs are largely those which have been used and developed at Sandia during the past several years. All principal programs are written in FORTRAN IV, with a few specialized machine-language segments called as subroutines.

A-D Layout, 17-m Low-Cost VAWT

<u>A-D Channel</u>	<u>Data Description</u>	<u>Cal. Factor</u>	<u>Notes</u>
1	Turbine Power	kW/V.	D
2	Turbine Current	RMSAMP/V.	
3	Phase Voltage	RMSV./V.	
7	Ambient Temperature	DEG.C./V.	I
10	Ambient Pressure	MB./V.	I
11	Turbine Brake Release	1 V./V.	
12	Turbine Vibration Switch	1 V./V.	
16	High Speed RPM	RPM/V.	D
17	Turbine Windspeed	MPH/V.	D
18	Sandia Windspeed	12 MPH/V.	D
19	Sandia Wind Direction	108 DEG./V.	D

I - Denotes analog display from instrument

D - Denotes planned panel display

FIGURE 3

During the first weeks of testing, it is expected that our principal analysts will serve as operators, and will do at least "first look" analysis on the site. For this period of time, we will be using routines we have used many times, and which require only trivial modifications to be fully applicable.

In the second phase of testing, we expect to use sequenced, automatically called routines for data acquisition. During this period, it should only be necessary to verify that the turbine is operating, that data acquisition is proceeding, and to exchange cartridge discs. Reduction and detailed analysis of the accumulated data will be accomplished at Sandia during this period, with "quick looks" only at the test site to assure that instrumentation failures have not occurred.

Siting and Site Preparation

At the moment of writing, only one installation site for a low-cost 17 meter VAWT has been chosen: the Wind Systems Test Center at Rocky Flats, near Boulder, Colorado, operated for the DOE by Rockwell International.

As a "friendly" location, this choice could not be improved upon. The Rocky Flats personnel are familiar with testing and test problems. Since they will, following successful acceptance testing, take charge of the machine for long-term evaluation, they have been most cooperative in assisting with siting and preparations for installation.

The principal power on this site is a 13.2 kV line from Colorado Power and Light, distributed in underground conduit on the test site. Since the nearest existing distribution transformer is some distance from the chosen site (Station 4.1), a new 13.2 kV/480 V, 3-phase, 300 kVA transformer will be installed near the turbine controller, as shown in Fig. 4.

TENTATIVE PLAN - 17M LOCo VAWT
 ROCKY FLATS WIND TEST SITE

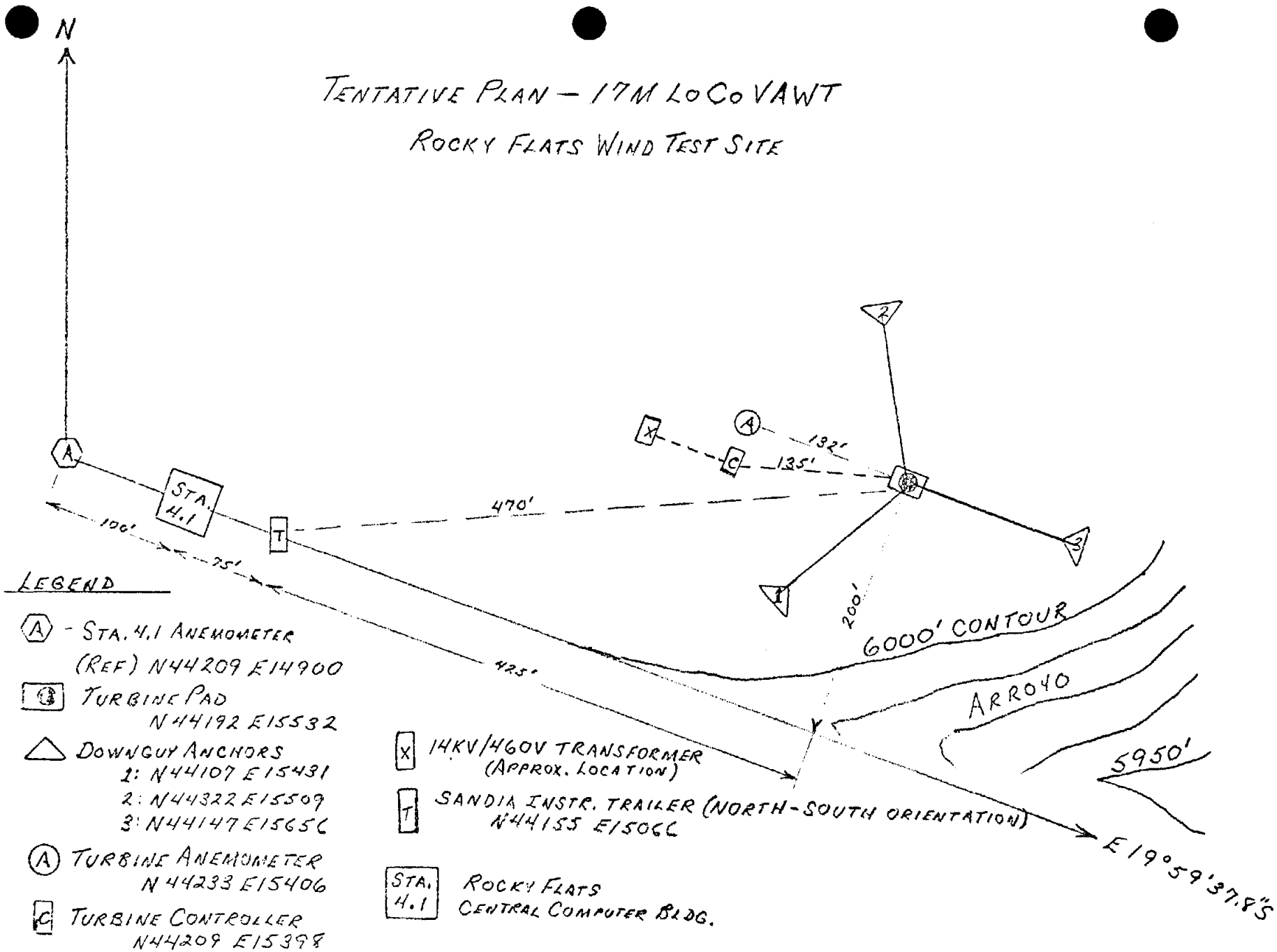


FIGURE 4

The Sandia instrumentation trailer will be spotted near the Station 4.1 pad, which currently houses the site computer facility. In accordance with site practice, Rocky Flats will provide concrete tiedown pads for the trailer; destructively high winds are common in this area. A 480 V, 3-phase line, terminating in utility outlets, will be provided near the trailer. (For later testing, under less favorable conditions, we have provided for runs of 500 feet of trailer cable.) Rocky Flats has also kindly agreed to provide telephone service. A roving guard force, working out of the nearby main plant, will provide protection for both the turbine and trailer. These and other site amenities, which would otherwise have to be arranged at considerable time and expense during site preparation, are very welcome. In return, we hope to be of service in smoothing preparation for the Rocky Flats tests, before we move to the next site.

CURRENTLY AVAILABLE INSTRUMENTATION SOFTWARE COLLECTION AND ANALYSIS PACKAGES ON THE 17-M RESEARCH TURBINE

Gerald M. McNerney

The DOE/Sandia vertical axis wind turbine (VAWT) experimental site is equipped with a mini-computer system which is used primarily for data acquisition, data reduction, and automatic control. The initial software development was aimed at "method of bins" type¹ reduction of real time aerodynamic performance data. Since the early stages of development, the software system has been expanded to perform a variety of jobs useful to the wind energy program. At the present time, there are more than 80 software packages available to perform primary and supporting jobs that fall into the following six categories:

1. Mathematical Functions
2. Aerodynamic Performance Testing
3. Structural Data Analysis
4. Automatic Control and Related Functions
5. Communicating Information to and from Other Computer Systems
6. Miscellaneous

In this paper, the six categories will be discussed in the context of the Sandia wind energy program and the types of programs available in each category will be reviewed.

Discussion of the Categories of Software Packages

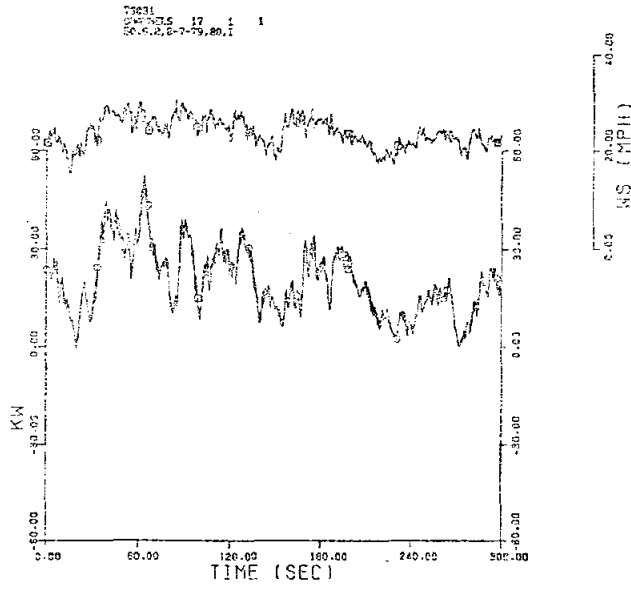
1. Mathematical Functions - The computational and storage capacity of the mini-computer system is sufficiently large for many calculations useful in wind turbine studies. Most notably,

the ability to store time resolved records from the Pulse Code Modulator (PCM) and the Analog to Digital Converter (A/D) has been introduced as software packages on the mini-computer. Along with the storage of time series records, the usual methods of time series analysis including plots, the calculation of spectral densities and cross correlation, and digital filtering are available. Figure 1 shows examples of time series plots, and Fig. 2 shows an example of a spectral density plot.

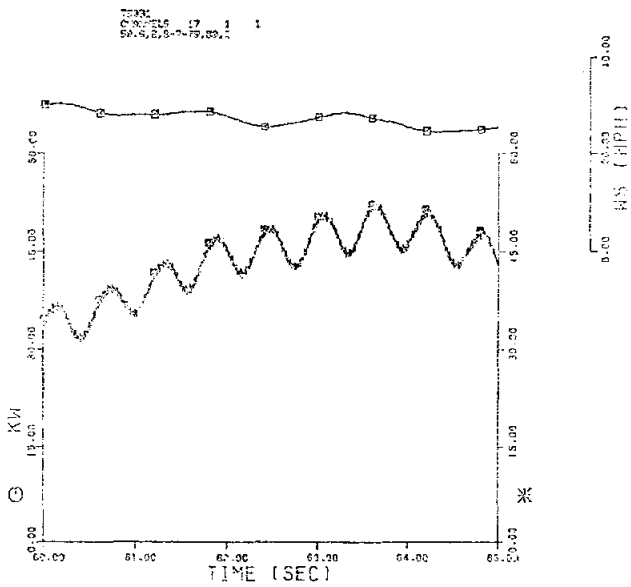
In a more theoretical setting, functions that are purely periodic are a special case of time series, and some packages have been developed to deal with this case. For a given periodic function, the first several Fourier coefficients can be calculated, which have use in torque ripple studies. In the opposite direction, a periodic function can be composed from its first few Fourier coefficients, and a periodic time series can be created from any number of input values.

Although most modern aerodynamic codes are too complicated to be useful on a mini-computer, a version of the single streamtube model is available and has been used to prepare predictions of the aerodynamic torque and resultant tower force functions. These predictions have been used to compare with actual measurements on the 17-m system.

2. Aerodynamic Performance Testing - Evaluation of the aerodynamic performance of the VAWTs is one of the most important functions of the DOE/Sandia VAWT program. The method of bins amounts to dividing the windspeed range into delta v's (Δv), and averaging all the readings of the torque meter taken in each Δv , and was developed here exactly for aerodynamic performance testing. The method is quite well suited for reducing large quantities of real time data since the fluctuations due to wind variations are averaged out, and very little storage space is required.



Time Series Long Time Scale



Time Series Short Time Scale

FIGURE 1

T1033
CHANNEL NUMBER 16
UPPER INSIDE FLATWISE

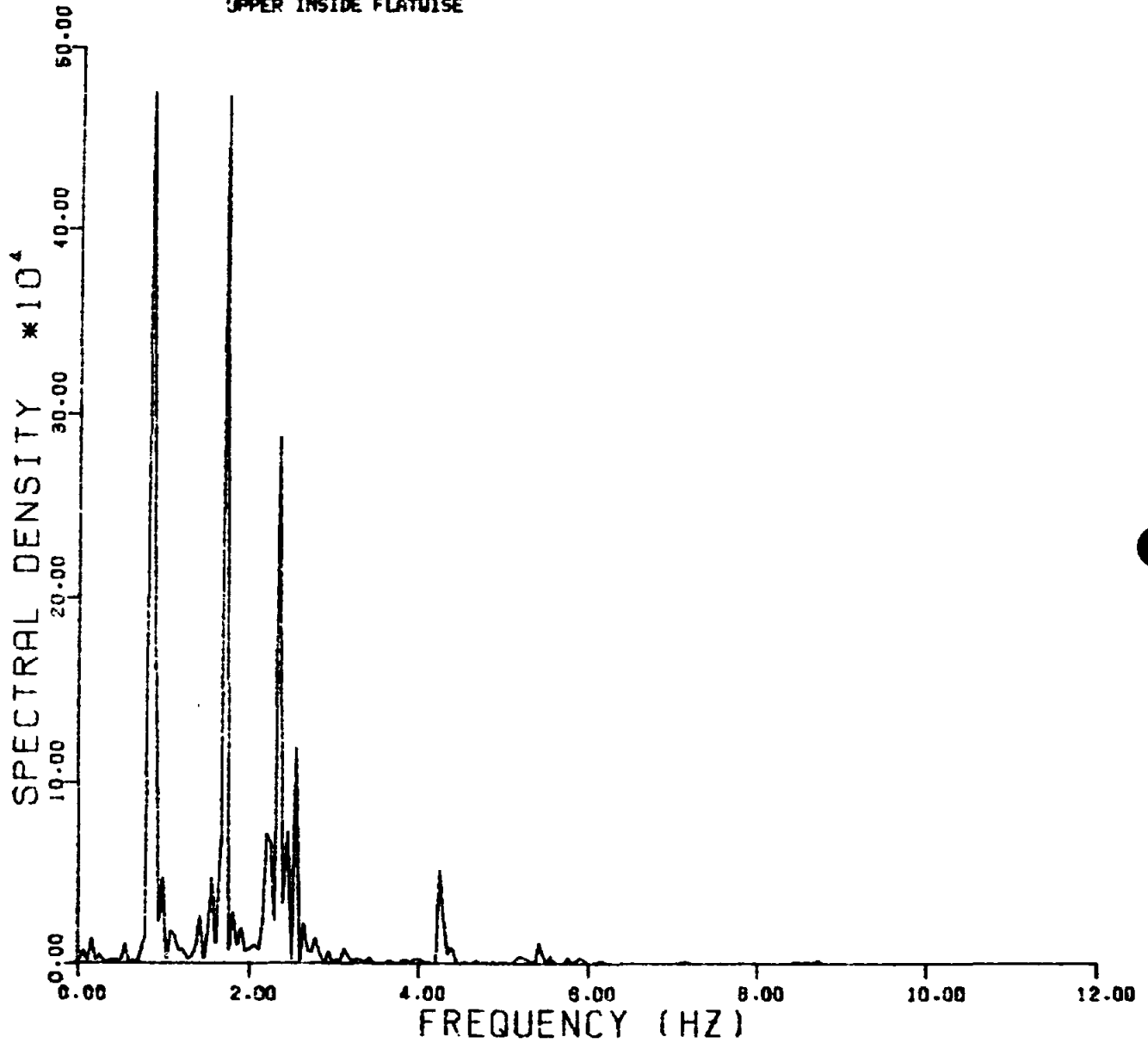


FIGURE 2. Blade Strain Spectral Density

The method of bins software package for reduction of aerodynamic data is a powerful one. Real time reduction on the 17 meter turbine is generally performed on two torque meters and an electric power transducer at the same time together with readings of 2 or 3 of the 10 anemometers available. Once the data are real time reduced, they can be stored on a disc file so that the results of many tests can be combined together. This gives the ability to see performance data over the whole range of winds normally available at a site. An example of the typical output of combined records is in Fig. 3. Bins reduction can also be performed on any combination of the 3 turbines on site simultaneously. In addition, the bins package can reduce a record of time series data and treat the results the same as real time data.

3. Structural Data Analysis - There are two aspects of concern in structural measurements. First is the immediate question of determining the structural integrity of the machine. Once integrity is established, a detailed analysis of the measurements is desired to provide a basis for confirming and/or redirecting our analysis tools.

The immediate question is naturally of concern when the turbine is turned on for the first time or when the turbine is operating under extreme or unusual conditions. To help answer this and to give turbine operators some guidance, a program was written which monitors in real time strain measurements from all the strain gauges. The program outputs the average and vibratory strain levels over ten seconds of readings, and continually updates a display of this information.

Detailed structural data analysis is generally post-processed from time resolved data stored from the PCM and A/D. For example, spectral analysis is performed on blade strain readings. This gives blade and tower vibrational information which has been used in conjunction with finite element analysis

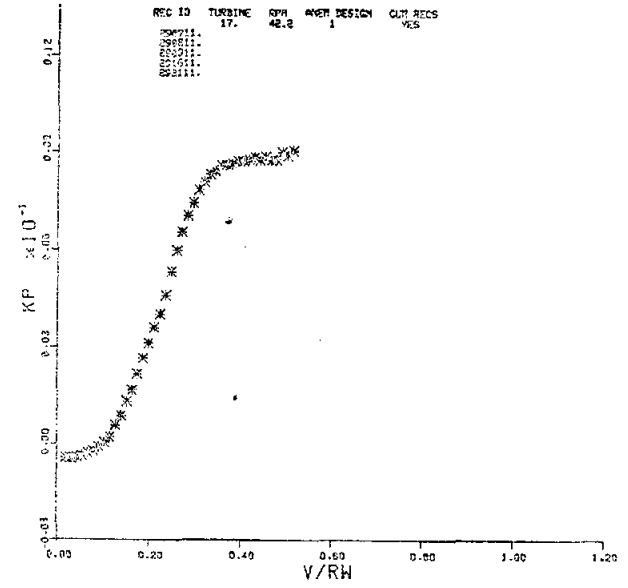
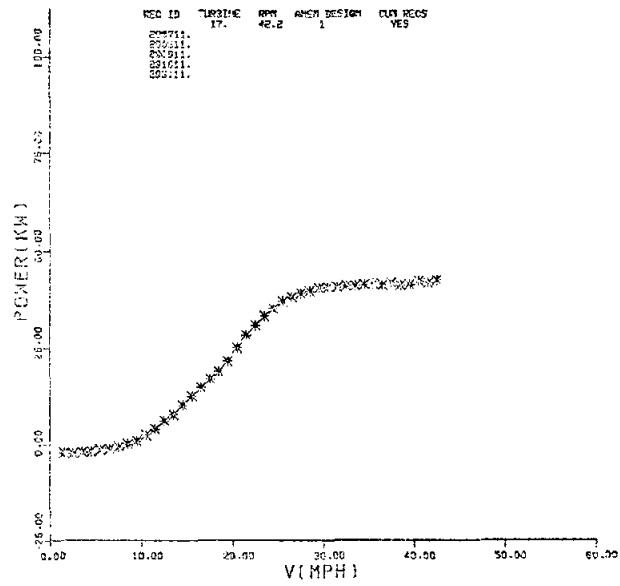
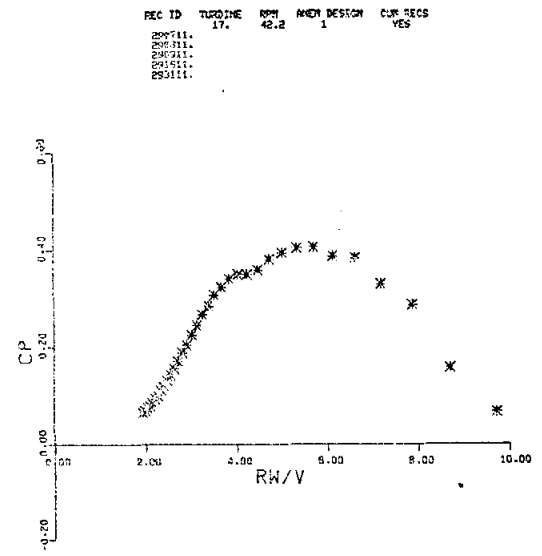
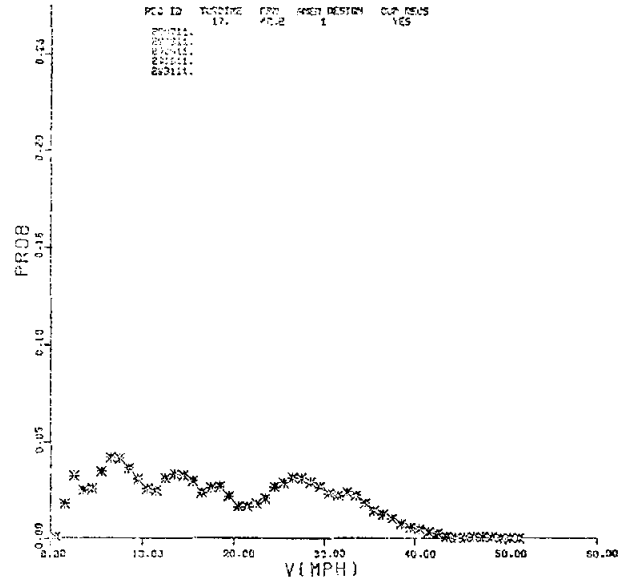


FIGURE 3. Aerodynamic Performance from Method of Bins

to help avoid conditions leading to excitation of the turbine's natural frequencies.

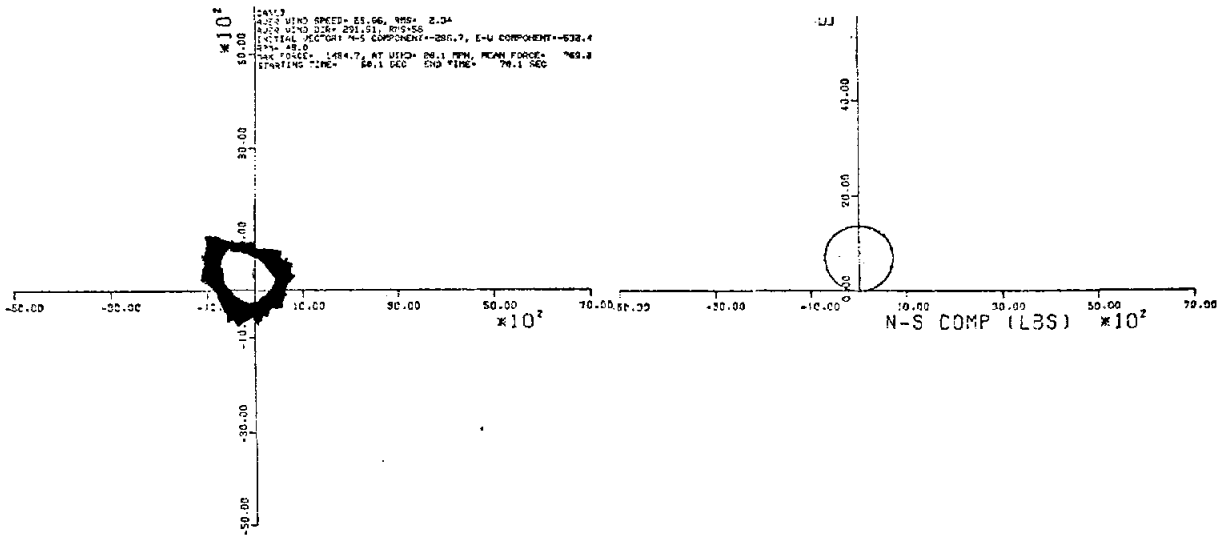
The resultant force experienced by the top of the tower as measured by guy wire tension is also of interest in checking for tower vibrations and aerodynamic load modeling. A package is available which calculates the resultant tower force versus time and outputs the results in polar plots. Two examples of polar plots appear along with the corresponding predictions from the single streamtube aerodynamic model in Fig. 4. The bottom figure was instrumental in spotting a tower vibration in the three-bladed configuration. For obvious reasons, these plots have been nicknamed "black holes" by the wind group.

The method of bins has been expanded from its original function of real time aerodynamic performance testing to reduce stored time series records of other quantities that are functions of windspeed. Transverse guy cable vibrational acceleration and guy cable tension have been found to depend on windspeed for an operating wind turbine. A bins type reduction package has thus been developed for guy cable analysis. For the cable acceleration, the additional feature is available that will calculate acceleration in any of the first three vibrational frequencies. Results of these measurements and calculations have been presented earlier in the conference.

In structural analysis, the phenomenon of torque ripple has been found to have a significant effect on turbine design. A program is available which calculates the torque ripple versus windspeed using a method of bins type of reduction. Also, the number of times the torque changes sign over a torque cycle may be calculated by a bins type reduction.

Although the method of bins is excellent for evaluating the magnitude of a phenomenon versus windspeed, the results are quite quantitative and lack any qualitative information.

2-Bladed Rotor, Tiedown Cable Resultants



3-Bladed Rotor, Tiedown Cable Resultants

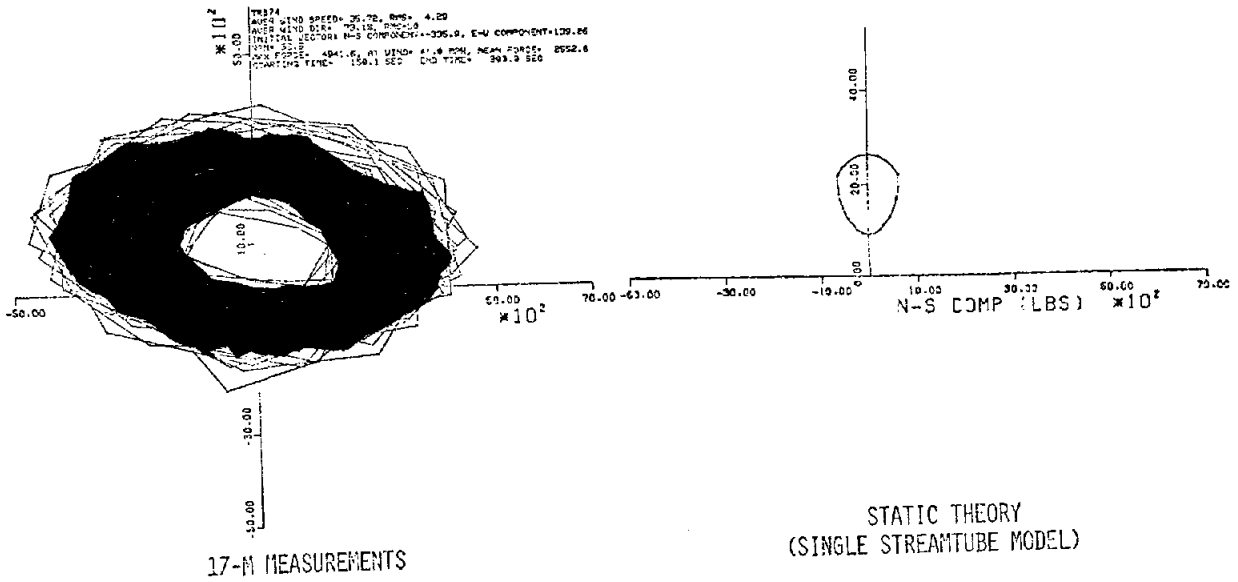
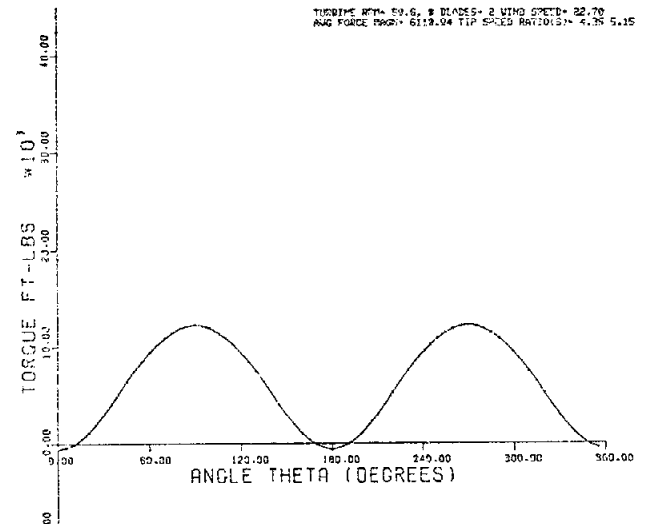
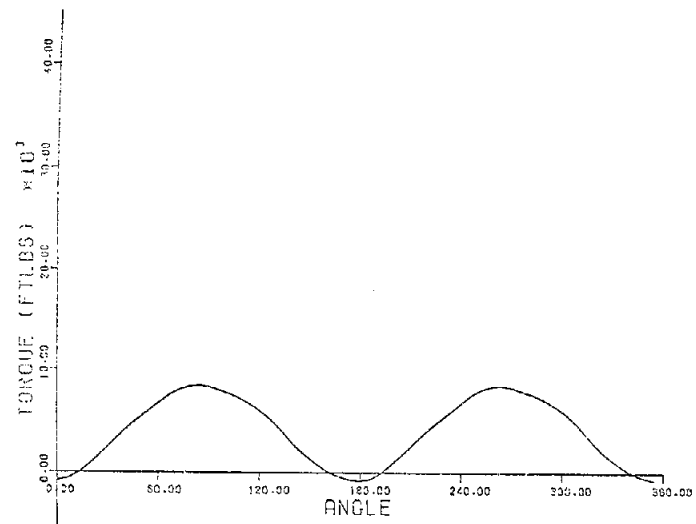
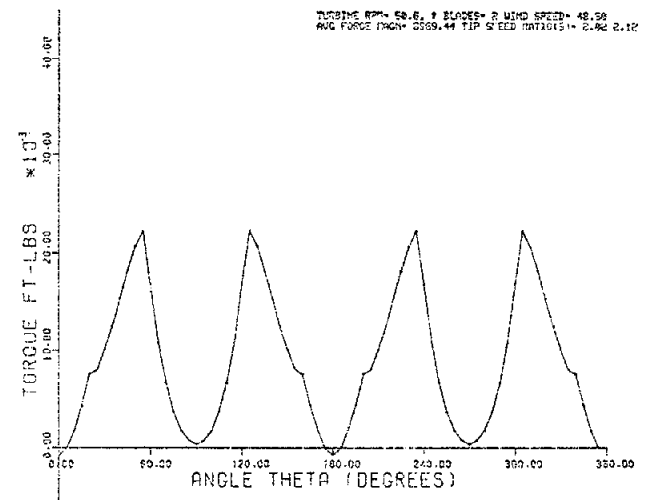
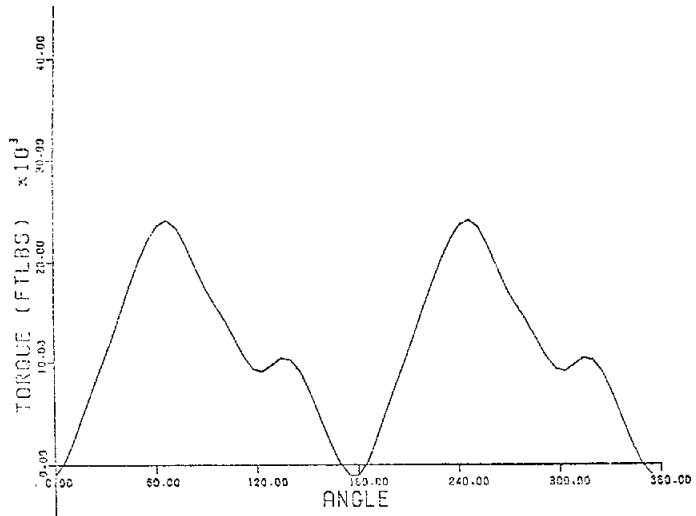


FIGURE 4

In the torque ripple study, a need exists to use the exact form of the torque function versus rotational angle relative to the wind direction for fixed windspeeds. In response to this need, a test was devised using accelerometers on the blades in conjunction with torque meter readings to obtain a true picture of aerodynamic torque. A set of computer programs was developed along with the test to massage the test results into what is considered the average torque cycle for several tip speed ratios. The computed average cycles for two tip speed ratios at 50.6 rpm appear in Fig. 5.

4. Automatic Control and Related Functions - Most of the emphasis at the DOE/Sandia VAWT site is on performance and structural testing, and tests are always run with an operator present to insure that proper conditions are met. However, the means of achieving automatic unattended operation of wind turbines is an important research issue and this has been investigated with the 17-m system.

A software package has been developed to run the 17-m turbine automatically and is being run during periods when the turbine is unattended. The control system continuously monitors windspeed, rpm, cable tension, and blade stress to insure safe operation. In addition, the control panel requires the mini-computer to answer a trivial question every 2 seconds. If the mini-computer fails to answer this question, the emergency brake is applied. This feature guards against turbine operation under computer failure. During turbine operation, aerodynamic performance, windspeed time series, and power output may be recorded. After every turbine stop, all stopping parameters are recorded. The computer control system has been successful thus far and demonstrates the possibility of operating the VAWT automatically.



17-m Measurements

Static Theory
(Single Streamtube Model)

FIGURE 5

5. Communicating Information to and from Other Computer Systems - The need for communication between the mini-computer at the VAWT site and other computers first arose as a result of the software package on the mini-computer that calculates the Fourier coefficients of a periodic time series. Since then, it has been desirable to transfer time series records to larger computers for more complete time series analysis than is available on the mini-computer. To accomplish the information transfers, the mini-computer is equipped with a 9 track magnetic tape unit. Programs are available to write time series to magnetic tape in card image format and read time series records either unformatted or in card image format.

A cassette tape system is also in use at the wind turbine site. Data may be recorded by a mobil cassette data logger, and then read by the mini-computer and either printed on hard copy or written on a 9 track magnetic tape. So far, meteorological data have been recorded by cassette tape from various sites including Sandia Crest.

6. Miscellaneous - Some localized wind related phenomenon are generally important to wind energy generation. In particular, the wind shear due to boundary layer effects near the earth's surface have an effect both on structural analysis and performance evaluation. The usual formula used in wind shear calculations is the one seventh exponent law. This law is empirical and is not universally valid. At the VAWT site, a meteorological tower has been erected and is instrumented with several anemometers. These anemometers along with anemometers located near each of the turbines are used to determine the wind field in the vicinity of the test site. This information is used to determine wind shear dependence on windspeed and direction, and to study the turbine wake characteristics of the 17-m turbine.

The growing interest in time resolved stored data over the last two years has resulted in a proliferation of stored data on disc files. Consequently, a method of keeping track of what data are available and where to find them has been developed in the form of a data file directory. The directory, itself a disc file together with user software, is a catalogue of each known record along with information as to what A/D or PCM channels are recorded, turbine characteristics, atmospheric conditions, test nature, and file location. The user can either ask for all information about a specific record, or can ask for a list of all records satisfying any number of 18 conditions. This facilitates data searches that are commonly required of time series records.

Reference

1. R. E. Akins, Performance Evaluation of Wind Energy Conversion Systems Using the Method of Bins - Current Status, SAND77-1375 (Albuquerque, NM: Sandia Laboratories, 1978).

VAWT Design Technology Seminar for Industry
 April 1-3, 1980
 Status
 Seminar Brochure Invitations and Response

<u>Mailing List Companies</u>	<u>Total</u>	<u>Response Seminar Attendees</u>
Small Business	86	13
Large Business	44	23
Universities	11	11
Small Consulting Firms	8	6
News, Dailies, PR	63	4
Electric Companies/Utilities	46	3
Government Federal/State	27	38
Foreign	29	11
TOTAL	<u>314</u>	<u>109</u>

Comments on Attendance

Documented in Registration Log: 107

VAWT (Estimated) Visitors, SNL, etc. Total: 135

SNL Technical Documents Requested and Delivered: Approximately 600

APPENDIX B

DOE/SNL: VAWT INDUSTRY SEMINAR APRIL 1-3, 1980 ATTENDANCE
INDUSTRY PERSONNEL REPRESENTING AND AFFILIATION

<u>Affiliation Representation</u>	<u>Representatives</u>	<u>Remarks</u>
1. R&D Industry	20	
2. Fabrication Industry	17	
3. R&D Fabrication Industry	7	
4. Consulting Specialty Firm	17	
5. Component Supplier	9	
6. Private Utility	2	
7. Public Utility	2	
8. Government Agency	13	
9. Government Laboratory	37	
10. Other	7	Sales, Agriculture, System Integration
 <u>Primary Interest of Representative</u>		
1. Prime Contracting	12	
2. Subcontracting	7	
3. Users	3	
4. Other	6	Engineering Design, etc.

BIBLIOGRAPHY

1. Advanced Energy Projects Division. Sandia Vertical Axis Wind Turbine Project Technical Quarterly Report -- April-June 1976, SAND76-0581. Albuquerque, NM: Sandia Laboratories, 1977.
2. Akins, R. E. Performance Evaluation of Wind Energy Conversion Systems Using the Method of Bins - Current Status, SAND77-1375. Albuquerque, NM: Sandia Laboratories, 1978.
3. Akins, R. E. Wind Characteristics for Field Testing of Wind Energy Conversion Systems, SAND78-1563. Albuquerque, NM: Sandia Laboratories, 1979.
4. Akins, R. E. Wind Characteristics at the VAWT Test Facility, SAND78-0760. Albuquerque, NM: Sandia Laboratories, 1978.
5. Auld, H. E. and Lodde, P. F., Civil Engineering Research Facility. A Study of Foundation/Anchor Requirements for Prototype Vertical Axis Wind Turbines, SAND78-7046. Albuquerque, NM: Sandia Laboratories, 1979.
6. Banas, J. F., Kadlec, E. G., and Sullivan, W. N. Application of the Darrieus Vertical Axis Wind Turbine to Synchronous Electrical Power Generation, SAND75-0165. Albuquerque, NM: Sandia Laboratories, 1975.
7. Banas, J. F., Kadlec, E. G., and Sullivan, W. N. Methods for Performance Evaluation of Synchronous Power Systems Utilizing the Darrieus Vertical Axis Wind Turbine, SAND75-0204. Albuquerque, NM: Sandia Laboratories, 1975.
8. Banas, J. F. and Sullivan, W. N. Engineering of Wind Energy Systems, SAND75-0530. Albuquerque, NM: Sandia Laboratories, 1976.
9. Banas, J. F. and Sullivan, W. N., Editors. Sandia Vertical Axis Wind Turbine Program Technical Quarterly Report -- October-December 1975, SAND76-0036. Albuquerque, NM: Sandia Laboratories, 1976.
10. Blackwell, B. F. The Vertical Axis Wind Turbine - How It Works, SLA-74-0160. Albuquerque, NM: Sandia Laboratories, 1974.
11. Blackwell, B. F., Sheldahl, R. E., and Feltz, L. V. Wind Tunnel Performance Data for the Darrieus Wind Turbine with NACA 0012 Blades, SAND76-0130. Albuquerque, NM: Sandia Laboratories, 1977.

12. Blackwell, B. F., Sheldahl, R. E., and Feltz, L. V. Wind Tunnel Performance Data for Two- and Three-Bucket Savonius Rotors, SAND76-0131. Albuquerque, NM: Sandia Laboratories, 1977.
13. Blackwell, B. F., Sullivan, W. N., Reuter, R. C., and Banas, J. F. Engineering Development Status of the Darrieus Wind Turbine, SAND76-0650. Albuquerque, NM: Sandia Laboratories, 1977.
14. Blackwell, B. F. and Reis, G. E. Blade Shape for a Troposkien Type of Vertical Axis Wind Turbine, SLA-74-0154. Albuquerque, NM: Sandia Laboratories, 1974.
15. Braasch, R. H. The Design, Construction, Testing and Manufacturing of Vertical Axis Wind Turbines, SAND78-1253. Albuquerque, NM: Sandia Laboratories, 1978.
16. Dodd, C. W. Lightning Protection for the Vertical Axis Wind Turbine, SAND77-1241. Albuquerque, NM: Sandia Laboratories, 1977.
17. Dodd, C. W. and Sullivan, W. N. The Brake System for the 17 Meter Vertical Axis Wind Turbine, SAND77-1331. Albuquerque, NM: Sandia Laboratories, 1978.
18. Grover, R. D. and Kadlec, E. G. Economic Analysis of Darrieus Vertical Axis Wind Turbine Systems for the Generation of Utility Grid Electrical Power, Volume III - Point Designs, SAND78-0962. Albuquerque, NM: Sandia Laboratories, 1979.
19. Grover, R. D. and Veneruso, A. F. Sandia Vertical Axis Wind Turbine Program Technical Quarterly Report -- July-September 1976, SAND77-0711. Albuquerque, NM: Sandia Laboratories, 1977.
20. Ham, N. D. Aeroelastic Analysis of the Troposkien-Type Wind Turbine, SAND77-0026. Albuquerque, NM: Sandia Laboratories, 1977.
21. Hinrichsen, E. N., Power Technologies, Inc. Induction and Synchronous Machines for Vertical Axis Wind Turbines, SAND79-7017. Albuquerque, NM: Sandia Laboratories, 1979.
22. Kadlec, E. G. Characteristics of Future Vertical Axis Wind Turbines, SAND79-1068. Albuquerque, NM: Sandia Laboratories, 1978.

23. Klimas, P. C. and Sheldahl, R. E. Four Aerodynamic Prediction Schemes for Vertical Axis Wind Turbines: A Compendium, SAND78-0014. Albuquerque, NM: Sandia Laboratories, 1978.
24. Leonard, T. M. A User's Manual for the Computer Code, PAREP, SAND79-0431. Albuquerque, NM: Sandia Laboratories, 1979.
25. Reed, J. W. Some Variability Statistics of Available Wind Power, SAND78-1735. Albuquerque, NM: Sandia Laboratories, 1979.
26. Reed, J. W. Wind Power Climatology of the United States - Supplement, SAND78-1620. Albuquerque, NM: Sandia Laboratories, 1979.
27. Reed, J. W. Wind Speed Distribution Changes with Height at Selected Weather Stations, SAND76-0714. Albuquerque, NM: Sandia Laboratories, 1978.
28. Reed, J. W. Wind Time Series Analyses for WECS Applications, SAND77-1701. Albuquerque, NM: Sandia Laboratories, 1978.
29. Reuter, R. C., Jr. Tie-Down Cable Selection and Initial Tensioning for the Sandia 17 Meter Vertical Axis Wind Turbine, SAND76-0616. Albuquerque, NM: Sandia Laboratories, 1977.
30. Reuter, R. C., Jr. and Worstell, M. H. Torque Ripple in a Vertical Axis Wind Turbine, SAND78-0577. Albuquerque, NM: Sandia Laboratories, 1978.
31. Reuter, R. C., Jr. Vertical Axis Wind Turbine Tie-Down Design with an Example, SAND77-1919. Albuquerque, NM: Sandia Laboratories, 1977.
32. Sheldahl, R. E. and Blackwell, B. F. Free-Air Performance Tests of a 5 Meter Diameter Darrieus Turbine, SAND77-1063. Albuquerque, NM: Sandia Laboratories, 1977.
33. Stiefeld, B. Wind Turbine Data Acquisition and Analysis System, SAND77-1164. Albuquerque, NM: Sandia Laboratories, 1978.
34. Strickland, J. H. The Darrieus Turbine: A Performance Prediction Model Using Multiple Streamtubes, SAND75-0431. Albuquerque, NM: Sandia Laboratories, 1975.

35. Sullivan, W. N. Economic Analysis of Darrieus Vertical Axis Wind Turbine Systems for the Generation of Utility Grid Electrical Power, Volume I - Executive Summary, SAND78-0962. Albuquerque, NM: Sandia Laboratories, 1979.
36. Sullivan, W. N. Economic Analysis of Darrieus Vertical Axis Wind Turbine Systems for the Generation of Utility Grid Electrical Power, Volume II - The Economic Optimization Model, SAND78-0962. Albuquerque, NM: Sandia Laboratories, 1979.
37. Sullivan, W. N. Preliminary Blade Strain Gage Data on the Sandia 17 Meter Vertical Axis Wind Turbine, SAND77-1176. Albuquerque, NM: Sandia Laboratories, 1977.
38. Sullivan, W. N. and Nellums, R. O. Economic Analysis of Darrieus Vertical Axis Wind Turbine Systems for the Generation of Utility Grid Electrical Power, Volume IV - Summary and Analysis of the A. T. Kearney and Alcoa Laboratories Point Design Economic Studies, SAND78-0962. Albuquerque, NM: Sandia Laboratories, 1979.
39. Weingarten, L. I. and Blackwell, B. F. Sandia Vertical Axis Wind Turbine Program Technical Quarterly Report -- January-March 1976, SAND76-0338. Albuquerque, NM: Sandia Laboratories, 1976.
40. Weingarten, L. I. and Nickell, R. E. Nonlinear Stress Analysis of Vertical Axis Wind Turbine Blades, SAND74-0378. Albuquerque, NM: Sandia Laboratories, 1975.
41. Worstell, M. H. Aerodynamic Performance of the 17 Meter Diameter Darrieus Wind Turbine, SAND78-1737. Albuquerque, NM: Sandia Laboratories, 1978.

DISTRIBUTION:

TID-4500-R66, UC-60 (289)

D. K. Ai
Alcoa Technical Center
Alcoa Laboratories
Alcoa Center, PA 15069

A. Akhil
Public Service Company of
New Mexico
P.O. Box 2267
Albuquerque, NM 87103

J. M. Alcone (2)
Science Applications, Inc.
200 Lomas NW
Suite 600
Albuquerque, NM 87102

C. E. Alford
Rockwell International
Rocky Flats Plant
P.O. Box 464
Golden, CO 80401

R. L. Ayers
New Mexico New Energy
Systems, Inc.
80 E. San Francisco St. #6
Santa Fe, NM 87501

E. E. Bange
Rockwell International
Rocky Flats Plant
P.O. Box 464
Golden, CO 80401

W. J. Barattino
DOE-AFESC Liaison Office
DOE/Albuquerque Operations
Office
Albuquerque, NM 87185

K. Barnett
New Mexico Solar Energy
Institute
Box 3SOL
Las Cruces, NM 88003

G. Beaulieu
IREQ, Hydro-Quebec
P.O. Box 1000
Varenes, Quebec
Canada JOL 2P0

W. Bogaerts (5)
Hansen Transmissions, Inc.
P.O. Box 710
Branford, CT 06405

H. T. Clark (5)
McDonnell Douglas
P.O. Box 516
Dept. 337, Bldg. 32-2
St. Louis, MO 63166

A. G. Craig, Jr.
Alcoa Technical Center
Alcoa Laboratories
Alcoa Center, PA 15069

K. Craig
Indiana Analytical Laboratories
P.O. Box 87
Shelocta, PA 15774

G. Curtis
Tumac Industries, Inc.
650 Ford St.
Colorado Springs, CO 80915

R. E. Donham
Lockheed California Co.
P.O. Box 551
Burbank, CA 91520

R. Duke
Tumac Industries, Inc.
650 Ford St.
Colorado Springs, CO 80915

B. N. Ellis
Bendix Corporation
Executive Offices
Southfield, MI 48076

R. E. Feldges
Safeguard Power Transmission Co.
P.O. Box 1089
Aberdeen, SD 57401

D. J. George
Alcoa Technical Center
Alcoa Laboratories
Alcoa Center, PA 15069

R. A. Golobic
Centennial Sciences, Inc.
3720 Seaton Road
Suite 205
Colorado Springs, CO 80907

M. W. Hall
Reynolds Metals Co.
6601 W. Broad St.
Richmond, VA 23261

B. Hibler (2)
Central New Mexico Electric
Coop, Inc.
P.O. Box 669
Moriarty, NM 87036

S. Hightower
U.S. Water Power Resources
Service
Mail Code 1500E
P.O. Box 25007
Denver, CO 80225

L. J. Hill
Kearns Machinery Co.
3201 N. Louise Avenue
Sioux Falls, SD 57101

R. B. Hobbs, Jr.
General Electric Co.
P.O. Box 8661
Building 11
Philadelphia, PA 19035

C. W. Hosey (3)
XTEK, Inc.
201 E. Southern Avenue
Suite 203I
Tempe, AZ 85282

T. C. Jameson
Battelle Pacific Northwest
Laboratories
P.O. Box 999
Richland, WA 99352

J. R. Jombock
Alcoa Technical Center
Alcoa Laboratories
Alcoa Center, PA 15069

M. Katz
U.S. Department of Energy
600 E Street NW
Washington, DC 20545

T. S. Kawahigashi
Austin-Tsutsumi and
Associates, Inc.
745 Fort St. Mall
Suite 900
Honolulu, HI 96813

T. C. Kennedy
Oregon State University
Corvallis, OR 97331

H. Kirlin
Central New Mexico Electric
Coop, Inc.
P.O. Box 669
Moriarty, NM 87036

J. Klose (2)
Solar America, Inc.
2620D San Mateo NE
Albuquerque, NM 87110

T. E. Kullgren
U.S. Air Force Academy
Department of Engineering
Mechanics
USAF Academy, CO 80918

A. Lemnios
Kaman Aerospace Corporation
Old Windsor Road
Bloomfield, CT 06003

O. Ljungström
FFA, The Aeronautical Research
Institute of Sweden
Box 11021, S-16111
Bromma, Sweden

A. Lober
Southwestern Energy Resources
1900 Chamisa St.
Santa Fe, NM 87501

T. Lonnbord
Falk Corporation
3001 W. Canal St.
P.O. Box 492
Milwaukee, WI 53201

S. Maekawa
Tetra Tech, Inc.
630 N. Rosemead Blvd.
Pasadena, CA 91197

B. Masse
IREQ, Hydro-Quebec
P.O. Box 1000
Varenes, Quebec
Canada J0L 2P0

R. D. McConnell
Solar Energy Research Institute
1617 Cole Blvd.
Golden, CO 80401

J. G. Melvin
General Dynamics Corporation
9841 Airport Blvd.
Suite 512
Los Angeles, CA 90045

P. W. Metcalfe (2)
Unarco-Rohn
P.O. Box 2000
Peoria, IL 61656

J. E. Murphy (2)
Rockwell International, Inc.
8900 De Soto Avenue
Canoga Park, CA 91304

D. R. Neill
University of Hawaii
2540 Dole Street
Honolulu, HI 96822

R. L. Nielsen
Boeing Engineering and
Construction Co.
P.O. Box 3707, M/S IE-10
Seattle, WA 98124

J. W. Oler
Texas Tech University
P.O. Box 4289
Lubbock, TX 79409

R. Q. Palmer
5027 Justin NW
Albuquerque, NM 87114

H.-Reinhard Meyer-Piening
ERNO Raumfahrttechnik GmbH
Huenefeldstr. 1-5
Bremen, West Germany
D-2800

J. L. Prohaska
Alcoa Technical Center
Alcoa Laboratories
Alcoa Center, PA 15069

R. L. Puthoff
NASA-Lewis Research Center
21000 Brookpark Road
Cleveland, OH 44135

S. Quraeshi (2)
The Shawinigan Engineering
Company Limited
620 Dorchester Blvd. West
Montreal, Quebec
Canada, Station B H3B 3L7

R. S. Rangi (2)
National Research Council
Montreal Road M-2
Ottawa, Ontario
Canada K1V 8N2

W. C. Reddick
U.S. Department of Energy
600 E Street NW
Washington, DC 20545

H.-G. Reimerdes
Aachen Technical University/
Inst. f. Leichtbau
Wullnerstr. 7
5100 Aachen, West Germany

B. Richards (2)
The Shawinigan Engineering
Company Limited
620 Dorchester Blvd. West
Montreal, Quebec
Canada, Station B H3B 3L7

H. R. Riley
City of Tucumcari
P.O. Box 1188
Tucumcari, NM 88401

L. P. Rowley (2)
Canadair Ltd.
P.O. Box 6087 Station A
Montreal, Quebec
Canada H3C 3G9

L. Schienbein
DAF Indal, Ltd.
3570 Hawkestone Road
Mississauga, Ontario
Canada L5C 2V8

R. Schoenmackers
New Mexico Solar Energy
Institute
Box 3SOL
Las Cruces, NM 88001

D. J. Sharpe
Kingston Polytechnic
Canbury Park Centre
Canbury Park Road, Kingston
upon Thames
Surry, England KT2 6LA

R. W. Sherwin
Enertech Corporation
P.O. Box 420
Norwich, VT 05055

K. Sivier (2)
University of Illinois
105 Transportation Blvd.
Urbana, IL 61801

H. P. Sleeper
Kentron International, Inc.
2003 Byrd Spring Road
Huntsville, AL 35802

P. South
Solar Energy Research Institute
1617 Cole Blvd.
Golden, CO 80401

W. J. Steeley (2)
Pacific Gas and Electric Co.
3400 Crow Canyon Road
San Ramon, CA 94583

G. Stricker (5)
Windfarms, Ltd.
301 S.W. Lincoln
Suite 1016
Portland, OR 97201

J. H. Strickland
Texas Tech University
P.O. Box 4289
Lubbock, TX 79409

J. L. Tangler
Rockwell International
Rocky Flats Plant
P.O. Box 464
Golden, CO 80401

C. J. Todd
Water and Power Resources
Service
Denver Federal Center
Denver, CO 80225

F. M. Townsend (2)
Venture Manager for Alcoa Vertical
Axis Wind Turbine Systems
1501 Alcoa Bldg.
Pittsburgh, PA 15219

P. K. C. Tu
Rockwell International
Rocky Flats Plant
P.O. Box 464
Golden, CO 80401

Solar Energy Research Institute(4)
1617 Cole Blvd.
Golden, CO 80401
Attn: I. E. Vas
P. Weis
Library (2)

M. C. Wehrey (3)
Southern California Edison Co.
P.O. Box 800
Rosemead, CA 91770

M. H. Williams
Alcoa Technical Center
Alcoa Laboratories
Alcoa Center, PA 15069

R. E. Wilson
Oregon State University
Corvallis, OR 97331

C. F. Wood
DAF Indal, Ltd.
3470 Hawkestone Road
Mississauga, Ontario
Canada L5C 2V8

M. K. Wright
Westinghouse
P. O. Box 10864
Pittsburgh, PA 15236

R. A. Zacharski
Rockwell International
Rocky Flats Plant
P.O. Box 464
Golden, CO 80401

New Mexico Engineering Research
Institute
University of New Mexico
P. O. Box 25
Albuquerque, NM 87131
Attn: Dr. Gerald Leigh

P. P. Zemanick
Westinghouse
P. O. Box 10864
Pittsburgh, PA 15236

4700 J. H. Scott
4710 G. E. Brandvold
4710 C. J. Mora
4715 R. H. Braasch (300)
4720 V. L. Dugan
3141 T. L. Werner (5)
3151 W. L. Garner (3)
For DOE/TIC
(Unlimited Release)